Fifteenth Edition

# Photovoltaics International

THE TECHNOLOGY RESOURCE FOR PV PROFESSIONALS

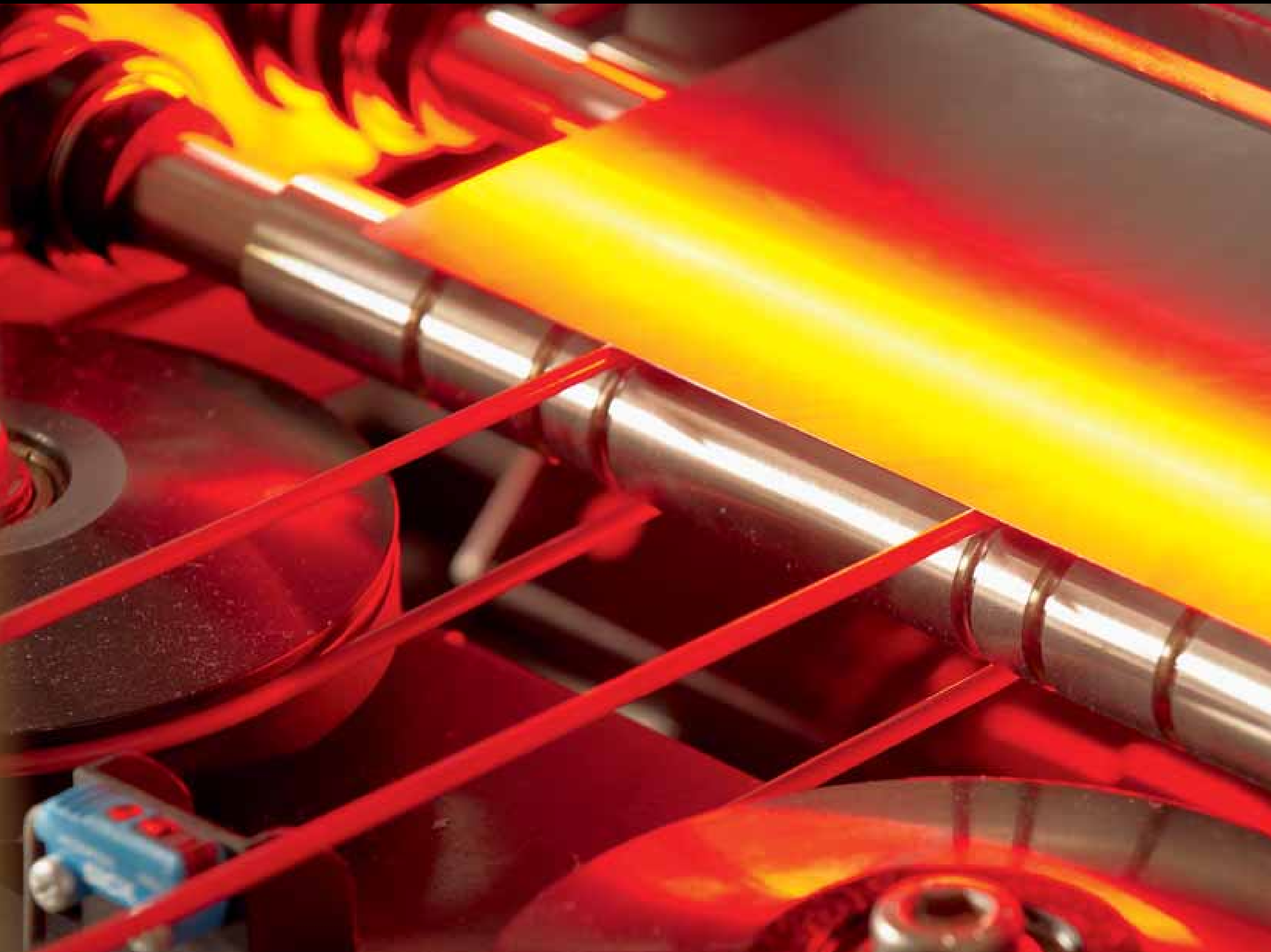

**CEA-INES:** an in-depth look at the pros and cons of diamond wire sawing
**MIT:** expounding the benefits of TCAD for impurity evolution modelling in PV
**REC ASA:** life cycle analysis of multicrystalline Si modules
**ISFH & LUH:** new schemes for rear-surface passivation of screen-printed PERC cells
**Max Planck Institute:** an all-inorganic approach to thin-film solar on glass
**AIT on module quality:** EL imaging and infrared thermography methods

First Quarter, February 2012

www.pv-tech.org

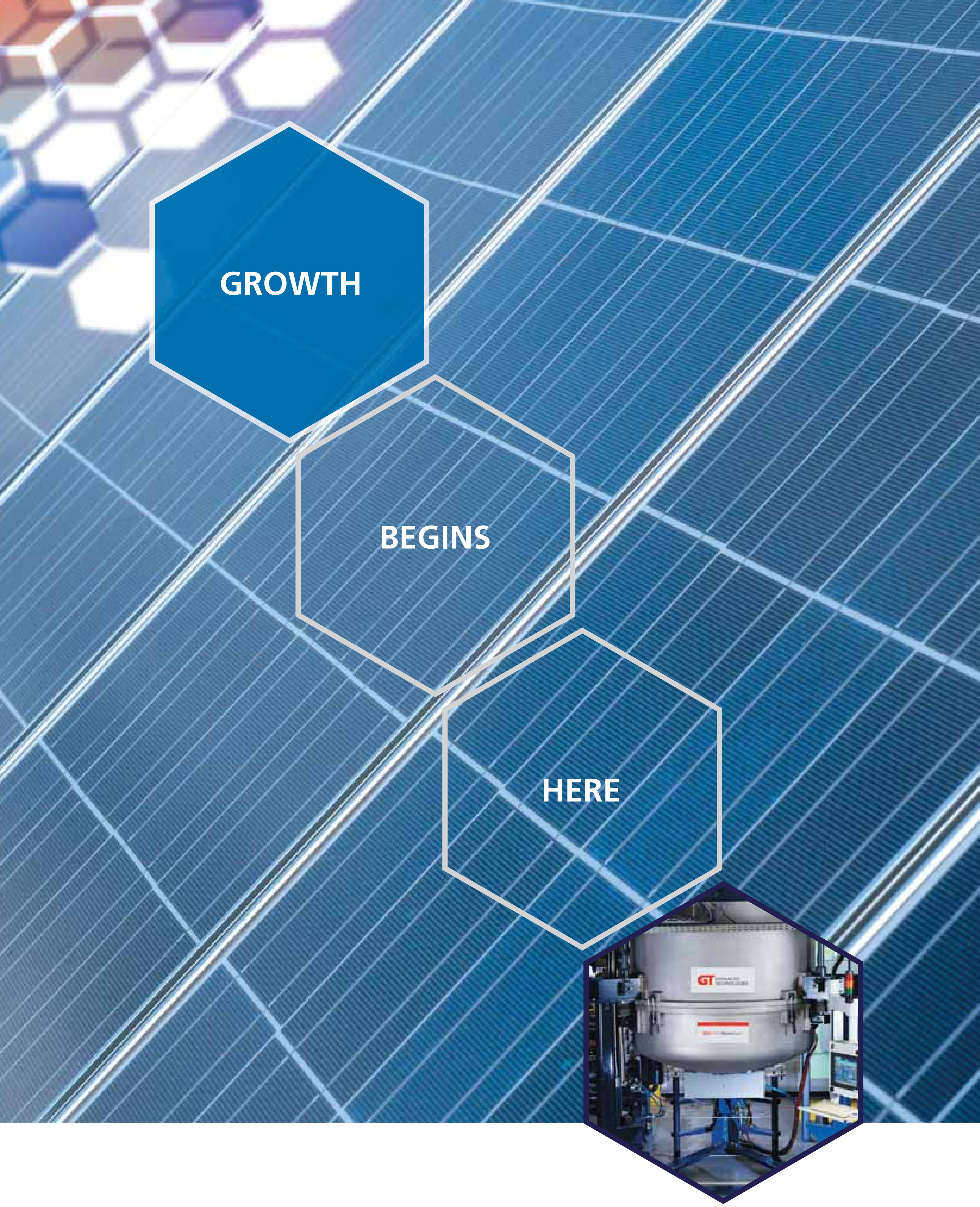
GROWTH
BEGINS
HERE

Photovoltaics International

Published by:
Solar Media Ltd.,
Trans-World House, 100 City Road, London
EC1Y 2BP, UK
Tel: +44 (0) 207 871 0123
Fax: +44 (0) 207 871 0101
E-mail: info@pv-tech.org
Web: www.pv-tech.org

Publisher: David Owen

Managing Editor: Síle Mc Mahon

Design & Production: Daniel H Brown
Production: Viki Hämmerle
Senior News Editor: Mark Osborne
Web & Publications Editor: Nilima Choudhury
News Editor: Syanne Olson
Contributing Editors: Felicity Carus,
Emma Hughes & Pete Bennett

Sub-Editor: Steve D. Brierley
Commissioning Editor: Adam Morrison

Sales Director: David Evans
Account Managers: Adam Morrison, Graham
Davie, Daniel Ryder, Gary Kakoullis,
Nick Richardson, Ben Irving & Peter Gibson
Germany Office Representative: Martin Lehmann
Marketing & Operations Director:
Joy-Fleur Brettschneider
Marketing & PR Executive: Laura Pleasants



Cover image shows a wafer passing through an in-line quality control tool. Image courtesy of Fraunhofer CSP Halle (Saale), Germany Saxony-Anhalt.

Printed by Buxton Press
Photovoltaics International
Fifteenth Edition
First Quarter 2012
Photovoltaics International is a quarterly journal published in February, May, August and November.

Distributed in the USA by Mail Right International, 1637 Stelton Road B4, Piscataway, NJ 08854.

ISSN: 1757-1197



USPS Information
USPS Periodical Code: 025 313

Periodicals Postage Paid at
New Brunswick, NJ
Postmaster: Send changes to:
Photovoltaics International,
Solar Media Ltd., C/o 1637 Stelton
Road, B-4, Piscataway, NJ 08854, USA

# Foreword

As the saying goes, *do not fear the winds of adversity: a kite rises against the wind, not with it*. This advice should be well heeded by the struggling photovoltaics industry this year, as the winds of adversity up the ante in what has come to be known as the 'solar shakeout.' With numerous facility closures, ensuing job losses and continued polysilicon price declines, it looks like 2012 will see the overcapacity situation persist in separating out those companies whose cost models have been shown to be lacking the backbone necessary to survive in such a cut-throat market.

So what is to become of the small- to medium-sized suppliers? 2011 saw relatively weak demand in the first half of the year, leading to high channel inventory and collapsing prices in the latter part of the year. As a result, many suppliers were forced to sell at a loss, a situation that has left many licking their wounds in early 2012.

We have already seen job layoffs from Bekaert, Roth & Rau and Sanyo, while rumours of bankruptcy surrounding former stalwart Q-Cells made many in the industry sit up and take stock of their operations. Many Chinese PV manufacturers have gone down the fully-integrated business model route in order to avoid pitfalls along the way, and several of the key industry players have reshuffled their operations in a bid to shake off the less-profitable business segments in an attempt to remain competitive. Those that don't have such an option will either struggle to survive or will fall by the wayside.

One approach to coping with the current situation is to tackle key factors such as cell efficiency, materials costs and process quality. And what better way to do so than to consult the pages of this edition of *Photovoltaics International*, which delivers some remarkable insights into efficiency improvements and quality control from some of the most esteemed researchers, engineers and analysts in this ever-changing industry.

We've got a strong focus on PV materials in this issue. On p. 36, **Alternative Energy Investing** presents a comprehensive look at materials cost and availability; quality control of Cz-Si wafers is discussed by **Fraunhofer ISE** on p. 50, while **CEA-INES** delivers perspectives on diamond wire sawing processes (p. 60).

Efficiency improvements on bifacial n-pasha cells are under consideration at **ECN** (p. 81), and we've got a contribution from **Massachusetts Institute of Technology (MIT)** on TCAD as an ideal method for modelling metal impurity evolution on p. 91. Regular contributors **imec** propose a meeting of minds of c-Si materials and thin-film processing developments on p. 107, while module lifetime is under the microscope in two papers by **REC Solar & ECN** (p. 136) and **Tata BP Solar** (p. 141).

Further downstream, **Fraunhofer IWES & DERlab** present approaches for long-term energy yield measurements (p. 178), while the merits of CPV technology are weighed up in an article by **Amonix** (p. 169). Rounding off this edition, **Solar Power Portal** outlines the UK solar market's current position (p. 192), and **IMS Research** gives us a brief run-down of what to expect from global markets in 2012 (p. 195).

As always, we're looking forward to another year of exciting industry events, and hope to see you at this year's SNEC PV Power Expo, for which Solar Media Ltd. is a Platinum Media Partner. Keep an eye out for our new publications this year: PV-Tech *PRO*, our new Chinese-language publication; *Solar Business Focus*, published bi-monthly and distributed digitally and in person at trade shows around the world; and of course the Photovoltaics International PV Production Annual 2012, which will be available for purchase online very soon!

Best of luck for 2012,

**Síle Mc Mahon**
Managing Editor
*Photovoltaics International*

# Photovoltaics International

Photovoltaics International's primary focus is on assessing existing and new technologies for "real-world" supply chain solutions. The aim is to help engineers, managers and investors to understand the potential of equipment, materials, processes and services that can help the PV industry achieve grid parity. The Photovoltaics International advisory board has been selected to help guide the editorial direction of the technical journal so that it remains relevant to manufacturers and utility-grade installers of photovoltaic technology. The advisory board is made up of leading personnel currently working first-hand in the PV industry.

## Editorial Advisory Board

Our editorial advisory board is made up of senior engineers from PV manufacturers worldwide. Meet some of our board members below:

*Gary Yu, Senior Vice President, Operations*

Mr. Yu served as Trina Solar's Vice President of Manufacturing since May 2007 and in July 2010 was promoted to the position of Senior Vice President of Operations. Mr. Yu has 17 years' manufacturing management experience in semiconductor-related industries. Before joining Trina Solar, he was Managing Director of Wuxi Lite-On Technology, an LED assembly company based in China. Prior to Wuxi Lite-On Technology, he served as a Director of Manufacturing for 1st Silicon Sdn. Bhd. in Malaysia, prior to which he worked at Macronix International, a semiconductor integrated device manufacturer in Taiwan. Mr. Yu has a master's degree in Industrial Engineering and Management from National Chiao Tung University in Taiwan and a bachelor's degree in Chemical Engineering from Tunghai University.

*Takashi Tomita, Senior Executive Fellow, Sharp Solar*

Takashi Tomita has been working at Sharp for 34 years and is widely recognised as a fore-father of the solar industry in Japan. He was responsible for setting up Sharp's solar cell manufacturing facilities in Nara and silicon production in Toyama. Takashi's passion for solar power has led him to hold numerous posts outside of his roles at Sharp, including: Vice Representative at the Japan Photovoltaic Industry Association; Committee Member of Renewable Energy Portfolio Standard of METI; Adviser Board Member of Advanced Technology of Nara; Visiting Professor of Tohoku University; Adviser of ASUKA DBJ Partners (JAPAN) and Adviser of Global Catalyst Partners (US).

*Dr. Kuo En Chang, President of Solar Division, Motech Industries, Inc.*

Dr. Kuo En Chang joined Motech in 1999 as Chief Technology Officer and became President of the Solar Division in 2008, with responsibility for all technology and manufacturing. Motech is the sixth largest solar cell producer in the world. Before Dr. Chang joined Motech Solar, he worked on secondary battery research at the Industrial Technology Research Institute (ITRI) for more than three years. Dr. Chang holds a Ph.D. degree in Metallurgical & Materials Engineering from the University of Alabama.

*Professor Eicke R. Weber, Director of the Fraunhofer Institute for Solar Energy Systems ISE in Freiburg*

Professor Eicke R. Weber is the Director of the Fraunhofer Institute for Solar Energy Systems ISE in Freiburg. Weber has earned an international reputation as a materials researcher for defects in silicon and III-V semiconductors such as gallium arsenide and gallium nitride. He spent 23 years in the U.S. in research roles, most recently as Professor at the University of California in Berkeley. Weber is also the Chair of Applied Physics, Solar Energy, at the University of Freiburg, and during his career has been the recipient of several prestigious awards including the Alexander von Humboldt Prize in 1994, and the German Cross of Merit on ribbon in June 2006.

*Dr. Zhengrong Shi, Chief Executive Officer, Suntech*

Dr. Zhengrong Shi is founder, CEO and Chairman of the board of directors of Suntech. Prior to founding Suntech in 2001, he was a Research Director and Executive Director of Pacific Solar Pty., Ltd., the next-generation thin-film technology company, before which he was a Senior Research Scientist and leader of the Thin Film Solar Cells Research Group in the Centre of Excellence for Photovoltaic Engineering at the University of New South Wales in Australia. Dr. Shi holds 11 patents in PV technologies and is a much-published author in the industry. His work has earned him such accolades as "Hero of the Environment" (TIME magazine 2007) and "Corporate Citizen of the Year" at the China Business Leaders Awards 2007. A member of the NYSE advisory board, Dr. Shi has a Bachelor's degree in optical science, a Master's degree in laser physics and a Ph.D. in electrical engineering.

*Dr. Sam Hong, President and COO of Neo Solar Power*

Dr. Hong has more than 30 years of experience working in the solar energy industry. He has served as the Research Division Director of Photovoltaic Solar Energy Division at Industry Technology Research Institute (ITRI), a research organization that serves to strengthen the technological competitiveness of Taiwan, and Vice President and Plant Director of Sinonar Amorphous Silicon Solar Cell Co., which is the first amorphous silicon manufacturer in Taiwan. In addition, Dr. Hong was responsible for Power Subsystem of ROCSAT 1 for the Taiwan National Space Program. Dr. Hong has published three books and 38 journal and international conference papers, and is a holder of seven patents. Dr. Hong was the recipient of Outstanding Achievement Award from the Ministry of Economic Affairs, Taiwan, and was recently elected as chairman of the Taiwan Photovoltaic Industry Association.

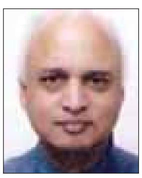

*Dr. G. Rajeswaran, President and CTO of Moser Baer Photovoltaic Ltd*

Raj served as President and CTO of Moser Baer Photovoltaic Ltd. from July 2007 until October 2008, since which time he has been Group CTO for all the Moser Baer business units and holder of the CEO function for launching new businesses. He spent 22 years with Eastman Kodak Company as the Vice President of Advanced Development & Strategic Initiatives, where he managed Kodak's Japan display operations including technology & business development in Japan, Taiwan, Korea and China. He has also served as Vice President and on the board of SK Display Corporation, and worked in technology development with Brookhaven National Laboratory. Raj has a Ph.D., an M.Tech. and a B.E. in electrical engineering. A much-published author, speaker and patent holder, Raj is a member of the Society for Information Display (SID) and has chaired several international conferences in the field of OLEDs.


WE GO FURTHER
dyMat PYE®
THERE'S NO BETTER BACKSHEET


**Giorgio Longoni**
*Coveme Business Manager Asia*

# Contents


8 Section 1
Fab & Facilities
+ NEWS

Page 13
**Environmental footprinting of photovoltaic module production**
**Mariska de Wild-Scholten**, SmartGreenScans, Groet, The Netherlands

Page 23
**US environmental permitting for PV manufacturing facilities – requirements and strategies for success**
**John Browning**, P.E., CH2M HILL, Denver, Colorado, USA

32 Section 2
Materials
+ NEWS
35 PRODUCT REVIEWS

Page 36
**PV manufacturing materials: Technological and process-related options for cost reduction**
**Joseph Berwind**, AEI Research & Consulting, NJ, USA

Page 50
**Cz-Si wafers in solar cell production: Efficiency-limiting defects and material quality control**
**Jonas Haunschild**, **Juliane Broisch**, **Isolde Reis** & **Stefan Rein**, ISE, Freiburg, Germany

Page 60
**Diamond wire sawing: State of the art and perspectives**
**Fabrice Coustier** & **Jean-Daniel Penot**, CEA-INES, LMPS, Le Bourget-du-Lac, & **Gérald Sanchez** & **Michel Ly**, Thermocompact, Pringy, France


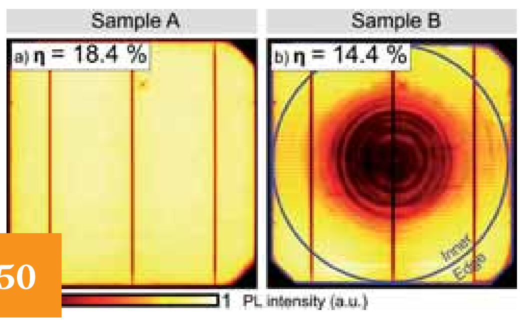


50


66 Section 3
Cell Processing
+ NEWS
70 PRODUCT REVIEWS

Page 73
**Firing stability of $SiN_y/SiN_x$ and $Al_2O_3/SiN_x$ stacks for the rear-surface passivation of industrial-type crystalline silicon solar cells**
**Sebastian Gatz**[1], **Jan Schmidt**[1,2], **Boris Veith**[1], **Thorsten Dullweber**[1] & **Rolf Brendel**[1,2]
[1]ISFH, Emmerthal; [2]Institute of Solid-State Physics, LUH, Hanover, Germany

Page 81
**Industrial n-type solar cells: Towards 20% efficiency**
**Ingrid Romijn**, ECN Solar Energy, Petten, The Netherlands, **Lang Fang**, Yingli Solar, Baoding, China, & **Ard Vlooswijk**, Tempress Systems BV, Vaassen, The Netherlands

Page 91
**TCAD for PV: A fast method for accurately modelling metal impurity evolution during solar cell processing**
**Douglas M. Powell**[1], **David P. Fenning**[1], **Jasmin Hofstetter**[1], **Jean-François Lelièvre**[2], **Carlos del Cañizo**[2] & **Tonio Buonassisi**[1]
[1]Massachusetts Institute of Technology, Cambridge, MA, USA; [2]Instituto de Energía Solar, Universidad Politécnica de Madrid, Madrid, Spain

101 Section 4
Thin Film
+ NEWS
106 PRODUCT REVIEWS

Page 107
**Crystalline silicon thin foils: Where crystalline quality meets thin-film processing**
**Frédéric Dross**, **Kris Baert** & **Jef Poortmans**, imec, Leuven, Belgium

Page 114
**Si nanorod-based thin-film solar cells on glass: A potentially low-cost and high-efficiency all-inorganic approach**
**Silke Christiansen** & **Michael Kiometzis**, **Max Planck** Institute for the Science of Light (MPL), Erlangen, and Institute of Photonic Technology (IPHT), Jena, Germany

120 Section 5
PV Modules + NEWS

125 PRODUCT REVIEWS

Page 126
**Non-destructive techniques for quality control of photovoltaic modules: Electroluminescence imaging and infrared thermography**
**Shokufeh Zamini**, **Rita Ebner**, **Gusztáv Újvári** & **Bernhard Kubicek**, Austrian Institute of Technology, Vienna, Austria


121

Page 136
**Life cycle analysis of modules: A multicrystalline silicon case study**
**Trond Westgaard**, REC, Sandvika, Norway, & **Carol Olson** & **Ton Veltkamp**, ECN, Petten, The Netherlands

Page 141
**Studying the lifetime of crystalline PV modules by interpreting the acceleration test data with statistical reliability models**
**Sreenivasa Murty Dasari**, **K. V. Nagaraj**, **S. Saravanan**, **Prakash Suratkar** & **T. S. Keshav Prasad**, TATA BP Solar India Ltd, Bangalore, India

Page 148
**A novel glue-membrane integrated backsheet for PV modules**
**Wenjin Xia**[1], **Yuzheng Zhang**[1], **York Yu**[1], **Hong Liu**[2], **Wenzhong Shen**[2] & **Jianwei Lin**[1]
[1]Jolywood (Suzhou) Sunwatt Co., Ltd.; [2]Institute of Solar Energy, Shanghai Jiaotong University, Shanghai, P. R. China

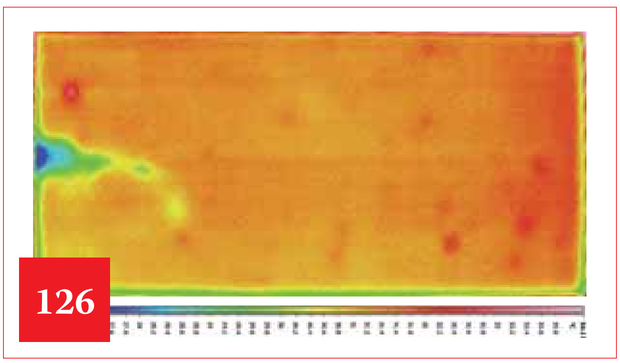
126

158 Section 6
Power Generation + NEWS

165 PRODUCT REVIEWS

Page 169
**Weighing the merits of solar power plants using concentration photovoltaics (CPV)**
**Geoffrey S. Kinsey**, Amonix, Seal Beach, California, USA

Page 178
**Harmonized procedures for long-term energy yield measurements and performance evaluation of PV modules in outdoor conditions**
**Vincent Helmbrecht**[1], **Diana Craciun**[1], **Abraham Ellis**[2], **Jennifer Granata**[2], **Stathis Tselepis**[3], **Anastasios Kyritsis**[3] & **Nikos Hatziargyriou**[4]
[1]DERlab e.V., Kassel, Germany; [2]Sandia National Laboratories, Albuquerque, New Mexico, USA; [3]Centre for Renewable Energy Sources and Saving (CRES), Pikermi, Greece; [4]Institute of Communication and Computer Systems - National Technical University of Athens (ICCS-NTUA), Athens, Greece

186 Section 7
Market Watch + NEWS

Page 190
**Tariff Watch**
**Nilima Choudhury**, *Photovoltaics International*

Page 192
**The global PV market – predictions for 2012**
**Ash Sharma**, **Sam Wilkinson** & **Frank Xie**, PV Research Group, IMS Research, Wellingborough, UK and Shanghai, China

Page 195
**The UK solar market's position worldwide in the face of changing FiT policy**
**Emma Hughes**, Solar Power Portal, London, UK

198 Advertisers & Web Index

199 Subscription Form

200 The PV-Tech Blog

# Fab & Facilities


**Page 9**
**News**

**Page 13**
**Environmental footprinting of photovoltaic module production**

Mariska de Wild-Scholten, SmartGreenScans, Groet, The Netherlands

**Page 23**
**US environmental permitting for PV manufacturing facilities – requirements and strategies for success**

John Browning, P.E., CH2M HILL, Denver, Colorado, USA




# News



## Trina Solar remains committed to 500MW solar cell and module capacity expansion

Plans by Trina Solar to build out its next-generation cell technology – despite industry conditions – have been secured with a structured term loan facility of up to US$100 million with Standard Chartered Bank. With the PV industry suffering from overcapacity, most PV manufacturers are in cash preservation mode and have put holds on capital spending. This loan will be used exclusively for Trina's East Campus project, which includes the addition of 500MW of cell and module capacity.

The news delivers some hope to equipment suppliers in what is expected to be a lean year for sales. NPD Solarbuzz had recently said that it expected a significant fall in capital spending in 2012 and that equipment suppliers were at risk of experiencing year-on-year revenue declines in the 60–70% range.

The Trina Solar expansion plans are among the few that have not been postponed.

### Capacity News Focus

## Silex Systems restarts production at its Sydney solar module facility

Silex Systems is said to have restarted production at its solar module facility in Sydney, Australia. The company announced in November that it would be halting production as it was hard hit by the rooftop solar market and was looking for ways to restructure its business. The report states that Silex decided to start operation again, upon publication of Tindo Solar's plans to begin commercial production. Plans to continue ramping up capacity at the company's Sydney site are being considered.

Michael Goldsworthy, CEO of Silex Systems, was said to have hinted that the company would more than likely bid into the ACT Government's proposed reverse auction for utility scale solar. The CEO further conceded that commercial and utility-scale solar PV is being propelled by significant drops in the prices of solar panels, coupled with growing electricity costs.

## First Solar cuts output but attempts to safeguard jobs at German plant

Last November, First Solar celebrated the production of its one millionth module at its Frankfurt (Oder) plant. This year, the company has announced plans to reduce production as declining subsidies reduce European demand.

Module production at First Solar's Frankfurt (Oder) plant.

*Source: First Solar*

In a climate of job losses, First Solar has applied for government assistant to place its 1,200 employees on a part-time contract. The thin-film manufacturer intends to cut output in half for six months, commencing in March, whilst waiting for approval of a government grant. A spokesman was cited as having attributed the cuts to the company's original 2012 guidance to scale back to 80% of the company's global production capacity.

## PPG Industries to expand Fresno-based manufacturing of Solarphire PV glass

PPG Industries has advised that its flat glass business in Fresno will be expanding its production capability in order to better allow the manufacturing of the company's Solarphire PV glass. The move aims to serve solar customers throughout California, the West Coast and even Asia with a faster shipping timeframe.

## Construction postponed on Bosch's €520 million PV plant in Penang, Malaysia

Bosch has revealed plans to delay the building of its €520 million integrated solar module manufacturing plant in Penang, Malaysia. Construction was due to commence at the end of last year, with completion scheduled for 2013. Bosch has attributed this news to the current market of overcapacity, falling module prices and government subsidy cuts.

The company hopes to have a revised timetable by the end of the year. To date, Bosch has invested around €2 billion in photovoltaics.

## Schneider Electric selected to construct 130MW Hevel Solar module factory in Russia

Schneider Electric has signed on to provide construction services for Hevel Solar's 130MW factory in Novocheboksarsk, Russia. The company will design and install the in-plant electric power, supply medium- and low-voltage equipment and training of the technical personnel in the plant. The plant is expected to be completed in the first quarter of 2012.

### Other News

## New business strategy for Italian Solon SpA

The Italian subsidiary of Solon SpA has announced it has suspended module production at its plant in Carmignano del Brenta, in the northern Italian region of Veneto. It has redeveloped its business plan in order to become a specialist systems integrator.

The company will focus primarily on the system integration business, providing engineering, procurement and construction (EPC) services for turnkey PV installations, alongside its current position of module distribution. The factory closure will affect about 70 workers.

## REC's solar wafer and cell plants in Norway set to be sold off by GoIndustry DoveBid

GoIndustry DoveBid, an asset manager company, has been retained by Renewable Energy Corporation (REC) to handle the disposal of three solar manufacturing plants in Norway. GoIndustry has placed the factories on the global market with a total estimated value of €50 million. REC initially disclosed in October 2011 that it was closing its 500MW capacity wafer plant in Herøya, its 275MW wafer multi-plant in Glomfjord and its 200MW capacity solar cell plant in Narvik.

The companies describe the equipment for sale as being state-of-the-art and highly automated with low labour requirements.

Solarphire's PV glass is manufactured in PPG Industries' flat glass plant in Fresno, California.

*Source: PPG Industries*

Scott Follett, global director of PPG Solar Performance, noted that the most prominent benefit of making Solarphire PV glass in Fresno will be reduced delivery times.


REC Wafer's plant in Herøya is one of three that has been placed on the market by the company.

*Source: REC Wafer*

GoIndustry Project Director Nick Schofield noted, "Some of the equipment was installed as late as 2009. The wafer plants have a capacity of around 775MW and the cell plants approximately 200MW."

## Jobs lost as Sanyo decides to shut down California factory

Falling solar panels and raw materials prices are claiming 140 jobs at Sanyo Electric's solar wafer factory in Carson, California, as it prepares to start up operations at a plant in Malaysia. The plant, opened in 2003, makes the equivalent of 30MW of silicon ingots and wafers for solar cells each year and is expected to close in October.

Production on the plant in northern Malaysia is due to start in December. Panasonic, who bought a majority stake in Sanyo in 2009, is to invest ¥45 billion (US$587 million) to build the 300MW plant for wafers, solar cells and modules in the Kulim Hi-Tech Park in Kedah.

## Portuguese Institute for Solar Energy founded

Portugal's University of Évora and a number of renewable energy companies and organizations have founded the Portuguese Institute for Solar Energy (IPES). The IPES will be a research and development institute at the university that will develop solar technologies and design strategies for deploying solar throughout the country. IPES also intends to work with the government to help shape solar energy policy in Portugal.

Founding members include Martifer Solar, Efacec, Dreen/DeViris, Siemens Solar, Magpower, Open Renewables and WS-Energia. The university's Manuel Collares Pereira has been named director of IPES.

## Saita installs PV wastewater treatment plant for Belgian cell producer

Industrial wastewater treatment (IWT) system manufacturer Saita srl has successfully installed an IWT for an unnamed Belgian solar cell manufacturer. This installation, which claims to recycle 97% of the wastewater used in the multicrystalline cell manufacturing process, marks the second system installed by Saita, and the Italian company has set its sights on expanding the uptake of such systems across the PV manufacturing industry.

The first of these IWT systems was built in 2008 for an unnamed Italian solar cell manufacturer that has an annual production capacity of 60MW. The system consists of a closed-loop circuit that treats the acid and alkaline wastewater streams to yield high-quality water for use in chemical wet bench applications, and produces an inert solid sludge as a waste product. The closed-loop system collects and treats both the water from the production process and the water from utility equipment, thus enabling the IWT to achieve recycling levels of 97% of the entire water needs of a solar cell manufacturing plant.

Portugal's University of Évora was instrumental in the establishment of the Portuguese Institute for Solar Energy (IPES).

*Source: Saita*

The Italian company has plans to expanding the uptake of IWT systems across the PV manufacturing industry.

## Tianwei gives loan extensions to Hoku

Struggling to complete and start polysilicon production at its first facility in Pocatello, Idaho, Hoku has received another financial lifeline with major investor, Tianwei New Energy, agreeing to extend loan payment terms of US$50 million, potentially to the first quarter of 2014. Two loans totalling US$50 million were due to be repaid to Tianwei this quarter but delays, mainly as a result of financial woes, have dogged the project from the start.

"The extension of the loans reaffirms Tianwei's continuing commitment to Hoku's long-term success," said Scott Paul, CEO of Hoku Corporation. "Although the extension does not provide Hoku with any additional cash, it does allow us to better manage our liquidity, as we would otherwise be obligated to pay US$50 million to Tianwei this quarter. As we source additional funds, our first priority is to pay our polysilicon plant vendors and to continue with plant commissioning activities."

Polysilicon prices have declined by over 200% since Hoku broke ground at Pocatello, reaching spot market process below US$30/kg at the beginning of February 2012. Some small volume producers in Europe and Asia have already shuttered polysilicon plants as prices fell below production costs.

*Source: Hoku Materials*

Hoku has been struggling to complete and start polysilicon production at its first facility in Pocatello, Idaho.

# Environmental footprinting of photovoltaic module production

**Mariska de Wild-Scholten**, SmartGreenScans, Groet, The Netherlands

ABSTRACT

Several PV module producers have performed a carbon footprint analysis and published a sustainability report as part of their corporate social responsibility policy. Comparison of carbon footprint results is difficult because several international standards and life cycle assessment (LCA) databases are used. No product footprint category rules (PFCR) or product category rules (PCRs) for photovoltaics exist, so LCAs are performed with varying underlying assumptions. Furthermore, a fair comparison can only be made when all environmental footprints of a product are taken into account.

## Sustainability reporting

One important step in corporate social responsibility (CSR) policy is publishing a sustainability report. The most used reporting framework is that of the Global Reporting Initiative (GRI) [1]. The content of the report is selected on the basis of the principles of materiality (significance), stakeholder inclusiveness, sustainability context and completeness. To ensure the quality of the report it must be well balanced, comparable, accurate, timely, clear and reliable.

"One way to determine the significance of an environmental performance indicator is to carry out an LCA of the PV module."

## Environmental performance indicators

How does one go about selecting the key GRI environmental performance indicators to be included in the report? First of all, the environmental issue must be significant. One way to determine the significance of an environmental performance indicator is to carry out an LCA of the PV module and analyze the possible environmental impacts from cradle to grave. The environmental impact assessment method ReCiPe [2] can be used for this purpose.

Fig. 1 shows the ReCiPe steps from calculating the inventory of life cycle emissions, through determining midpoint environmental impacts, to evaluating endpoint damages to human health and ecosystems and depletion of resources. After normalization of midpoint environmental impacts to the impact of one citizen, the researcher has an idea of which indicators are significant. For a multicrystalline silicon PV module produced in China these are (see Fig. 2):

1. Fossil depletion
2. Climate change (human and ecosystem)
3. Particulate matter formation
5. Human toxicity

In this case the solar cell is the largest contributor to all impacts.

Stakeholders – such as governments/policy makers, suppliers, employees, customers, competitors, neighbouring communities, banks, investors, advocacy NGOs, media and scientists – can be asked which environmental issues they would like to see reported. One environmental advocacy organization is the Silicon Valley Toxics Coalition (SVTC). They envision a safe and sustainable solar PV industry that

- takes responsibility for the environmental and health impacts of its products throughout their lifecycles, including adherence to a mandatory policy for responsible recycling;
- implements and monitors equitable environmental and labour standards throughout product supply chains;
- pursues innovative approaches to reducing toxic chemicals in PV module manufacturing.

Each year, SVTC publishes a solar scorecard based on questionnaires sent to PV module manufacturers. The 2010 results of the top 10 PV module manufacturers are given in Fig. 3 [3]. This 2011 solar scorecard represents 46.6% of the industry market share, based on solar PV module

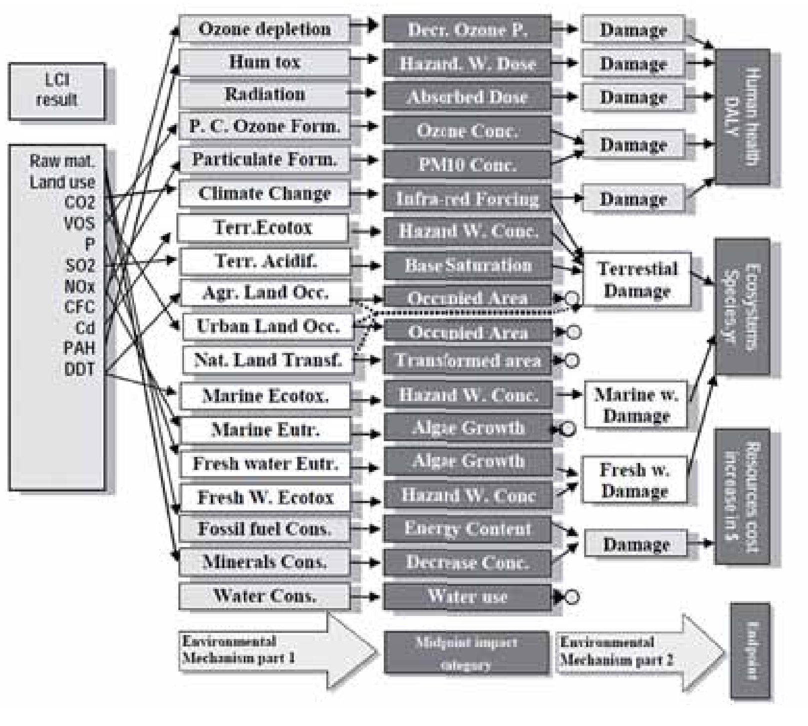


Figure 1. ReCiPe environmental impact assessment method [2].

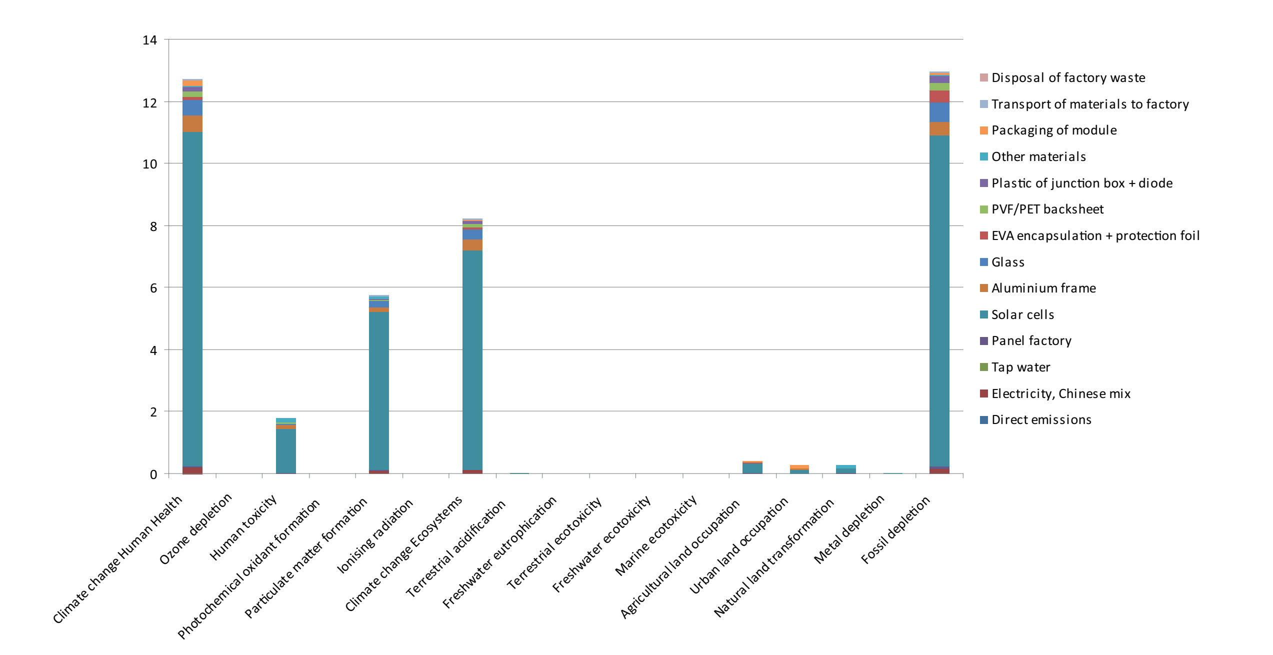


**Figure 2. Environmental impact assessment of a multicrystalline silicon PV module produced in China using the ReCiPe H endpoint method and Europe ReCiPe H/A [2] normalization with weighting in Simapro software. The y-axis units are ReCiPe points.**

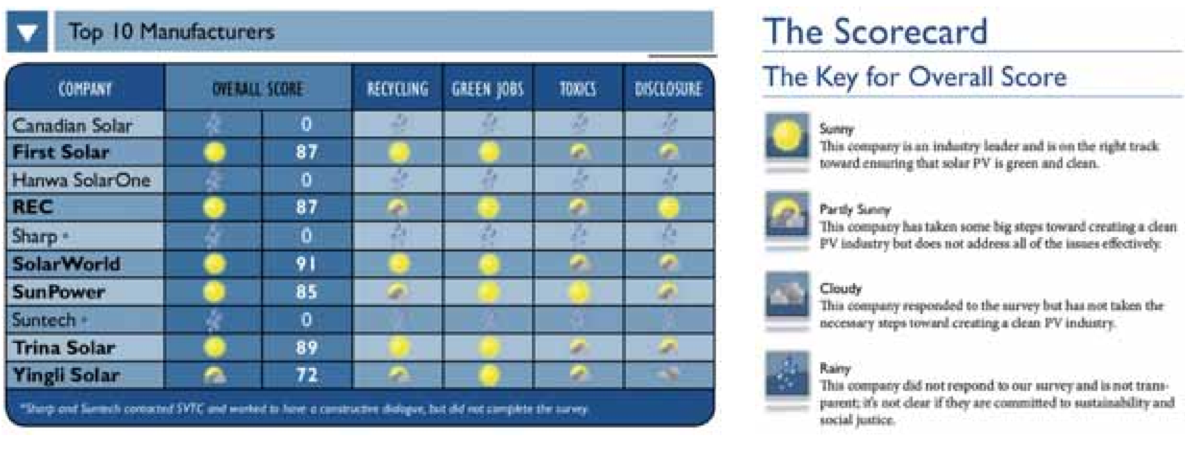

Top 10 Manufacturers

| COMPANY | OVERALL SCORE |
|---|---|
| Canadian Solar | 0 |
| First Solar | 87 |
| Hanwa SolarOne | 0 |
| REC | 87 |
| Sharp * | 0 |
| SolarWorld | 91 |
| SunPower | 85 |
| Suntech * | 0 |
| Trina Solar | 89 |
| Yingli Solar | 72 |

*Sharp and Suntech contacted SVTC and worked to have a constructive dialogue, but did not complete the survey



**Figure 3. Overall score in the 2011 solar scorecard of the top 10 PV module manufacturers [3].**

shipment statistics for 2009. The indicators put forward by SVTC can be considered to be important for environmental advocacy stakeholders. Table 1 gives an overview of the 2012 PV module manufacturer survey by SVTC, and a mapping with the paragraphs and performance indicators of the GRI sustainability reporting structure.

> "Knowing your environmental profile is the first step in the implementation of improvements, which reduce costs as well."

Ecodesigners need to know the most significant contributors to the environmental impacts as revealed by a full LCA. Knowing your environmental profile is the first step in the implementation of improvements, which reduce costs as well.

## Carbon footprinting

One of the most significant environmental impacts from the production of PV modules is climate change, and this is the reason why life cycle greenhouse gas emissions need to be considered. There are several *international* standardization initiatives for creating a standard for product carbon footprint, including:

- ISO 14067, expected in 2012 [4]
- Greenhouse Gas Protocol (GHG Protocol), published in September 2011 [5]

In 2010 more than 85% of the 2487 respondents to the Carbon Disclosure Project survey used the GHG Protocol Corporate Standard to measure and report their emissions. The Carbon Disclosure Project is globally the largest collection of self-reported climate change data [6]. There is also a British specification called PAS2050 that is applied by several solar cell and PV module producers (Motech, AOU, Upsolar, Yingli Solar, NexPower), but PAS2050 is *not* a standard [7].

Special attention is required when gases such as $NF_3$, $SF_6$, $C_2F_6$, $CF_4$ and $N_2O$ are used in solar cell and module manufacturing, since they have high global warming effects that are, respectively, 17200, 22800, 12200, 7390 and 298 times that of $CO_2$ [8]. Control of emissions by the installation of abatement systems is necessary.

## Water footprinting

The consumption of water in the manufacturing of PV modules and their components may also be important for

| Aspect | Paragraph / Indicator | | | Question | |
|---|---|---|---|---|---|
| **Standard disclosure: profile** | | | | | |
| Strategy and analysis | in 1.2, section 2 | Targets and goals | | III-2 | Does your company post on its website annual hazardous chemical reduction targets? |
| | | | | V-6 | Has your company set any 'zero waste' and/or annual waste diversion targets for PV modelling facilities? |
| | | | | V-7 | Does your company set goals for improving recyclability or reducing the amount of packaging materials used for shipping PV modules? |
| Organizational profile | 2.5 | Number of countries in which the organization operates, and names of countries either with major operations or that are specifically relevant to the sustainability issues covered in the report | | | Countries where PV module manufacturing occurs |
| | in 2.8 | Quantity of products or services provided | | | Total volume of PV modules manufactured in 2011 in MWp |
| | | | | | PV module manufacturing capacity in MWp as of January 1st 2012 |
| **Environmental performance indicators** | | | | | |
| Materials | EN1 | Materials used by weight or volume | CORE | III-4 | Do your PV modules contain cadmium, lead or selenium? |
| | | | | III-5 | Do your processes or products use, generate or contain engineered nanoparticles? |
| | | | | IV-7 | Can you verify that your supply chain does not contain conflict materials? 'Blood diamonds', coltan, tungsten, cassiterite (tin ore) and gold from the Great Lakes Region of Africa are widely considered the most common conflict materials. |
| | EN2 | Percentage of materials used that are recycled input materials | CORE | V-2 | What percentage of your PV module (by weight) is made from recycled materials? |
| Energy | EN3 | Direct energy consumption by primary energy source | CORE | V-4 | Do you report your company's overall direct and indirect energy consumption by primary energy source (via your own website or a third party such as Carbon Disclosure Project or Global Reporting Initiative)? |
| | EN4 | Indirect energy consumption by primary energy source | CORE | | |
| | | | | V-3 | Have you conducted a life cycle analysis on your PV modules (energy payback time)? |
| | EN5 | Energy saved due to conservation and efficiency improvements | ADD | | |
| | EN6 | Initiatives to provide products and services that are energy-efficient or based on renewable energy, and reductions in energy requirements as a result of these initiatives | ADD | V-8 | What percentage of your manufacturing operations is conducted in LEED-certified, zero-energy or green buildings? |
| | EN7 | Initiatives to reduce indirect energy consumption and the reductions achieved | ADD | | |
| Water | EN8 | Total water withdrawal by source | CORE | III-6 | Do you post on your website the volume of water that is used in production each year? |
| | EN9 | Water sources significantly affected by withdrawal of water | ADD | | |
| | EN10 | Percentage and total volume of water recycled and reused | ADD | | |
| Biodiversity | EN11 | Location and size of land owned, leased, managed in (or adjacent to) protected areas and areas of high biodiversity value outside protected areas | CORE | | |

**Table 1. Mapping of performance indicators in a GRI sustainability report and questions from a 2012 survey by the Silicon Valley Toxics Coalition (SVTC) for the solar scorecard.**

| | | | | | |
|---|---|---|---|---|---|
| | EN12 | Description of significant impacts of activities, products and services on biodiversity in protected areas and areas of high biodiversity value outside protected areas | CORE | V-9 | Describe significant impacts of activities from your company or its subsidiaries on biodiversity in protected areas and areas of high biodiversity value outside protected areas. |
| | EN13 | Habitats protected or restored | ADD | | |
| | EN14 | Strategies, current actions and future plans for managing impacts on biodiversity | ADD | | |
| | EN15 | Number of IUCN Red List species and national conservation list species with habitats in areas affected by operations, by level of extinction risk | ADD | | |
| Emissions, effluents and waste | EN16 | Total direct and indirect greenhouse gas emissions by weight | CORE | III-1 | Do you post on your website the following environmental releases: greenhouse gases/ $CO_2e$; perfluorocarbons, $SF_6$, $NF_3$, $CHF_3$, $CF_4$, $C_2F_6$? |
| | EN17 | Other relevant indirect greenhouse gas emissions by weight | CORE | V-3 | Have you conducted a life cycle analysis on your PV modules (greenhouse gas/carbon footprint)? |
| | EN18 | Initiatives to reduce greenhouse gas emissions and reductions achieved | ADD | | |
| | EN19 | Emissions of ozone-depleting substances by weight | CORE | | |
| | EN20 | NO, SO and other significant air emissions by type and weight | CORE | III-1 | Do you post on your website the following environmental releases: air emissions - SOx, NOx, VOCs, PM10, hazardous; total heavy metal emissions? |
| | | | | V-3 | Have you conducted a life cycle analysis on your PV modules: criteria - air pollutants (according to US EPA: ozone, particulate matter, carbon monoxide, nitrogen oxides, sulphur dioxide, lead)? |
| | EN21 | Total water discharge by quality and destination | CORE | | Do you post on your website your annual volume of waste water discharged? |
| | | | | | Do you post on your website the following waste water discharge quality indicators: chemical oxygen demand, biological oxygen demand, heavy metals, total suspended solids? |
| | | | | III-1 | Do you post on your website the following environmental releases: total heavy metal emissions? |
| | EN22 | Total weight of waste by type and disposal method | CORE | I-4 | What is the final destination for end-of-life and defective PV modules (by weight)? |
| | | | | I-5 | Are waste or scrap PV modules recycled at a facility with a documented environmental management system and worker safeguards and protection that is consistent with ISO 14001? |
| | | | | I-6 | Have you performed a hazardous waste determination for your PV modules? |
| | | | | III-1 | Do you post on your website the following environmental releases: landfill disposal by weight; weight of hazardous waste released and transferred? |
| | EN23 | Total number and volume of significant spills | CORE | | |
| | EN24 | Weight of transported, imported, exported or treated waste deemed hazardous under the terms of the Basel Convention Annex I, II, III and VIII, and percentage of transported waste shipped internationally | ADD | | |

**Table 1. Mapping of performance indicators in a GRI sustainability report and questions from a 2012 survey by the Silicon Valley Toxics Coalition (SVTC) for the solar scorecard.**

SNEC 6th (2012) International Photovoltaic Power Generation Conference & Exhibition

# SNEC PV POWER EXPO 2012
Conference & Exhibition

The Only Official Website www.snec.org.cn

## May 16-18, 2012

**Shanghai New International Expo Center**

(2345 Longyang Road, Pudong District, Shanghai, China)

**230,000**sqm Exhibition Space | **2,000+** Exhibitors | **5,000** Professionals | **200,000** Visitors Attendances

· Gather worldwide PV industry leaders and enterprises.

· Grasp the newest trends in PV technologies and the PV industry.

· Build international co-operation and trade platforms for the PV industry.

· Attract tens of thousands of powerful buyers.

member of GLOBAL SOLAR ALLIANCE


◎**Hosted by**: Shanghai New Energy Industry Association

◎**Show Management**: Follow Me Int'l Exhibition (Shanghai), Inc.

Add: Room 902, Building No.1, Hua Yi Plaza, 2010 West Zhongshan Road, Shanghai 200235, China

Tel: +86-21-64276991 +86-21-33561099 Fax: +86-21-64642653 +86-21-33561089

◎**Contact**: *For Exhibition*: Ms. Shirley Chan E-mail: shirley@snec.org.cn

*For Conference*: Ms. Qun Wang E-mail: alywang@snec.org.cn

◎**International Agent**: Follow Me Int'l Exhibition (USA), Inc. Peter Xu : Tel/Fax: +1-(408)-434-1993

2055 Junction Ave 225, SanJose, CA, 95131 E-mail: petersnec@gmail.com

| | | | | | |
|---|---|---|---|---|---|
| | EN25 | Identity, size, protected status and biodiversity value of water bodies and related habitats significantly affected by the reporting organization's discharges of water and runoff | ADD | | |
| Products and services | EN26 | Initiatives to mitigate environmental impacts of products and services, and extent of impact mitigation | CORE | | |
| | EN27 | Percentage of products sold and their packaging materials that are reclaimed by category | CORE | | |
| Compliance | EN28 | Monetary value of significant fines, and total number of non-monetary sanctions for non-compliance with environmental laws and regulations | CORE | | How many sanctions for non-compliance with health, safety or environmental violations occurred in the past three years at facilities where you operate or that manufacture your brand-name products? |
| Transport | EN29 | Significant environmental impacts of transporting products and other goods and materials used for the organization's operations, and transporting members of the workforce | ADD | | |
| Overall | EN30 | Total environmental protection expenditures and investments by type | ADD | I-2 | Does your company currently set aside money to finance the collection and management of end-of-life PV modules? |
| | | | | V-3 | Have you conducted a life cycle analysis on your PV modules (toxicity)? |
| | | | | V-5 | Has your company offered 'design for recycling', 'cradle-to-cradle' or similar training to product designers in the past three years? |
| Product responsibility performance indicators | | | | | |
| Product and service labelling | PR3 | Type of product and service information required by procedures, and percentage of significant products and services subject to such information requirements | CORE | I-3 | Does your website let customers know how to recycle/take back their PV modules? |

**Table 1. Mapping of performance indicators in a GRI sustainability report and questions from a 2012 survey by the Silicon Valley Toxics Coalition (SVTC) for the solar scorecard.**

certain factory locations. Tap water and/or (for example) river or lake water are withdrawn from nature. The cooling water is heated up during use, and this heat is removed in the cooling tower by evaporating water. The remaining liquid water is discharged to the municipal water system, and then back to nature after on-site wastewater treatment.

At the moment, the calculation of life cycle water consumption is hindered by the fact that in the ecoinvent database [9] the water discharged is not included, so it is only possible to model water withdrawal and not the net water consumption. Fair comparisons cannot be made on the basis of water withdrawal alone.

## Fair comparison of environmental footprints

A fair comparison of environmental impacts of PV modules is only possible when:

- the same standard is used
- the same impact assessment method is used
- underlying LCAs used are transparent
- underlying assumptions are the same

### Category rules for PV modules

Unfortunately no environmental product footprint category rules (PFCRs) or product category rules (PCRs) exist for PV modules. PFCRs provide detailed technical guidance and complement general methodological guidance for environmental footprinting by providing further specification at the product level.

As defined in ISO 14025(2006), PCRs include sets of specific rules, guidelines and requirements that are aimed at developing Type III environmental declarations (quantitative, LCA-based claims of the environmental aspects of a certain product or service). Since PV modules are sold to many different countries, what installation location should be assumed when analyzing the use phase of the PV module? Transport distances, irradiation on the module and the electricity mix replaced all depend on the location. The IEA PVPS task 12, which deals with environmental health and safety aspects of photovoltaics, has published guidelines [10], but these are not official PFCRs or PCRs.

### LCA databases

Only the ecoinvent database is transparent and discloses all underlying data such as the energy and material consumption and waste and emissions of all data sets. The ELCD and Gabi databases [11,12] are not transparent because they are only available as data sets in which all life cycle resources from nature and emissions to the environment are aggregated. The ELCD database currently contains only very little data. A transparent database is the most suitable if it is desired to tweak a data set with one's own collected data. Using a transparent database is also the fastest way of generating LCA results that show all contributions from upstream process steps.

Different LCA databases will generate different results because all underlying data are different. Understanding these differences is impossible when the data sets are not transparent.

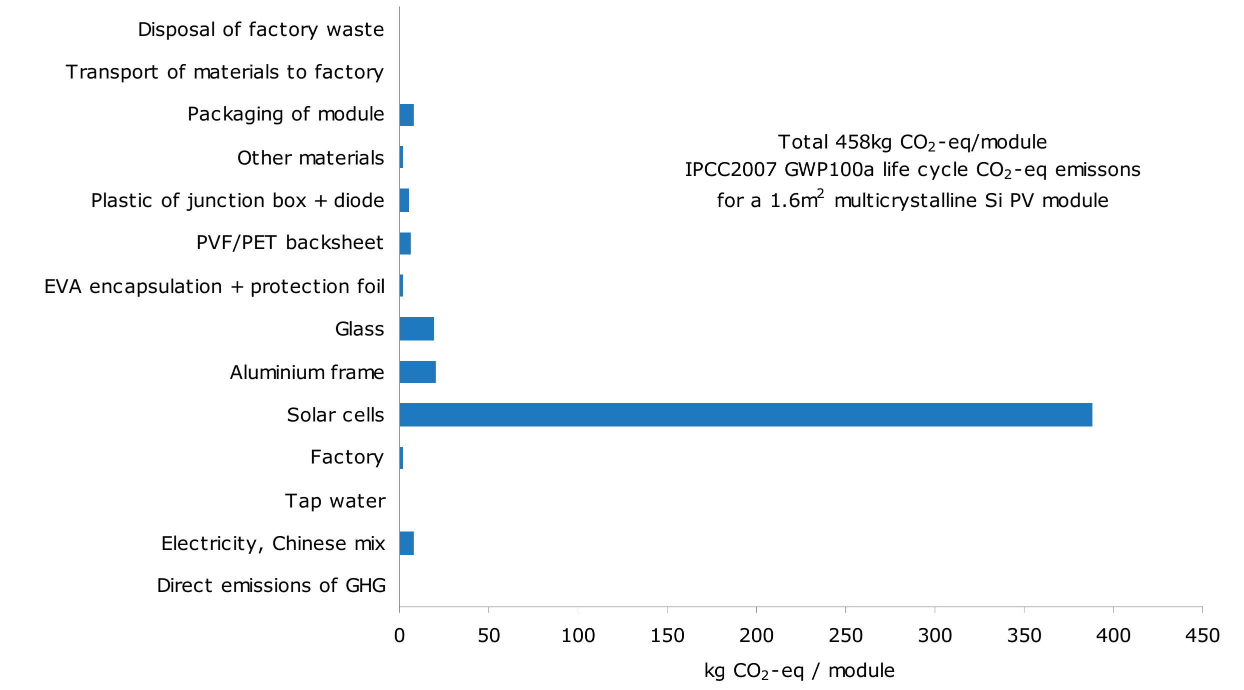


**Figure 4. Carbon footprint in kg $CO_2$-eq/module of a 1.6m$^2$ commercial multicrystalline Si PV module made from polysilicon, ingot, wafer, cell and module produced in China (ecoinvent 2.2 data for other materials).**

### LCA data for commercial PV modules

Data collection for LCA is a time-consuming process. PV module manufacturers must set up a systematic data-monitoring system on different levels. First, data need to be collected on the entire factory level. However, for product environmental footprinting, operational data need to be broken down from total factory level to module type. The data required for LCA are basically the input and outputs from the factory: amounts of materials and energy consumed, waste streams, emissions to the environment (to air and water) and products produced. In addition, data need to be collected about the means of transport and distances covered for all materials transported to the factory. It is even more challenging to obtain these types of data from suppliers.

LCA data for PV module production are available in the ecoinvent 2.2 database and also in a compilation from the IEA PVPS task 12 [13]; unfortunately, these data sets are outdated. This year, SmartGreenScans [14] will publish a new data set for commercial production of PV modules and their components, namely polysilicon, crystals/ingots, wafers and solar cells for the following technologies: crystalline silicon, silicon thin-film, CdTe and CIGS. Public data on module recycling are lacking at the moment.

### LCA results for commercial PV modules

The current globalization trend is that production of PV modules and their components is shifting to Asia. In order to calculate actual environmental impacts, the actual electricity mixes need to be used. Energy payback time and carbon footprint results were calculated on the basis of actual electricity mixes used in the production of polysilicon, ingots/crystals, wafers, solar cells and modules [15]. Fig. 4 shows the carbon footprint of a 1.6m$^2$ PV module for which the polysilicon, ingot, wafer and solar cells are all produced in China. The other materials are all taken unmodified from the ecoinvent 2.2 database.

> "The number of PV module manufacturers publishing sustainability reports and performing carbon and water footprinting is increasing and shows their corporate social responsibility."

## Conclusions

The number of PV module manufacturers publishing sustainability reports and performing carbon and water footprinting is increasing and shows their corporate social responsibility. A comparison of carbon footprint results is difficult because several international standards and LCA databases are used. No product rules for photovoltaics exist, so LCAs are performed with varying underlying assumptions. A fair comparison can only be made when all environmental footprints of a product are taken into account.

### References


[1] Global Reporting Initiative 2011, *The GRI Sustainability Reporting Cycle: A handbook for small and not-so-small organizations.*

[2] Goedkoop, M.J. et al. 2009, "ReCiPe 2008: A life cycle impact assessment method which comprises harmonised category indicators at the midpoint and the endpoint level. First edition. Report I: Characterisation" [see http://www.lcia-recipe.net/].

[3] Silicon Valley Toxics Coalition 2011, "Solar Scorecard 2011" [see http://solarscorecard.com/].

[4] ISO 14067 (under development), "Carbon footprint of products: Requirements and guidelines for quantification and communication".

[5] World Resources Institute and World Business Council for Sustainable Development 2011, "Greenhouse Gas Protocol: Product life cycle accounting and reporting standard".

[6] Carbon Disclosure Project [see http://www.cdproject.net/].

[7] BSI 2011, PAS 2050:2011, "Specification for the assessment of the life cycle greenhouse gas emissions of goods and services".

[8] Schottler, M. & de Wild-Scholten, M.J. 2008, "Carbon footprint of PECVD chamber cleaning", *PVI*, 2nd edn, pp. 64–69.

[9] ecoinvent database [see http://www.ecoinvent.ch].

[10] Fthenakis, V. et al. 2011, "Methodology guidelines on life cycle assessment of photovoltaic electricity", International Energy Agency Photovoltaic Power Systems (IEA PVPS) Programme Task 12, Report T12-03:2011 [available online at http://www.iea-pvps.org/fileadmin/dam/public/report/technical/rep12_11.pdf].
[11] ELCD database [see http://lca.jrc.ec.europa.eu].
[12] Gabi database [see http://www.gabi-software.com].
[13] Fthenakis, V. et al. 2011, "Life cycle inventories and life cycle assessment of photovoltaic systems", IEA PVPS Task 12, Report T12-02:2011 [available online at http://www.iea-pvps.org/fileadmin/dam/public/report/technical/rep12_10.pdf].
[14] de Wild-Scholten, M.J. & van der Meulen, R. 2012, "Carbon and environmental footprint of PV module production", submitted for the 27th EU PVSEC conf., Frankfurt, Germany.
[15] de Wild-Scholten, M.J. 2011, "Environmental profile of PV mass production: Globalization", *Proc. 26th EU PVSEC*, Hamburg, Germany.

## Acknowledgements

Part of this work was supported by the German Federal Ministry for the Environment, Nature Conservation and Nuclear Safety (BMU) within the project "Aktualisierung von Ökobilanzen für Erneuerbare Energien im Bereich Treibhausgase und Luftschadstoffe" (Förderkennzeichen 0325188) and by Certisolis in France.

## About the Author

**Mariska de Wild-Scholten** is a self-employed consultant for SmartGreenScans in The Netherlands and an expert on LCAs of photovoltaics. She is an active member of the IEA PVPS Task 12 on Environmental Health and Safety of PV, and an editor in photovoltaics for the *International Journal of Life Cycle Assessment*. Mariska has been a member of PV CYCLE since 2012.

## Enquiries

SmartGreenScans
Wagenmakersweg 22
1873 GH Groet
The Netherlands

Tel: +31 72 5621628
Email: mariska@smartgreenscans.nl
Website: www.smartgreenscans.nl

# US environmental permitting for PV manufacturing facilities – requirements and strategies for success

**John Browning, P.E.**, CH2M HILL, Denver, Colorado, USA

ABSTRACT
As a relative newcomer to the industrial world compared to more mature manufacturing sectors, the PV industry has not yet been subject to consistent environmental regulatory standards internationally. Like all industries that have preceded it, PV manufacturing is seeing its regulatory future evolve as PV producers migrate to different regions of the world. With this global expansion come significantly different levels of regulatory stringency, reflective of local conditions and cultures.

## Introduction

Despite the clean-energy products made by the PV manufacturing industry, PV manufacturing processes and support systems can generate pollution [1,2]. As PV manufacturing facilities continue to become more widespread around the world, history suggests that the trend of tightening environmental regulations will accompany the industry's global growth [3]. For that reason, this paper uses its analysis of US environmental permitting criteria and processes as a basis of comparison that, it is believed, can be useful for solar manufacturers in other parts of the world, since the tightening of US environmental standards for manufacturers often foreshadows the imposition of more demanding regulations in other countries.

"If manufacturers can plan their PV manufacturing projects accordingly, they may be spared the negative consequences of finding their manufacturing facilities unable to comply with future permitting standards."

Several factors that can influence a more favourable and expeditious environmental permitting process for PV manufacturing projects outside the US will also be discussed in this paper. However, PV manufacturers can expect the demands of the US-based permitting issues identified below to become increasingly common as the industry matures. This paper aims to share these permitting particulars in the spirit of 'forewarned is forearmed,' to help PV manufacturers anticipate this expected trend of increasing permitting rigour. If manufacturers can plan their PV manufacturing projects accordingly, they may be spared the negative consequences of finding their manufacturing facilities unable to comply with future permitting standards.

## The US model for PV manufacturing environmental permitting

Before regulated pollutants can be discharged to the environment from an industrial source, US state and local environmental laws and regulations require the source to obtain environmental permits. Even before manufacturing operations commence, environmental permits must be sought by greenfield developments that might impact sensitive environmental resources (e.g. wetlands, endangered species, nesting migratory birds and archaeological/cultural/historical resources). Permits associated with such sensitive resources generally trigger review and approval periods that exceed the time-to-market goals of a new PV manufacturing facility. In this case, site selection efforts should seek to avoid areas where such sensitive resources may exist.

This section describes the four primary environmental permits anticipated for nearly any large-scale industrial development to establish a PV


Figure 1. Efficient environmental permitting of any large-scale industrial development requires early engagement and planning in three main areas: air emissions, stormwater discharge and wastewater discharge.

| Potential pitfall | Mitigation measure |
|---|---|
| Site layout and thus civil plans remain undefined, making preparation of E&SC plans difficult. | Go with the best available information given the time frames to get through the regulatory process. Most authorities have procedures for updating construction plans, without having to reapply for a permit. |
| A construction SWPPP requires details such as name and telephone number of site E&SC inspector that are not known at the time of permit application submission. | The site developer or engineer of record may need to be identified as the inspector until such time that the grading contractor has been identified. |
| The duty to comply with the construction stormwater permit usually falls on the 'owner/operator'. Therefore the PV developer can be culpable for violations made by an on-site contractor. | Have processes in place to monitor contractor activities during construction. |

**Table 1. Overcoming difficulties in obtaining construction stormwater permits.**

manufacturing facility in the United States, specifically permits for:

- Construction stormwater discharge
- Air emissions
- Wastewater discharge
- Industrial stormwater discharge

In addition, strategies for obtaining, in a timely manner, permits that have reasonably attainable compliance requirements are reviewed. Permitting applicability, general steps involved in obtaining the permits and schedule considerations are briefly discussed, and a series of potential pitfalls and avoidance manoeuvres are provided. Environmental permitting outside the US is then considered in a subsequent section.

## Construction stormwater permits

Under the US Federal Clean Water Act, stormwater discharge permits are required for construction activities, including clearing, grading, excavation, materials or equipment staging, and stockpiling that will disturb one or more acres of land. This permitting programme also applies to construction activities that will disturb less than one acre when they form part of a common plan of development or sale, if the larger common plan of development or sale will ultimately disturb one or more acres. One acre comprises 43,560 square feet, so most PV manufacturing development projects trigger this permit requirement. The permit is required prior to commencing earth-disturbing activities. While a few US states have not been delegated authority to administer this federal programme, most often the permit is obtained from the state or local environmental authorities. The majority of construction stormwater permits are 'general' permits, meaning that there is one permit in the jurisdiction to cover all potential permittees.

In general, the steps associated with obtaining this permit include:

1. Develop a site civil grading, and an erosion and sediment control (E&SC) plan.
2. Dovetail the civil plan into a construction stormwater pollution prevention plan (SWPPP).
3. Develop a construction SWPPP. The plan includes inventorying all 'significant' materials, describing best management practices to prevent stormwater pollution, and preparing detailed spill response procedures.
4. Submit a notice of intent (NOI) (after the SWPPP has been developed) to the permitting authority to obtain permit coverage.
5. Permit coverage is usually obtained within 15–60 days, depending on local agency processes.
6. Submit a construction completion report within 30–60 days (depending on local agency processes) to the permitting authority once construction is complete and the site has been permanently stabilized in accordance with the general permit.

Because of the large number of construction projects and NOIs submitted under this programme, there is usually little, if any, 'back and forth' with the permitting authority in obtaining a construction stormwater permit.

## Air emission permits

For a PV manufacturing facility, air emission permits are typically required for process sources, e.g. etch processes releasing acid gases or screen-printing operations releasing volatile organic compounds (VOCs), and for process support systems, such as natural gas-fired boilers or diesel-fired emergency standby generators. Broadly speaking, air permits can be divided into 'major' source permits and 'minor' source permits. 'Major' source air permits can be required when facility emission rates are more than 100 tons per year (tpy) of criteria pollutants (particulate matter, carbon monoxide, oxides of nitrogen, sulphur dioxide or VOC), or exceed 10 tpy of an individual hazardous air pollutant or 25 tpy of combined hazardous air pollutants (HAPs – there are 188 of these listed in the Clean Air Act). Recently, the US Environmental Protection Agency (EPA) promulgated regulations that also define a 'major source' as one that can emit 100,000 tpy or more of greenhouse gases (as carbon dioxide equivalents – $CO_2e$). Minor sources have the potential to emit regulated air pollutants at rates less than these major source thresholds [4]. All but the very largest PV manufacturing operations will most likely be 'minor' sources of air pollutants.

The tipping point for when an air permit needs to be in place for a minor source is not often defined in state regulations and may only be understood in a written or an unwritten policy. Some agencies request, without exception, that the permit be in place prior to construction activities, such as ground breaking or the pouring of foundations, while other agencies may allow a project to proceed 'at risk' up to the point where an emission source gets connected and becomes operable. Either way, early regulatory agency involvement and planning can circumvent schedule surprises. Typical agency review and approval periods for minor source air permits are 4–6 months.

In general, the steps necessary for obtaining an air permit are:

1. Prepare a preliminary air emissions inventory to estimate the annual emission rates of regulated air pollutants.
2. Hold a pre-application meeting with the regulatory agency to define permit application expectations and processes, including triggers for public comment periods, which often accompany air permit applications.
3. Collect additional details from the design team about air emission sources (parametric monitoring capabilities,


Innovative backsheets.
Proven experience.
+25
years
practical
experience

| Potential pitfall | Mitigation measure |
|---|---|
| The availability of detailed design information falls well behind the due date for the air permit application. | Go with the best available information. Be creative and conservative with estimates of chemical and fuel use and thus emissions. Making a future permit modification will be easier if more emissions rights are not requested. |
| The project is phased, but the timing and capacity of each phase is not well defined. | Always attempt to permit for maximum projected full build-out. Arguably, permitting for anything less could be considered 'sham' permitting that contravenes the Clean Air Act. Permitting for full build-out usually leads to maximum operating flexibility. |

Table 2. Overcoming difficulties in obtaining air emission permits.

chemical and fuel consumption rates, stack parameters, etc).

4. Refine the air emission inventory, prepare the agency forms and submit.

5. Carefully review the draft permit and conditions. Air permits can be issued for five years and are not always easily modified!

### Wastewater discharge permits

A variety of PV module manufacturing activities generate wastewater, including acid-etch processes and rinses, chemical bath deposition and rinses, electroplating, and scrubber or cooling tower blow-down. Wastewater discharges can be 'direct', i.e. direct to surface waters, or 'indirect', such as when wastewater is discharged to the local municipal wastewater treatment plant.

Direct discharges normally require a national pollutant discharge elimination

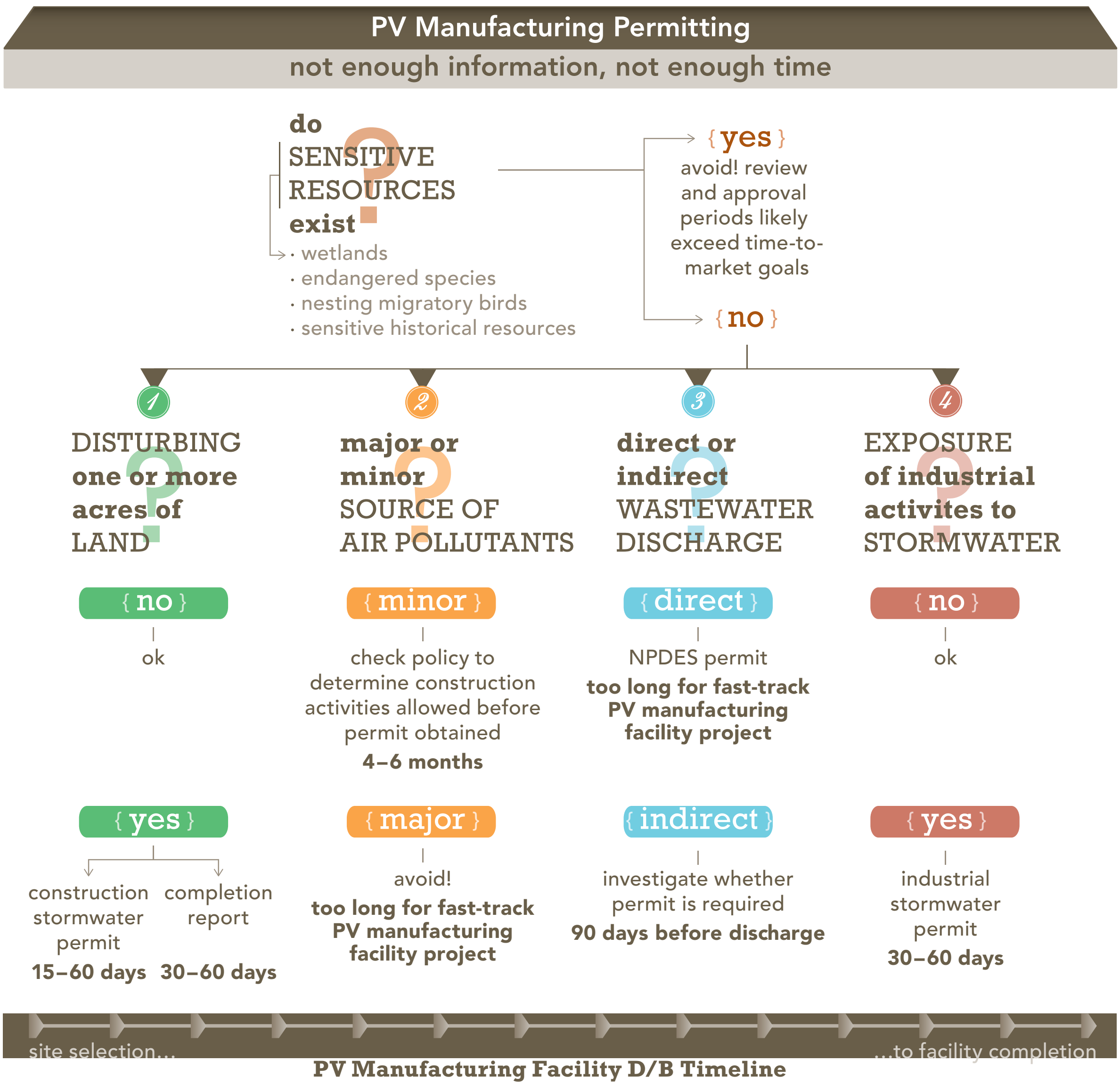


Figure 2. Permitting in PV manufacturing necessitates the collection and preparation of information in four main areas, each with its own timeline during the design-build process. Early planning will help ensure that permitting is well integrated into that timeline.


www.hyundaisolar.com
Imagine
How a single Solar Module
Can save a polar bears home
With a 240Wp solar module
It can replace 3 barrels of oil energy
Solar Energy, that reduces risks of global warming…
Supports a younger, healthier earth
We need Solar!

| Potential pitfall | Mitigation measure |
|---|---|
| In addition to a permit application, the wastewater authority requires an 'Engineer's Report' with final, stamped engineering drawings of the pre-treatment system. The project is fast track, and the wastewater collection and treatment system is designed by multiple entities. | Scheduling and coordinating the preparation of an 'Engineer's Report' can be a challenge for a fast-track project. Advise the agency on how the system is being designed and check if early reviews of system components can be performed. |
| No representative sampling data for characterizing the wastewater effluent exists, because the process operations and chemistry are still evolving. | Use mass-balance engineering calculations to generate estimates. These will very likely be conservative, but they offer a way of initially evaluating how operations may bump up against permit limits. |
| The permit application demonstrated compliance with known wastewater discharge limits, but additional parameters were identified during the review process. | Local treatment plants also have discharge permits with which they must comply. Reviewing these permits and, of course, asking the agency for any 'off-the-books' parameters that may be regulated is important. Such typical parameters that may affect the PV industry include nitrogen compounds, fluorides or phosphorus compounds. |

**Table 3. Overcoming difficulties in obtaining wastewater discharge permits.**

system (NPDES) permit, and, as in the case of the aforementioned sensitive resource permits, have long lead times that are not amenable to fast-track PV manufacturing facility projects. Consequently, these types of permit are not discussed in this paper.

For indirect wastewater discharges, there are a number of triggers that would require a facility to obtain industrial wastewater discharge permits from a local municipality. These triggers include:

- The facility's activities are subject to Federal EPA 'Categorical Source' requirements. Historically, certain PV manufacturing technologies have been subject to the EPA's 'Electrical and Electronic Components Point Source Category' and/or the 'Metal Finishing Point Source Category.'
- Wastewater flow rates are expected to exceed 25,000 gallons per day.
- Pre-treatment activities are required to meet discharge limits.
- The wastewater authorities perceive that operations at the facility may have an adverse effect on the municipal system, and therefore request that the facility go through the permitting process.

Typically, for an industrial source discharging wastewater to a local treatment plant, the municipality is also the permitting authority. A wastewater discharge permit application should be submitted at least 90 days prior to discharging wastewater; however, certain US states also require a state permit to be obtained and this can increase the required lead times for obtaining a permit.

In general, the steps required to obtain an industrial wastewater discharge permit include the following:

1. Inventory all wastewater sources, including flow rates and potential chemical concentrations.
2. Identify 'local limits' or other regulatory limits such as EPA Categorical Source limits.
3. Work with wastewater treatment vendors in designing a pre-treatment system as necessary.
4. Hold a pre-application meeting with the wastewater authority.
5. Compile and submit a permit application (common elements include a water balance diagram, a mass balance or analytical testing to determine constituent concentrations, and engineering details of the pre-treatment system).

### Industrial stormwater permits

Probably the final permit received prior to the start-up of a new PV manufacturing facility is the industrial stormwater permit. Under the Clean Water Act and the associated NPDES programme, certain industrial sectors must obtain a stormwater discharge permit for their 'industrial activities' unless they can demonstrate and certify that there is 'no exposure' of those activities to stormwater. This permitting programme applies to numerous types of industrial source categories, including those with a Standard Industrial Classification (SIC) code of 36, which many PV manufacturing facilities have been designated.

> "It is vital to have someone on your facility development project team who has expertise in permitting issues in international locations."

As a rule, the state environmental authority is the permitting agency for this type of permit; the review and approval periods can be 30–60 days. Similarly, the construction stormwater permit is typically a 'general' permit.

The steps associated with obtaining this permit usually include:

1. Review a copy of the general industrial stormwater permit applicable to the project.
2. Develop an operational industrial stormwater pollution prevention plan (SWPPP). This is the most extensive

| Potential pitfall | Mitigation measure |
|---|---|
| The criteria for certifying the facility for 'no exposure' seem vague. | Carefully evaluate the 'no exposure' criteria for your state. Even something as simple as an outdoor loading dock can invalidate 'no exposure' certification. Go ahead and apply for permit coverage. |
| The start of 'industrial activities' is difficult to define for a new facility start-up. | Apply for permit coverage as soon as an SWPPP can be reasonably drafted for the new facility. Have the permit in place in advance of process chemicals arriving on site. |

**Table 4. Overcoming difficulties in obtaining industrial stormwater permits.**

activity associated with the permit. The plan includes inventorying all 'significant' materials, describing best management practices to prevent stormwater pollution, and preparing detailed spill response procedures.

3. Submit an NOI to the permitting authority to obtain permit coverage.

4. Permit coverage is usually obtained within 30–60 days, depending on local agency processes.

## International considerations

With the exception of the stormwater discharge permitting programme, similar environmental permitting programmes exist for industrial projects outside the US. While a complete description and comparison of non-US environmental permitting programmes is beyond the scope of this paper, here are some general observations related to international environmental permitting derived from the author's direct experience:

- In general, there is less opportunity for public involvement in many international locations.

- There tends to be a greater prevalence of numerical discharge standards 'on the books' that can be used to understand requirements before the permitting process begins.

- Environmental authorities have significantly more opportunities to subjectively interpret regulations during the permitting process, potentially generating ambiguity and increasing permitting durations.

- In some locations, multilayered regulatory bureaucracies can protract permitting processes and jeopardize a project's schedule. Be aware of the permitting climate in the country of interest so that the amount of time that the permitting process may require in a given location can be factored in.

- In many locations (including the US), it is vitally important to work collaboratively with regulatory officials in the knowledge that regulatory issues pertaining to advanced technology manufacturing facilities can evolve as rapidly as the processing technologies used in these facilities. There have been many instances in which a jurisdiction's permitting criteria were revised in response to a new type of processing technology, once the environmental circumstances related to that technology were shared with local regulatory officials. Officials around the world are often very accommodating to regulatory flexibility as long as these issues are addressed respectfully and honestly.

- Understand the 'environmental climate' of the country in which a development is planned. There have been cases in which owners have built a manufacturing facility compliant with existing permitting criteria, only to experience repercussions later when regulatory criteria tightened. Before committing to a specific location, owners should seek to determine, to the extent possible, any trends of tightening local environmental regulations related to particular manufacturing processes. In some cases, insight into the local level of environmental sensitivity can become the central determining issue of how or if you should choose to develop your facility in a specific location.

- For the reasons noted above, as well as many others, permitting processes are notorious bottlenecks that can impede a facility development schedule. It is vital to have someone on your facility development project team who has expertise in permitting issues in international locations. Permitting experts have proved countless times to be 'unsung heroes' who used their understanding of regulatory issues and the negotiation of permitting timelines to expedite permitting processes that would otherwise have seriously delayed project schedules.

> "Engage regulatory authorities in good time."

## Conclusion

Most new PV manufacturing facilities will need to obtain construction stormwater, air emission, wastewater and industrial stormwater permits. For fast-track projects, one major constraint on preparing the permit applications is having available information on what is to be built, and thus what the environmental discharges will be. While multiple mitigation strategies exists, several stand out:

1. Engage regulatory authorities in good time.

2. Maintain close access to the design team to get the latest information.

3. Be proactive and resourceful in closing information gaps.

### References


[1] Fthenakis, V.M, Kim, H.C. & Alsema, E. 2008, "Emissions from photovoltaic life cycles", *Environ. Sci. & Tech.*, Vol. 42, No. 6, pp. 2168–2174.

[2] Fthenakis, V.M. 2004, "Life cycle impact analysis of cadmium in CdTe PV production", *Renew. & Sust. Energy Rev.*, Vol. 8, No. 4.

[3] Detsky, M. 2003, "The global light: An analysis of international and local developments in the solar electric industry and their lessons for United States energy policy", *Colo. J. Int. Environ. Law & Policy*, Vol. 14, No. 301.

[4] Chappel, L.M. 2010, "Regulatory impact analysis for the final prevention of significant deterioration and Title V Greenhouse Gas Tailoring Rule", US EPA Final Report.


### About the Author

**John Browning, P.E.**, has over 17 years of experience providing environmental consulting services for a wide range of international projects, including performing chemical mass balances of manufacturing facility process and support systems, characterizing environmental discharges from industrial facilities, obtaining environmental approvals and permits, and evaluating environmentally related operational plans. He has helped regulatory officials prepare environmental permits for advanced-technology manufacturing industries and approvals for a broad variety of manufacturing facility developments.

### Enquiries


CH2M HILL
2020 SW Fourth Ave, 3rd floor
Portland
OR 97201
USA
Email: John.Browning@ch2m.com
Website: www.ch2mhill.com

# Materials


Page 33
News

Page 35
Product Reviews

Page 36
PV manufacturing materials: Technological and process-related options for cost reduction

Joseph Berwind, AEI Research & Consulting, Millburn, New Jersey, USA

Page 50
Cz-Si wafers in solar cell production: Efficiency-limiting defects and material quality control

Jonas Haunschild, Juliane Broisch, Isolde Reis & Stefan Rein, Fraunhofer ISE, Freiburg, Germany

Page 60
Diamond wire sawing: State of the art and perspectives

Fabrice Coustier & Jean-Daniel Penot, CEA-INES, LMPS, Le Bourget-du-Lac, & Gérald Sanchez & Michel Ly, Thermocompact, Pringy, France


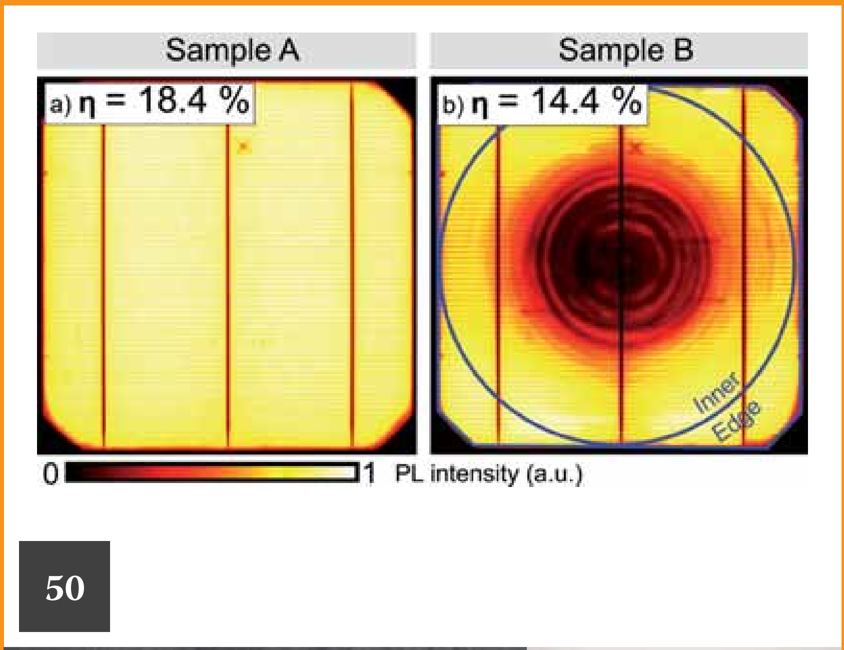


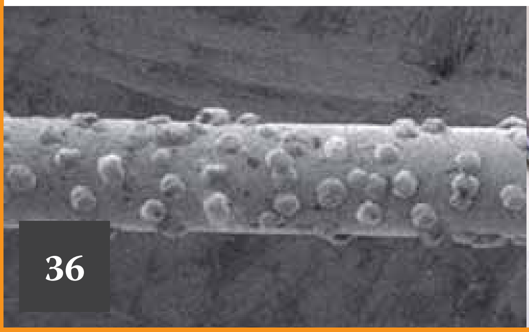


# News



## Sumco exits solar wafer market with 1,300 job losses

Citing 'structural' overcapacity, 'significant price declines' and a fall in demand of crystalline silicon wafers, Sumco has decided to completely exit the wafer market. The company expects to incur charges of ¥5 billion, folding both wafer subsidiaries, Sumco Solar Corporation and Minimata Denshi, and noted that it would report a significant operating loss in its fiscal fourth quarter results. Sumco said that wafer prices had declined by 70% from January 2011.

Solar wafer segment losses for the fourth quarter had been guided at -¥7.2 billion and full-year losses of -¥6 billion.

Sumco is also restructuring and consolidating its semiconductor wafer operations. The reduction in demand for 200mm wafers was cited as one of the reasons for the changes. Sumco said it would close its Ikuno 200mm plant and transfer production to its Imari and Nagasaki facilities. However, the company is also closing its 300mm wafer line at its Nagasaki plant, while a 150mm wafer line at its Imari plant will also close.

Sumco said that wafer prices had declined by 70% from January 2011.

In total, Sumco expects to incur charges related to the restructuring charges of approximately -¥58.2 billion, with 1,300 job losses, or 15% of its workforce. The company had used a proprietary 'Electromagnetic Casting Method,' which produced seven-metre long ingots with extremely high purity.

**Business News Focus**

## Targray to offer full range of SiC slicing materials to portfolio for Taiwanese market

Targray Technology has added a high-quality silicon carbide (SiC) material to its range of products on offer to the Taiwan market following the establishment of a new distribution agreement with Washington Mills AS. Targray will exclusively offer the Carborex silicon carbide product as part of its portfolio for its Taiwan-based customers.

Washington Mills' Carborex range of SiC micro grits go through a rigorous processing regime of steps such as crushing, shaping, flotation, chemical treatment to remove impurities, drying, magnetic separation, dust removal and sieving, and are then milled in jet-mills, and then classified by sieving, air classification and/or sedimentation in water.

The grits are then measured for chemistry, size distribution, surface area, bulk density, grain shape and abrasive efficiency in order to ensure they are of the exacting standards required of the solar wafer manufacturing industry.

SiC is an agent for use in the high-precision ultra-thin slicing of silicon wafers.

## Wacker notes polysilicon supply contract terminations and abrupt demand decline

Polysilicon producer Wacker Chemie saw an abrupt demand decline in the fourth quarter of 2011 as PV customers reduced inventory levels and cancelled contracts due to some customers exiting the industry. Polysilicon spot prices fell below Wacker's long-term pricing levels for the first time in many years, sparking price renegotiations.

Source: Wacker Chemie AG

Wacker Chemie's polysilicon division saw sales fall 32% in the fourth quarter of 2011.

The polysilicon division reported total sales of some €255 million in the fourth quarter, down 32% compared to the year before. EBITDA fell approximately 22% to about €165 million, compared to €211 million in the fourth quarter of 2010. However, EBITDA margin increased to 64.7% in Q4, compared to 56.6% in the prior year.

Wacker had posted polysilicon sales of €378.2 million in the third quarter of 2011. The third-quarter EBITDA margin had been 47.4%, down from 54.3% in the same quarter of 2010. Overall, polysilicon revenue has declined sequentially each quarter in 2011.

Wacker noted that it had benefited from advance and indemnity payments totalling €65 million due to the termination of supply contracts with customers exiting the solar business, though the company did not identify those customers.

## Praxair Electronics to supply its gas delivery system for Applied Materials' ion implant platform

Applied Materials' Varian VIISta ion implant platform will be using Praxair Electronics' UpTime sub-atmospheric dopant gas delivery system. Praxair Electronics noted that it is also the preferred sub-atmospheric dopant supplier for the Solion implant tool developed by Varian Semiconductor Equipment.

## DuPont and Yingli Green disclose N-type 'Panda' technology collaboration

An RD&E collaboration between DuPont Photovoltaic Solutions and Yingli Green Energy has been disclosed. Although the companies reiterated previous collaboration on Yingli Green's first generation 'Panda' cell technology now entering volume production, the companies are also working together to customize metallization materials for the Panda series modules, made with an N-type cell design, which is claimed to achieve a conversion efficiency of over 19%, based on current lab testing.

Yingli Green has been developing the Panda technology since 2009 with the Energy Research Center of the Netherlands (ECN) and recently announced efforts in the project with Amtech Systems' solar division Tempress Systems, which revealed that its N-type metal wrap through (N-MWT) PV cell and module technology had reached a cell efficiency of 19.7% and a module efficiency of 17.6%. Yingli has now highlighted that it was integrating DuPont's metallization paste (Solamet PV17x) via an advanced cell diffusion process for greater efficiency increases.

## Yingli Green signs US$100 million materials deal with DuPont

Following-on from an RD&E collaboration between DuPont Photovoltaic Solutions and Yingli Green Energy in January 2011, the companies have signed a new US$100 million strategic agreement. The new contract will see Yingli Green purchase DuPont's Solamet metallization pastes and Tedlar polyvinyl fluoride backsheet for its solar modules. The agreement is designed to extend DuPont and Yingli's commercial relationships and material supply availability.

At the beginning of February 2012, DuPont also entered into a strategic agreement with Suntech, which specifically focused on technology advancements, supply chain optimization and cost reduction in relation to DuPont's Tedlar polyvinyl fluoride film supply.

## Polysilicon business bolsters order backlog at GT Advanced Technologies

Third-quarter revenue at GT Advanced Technologies (GTAT) was inline with guidance at US$153.0 million, compared to US$217.7 million in the second quarter of fiscal 2011 and US$262.9 million in the third quarter of fiscal 2011. The polysilicon equipment segment continued to be the key earner, generating revenue of US$87.4 million. Recent new orders in this segment pushed its order backlog to US$2.2 billion. GTAT had a book to bill ratio of 1.3.

GTAT expects that revenue for the first nine months of FY2012 will reach US$601.8 million, compared to US$627.4 million of revenue for the first nine months of fiscal 2011. Gross profit in the quarter reached US$66.0 million, compared to US$95.1 million in the second quarter.

GTAT revenue by business segment for the quarter was US$87.4 million in polysilicon, US$34.4 million in photovoltaic and US$31.2 million in the sapphire segment.

Source: Centrotherm SiTec

Centrotherm SiTec will equip the Saudi Arabia-based company's new polysilicon plant.

## centrotherm SiTec wins Saudi Arabian polysilicon plant contract

IDEA Polysilicon Company has selected centrotherm SiTec to provide basic engineering and technology concepts for its first 10,000MT capacity polysilicon plant to be built in the city of Yanbu, Saudi Arabia. Actual construction timelines were not disclosed.

Centrotherm noted that future collaboration with IDEA could expand to include the production of metallurgical silicon and the manufacturing of ingots and wafers as well as modules.

# Other News

## Fraunhofer ISE develops MWT/PERC solar cell using special Heraeus metallization paste

Work undertaken on a conventional but advanced solar cell employing metal wrap-through (MWT) and passivated emitter and rear cell (PERC) technology exceeded 20% efficiencies that were supported by a specially developed and formulated metallization paste from Heraeus metallization paste, according to the company. In 2011, Heraeus introduced a new series of pastes for low temperature processing.


Source: Heraeus

Heraeus's SOL315 solar cell paste.

In April 2011, the Photovoltaic Technology Evaluation Centre PV-TEC of the Fraunhofer Institute for Solar Energy Systems ISE in Freiburg initially announced development work on a MWT/PERC solar cell. Efficiencies up to 20.2% were reported at the time.

## BioSolar claims first customer prepping its backsheet material for recertification by UL

Bio-based PV module backsheet developer, BioSolar claims that a customer is preparing a batch of solar panels with its 'BioBacksheet' material for full panel recertification by Underwriters Laboratories (UL). In March, 2011 the company announced it was supplying sample material for PV module manufacturers based in Asia for evaluation. BioSolar did not say when the recertification process would actually start or expected completion timeline.

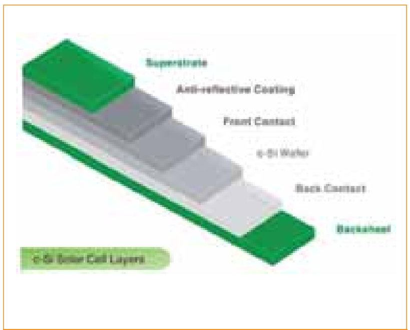


Source: BioSolar

The BioBacksheet is designed specifically for c-Si PV module manufacturers.

## DuPont expects PV materials destocking to correct by mid-year

DuPont reported Electronics & Communications segment sales of US$630 million in the fourth quarter, a decline 18% compared to the same period last year, with 33% lower volume which was offset by 15% higher prices. PV related revenue represent about 40% of DuPont's electronics segment sales. Management noted that material destocking at PV manufacturers had continued in the fourth quarter due to inventory issues, impacting pre-tax earnings, which were down from US$56 million in the fourth quarter of 2010 to US$42 million in the fourth quarter of 2011.

However, management noted in a conference call to discuss quarterly and full-year results that the PV destocking is expected to have been completed by mid-2012 or perhaps sooner as the company still expected the PV sector to grow approximately 10% this year. Management also expected sales in the sector to be down modestly in the first quarter from fourth quarter levels with limited restocking.

# Product Reviews



## GT Advanced Technologies

### GTAT DSS 450 MonoCast technology offers 19% plus cell efficiencies

**Product Outline:** GT Advanced Technologies' DSS 450 MonoCast crystal growth system furnace incorporates a number of new features that result in ≥80% mono volume yield per slabbed ingot and significantly increases Grade I wafers (>90% mono area/wafer) per ingot than other cast mono technologies.

**Problem:** GTAT claims that although boron-doped batch CZ monocrystalline wafers offer higher purity and provide higher cell efficiencies compared to conventional multicrystalline wafers, production costs are significantly higher. Currently there is no quasi-mono technology in the market capable of producing 100% mono ingots.

**Solution:** A typical MonoCast ingot produces three grades of wafers: Grade I is nearly all mono, Grade II is a hybrid wafer with more mono than multi, and Grade III wafers are more multi than mono. Georgia Institute of Technology claims MonoCast material, when combined with advanced cell processing technology, can deliver efficiency conversions of greater than 19%.

**Applications:** MonoCast or quasi-mono wafer production.

**Platform:** The MonoCast eliminates dipping and operator intervention between melt and growth. When combined with GT's new Acuity performance software, it can produce high quality ingots run after run.

**Availability:** The MonoCast technology is being offered first on GT's DSS450 and DSS450HP systems. Customers currently operating these DSS furnaces can migrate to the new DSS450 MonoCast system through a field upgrade, which is expected to be at a cost below US$100,000 per system.

## GT Advanced Technologies

### GTAT Acuity software has key performance indicators

**Product Outline:** GT Advanced Technologies has developed the Acuity software, a comprehensive performance management solution that lets operators optimize the performance of GT's DSS family of crystal growth furnaces. Acuity performance software monitors DSS production data providing PV manufacturers with real-time insight into actual versus ideal equipment performance. By understanding these performance gaps, companies can make more informed decisions to ensure that DSS furnaces perform at optimal levels of efficiency run after run.

**Problem:** Over the past several years, PV manufacturers have made significant investments in DSS crystalline growth systems. These manufacturers are being driven to lower their cost of manufacturing to remain competitive. Understanding how their DSS equipment assets perform is a critical step toward achieving this goal.

**Solution:** Acuity software is an application that puts real-time production data into the hands of production managers. The software allows manufacturers to establish key performance indicators that are most critical to achieving optimal performance of their DSS assets.

**Applications:** GT's DSS family of crystal growth furnaces.

**Platform:** DSS Acuity performance software offers a wide range of features such as configurable KPI dashboards, historical trend analytics, remote monitoring of alarm data, detailed run-to-run performance data and recipe management.

**Availability:** January 2012 onwards.

## Tanaka Precious Metals

### Tanaka Precious Metals provides irradiated hardened UV silver ink

**Product Outline:** Tanaka Precious Metals has introduced what it claims is the world's first conductive silver ink capable of forming electronic circuits hardened by UV light rather than heat. Three silver inks using different types of resin and reaction initiator will be available. Users can select the materials according to their manufacturing equipment and application.

**Problem:** Heating conditions for ink hardening may have been an issue because they all require heating to supplement hardening by UV irradiation.

**Solution:** This conductive silver ink is formed through irradiation from UV light under room temperature without heating due to optimization of the composition and mixture of resin containing silver particles and reaction initiator. As there is no need for large equipment or thermal processing time, it is possible to significantly improve production speed per unit of area.

**Applications:** Solar cells including silicon and dye-sensitized cells on thin-film flexible plastic substrates.

**Platform:** After printing a circuit on base material using this ink and exposing it to UV light for approximately 0.3 seconds, the user can instantly harden the printed film even at room temperature to form a circuit that carries current. At a film thickness of 5μm or more, it is possible to form wiring on the same level as the conductive material generally used at present, with electrical resistivity of $10^{-3}\Omega$cm. By using this ink, it is possible to perform wiring not only on glass-based material and substrates, but also flexible base material such as polyvinyl chloride film and polyester film.

**Availability:** Samples are available from January 2012.

# PV manufacturing materials: Technological and process-related options for cost reduction

**Joseph Berwind**, AEI Research & Consulting, Millburn, New Jersey, USA

ABSTRACT

The PV industry is undergoing dramatic changes. Like a carnival ride gone dreadfully wrong, exhilaration has been supplanted by dread; joy has been replaced by fear. Just look around you – provided you are able to turn your head to defy the g-forces acting upon you as we bank and turn wildly along. You will see PV companies closing their doors for good. You will see extraordinarily talented people throughout the supply chain, shifting positions everywhere and looking for safe-haven jobs. And you will also see once-leading PV companies burning cash and losing their status as 'bankable.' Everywhere we turn, we see companies in the supply chain shuttering production as if to balance markets. Then it happens again. Another wheel comes off the roller coaster. While we all want this reckless ride to end safely, optimism that was once universal has been replaced by threats of bankruptcy, failing policy support and a looming trade war. Indeed, it is hard not to be concerned about what lies ahead. However, despite all the neck-snapping gyrations, there remain three keys to surviving and prospering in the long run. The first is cost reduction: now, more than ever, the industry must reduce the cost of everything, from upstream to downstream, in order to bridge the gap to grid parity. The second key is quality: there is nothing more harmful to the industry's potential than cutting corners and sacrificing quality. And, finally, there is the third key – profitable volume. A degree of cost reduction for the industry that delivers on these three key mandates of cost, quality and profitability will be discussed in this paper by taking a fresh look at which processes, as well as which technologies, show the most promise.

## Global demand-supply dynamics

According to most estimates, demand surprisingly grew in 2011. This growth came in spite of subsidy cuts, less financing and Europe's sovereign debt crisis. As there are only a few countries reporting official installation numbers for 2011 thus far, AEI maintains that the global market for installations was 21.5GW and 23.8GW (Fig. 1), a maximum increase of approximately 20% from 2010. Yet another year-end rush, or 'pull-in,' seems to have created even more disagreement than is usually the case among estimators with some full-year estimations in excess of 28GW, expressed after German officials registered a whopping 3GW of installations in December alone. With growth estimates for 2011 ranging from 'up to 20%' to 'over 40%,' it would seem that the industry should be doing quite well, but that is not the case. Perhaps an estimator is off the mark, ourselves included – or is something else going on here?

"With growth estimates for 2011 ranging from 'up to 20%' to 'over 40%,' it would seem that the industry should be doing quite well, but that is not the case."

There is, however, one issue without much debate. Prices and profits for everything throughout the supply chain fell dramatically, and the fallout has resulted in an industry-wide requirement for everyone to reset their business models at this new lower level. While some of this need is taken up through supply-chain price discounting, the remainder must come from the adoption of processes that support production and result in restoring profits. Not an easy task given that pricing for everything moves so much and with very little warning, and often down as it has in the last three years.

The widening gap between supply and demand seems to have at last set

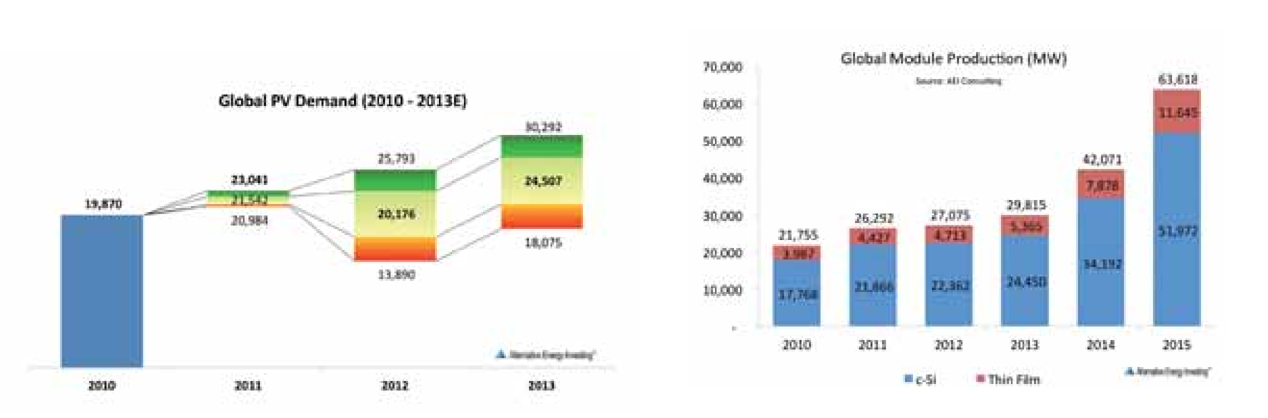


Figure 1. Global PV module supply and demand scenarios. The demand chart (left) illustrates the estimated outcomes corresponding to a 'worst-case,' 'base-case' and 'best-case' scenario. This chart and the production chart (right) together characterize the supply/demand situation.

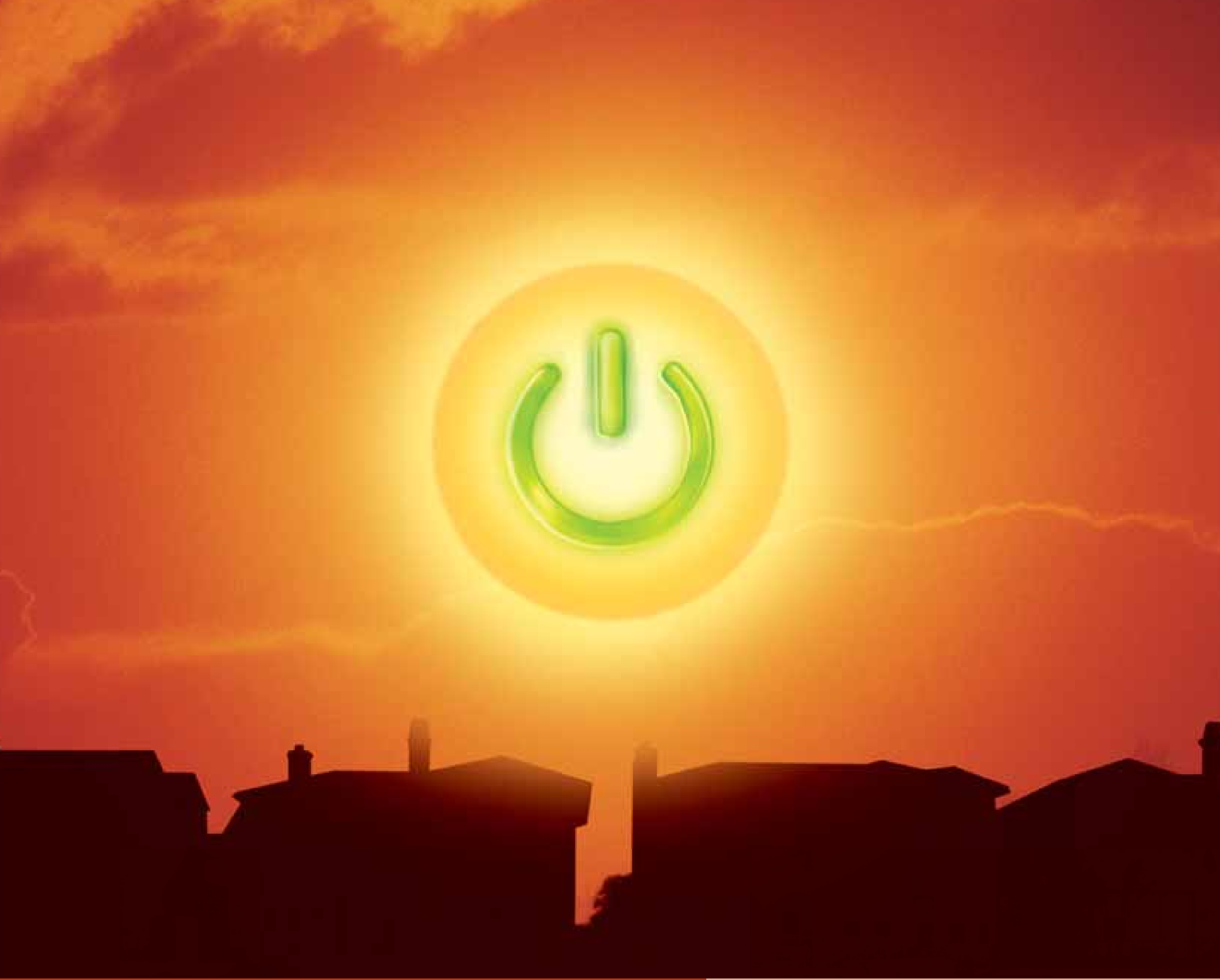

# One day soon, solar power will just be power.

**With SunSource™ materials and turnkey solutions, your PV investment looks brighter than ever.**

For fast fab ramp-up and grid parity acceleration, it's hard to beat the experience behind Air Products' SunSource portfolio of gases, chemicals, equipment, on-site chemical services and project management. We've been providing materials and expertise to Silicon Valley since the beginning of Silicon Valley. Today we serve all market segments in the global electronics industry, including thin-film and crystalline PV manufacturing. Which makes our experience directly applicable to your PV fab.

Visit airproducts.com/SunSource2 to see our interactive back-pad demo. And see for yourself how the SunSource portfolio can energize your PV investment.

AIR PRODUCTS

**tell me more**

www.airproducts.com/SunSource2

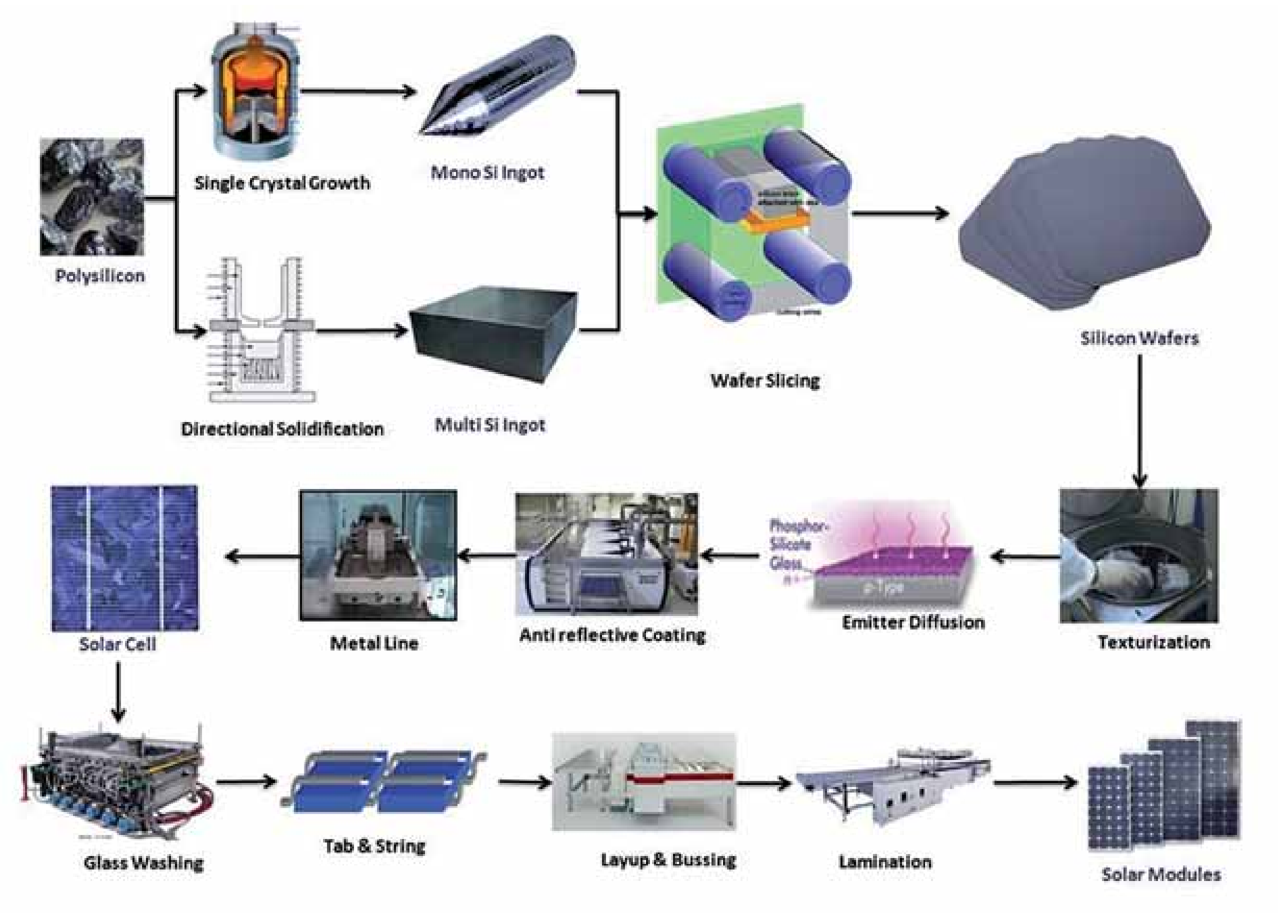


Figure 2. The standard crystalline silicon module manufacturing process sequence.

an expectation in the marketplace that average selling prices of modules will continue to fall. In 2011 alone we witnessed a 25% drop in the average selling prices (ASPs) of multicrystalline silicon (mc-Si) modules from Tier 1 Chinese companies. With prices hovering near $1/Wp, the ever-constant pressure to drive out costs reached the breaking point for practically every monocrystalline silicon (c-Si) module company except the Tier 1 cohort in China. Alas, to retain margins, and indeed hang on to their own survival, SolarWorld and others allege that Chinese module makers are dumping and a trade war looms. Given this as a backdrop, the key technological developments happening across the c-Si PV value chain will be reviewed, and areas for cost reduction with the potential for a 43% reduction in the medium term will be identified. Combined with falling polysilicon prices seen in the market today, total cost reductions for the industry may exceed 60% in the near term.

Whether installations grew at the high end or the low end of the range, the whopping growth of 200%+ during 2010 is over and we now face a slowdown in global demand growth, largely attributable to subsidy cuts in key regions – Germany, Italy and Spain – and persistent negative macroeconomic factors. Supply, on the other hand, for everything has continued to increase in the face of crippling news on the demand front. If announced capacities are adjusted to account for ramp-up delays and misinformation, etc., then it is still possible to arrive at a base level of module production of 26.3GW in 2011, 27.1GW in 2012 and 29.8GW in 2013, should companies proceed on their expansion plans. However, since supply continues to greatly exceed demand, more reductions in module prices are to be expected in the near future.

## c-Si PV standard manufacturing process

The crystalline silicon module production process starts from polysilicon raw material. A PV module can be manufactured from the more costly and more efficient c-Si or from the less expensive but less efficient mc-Si. A c-Si ingot is manufactured using Czochralski (CZ) or float zone (FZ) processes, whereas an mc-Si ingot is manufactured using directional solidification (DSS). Processing a wafer from ingots and bricks requires slicing, which is done with wire saws using wires of up to 400km in length. The real cutting work is carried out by what is known as slurry – a mixture of oil and silicon carbide grains – while the wire is wound on guides that form a horizontal 'web' of up to 1000 wires in parallel. Motors rotate the wire guides, causing the entire web to move at a speed of 5 to 25 metres per second. The wire speed and the back-and-forth motion are adjusted throughout the cut as nozzles continuously spray the wires with slurry. The silicon blocks are mounted to cutting tables, which then travel vertically through the web, cutting blocks into wafers. The wafers are then processed into cells.

Through a series of chemical and physical stages, wafers are processed to make them sensitive to solar radiation and absorb photons of light, which then creates free electrons within a newly made solar cell. Since cutting silicon into wafers leaves the surface of the wafer covered with cutting slurry and damaged due to the action of the saw, the wafers are cleaned in a hot solution of sodium hydroxide that removes the surface contamination and the first 10μm of damaged silicon. The wafers are then textured in a more dilute solution of sodium hydroxide with isopropanol as a wetting agent.

The p-n (positive-negative) junction is finally created by exposing the wafer to heat in a thermal diffusion step in a high-temperature oven (about 1000°C) with a controlled and highly purified atmosphere. During this process, the first 0.5μm of the wafer is doped with phosphorous, turning its conductivity into n-type and thus creating a p-n junction. The rest of the wafer maintains

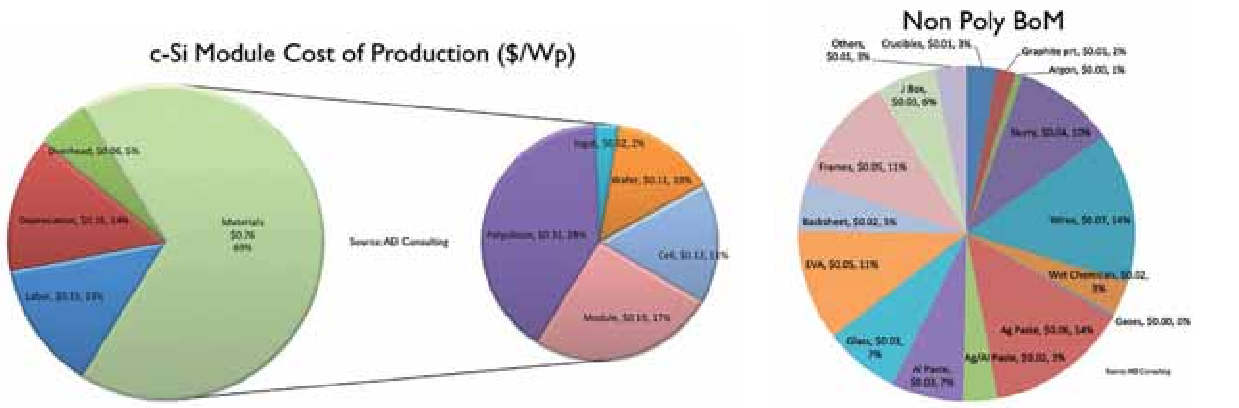


Source: AEI Consulting

Figure 3. c-Si module manufacturing cost.

a p-type conductivity, which acts as a separator for the electric charges created by the photons absorbed into the cell.

A very thin anti-reflecting coating (60–80nm) of silicon nitride ($SiN_x$) is applied through a plasma-enhanced chemical vapour deposition (PECVD) step to further reduce reflection and maximize the cell's light-absorption characteristics. Finally, electrodes are formed by printing silver paste grid lines on the front and aluminium paste on the back by means of a screen-printing process.

Once the solar cells are ready, individual cells are interconnected and laminated into a module. In this basic process, first using ribbon wire, individual cells are electrically connected into a solar cell string. The strings are then placed onto the glass panel and interconnected with bus ribbon, and encapsulated in EVA and a backsheet before aluminium frames are arranged around the laminated module stack. As a final step, junction boxes are put in place and final tests carried out.

> "Given the cost of materials to make a module, the industry is lowering the key cost contributors and has identified potential areas of cost-reduction across the value chain."

In 2011 around 75% of silicon PV modules were made from multicrystalline silicon and the balance of 25% from monocrystalline silicon. The average cell efficiency for multi was 14.85%, while for mono it was 15.15%; the market-weighted average cell efficiency was therefore approximately 14.93%. The average wafer thickness in 2011 is estimated to have remained in a variable range of 180–200µm. Polysilicon consumption was 6.16g/W and the average price of polysilicon was $50/kg for the year. With these assumptions, the average cost of manufacturing a module is estimated to be $1.12/W, with the total cost approximately split up into 66% materials, 13% labour, 14% depreciation and 5% overheads. The biggest factor in the cost of materials is of course polysilicon, which accounts for approximately 28%. Non-polysilicon costs were approximately $0.45/W. Of these, slurry (10%), sawing wires (14%), metallic pastes (24%), EVA/PVB (11%), frames (11%), and glass (7%) were the bulk contributors. Given the cost of materials to make a module, the industry is lowering the key cost contributors (polysilicon, sawing wires, metallic pastes, etc.) and has identified potential areas of cost-reduction across the value chain.

## Cost reduction areas for PV materials and consumables

While there are numerous ways in which costs of materials and consumables throughout the c-Si supply chain can be reduced, there are several key focus areas

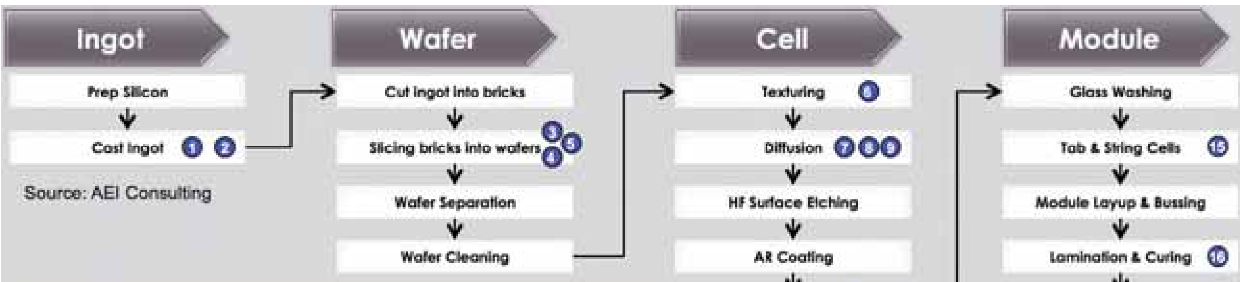


| No | Particulars | No | Particulars |
|---|---|---|---|
| 1 | Induction Melt Cold crucible | 9 | Selective Emitter |
| 2 | Mono cast Ingot | 10 | Double Printing – Esatto™ |
| 3 | Diamond Wire | 11 | Busbar Optimization |
| 4 | Structured Wire | 12 | Nickel film & Wet Metallization |
| 5 | SiGen PolyMax™ | 13 | Rear Passivated PoP |
| 6 | Plasma Etching Texturization | 14 | Direct Printing |
| 7 | Ion Implantation | 15 | Multiple Dye Doping of EVA |
| 8 | n-type Silicon | 16 | Backsheet Developments |

Source: AEI Consulting

Figure 4. Identified potential areas for cost reduction.

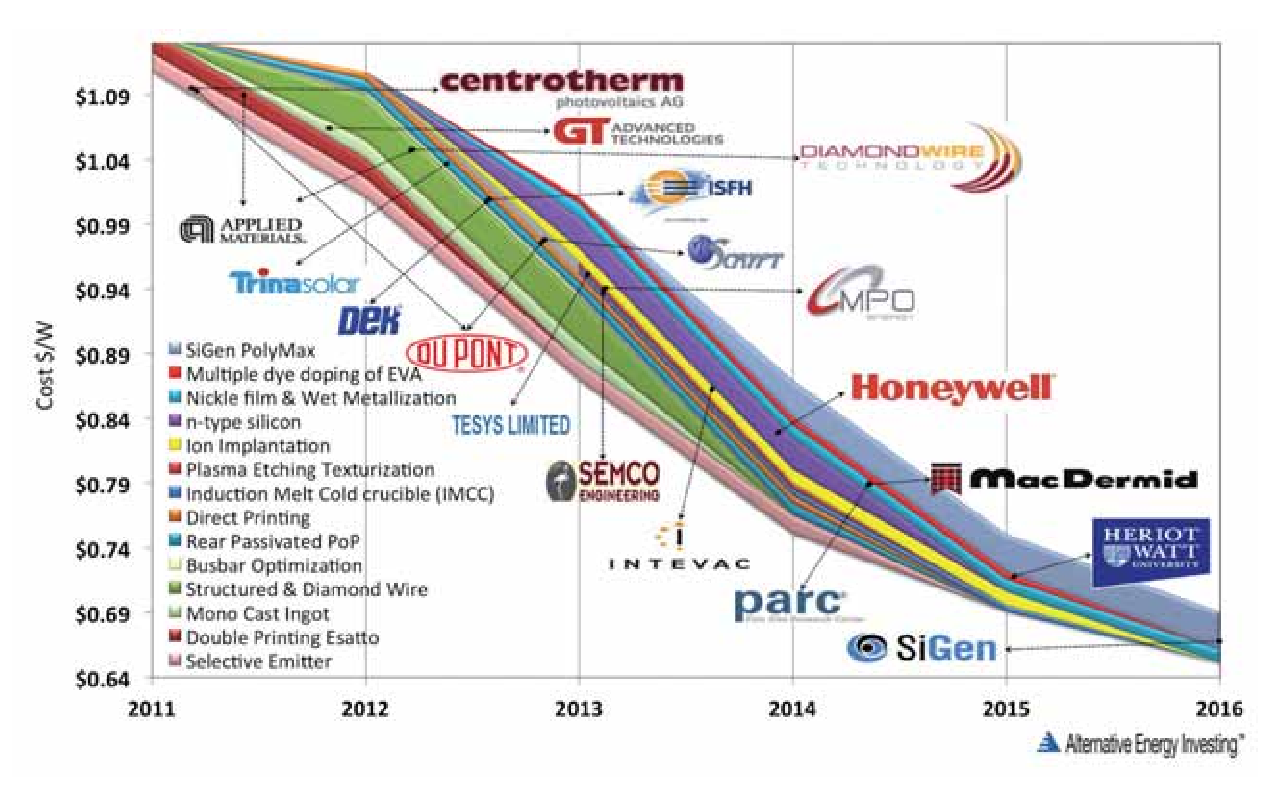


Source: AEI Consulting

Figure 5. Cost reduction potential.

for achieving this goal. Of these, the most critical are in the fields of improved wafer slicing, replacement of p-type silicon with n-type structures, and optimized metallization to reduce costly silver paste.

Given the current standard module manufacturing process, slurry and sawing wire together account for approximately a quarter of non-silicon material cost. Kerf loss associated with this process remains a big problem. Over the next two years, a sizable cost saving occurring in these areas alone through the replacement of conventional steel wires with structured and diamond wires should deliver a large part of the cost reduction. Beyond 2015, the sawing process itself may be replaced by novel and disruptive kerf-less wafering techniques that promise wafer thicknesses of 20µm, nearly a tenth of what can be achieved today on commercial production lines.

The replacement of p-type silicon with n-type silicon has been slowly gaining in importance because of the benefits of increased carrier lifetime and bulk resistivity, which lead to meaningful increases in cell efficiency. Process improvements and the introduction of innovative printable dopants are paving the way for potentially manufacturing n-type cells industrially on a large scale, a development which should contribute significantly to cost reduction in the coming years.

Metallic pastes account for approximately 24% of non-silicon material cost. Optimizing the screen-printing process is therefore critical to the overall cost-out equation. Techniques such as double printing, optimizing the busbar design, direct-printing technology, nickel film contact layers and so on are currently being used and tested or examined. These processes hold the potential for lowering costs by more than a third by 2016. Some of these process improvements are more popular and are being deployed much faster, which may result in accelerated cost reduction, depending on implementation and technology adoption. As noted, the standard manufacturing cost is currently $1.12/W, but it will be shown that this cost may drop to $0.64/W by 2016, given the adoption of improved technologies. Falling polysilicon prices may reduce costs for the industry beyond just those initiatives covered here. Assuming a $20/kg polysilicon price, with an average silicon usage of 5.01g/W by 2016 and a one percentage point increase in cell efficiency, the silicon cost could be $0.10/W, or 68% of the current level of $0.31/W. The combined effect of technological development and silicon price reduction may result in module manufacturing costs falling from $1.12/W to $0.43/W by 2016 – a 62% reduction from the current level.

## Diamond wire (3)

Diamond wire is intended to replace the conventional multiple-wire slurry saw (MWSS) of today; however, the process remains very expensive. The wire is coated with diamond particles and these particles become the abrasive element instead of the SiC particles found in today's conventional sawing technology. Diamond wires have very high cutting speeds (2–5× the speed of MWSS): certain companies – such as Read Co., Ltd., Japan – claim that their diamond wire cuts 5× faster than slurry-based steel wire. This obviously results in higher productivity, lower wire usage and ultimately a lower cost of ownership (CoO) as stated by the value proposition. Since diamond wires use fixed diamond grit, no slurry (SiC and PEG) is required and therefore this cost is avoided. Diamond wires also have very high tension strength and can be reused for several cuts, which obviously means less wire usage.

Meyer Burger has demonstrated wire consumption of under 3m/wafer (for 156mm wafers) on their DS265 sawing machine. But, as previously noted, diamond wire remains too expensive and, with the cost in the range of $375/km to $450/km (e.g. Read is selling at $400/km FoB Japan) and MWSS prices of $1–2/km, it is likely that we must wait for the cost of this technology to fall before it can contribute to the cost-out mandate of the industry. In 2011, the average MWSS cost $1.28/km and required 185m per 156mm wafer. The cost of slurry was $0.16 per wafer, and depreciation approximately $0.12 per wafer. Therefore, MWSS total CoO works out to be approximately $0.512 per wafer.

Diamond wire's high speed and tension strength means a usage of between 1 and 3m per wafer. Higher productivity and lower depreciation cost are calculated to be approximately $0.03/W, and there is

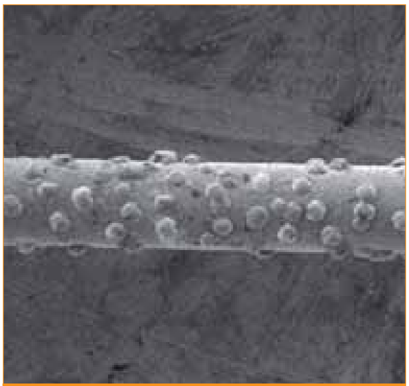

Source: Applied Materials

Figure 6. Diamond wire.

no slurry cost. Presuming a price of $250/km for diamond wire, the CoO works out to be approximately $0.32 per wafer. This implies that replacing MWSS with diamond wire could result in a net benefit of $0.19/wafer. Assuming market weighted average cell efficiency of 14.93%, this implies a net benefit of $0.05/W. A nickel does not purchase very much anymore, but in PV a nickel becomes disproportionally large as the cost per watt for modules falls below $1.

### Structured wire (4)

Today's state-of-the-art technology for c-Si wafering is based on the multi-wire saw method using abrasive grains as the cutting agent, suspended and transported in a liquid media ('slurry') as mentioned previously. The productivity and quality of the wafer slicing process essentially relies on the capability to transport slurry into the cutting channel. Applied Materials has developed a new process of using ultrathin, 120µm-diameter structured wire for slicing. This structured wire is a metal saw wire with a plurality of crimps or waves alternately oriented in two orthogonal planes. The idea here is to increase productivity by the more efficient transport of the slurry and by faster cutting speeds.

Applied Materials has demonstrated that structured wire can result in a 25–35% improvement in productivity over conventional MWSS. If structured wire results in 30% more productivity over MWSS, the wire use falls from approximately 0.185km/wafer to 0.142km/wafer, or a 23% reduction in wire consumption. Assuming structured wire costs 10% more than conventional MWSS, there is a net cost saving of $0.06/wafer. Again, assuming a market-weighted average cell efficiency of 14.93%, this implies a net benefit of $0.02/W.

### SiGen PolyMax kerf-less wafering (ion-beam-induced cleaving) (5)

Kerf-less silicon wafer-making equipment has been suggested as the cost-effective alternative to the wire saw method. The potential benefits include greater efficiency of materials utilization and lower cost. However, it seems that commercial efforts have been abandoned because of the poor electrical quality of kerf-less wafers and the method's inability to compete with the steadily improving performance of wire-saw-based wafering. To become competitive and gain traction against modern wire-saw-based wafering, the kerf-less method must support sub-100µm thicknesses and produce wafers possessing good electrical quality and mechanical strength.

SiGen is developing an ion-beam-induced cleaving technique that seems to hold some promise. This company is developing a novel technology called PolyMax, a potentially disruptive new capability for wafer generation by cleaving the wafers, in contrast to the destructive wire sawing process. In PolyMax technology, electron beam injections of H ions are used to peel the wafer from the silicon ingot without generating silicon losses. Gluing, wafer cutting, wafer separation and wafer cleaning process steps are also eliminated. This technology offers wafer thicknesses of as little as 20µm as against today's standard of ~180–200µm. Currently, the standard process consumes silicon at the rate of approximately 6.16g/W. Assuming a silicon price of $50 per kg, the silicon cost is $0.31/W. In comparison, if PolyMax is successful, with the potential for initially reducing the wafer thickness to 120µm, the silicon usage rate will drop to 3.70g/W, resulting in silicon costs decreasing from $0.31/W to $0.18/W.

Again, the wire saw technique involves a cost of around $0.13/W in respect of crucibles, graphite parts, saw wires and slurry, which can be completely avoided by switching to PolyMax technology. However, PolyMax could involve higher upfront capital which, it is estimated, may entail $0.17/W higher depreciation charges. However, on the whole, switching to PolyMax brings to the table a net benefit of $0.09/W initially and potentially $0.23/W later on, once wafer thicknesses gradually slim down to 30µm as the technology matures further. As one can see, kerf-less process technology is a huge contributor to the industry's overall cost reduction programme.

### n-type silicon (8)

Silicon is the most commonly used material in the production of solar cells. It is a non-conducting material, meaning that it does not conduct electrical current because it has wide energy bandgap. During material preparation, a dopant is introduced homogeneously into the silicon lattice to make it electrically semiconducting; in other words, it conducts electricity in only one direction, according to the type of dopant added. The most common dopants are phosphorous and boron. When a silicon lattice is doped with phosphorus, the electrical conduction is dominated by electrons and is called 'n-type'. Boron-doped silicon, on the other hand, is dominated by holes and is called 'p-type'. During cell fabrication, the electrical junction is formed by the thermal diffusion of oppositely charged impurities. For example, a junction is formed on the p-type substrate by phosphorous diffusion. The junction provides a built-in voltage that separates electron-hole pairs that flow through an external circuit.

Today most solar cells (whether mono or multi) are made from p-type (boron-doped) substrate on which phosphorous is diffused. There has been growing interest in developing a low-cost industrial cell manufacturing process based on n-type substrates. It has been successfully demonstrated that the use of n-type substrates could increase the minority carrier lifetime and bulk resistivity of devices, resulting in higher cell efficiency. Several studies have confirmed that efficiency improvements of 1–2% can be achieved by using n-type silicon instead of p-type standard silicon. Unfortunately, industrial manufacturing of n-type cells based on conventional architecture costs more than for conventional p-type silicon solar cells.

The process of manufacturing n-type cells usually involves two diffusion steps, including (for example) $BBr_3$ diffusion

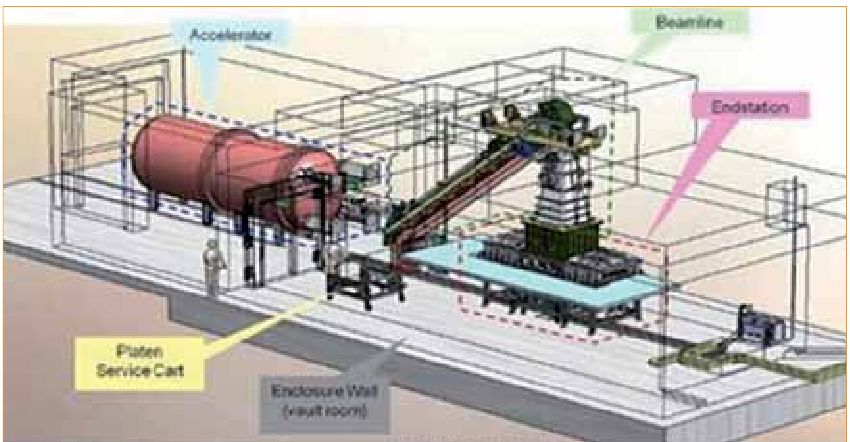


Source: SiGen

Figure 7. SiGen PolyMax ion-beam implanter tool.

for top emitter formation, and $POCl_3$ diffusion for back-surface field (BSF) formation. In addition to the associated equipment depreciation, energy costs and safety concerns involved in handling $BBr_3$ in volume manufacturing, the added thermal budget seems to put limits on the use of this process for creating very high quality Si substrates. Honeywell presented an approach using a co-diffusion of boron emitter and phosphorus BSF using printable dopants. These dopants can be applied by various techniques, including inkjet printing and screen printing. Under diffusion conditions of 60 minutes at 925°C, the new technique has been able to achieve a sheet resistance ($R_s$) below 60Ω/sq for a boron emitter, with good doping uniformity over the entire wafer.

It is estimated that replacing p-type silicon with n-type silicon could result in a 1–2% absolute efficiency gain. However, with $BBr_3$ diffusion, this could involve higher material cost and could involve higher capex due to the extra process steps involved. On the whole, it is estimated that switching to n-type could result in a net benefit of between $0.05/W and $0.06/W.

### Selective emitter (9)

Energy conversion in a silicon solar cell happens at its p-n junction, which is normally formed by firing the wafer in a phosphorus-rich atmosphere. The phosphorus diffuses into the upper zone of the wafer to form a layer that is uniform and planar, lies a few hundred nanometres under the surface, and extends across the wafer's entire area. This process is called 'emitter diffusion'. In this layer, photons of sunlight release electrons that migrate through the silicon to the cell's front face, where they are captured by the grid of silver conductor fingers printed on the cell's top side. The flow of electrons through this grid is the electrical current that constitutes the cell's power. These electrons then flow around the circuit back to the aluminium contact on the reverse side of the cell, where they once again join with atoms that are missing electrons (i.e. possess 'holes').

However, the top part of the cell where the phosphorus is most concentrated is essentially a 'dead layer' that reduces the cell's blue response. In other words, the electrons activated by blue light turn into charge carriers, but then, even before they leave the silver conductor grids, they recombine with the wafer's surface, generating heat rather than current. In order to resolve this problem it is desirable to deposit more phosphorus under the silver grid and less phosphorus between the grid fingers. This can be done through 'selective emitter' (SE) technology. Using SE approaches, it is possible to deposit more phosphorus directly under the silver grid to facilitate contact between the grid and the silicon, allowing the electrons to migrate efficiently. At the same time, by reducing the amount of phosphorus between the grid fingers, recombination losses are reduced and the cell's blue response is improved.

There are different ways in which selective emitters can be formed, such as doped silver paste, screen printing, selective diffusion, laser doping, etch back and buried contacts. Of these, laser doping may be the most promising. Centrotherm, together with its partners, has implemented a new SE process using laser doping in different industrial production lines in Asia. The company claims it has demonstrated a 0.50% absolute efficiency gain using its SE technique. The major task in laser-diffused selective emitters is to sufficiently increase the phosphorus concentration in the silicon close to the surface of the laser-treated areas, to enable a good contact resistance without causing too many crystal defects or contamination within the silicon.

Centrotherm's process flow for SE formation suggests that, in the current state-of-the-art process flow sequence, between the diffusion and the phosphorous silicate glass (PSG) etch, there is an additional process step. In this process step the contact resistance of the previously diffused emitter with high sheet resistance and inferior contacting properties is improved to a level of contact quality comparable to standard emitters. The two main cost drivers in SE technologies are the number of additional pieces of equipment added to the production line and the amount (and price) of additional consumables needed. In both respects Centrotherm's laser-diffused selective emitter seems to be very cost effective. There is only one additional piece of equipment – a laser – which needs almost no consumables. Apart from this, the cost structure of the standard process remains unchanged. Thus, the method used is probably one of the most economical SE processes available.

When calculating the cost-saving potential of SE technology, the overall cost structure remains more or less unchanged and so the efficiency gains determine the net benefit. In an alternative approach, DuPont Innovalight offers innovative silicon inks for screen printing selective emitters on the solar cells. The proprietary material comprises silicon nanoparticles dispersed in an environmentally friendly blend of chemicals. For the silicon ink SE cells, as-cut wafers are first cleaned and textured in an alkaline bath to create a random pyramid-textured surface. Silicon ink is deposited in a screen-printing step and heavily doped regions are required for good contact formation. This screen-printing step includes a simple drying process to drive off the remaining organic solvents and densify the printed silicon ink film. An n-type phosphorus diffusion is subsequently performed in a quartz diffusion tube: in this step, selectively doped regions are formed on the front surface of the wafer. Typically, heavily doped printed regions achieve sheet resistance values of 30–50Ω/sq, whereas unprinted areas remain at 80–100Ω/sq.

SE technology offers very good cost-saving potential by substantially increasing the cell efficiency: DuPont claims that, using Innovalight, efficiency can be improved by 2–3%. The Innovalight technology requires the additional cost of silicon ink dopant, and it is assumed that this could add 5% to material costs. The process also requires the silicon ink to be screen printed, for which new screen-printing equipment is needed. It is estimated that this could entail 30% additional capex. Our analysis suggests that there is a cost saving potential of $0.06/W.

### Double printing – Esatto (10)

In current state-of-the-art c-Si cell making, a screen-printing method is used to produce electrodes on the cells. In this method, a printing mask that has been formed with a predetermined pattern is placed at a fixed distance from the wafer, and paste (including an electrode material) is applied to the mask. The paste is spread on the printing mask by a squeegee, and only the paste on a meshed area is applied. The coated wafer is then baked at a predetermined temperature, depending on the electrode material, and the electrode is formed. The objective is then to print thin lines that reduce efficiency losses due to the 'shadowing' effect. On the other hand, if the lines are very narrow, increased sheet resistivity reduces cell efficiency. So, in order to optimize the printed line structure, and to increase efficiency and reduce cost, Applied Materials have introduced Esatto – a double-line printing technology.

Esatto was designed to allow the use of advanced contact-formation techniques, such as double-printed front-side metal lines, and the multiple process flows required to create selective emitters. Esatto enables manufacturers to print taller and narrower grid lines that reduce shadowing and improve conductivity. In a production environment, Esatto replaces single 120µm-wide lines with two-layer, double-height lines of width less than 80µm on the finished cell. Customers have demonstrated a 0.46% absolute cell efficiency gain using Esatto and up to a 14% reduction in silver printing paste consumption.

Currently, the front-side silver paste consumption is estimated to be 0.18g/cell (156mm), and the price for paste is approximately $1220/kg. Assuming an average cell efficiency of 14.93%, front-side paste costs \$0.06/W and the total module cost would be \$1.12/W. Given a 0.40% increase in efficiency and a 10% reduction in paste usage per cell, the incremental benefit of using Esatto is approximately \$0.03/W. Therefore, if the Esatto upgrade costs \$650,000, assuming 2000 wafers/hour throughput and 3520 days working per year, the added capita cost is approximately \$0.02/W. Given a 5-year system life the additional depreciation expense is 0.50¢/W, resulting in a net benefit of ~\$0.03/W when using Esatto.

### Direct-printing technology (14)

The challenge in front-contact grid-line printing is to reduce the grid width to limit shading losses without reducing line conductivity in the process. This is to increase the aspect ratio (height/width) while increasing cell efficiency. DuPont, nScrypt and others have presented a direct-printing technology that offers tools for patterning fine grid lines with high aspect ratios. This technology is based on micro dispensing and uses a special pump assembly and a printing head, which is able to handle screen-printable paste and thixotropic materials with very high viscosities. Printing as fast as half a metre per second is possible in some cases. Multiple nozzles enable this process to print each wafer in about 2 seconds.

To achieve fine lines with high aspect ratios, a silver paste for front-side metallization should be modified based on available screen-printing paste. In a typical case, the line is as small as 50µm wide by 30µm tall after firing. This is generally more precise than stencilling, which can usually only achieve a width of around 110–130µm. Direct printing effectively reduces the shading area while maintaining high grid-line conductivity and low contact resistance. The company claims that solar cells made with direct-printed grid lines show up to a 0.5% absolute efficiency increase over those with screen-printed grid lines, resulting in \$2–3 million annual savings for solar cell manufacturers.

If it is assumed that direct printing reduces the print width to 50µm from a current width of 120µm, the paste usage could be reduced from 0.184g/cell to 0.112g/cell. Again, this could increase overall cell efficiency by 0.50%. It is calculated that the incremental cost saving achieved by introducing direct printing could be \$0.06/W. An nScrypt direct-printing tool could cost 20% more than a normal screen-printing tool. In this case, assuming 2000 wafer/hour throughput, the capex could work out to be \$0.11/W. The assumption of a 10-year system life implies a depreciation cost of an additional \$0.01/W. Therefore, the net benefit of introducing direct printing could be \$0.05/W.

### Nickel film contact layer (12)

Reducing the contact resistance is one of the major challenges for the front-side metallization of crystalline silicon solar cells. Screen printing silver paste and firing through the silicon nitride antireflection coating layer is the most common technique for front-side metallization of today's industrial silicon solar cells, but it also produces a poor, very resistive metal-silicon contact.

Palo Alto Research Center has developed new approaches for the front-side metallization of crystalline silicon solar cells using a blanket sputtered nickel film as the contact layer, which is aimed at dramatically reducing the specific contact resistance between the metal grid line and the n+ emitter layer. One technique involves drilling the contact holes in the silicon substrate through the nitride layer using a laser ablation method, and then sputtering a thin nickel film on the whole surface. This is followed by screen printing silver grid lines which are aligned with the contact holes. Finally the uncovered nickel film is etched away using the silver grid lines as a protective mask. This approach could significantly reduce the specific contact resistance and it has been demonstrated that this equates to an absolute efficiency gain of as much as 0.9%. This improvement in efficiency implies that an additional 9W can be generated per $1m^2$ area, which translates to a cost saving of \$0.064/W. It is estimated that this could involve additional capex: for direct printing, the capex could be as high as 120% of that for current screen-printing tools. Nevertheless, this leaves a net benefit of \$0.05/W.

### Rear-passivated cells with print-on-print front contacts (13)

In current state-of-the-art cell manufacturing, the silver (Ag) front-side metallization with finger widths of around 90–100µm reflects about 7% of the incident solar radiation. Similarly, the screen-printed full area Al BSF exhibits only a moderate passivation quality. In addition, only about 70% of the infrared light reaching the Al rear contact is reflected back into the silicon wafer. With improvements in these areas, there is a great potential for significantly increasing the cell efficiency.

The Institute for Solar Energy Research Hamelin (ISFH) and DEK Printing Machines have suggested a new approach for overcoming these problems. Before texturing and phosphorus diffusion, a dielectric protection layer is deposited on the rear side of the solar cell. The dielectric layer acts as a barrier against the alkaline texturing process as well as the phosphorus diffusion. Accordingly, only the front side of the solar cell is textured and phosphorus doped, with a sheet resistance of about 70Ω/sq, whereas the rear side remains planar and boron doped. The PSG etch after the diffusion step is slightly adjusted in order to remove the dielectric layer at the rear in addition to the PSG at the front. In the case of $Al_2O_3$-passivated PERC cells, the wafers are coated with a 10nm plasma-assisted ALD-$Al_2O_3$ layer. To improve the front printing quality, a print-on-print (PoP) technique has been suggested. The number of fingers has to be increased for PoP in order to minimize resistive losses due to the significantly smaller finger width. The process flow of the PoP cells is identical to standard single-printed solar cells. However, the Ag front contact is deposited in two consecutive screen-printing steps.

Rear passivation and PoP together can result in an efficiency gain of 1% and a reduced silver paste usage by decreasing the print width. It is calculated that these could translate to a cost saving of \$0.08/W. However, extra steps are required because of additional chemical deposition and consequent printing; this entails additional capex, which is estimated to be \$0.20/W. Therefore, the proposed technological development could yield \$0.06/W net benefit.

### Busbar optimization (11)

With the price of silver material rising, the cost of screen-printed silver paste has become one of the major components of the total cost in \$/W for PV modules. In traditional H-grid front metallization pattern design, over a third of the total metallization area comes from busbars, which are required to be wide enough for terminal contacts in *I-V* measurements and for reducing the series resistance.

The State Key Lab of PV Science and Technology (Trina Solar) has presented a segmental busbar design which cuts down silver paste usage significantly (by over 30%), while the fill factor (*FF*) and maximum output power of the final module remain at the same levels. Experiments on 125mm × 125mm Cz-Si mono cells show that, because of the increase in resistive losses along the busbars, the segmental busbar design will lead to a 0.45% drop in the cell's *FF* and a 0.12% drop in cell efficiency. However, this loss can be compensated for by soldering ribbons in modules, which results in almost the same performance. This implies that over 30% of the cost of silver paste can be saved without any influence on the final module's output power.

Normally two busbars, each 2mm wide, are used in standard cells. Per cell, the busbars usually occupy $612.5mm^2$ of area and consume 60mg of silver paste. In the proposed optimization, the busbar regions between contact terminals have been hollowed out, while the regions corresponding to the positions of the *I-V*

PVGroup | semi

# 6$^{th}$ PV Fab Managers Forum

## Roadmap to manufacturing excellence and greater productivity in a challenging business environment.

25-27 March 2012 in Berlin, Hotel Kempinski Bristol

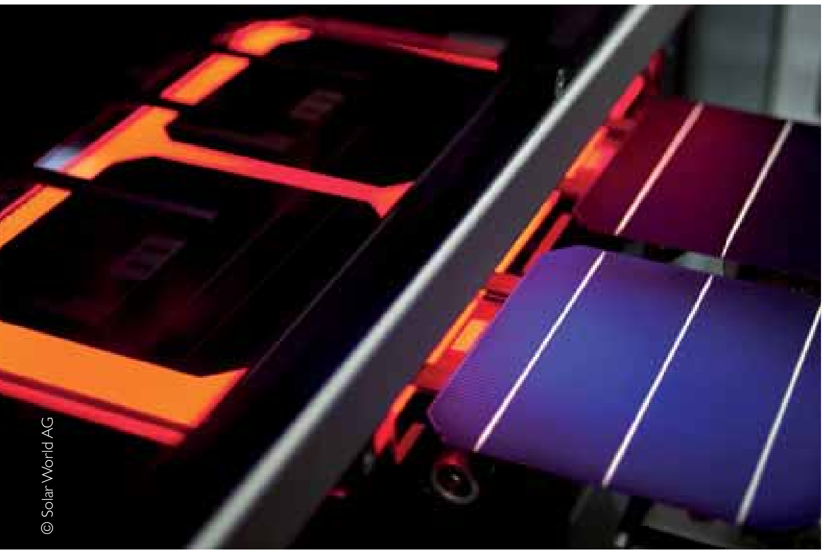


**The PV Fab Managers Forum is the most important forum where suppliers and manufacturers meet and discuss current challenges and future requirements.**
No other forum brings together the whole manufacturing supply chain better and offers such a dense line-up of presentations from industry professionals.

### Forum Topics:

- PV Market and Manufacturing Technology Outlook
- PV Technology Roadmap (ITRPV)
- Cost Reduction Potentials in Cell and Module Manufacturing
- Efficiency Increase Potentials in Cell and Module Manufacturing
- PV Standardization Update and Overview
- Total Cost of Ownership Models

For more information please visit our event website: www.pvgroup.org/pvfmf

### Who should attend?

The forum is attended by executives, senior management, fab managers, scientists and experts from the photovoltaic industry, research and academic organizations.

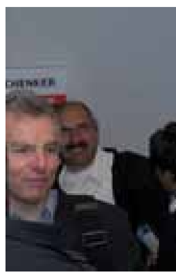

tester contact pins remain untouched. In this case, the current from the fingers flows through the edge of the busbar and reaches the contact terminals. Typically around 30% of the busbar area is hollowed out and hence 30% less silver paste is used. Therefore, the amount of paste used per cell busbar area can be reduced to 42mg. Assuming silver paste is priced at $1200 per kg, this implies a net cost saving of $0.01/W.

### Ion implantation (7)

In standard solar cell manufacture, the starting material consists of p-type boron-doped silicon wafers. The first process is an acid etch, to remove saw damage and texture the surface, which improves the absorption of incident light. The wafer is then heated in a furnace (800 to 1000°C) with a phosphorous atmosphere, causing a small amount of phosphorous to be incorporated in the outer layer of silicon. This is called 'thermal diffusion,' in which phosphorous doping is performed in a furnace with $POCl_3$ gas that creates a light n+ emitter region on the silicon surface. The diffusion causes the creation of PSG, and a hydrofluoric acid etch is done to remove PSG. Diffusion is performed in a furnace with a flow of gas running over the wafers. This step, as with the acid etch, is not selective, so the photoresist and patterning processes need to be done prior to this step.

Ion implantation is being evaluated as a replacement for the diffusion process. While diffusion uses the natural state of gas spreading to locations where there is no gas, ion implantation shoots the desired dopant ions into the wafer. Even though ion implantation has several advantages over diffusion – such as saving energy, time and chemicals – historical semiconductor-based ion implantation tools did not meet the performance and cost requirements of the solar industry.

Intevac recently developed a high-throughput ion implantation tool for solar application, in which wafers are transported horizontally in three columns on a conveyor belt. Despite having a smaller footprint than commercial ion implanters, the ENERGi tool is capable of processing 2400 wafers per hour, with low or high sheet resistivity. The implantation of either n-type or p-type dopants is possible, allowing for greater flexibility in emitter design. It has been demonstrated that the total CoO of this ion implantation tool could be $0.025/W, compared with $0.04/W for the conventional diffusion process. This implies a cost saving of ~$0.04W.

### Plasma-etching texturization (6)

Surface texturing is the first process to be carried out on incoming wafers in silicon cell manufacturing. Texturing also allows removal of the saw damage layer that develops during the slicing of the Si ingots into wafers. The defects induced by slicing with a wire saw (in the form of μ-cracks), well known for degrading cell performance, are removed during the texturing process. The isotropic etch in an acidic bath, based on a $HF/HNO_3$ mixture, is now a standard procedure in the photovoltaic industry for mc-Si with randomly oriented grains.

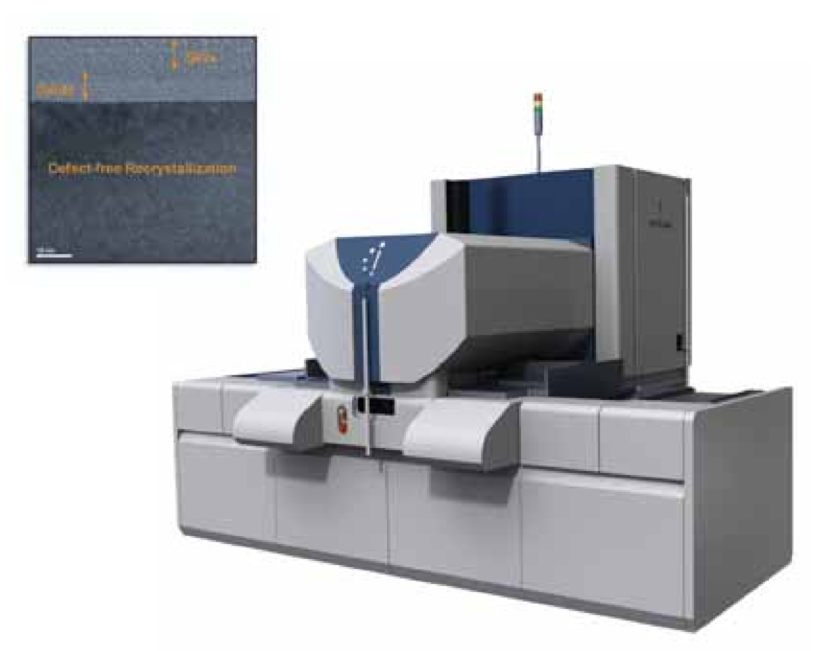


Source: Intevac

Figure 8. Intevac's ion implantation tool for manufacturing solar cells.

As an alternative to the well-established isotexture process, MPO Energy, Semco Engineering and others have developed a combination of a wet etch and a plasma process, for which a specific plasma chamber has been designed. The resulting texturing procedure was then successfully implemented in a solar cell process. Surface characterizations underlined the fact that no plasma damages occur during this texturing process. Solar cell results exhibit an increase in short-circuit current density and no drop in open-circuit voltage. This leads to a gain in efficiency for the plasma-texturing process, compared to the standard texture process (alkaline or acidic).

The new approach could result in an improvement of 0.15% in efficiency. This implies that an additional 1.5W can be generated per $1m^2$ area. This translates to $0.011/W in cost savings. Normally, a texturization tool could cost $2 million and it is assumed that the additional capex could be 50% of that amount. This implies that $0.002/W additional annual depreciation charges would be incurred in implementing this approach, therefore leaving a net benefit of ~$0.01/W.

### Mono-cast ingot (2)

Silicon ingots can be either mono or multi. Mono ingots are much more efficient than multi ingots, but are more expensive to manufacture. GT Advanced Technology has developed a new technique called 'MonoCast' to produce quasi-mono ingots at a very low cost. The DSS450 MonoCast furnace produces the industry's highest mono volume yield in production ingots comprised of up to 25 bricks. The new mono-cast technology uses a lower-cost multicrystalline ingot process to manufacture higher-quality, mono-like ingots, without the associated higher production costs. Cells produced from DSS450 MonoCast wafers are claimed to have lower light-induced degradation (LID). Moreover, the full-square surface dimension area across the MonoCast wafer provides greater surface area (~1.8% more) for electricity generating than the pseudo-square shape of traditional monocrystalline wafers. MonoCast ingots produce three grades of wafers: Grade 1 (mostly mono), Grade 2 (hybrid) and Grade 3 (mostly multi). Over 95% of the wafers produced are either Grade 1 or Grade 2.

Mono-cast technology offers sizable cost savings by increasing the ingot quality, which in turn results in greater cell efficiency. The current weighted-average cell efficiency is assumed to be 14.93%. It is believed that mono-cast quasi cells could increase the cell efficiency by 0.35%, which could result in a 10% reduction in ingot material usage. Our analysis suggests that there is potential for reducing the total cost by $0.03/W.

### Induction melting in cold crucibles (1)

The standard technology used for producing multicrystalline silicon ingots is the directional solidification method in quartz crucibles. This method has several drawbacks: inhomogeneity of ingots;

part of the material is contaminated with oxygen/metal impurities; the productivity of growing is rather low, etc.

To overcome these drawbacks, Tesys Ltd. and Piller Ltd. introduced the process known as induction melting in cold crucible (IMCC) as an alternative to directional solidification. The technology of producing multicrystalline silicon ingots by the IMCC method consists of induction heating and melting of silicon held in a water-cooled (cold) segmented copper crucible. Melting is accompanied by ingot formation via crystallization of the melt in the cross-sectional shape of the cold crucible, thus forming the ingot; the IMCC technology is consequently considered to be continuous casting. Application of induction heating provides a high concentration of energy in the melting zone, thus achieving a high rate of fusion and high-speed crystallization and formation of the ingot. At the same time, the resulting ingot has both a uniform structure and a homogeneous distribution of impurities along its entire length.

IMCC offers significant cost savings by increasing the productivity and reducing the consumption of disposable quartz crucibles and graphite components. A 20% productivity gain and 40% reduction in crucible usage are assumed and no graphite component consumption is required, resulting in a potential net benefit of $0.01/W.

## Multiple dye doping of EVA (15)

In a study the School of Engineering and Physical Sciences at Heriot-Watt University, Edinburgh, UK, have optimized the light-absorption properties of luminescent encapsulation layers made from (poly)ethylene vinyl acetate (EVA), by using multiple dye doping and varying the concentration of the most promising dye. These layers were used to encapsulate mc-Si solar cells. This led to a 25% enhancement of the external quantum efficiency (EQE) for the region 300nm $< \lambda <$ 400nm, leading to an efficiency increase of $\Delta\eta = 0.3\%$ absolute for a 59cm$^2$ single-cell mini-module.

By optimizing the light-absorption properties of EVA by dye doping, module efficiency could be increased by 0.3%; this implies that an additional 3Wp power can be produced per 1m$^2$ area. It is assumed that this multiple dye doping could cost 20% of the EVA cost, which would result in a potential saving of $0.02/W if this new approach were adopted.

## Backsheet developments (16)

Most backsheets are multilayer composites which enhance the performance of PV modules in many ways. They offer protection from the environment, provide electrical insulation and contribute to aesthetics. The backsheet has a dominant role in providing long-term protection for the solar module. It has been established that the main reasons for PV system failure include degradation of packaging materials, adhesional loss, degradation of interconnects, degradation due to moisture intrusion, and semiconductor device degradation. Improvements in backsheet quality are therefore reflected in improved system life, decreased degradation and, to some extent, improved yield, which could reduce the cost of production. Consequently, the best parameter to look at for expressing improvement in backsheet technology and quality is the levelized cost of energy (LCOE), because, as the backsheet improves, the LCOE can fall. Indeed, paradoxically, an increase in the per watt manufacturing cost may be offset by a decrease in degradation, resulting in increased system lifetimes.

Peel strength, water vapour transmission rate (WVTR), dimensional stability and dielectric strength are considered to be some of the critical factors in determining the quality of the backsheet; these factors have an impact on the LCOE of the module. An exhaustive database of backsheets, including 39 products offered by 13 companies, has been created. However, different companies may apply different chemistries, so, to assess them, the following assumptions have been made in order to calculate the LCOE for different backsheets.

To avoid delaminating effects in the long run, it can be assumed that peel strength should be higher for the backsheet. It has been noted that the average peel strength for the backsheets in the database is 4.84N/mm, with a minimum of 2.5 and a maximum of 12.0. A backsheet is considered to be 'excellent' if peel strength is greater than or equal to 6.0 and 'bad' if peel strength is less than 3.0. If peel strength is 'excellent', the annual power degradation can be reduced by 0.1% and the system life increased by 2 years; if it is 'bad', the annual power degradation can be increased by 0.1% and the system life reduced by 2 years.

It can also be assumed that WVTRs for the backsheet must be more effective in blocking water vapour in the air from entering the panels over time. The WVTRs averaged 2.75g/m$^2$ per day, with a minimum of 0.8 and a maximum of 9.0, in our database of backsheets. A backsheet is considered to be 'excellent' if the WVTR is less than or equal to 1.5 and 'bad' if the WVTR is greater than 3.5. When the WVTR is considered 'excellent', annual power degradation could be reduced by 0.2%; if the performance is 'bad', annual degradation may increase by 0.2%.

Dimensional stability is assumed to be a factor because, as a backsheet changes its shape, the manufacturing yield could be lower. An average dimensional stability of 1.21% was noted, with a minimum of 0.05% and a maximum of 5%. A backsheet is considered to be 'excellent' if its dimensional stability is less than or equal to 0.8% and 'bad' if its dimensional stability is greater than 1.5%. If the dimensional stability is 'excellent', the manufacturing cost could be decreased by 3%; if it is 'bad', the cost could be increased by 3%.

On the basis of these assumptions and frameworks for ranking this group of backsheets, the LCOE was calculated for a typical module incorporating these backsheets in Frankfurt, Germany. The analysis showed that the lowest LCOE is achieved for Solar Gard's backsheet (11 in Fig. 9), which uses PVF/PET/PVF chemistry; the highest dielectric strength is noticed for Krempel's backsheet (31 in Fig. 9), which uses PVDF/PET/PVDF chemistry. On the whole, Solar Gard (11 in Fig. 9) and DuPont (7 in Fig. 9) backsheets, with higher dielectric strength, have demonstrated relatively lower LCOEs. However, technology changes may rewrite the rankings observed here.

Most multilayer backsheets are constructed from laminated layers glued together, with distinct adhesive layers. An alternative to laminating different layers with adhesive is a coating process: coating one or more layers is a well-known way of producing highly functional multilayer structures. DuPont, Asahi and Daikin are some of the major companies developing this promising field of fluorinated coatings for photovoltaic backsheets. Coating-based backsheets can simplify their manufacturing process by dispensing with the need for an adhesive layer to bond the fluoropolymer to the PET. This allows a thinner construction.

In 2009 DuPont introduced PV2400, which is a system for making TPT by coating PVF formulations directly on PET. After coating, the formulations are heated and processed in a similar way to PV2100. However, in the case of PV2400, the dried PVF coating adheres to the coated substrate. At the end of 2011, DuPont developed TPNext – a solar backsheet technology based on a single protective layer – which improves adhesion for c-Si solar module encapsulants, resistance to UV light, and backsheet production throughput. The new laminate consists of Tedlar film, polyester and an extrusion-coated tie layer that reduces the use of organic solvent-based adhesives. An extrusion-coated process is used to put down the tie layer. Since no solvents are used, it can be done at much greater line speed than traditional means for putting down solvent-based adhesives. This results in enhanced productivity for the backsheet makers. DuPont expects to release TPNext in 2012.

| S No | Company | Chemistry | Peel Strength Ranking | WVTR Ranking | Dim Strength Ranking | Dielectric Strength | LCOE ¢/kWh |
|---|---|---|---|---|---|---|---|
| 1 | Krempel | PVF/PET/PVF | | | | | 19.74 |
| 2 | Krempel | PVF/PET/PVF | | | | | 19.53 |
| 3 | Krempel | PVF/PET/PVF | | | | | 19.53 |
| 4 | Krempel | PVF/PET/PVF | | | | | 19.53 |
| 5 | Dunsolar | PVF/PET/PVF | | | | | 21.14 |
| 6 | Dupont | PVF/PET/PVF | | | | | 19.98 |
| 7 | Dupont | PVF/PET/PVF | | | | | 18.51 |
| 8 | Haflon New energy | PVF/PET/PVF | | | | | 19.98 |
| 9 | Haflon New energy | PVF/PET/PVF | | | | | 19.98 |
| 10 | Haflon New energy | PVF/PET/PVF | | | | | 19.98 |
| 11 | Solar Gard | PVF/PET/PVF | | | | | 18.28 |
| 12 | Isovolta | PVF/PET/PVF | | | | | 19.74 |
| 13 | Madico | EVA/PET/EVA | | | | | 18.72 |
| 14 | Madico | EVA/PET/EVA | | | | | 18.72 |
| 15 | SFC | FPF/PTI/FPF | | | | | 19.74 |
| 16 | SFC | FPF/PTI/FPF | | | | | 19.74 |
| 17 | SFC | FPF/PTI/WPO/Primer | | | | | 19.95 |
| 18 | SFC | FPF/PTI/WPO/Primer | | | | | 21.35 |
| 19 | Madico | Protekt/PET/EVA | | | | | 18.72 |
| 20 | Madico | Protekt/PET/EVA | | | | | 18.72 |
| 21 | Krempel | PVF/AL/PET | | | | | 19.53 |
| 22 | Krempel | PVF/AL/PET | | | | | 19.29 |
| 23 | DNP Solar | ETFE / PET / Olefin | | | | | 18.51 |
| 24 | Dunsolar | Fluorinated Layer / PET / Primer | | | | | 21.14 |
| 25 | SFC | FPF/AL/PTI/Primer | | | | | 19.95 |
| 26 | Avery Dennison | FPF/PET/FPF | | | | | 19.53 |
| 27 | SFC | FPF/PTI/FPE | | | | | 19.74 |
| 28 | Dunsolar | PET / PET / Primer | | | | | 21.40 |
| 29 | Dunsolar | Primer / PET / Primer | | | | | 21.35 |
| 30 | Dunsolar | PVDF Film / PET / Primer | | | | | 21.14 |
| 31 | Krempel | PVDF/PET/PVDF | | | | | 19.53 |
| 32 | Madico | PVF/PET/EVA | | | | | 18.72 |
| 33 | Backfilm | PVF/PET/FPE | | | | | 19.74 |
| 34 | Coveme | PVF/PET/Primer | | | | | 19.49 |
| 35 | Filmcutter | SN/PET/SN | | | | | 19.74 |
| 36 | Isovolta | PA/PA/PA | | | | | 19.53 |
| 37 | Isovolta | PA/PET/PA | | | | | 19.29 |
| 38 | Isovolta | FPF/PET/PA | | | | | 18.29 |
| 39 | Isovolta | PVF/PET/PA | | | | | 18.29 |

PVF: poly vinyl fluoride

WPO: low - oligomer white polyester film

PTI: polyester film

ETFE: ethylene tetrafluoroethylene

PA: polyamide

Protekt: multi-layered laminate

FPF: fluoropolymer

PET: polyethylene terephthalate

SN: saturated nonwoven

PVDF: polyvinylidene fluoride

FPE: fluoropolyethylene resin

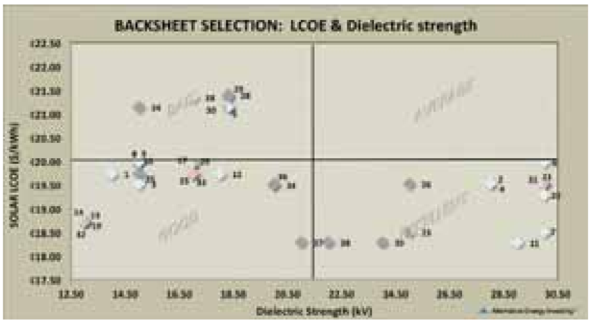


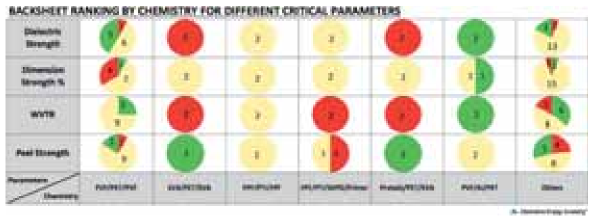


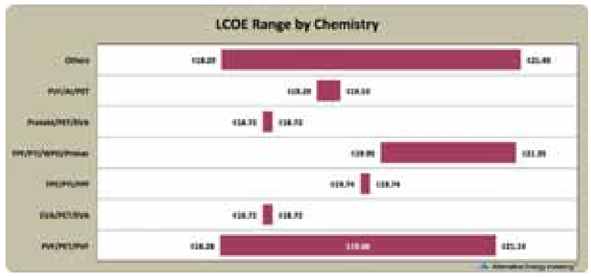


**Figure 9. Backsheet selection.**

> "The innovations discussed in this paper offer a way to bring the cost of modules down from the current $1.12/W level to $0.43/W by 2016."

## Conclusions

Now, more than ever, the industry must reduce the cost of everything, from upstream to downstream, to bridge the gap to achieving grid parity. Quality must also remain a critical component: there is nothing more harmful to the industry's potential than cutting corners and sacrificing quality. But these two requirements mean very little without profitable volume.

By taking a fresh look at which processes, as well as which technologies, show the most promise, a degree of cost reduction has been estimated for the industry in the near term that delivers on the three key mandates of cost, quality and profitability. PV demand is expected to soften before once again accelerating in the future. A widening gap between demand and supply is creating tremendous dislocations in the marketplace. On the basis of announced capacity expansion by major module makers, it is assumed that the gap could widen in the near future, resulting in additional price reductions. This increases the pressure on module makers to reduce the cost of production.

A number of innovative technological advancements that focus on cost reduction have been identified. The innovations discussed in this paper offer a way to bring the cost of modules down from the current $1.12/W level to $0.43/W by 2016. While many of these innovations may fail to transition into commercial production, those mentioned seem to be the most likely of the hundreds of others to be tested by the industry. Therefore, despite the risk of failure, they set the stage for c-Si module costs to reach a level that by any account opens natural markets for solar around the globe.

## About the Author

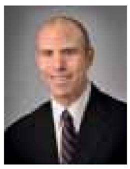

**Joseph Berwind** is a veteran researcher and consultant. As Managing Partner of AEI Research & Consulting, a company he founded in 2005, he has pioneered several industry-leading models for chemicals and materials used in photovoltaics, fabrication cost simulation, device demand, and volume, cost and price estimation. Joe has an MBA in finance from the Stern School of Business and a BA in economics from Columbia University.

## Enquiries

Joseph Berwind
Managing Partner
AEI Research & Consulting
Division of Alternative Energy Investing, LLC
343 Millburn Avenue, Suite 209
Millburn, NJ 07041
USA

Tel: +1 (973) 671 8191
Email: joe@aeiresearch.net
Website: http://aeiresearch.net

# Cz-Si wafers in solar cell production: Efficiency-limiting defects and material quality control

**Jonas Haunschild, Juliane Broisch, Isolde Reis** & **Stefan Rein**, Fraunhofer Institute for Solar Energy Systems (ISE), Freiburg, Germany

ABSTRACT
Most high-efficiency solar cells are fabricated from monocrystalline Czochralski silicon (Cz-Si) wafers because the material quality is higher than multicrystalline silicon (mc-Si) wafers. However, the material study presented in this paper reveals strong variations in the material quality of commercially available Cz-Si wafers, leading to a loss in solar cell efficiency of 4% absolute. The reason for this is the presence of defects, which appear as dark rings in photoluminescence (PL) images of the finished solar cells. It is shown that these efficiency-limiting defects originate from oxygen precipitation during emitter diffusion. It is demonstrated that an incoming inspection in the as-cut state is difficult, as strong ring structures in as-cut wafers turn out to originate most often from thermal donors. These are dissolved during high-temperature treatments and are therefore harmless, whereas moderate ring structures in the as-cut state may become severe. That is why critical wafers can be identified and sorted out reliably only after emitter diffusion, by using QSSPC-based lifetime measurements or PL imaging. The two-year statistics gathered from the research line at Fraunhofer ISE on the occurrence of ring defects in Cz-Si wafers indicate that ring defects are highly relevant in terms of material yield.

## Introduction

It was only six years ago that Fuyuki et al. [1] and Trupke et al. [2] proposed electro- and photoluminescence imaging (EL, PL) as characterization tools for solar cells and wafers. Since then, these techniques have become widely used. According to the yearly market survey by PHOTON [3], the number of companies selling EL tools is increasing and new companies are entering the market in the field of PL. Luminescence imaging owes its success to the fact that it is a very fast and non-destructive technique which allows electrical parameters to be characterized with high spatial resolution [4,5]. Defects do not appear as a single value, but as a pattern in the images. With knowledge of the specific pattern caused by a certain defect, the images can be interpreted in terms of physics, which allows a more precise quality and process control [6].

One of the most promising applications for PL imaging is the incoming quality control (IQC) of multicrystalline silicon (mc-Si) wafers in the as-cut state. In IQC all wafers whose mechanical or electrical quality is not sufficient for producing high-performance solar cells should be rejected or sorted into an adequate production process. However, in the as-cut state, bulk lifetime information is highly masked by surface recombination due to the saw damage of the wafers and is therefore almost invisible to state-of-the-art characterization tools. Approaches for overcoming this problem are currently being researched [7,8]. The limited lifetime information is also an issue for PL imaging, but fortunately most electrical defects formed during crystallization appear as very distinct patterns in PL images. By applying pattern recognition, it has been shown that open-circuit voltage, short-circuit current and efficiency can be predicted for a known solar cell process [9,10]. Current research aims at establishing a reliable wafer rating based on an automatic evaluation of PL images which can be acquired with high resolution at in-line speed.

In general, material quality of Czochralski-grown monocrystalline silicon (Cz-Si) is higher than that of multicrystalline silicon (mc-Si). That is why PL-based IQC has so far focused on mc-Si. However, recent studies have revealed that material quality in Cz-Si wafers may differ significantly as well [11,12]. Particularly when using Cz-Si wafers for high-efficiency solar cell concepts exceeding 20% efficiency, minor defects can already limit cell performance [13]. It has to be emphasized that the defects observed in these studies and discussed in this paper do not relate to the well-known metastable defect formed by boron–oxygen pairing (BO) [14,15], but rather to more severe background defects.

In a recent study [12,16] the varying impact of such oxygen-related defects on solar cell performance was evaluated and the possibility of detecting them by means of in-line measurements was investigated. The present paper gives an overview of these results and adds some new results from ongoing work. First, a short overview is given on oxygen-related defects, the material compilation underlying this study and the solar cell process applied. Before investigating the possibilities of detecting severe ring defects by different characterization techniques in different process steps, the impact of ring defects on the efficiency of finished solar cells will be demonstrated. Finally, new results concerning the identification of oxygen precipitates as the main defect are presented, together with data about the statistical relevance of these defects for the PV industry.

> "The most prominent defects are thermal donors, which strongly influence resistivity measurements, and the metastable boron–oxygen complex, which leads to light-induced degradation in the final solar cells."

## Oxygen-related defects in Cz-Si

Oxygen-related defects in Cz-Si have been characterized thoroughly for semiconductor devices [17,18]. The impact of these types of defect on solar cell performance is currently gaining in importance, as highly efficient solar cell concepts require materials of the highest

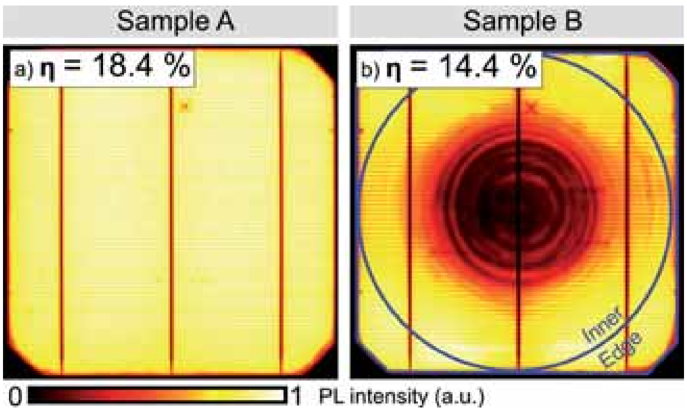


**Figure 1. PL images of two finished solar cells: (a) sample A, which yielded 18.4% efficiency, with no rings present; (b) sample B, which yielded only 14.4% efficiency, showing pronounced rings.**

quality. Typical oxygen concentrations in Cz-Si are of the order of $10^{17}$–$10^{18}$cm$^{-3}$. Oxygen enters into the silicon melt primarily by out-diffusion from the quartz crucible and is built into the silicon lattice during crystallization. Depending on temperature gradients and pulling speed during crystallization, interstitial- and vacancy-rich regions can form. These intrinsic defects have direct and different impacts on oxygen precipitation and the formation of oxygen defects [19]. The variety of these oxygen-related defects is wide and their influence on carrier lifetime varies. They can be activated and deactivated by high-temperature steps, depending on the plateau temperatures and the heating and cooling ramps of the high-temperature steps applied during solar cell processing. The most prominent defects are thermal donors [20,21], which strongly influence resistivity measurements, and the metastable boron–oxygen complex [14,15], which leads to light-induced degradation in the final solar cells.

In semiconductor technology, oxygen precipitation is another well-known effect [22,23]. If uncontrolled, precipitation may lead to severe defects which can cause failure of integrated circuits. However, by applying special thermal treatments during production, precipitate growth can be carefully controlled to take place only in the bulk, and impurities are gettered from the regions near the surface, thus increasing material quality in the so-called 'denuded zone.' In photovoltaics, however, both the bulk and the surface need to be free of precipitates. The formation of oxygen precipitates has only recently been observed with respect to solar cells [24], and has not yet been investigated in depth.

## Pre-characterization and solar cell processing

Definition of suitable IQC measures for Cz-Si first requires a representative picture of the defect classes present in Cz-Si. To obtain this, Cz-Si wafers were investigated from different crystal positions, manufacturers and crystallization processes within a broad material evaluation. Two hundred wafers with resistivities specified in the range 1–6Ωcm were grouped in different quality classes according to their appearance in the PL image taken in the as-cut state. Half of the wafers were fabricated into solar cells using a standard 156mm × 156mm solar cell process, which included alkaline texturing, two-sided emitter diffusion, phosphorus silicate glass etching, antireflection coating, screen-printing, fast firing and laser-edge isolation. The other half of the wafers, consisting of wafers adjacent to the processed wafers, were used for a more detailed characterization. Solar cells whose efficiency was limited by process-induced defects such as shunts or high series resistances were identified by applying thermographical measurements and quantitative PL imaging [25] and were excluded from the study in order to focus only on material-related issues.

PL imaging was performed on the setup build at Fraunhofer ISE, where a laser at 790nm irradiates the sample area with an illumination equivalent to up to two suns. The radiative band-to-band recombination of the excited charge carriers is detected by means of a Si-CCD camera with appropriate filters mounted in front of the camera lens to block reflected excitation light.

## Efficiency-limiting defects in Cz-Si solar cells

The results from *I-V* curve measurements reveal that the efficiency ranges from 14.4% up to 18.4% in the non-degraded state. PL images of a solar cell with a high efficiency and with a low efficency are shown in Fig. 1. As process-related problems can be excluded, efficiency is limited by the ring-like defect structure, which is highly recombination active and thus appears dark in the PL image of sample B in Fig. 1. The observed efficiency drop of 4% (absolute) can thus be attributed to poor material quality.

In order to find out if the differences in efficiency scale with the intensity of the rings visible in PL images, a simple metric – ring defect strength (RDS) – was set up in which the mean count rates of the edge region of the luminescence signal were divided by the mean count rates of the inner region under open-circuit conditions, as marked in Fig. 1(b). Both regions are symmetric with respect to the centre of the solar cells. The position of the circle was chosen to cover the largest extension of rings in this study and is applied to all solar cells. Note that this procedure is only feasible if the PL image is not completely covered by rings.

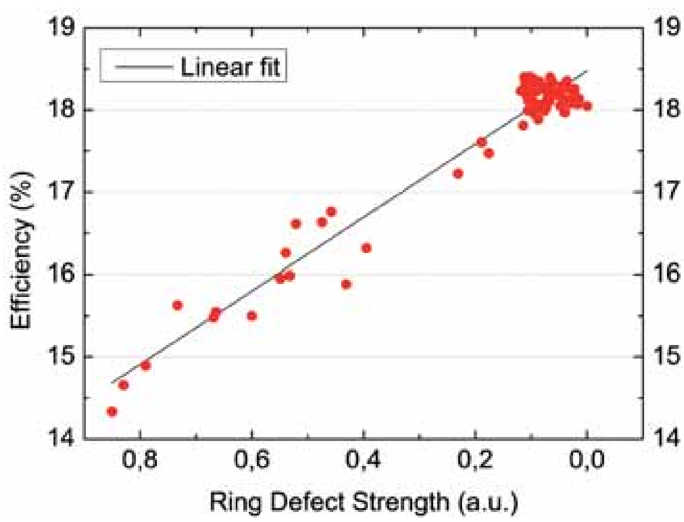


**Figure 2. Solar cell efficiency as a function of the ring defect strength (defined as the ratio of the average PL-intensities in the centre and the edge region shown in Fig. 1b) measured for finished Cz-Si solar cells.**

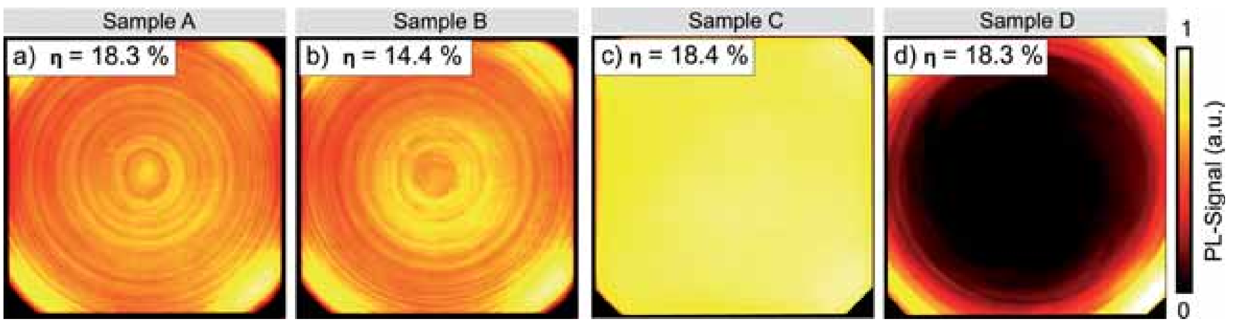


**Figure 3. PL images of Cz-Si as-cut wafers: a typical homogeneous image is shown in (c), while different kinds of ring patterns are shown in (a), (b) and (d). The rings are caused by lateral differences in lifetimes and doping levels. The efficiencies represent the values of the finished solar cells processed from these wafers.**

The ring defect strength is expressed as:

$$RDS = \frac{< I_{PL}(x,y) >|_{Edge}}{< I_{PL}(x,y) >|_{Inner}} \qquad (1)$$

Fig. 2 shows the correlation of RDS to the solar cell efficiency, with a correlation coefficient of $R^2 = 0.94$. The loss of efficiency in this batch can be therefore clearly attributed to material defects within the Cz-Si wafers which appear as concentric ring-like defect patterns in the PL images.

> "Strong material defects have been found in commercially available Cz wafers labelled as 'high quality.'"

It should be stressed that strong material defects have been found in commercially available Cz wafers labelled as 'high quality.' The difference in efficiencies of 4% absolute is not tolerable for industrial solar cell processing. High-efficiency solar cell concepts in particular can be expected to suffer even more if material quality limits the efficiency to below 15%. Now two questions arise:

1. Can these defects be detected in the early stages of production so that a reliable IQC can allow the wafers in question to be directly rejected?
2. What is their physical origin?

## Defect characteristics in different productions states

### As-cut characteristics

When characterizing Cz-Si wafers by PL, the resulting image is expected to look homogeneous, because no major material defects should be present. However, a random sampling from wafers from the storage at Fraunhofer ISE has revealed different kinds of ring- and swirl-structures. Four representative samples are presented in Fig. 3, along with their solar cell efficiencies. The images in Figs. 3(a) and 3(b) are the same samples as in Fig. 1 (but in the as-cut state here). Although the resulting efficiencies were quite different, both of these PL images show rings of medium intensity. Sample C in Fig. 3(c) looks homogeneous, as do most PL images of Cz-Si as-cut wafers, and resulted in a high efficiency. Fig. 3(d) shows bright edges, with the centre yielding almost no signal, but the finished solar cell surprisingly had a high efficiency.

All wafers in the batch can be sorted into one of four groups corresponding to the PL images in Fig. 3. Group A shows medium rings, resulting in high solar cell efficiency. Group B, also having medium rings but resulting in low efficiency, will be the main focus. Wafers from group C show no rings and result in high efficiency, while group D wafers have strong rings, but also result in highly efficient solar cells. It would be desirable to identify wafers with a material quality during incoming inspection that is too low (group B), in order to allow their direct rejection or their transfer to specially adjusted production lines. Fig. 3 demonstrates that this is not possible solely by PL imaging, as groups A and B yield the same ring pattern.

In Fig. 4(a), solar cell efficiency is plotted as a function of the effective charge carrier lifetime measured on the individual wafers in the as-cut state using the quasi-steady state photoconductance (QSSPC) technique. With the in-line setup used, the measurement is performed on a coil with a diameter of 55mm in the centre of the wafer, and the lifetime values are extracted at an injection density $\Delta n = 5\times10^{14}cm^{-3}$. The four wafer groups A–D are marked on the graph. For groups A and C, with as-cut lifetimes in the range of 0.7µs, the small differences in carrier lifetime do not correlate to small differences in cell

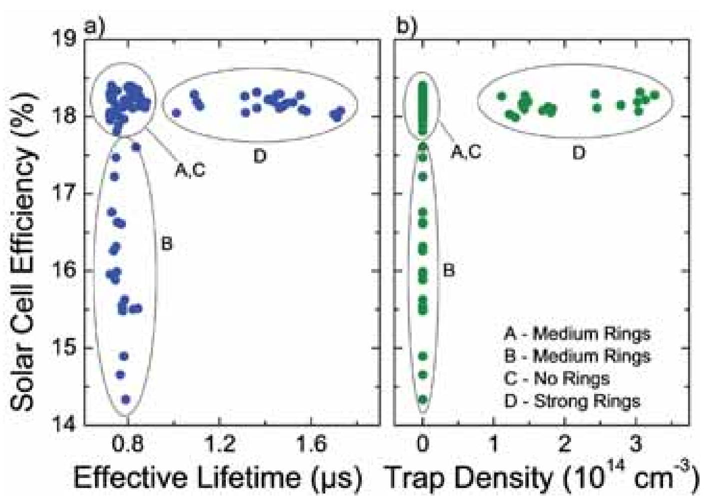


**Figure 4. (a) Solar cell efficiency as a function of effective carrier lifetime, measured by means of QSSPC on the as-cut wafers; (b) cell efficiency as a function of trap density. Lifetime is limited by surface recombination and increased by charge carrier trapping, which may be corrected.**

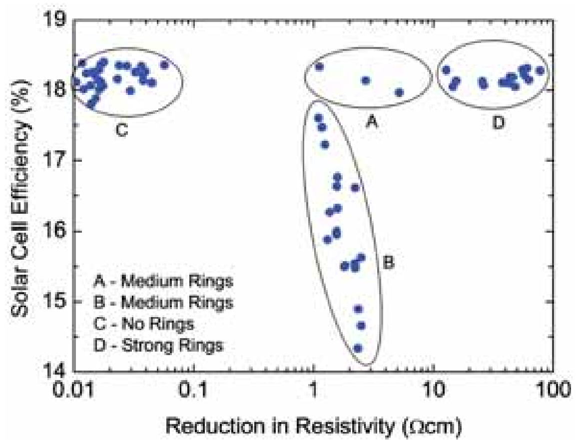


**Figure 5. Reduction in resistivity after annealing plotted against solar cell efficiency. Wafers from group C show the noise of the measurement, while resistivities of groups A, B and D are reduced by more than 1Ωcm.**

efficiency. In this case the lifetime of the finished cell is obviously high enough to reach the efficiency limit of the process. For group B, with as-cut lifetimes in the same range, cell efficiencies vary significantly, from 14.4% to 17.6%, which is not reflected in the lifetimes in the as-cut state. Group D wafers, with high as-cut lifetimes above 1.0µs, did not result in higher efficiencies.

In Fig. 4(b) trap density, extracted according to Sinton et al. [8], shows that the lifetime values of group D are increased by trapping artefacts, which cannot be completely removed despite a trapping correction, while wafers from groups A–C are not affected by trapping.

As in the case of PL imaging, lifetime measurements and the investigation of trap density do not allow a distinction to be made between groups A and B. This inability to distinguish between the groups is a result of either the surface limitation of carrier lifetime or a defect activation at a later process stage. If this is the case, the harmful effect from group B wafers may not be detected unambiguously in the as-cut state. Further research is required in this area.

## Check for thermal donors

An in-line measurement of the base resistance yields values between 1.19 and 82.7Ωcm, which falls outside the material specification (1–6Ωcm). Increased and inhomogeneous resistance values of as-cut wafers are (in most cases) caused by the well-known thermal donor (TD) defect. TDs can be destroyed in a high-temperature step (e.g. emitter diffusion) and should have no effect on final solar cell results.

The results of an in-line test before and after a thermal treatment, performed in an in-line furnace with a peak temperature of 800°C for 10 seconds, are plotted in Fig. 5. After the treatment, all TDs had dissolved and resistivity for all tested wafers was in the expected range. The graph shows the absolute reduction in resistivity after annealing plotted against the solar cell efficiency. If no rings in the PL images are present (group C), the resistivity of the wafers does not change significantly, whereas the change for wafers from groups A and B is of the order of 1–10Ωcm; for group D the difference is greater than 10Ωcm. Therefore, we can conclude that Groups A and B have weak TDs, group C has no TDs and group D has strong TDs.

Although groups A and B cannot be distinguished by their changes in resistivity, the rings in the PL images of group A vanish, while they get stronger for group B. The same effect occurs after emitter diffusion and is discussed in the following section.

## Characterization after emitter diffusion

Fig. 6 shows the PL images of the wafers from Fig. 3 in the as-cut state and the same wafers after emitter diffusion. Wafers from group A give homogeneous PL images, leading to the conclusion that the

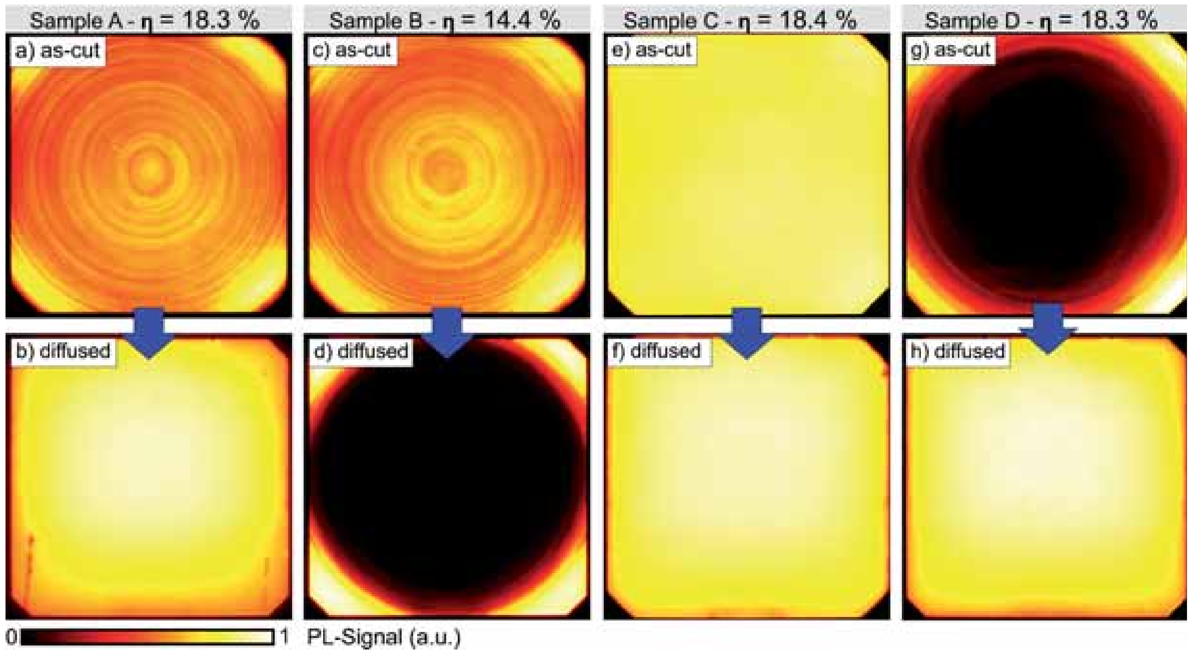


Figure 6. PL images of the as-cut wafers (the same ones as in Fig. 3) are displayed in the top row and PL images of the same wafers after emitter diffusion are displayed underneath. Whereas the rings vanish for samples A and D, they become stronger for sample B.

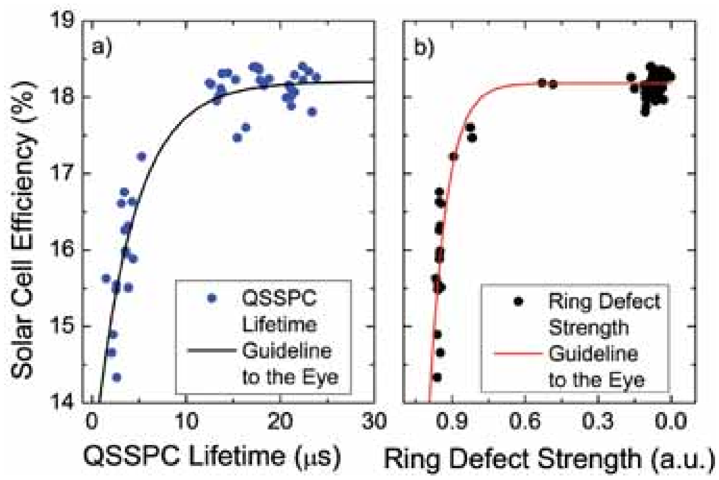


Figure 7. Solar cell efficiency plotted against (a) QSSPC lifetime, and (b) PL RDS, both measured after emitter diffusion. Wafers resulting in low efficiency can be identified reliably using both methods.

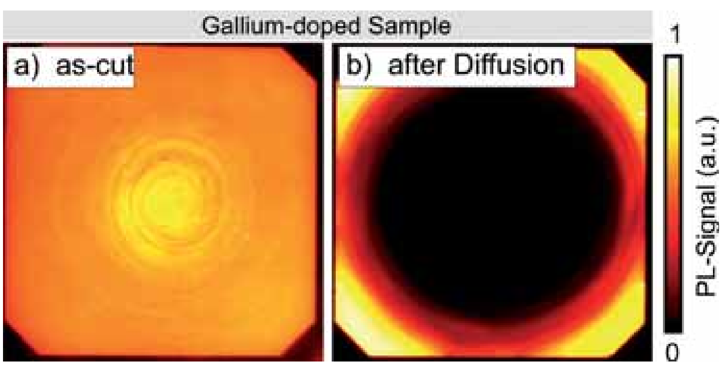


Figure 8. PL images of a Ga-doped Si wafer: (a) in the as-cut state; (b) after emitter diffusion.

ring effect in the as-cut state was caused by weak TDs. Wafers from group B, however, give a PL image with a dark centre of low lifetime. In addition to weak TDs, a more severe background defect must be present, which is activated during high-temperature processing. Group C wafers show no change, while the very dark rings of group D vanish. Pronounced rings in PL images of as-cut wafers can therefore be attributed to strong but harmless TDs.

Fig. 7 shows the solar cell efficiencies plotted as a function of the effective lifetime obtained from in-line QSSPC (Fig. 7a), and as a function of the ring defect strength extracted from PL images (Fig. 7b), both quantities measured after emitter diffusion. While low efficiencies can obviously be attributed to low carrier lifetimes, above approximately 20μs the cell efficiency is limited by the solar cell process. The PL RDS evaluation yields similar results and confirms that the low lifetimes originate from ring features. Therefore, both methods can be used for rating a wafer after emitter diffusion.

## Dopant dependency

In addition to the investigation of the boron-doped samples, a group of gallium-doped silicon wafers was analysed. As shown in Fig. 8(a), ring patterns were found in the PL images of the as-cut wafers during incoming inspection. After emitter diffusion (Fig. 8b), a circular low-lifetime region forms around the centre: it covers almost the entire wafer and resembles the defect structures observed in sample B of the boron-doped silicon (see Fig. 6d). The fact that the same defect structures are

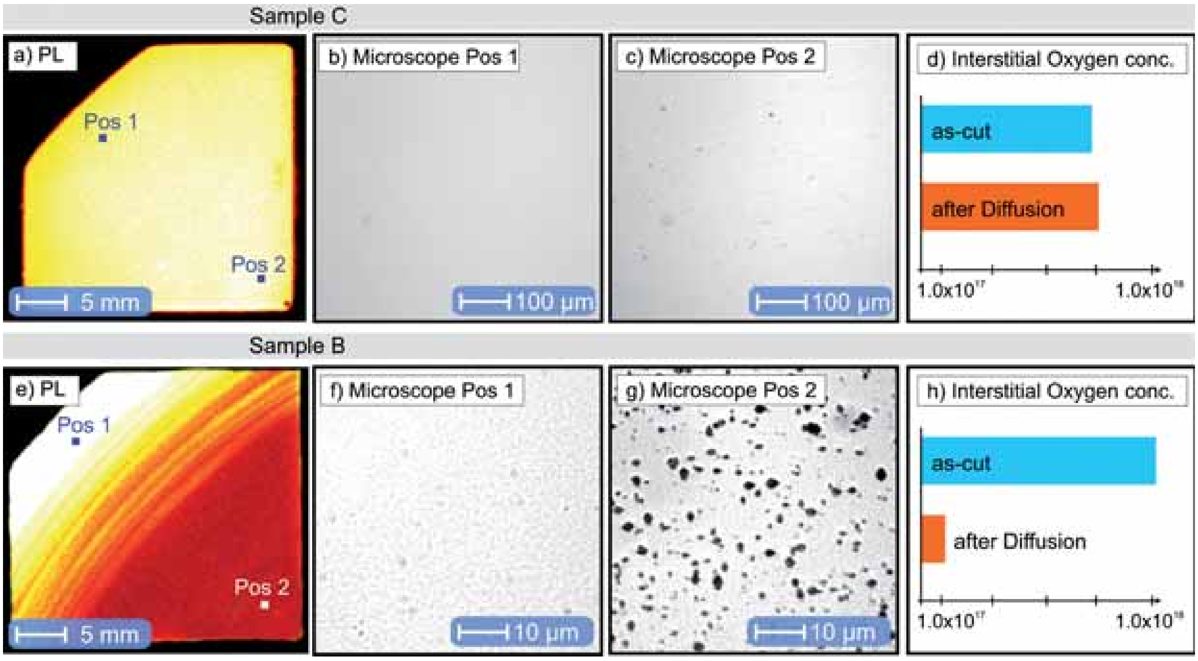


**Figure 9. (a) PL image of sample C after preferential etching; (b,c) optical microscope pictures of the marked positions – no precipitates can be observed; (d) interstitial oxygen concentration of neighbouring samples of sample C; (e) PL image of sample B after preferential etching; (f,g) optical microscope pictures of the marked positions – the darker the PL image, the higher the density of precipitates; (h) interstitial oxygen concentration of neighbouring samples of sample B.**

found in both gallium-doped and boron-doped silicon indicates that the formation of the observed severe ring defects is independent of the dopant, and is induced by more intrinsic effects such as oxygen precipitation after high-temperature treatments. Oxygen precipitates grow independently of the wafers' doping during high-temperature processing steps. That is why the observed phenomenon seems to be relevant for all Cz-Si materials.

> "Oxygen precipitates grow independently of the wafers' doping during high-temperature processing steps."

### Defect characterization

To shed some light on the physical origin of the observed defect structures, a more detailed defect characterization was performed on adjacent wafers for selected material types. By using Fourier transform infrared (FTIR) spectroscopy, the interstitial oxygen content of neighbouring samples was measured in the as-cut state and after emitter diffusion. For wafers similar to sample C (without rings), the interstitial oxygen concentrations were measured to be $[O_i]=7\times10^{17}cm^{-3}$ in both states; for wafers similar to sample B (with rings), the concentrations changed from $[O_i]=1\times10^{18}cm^{-3}$ in the as-cut state to $[O_i]=1\times10^{17}cm^{-3}$ after emitter diffusion (see Figs. 9d and 9h). For the sample with ring defects, the fact that the interstitial oxygen concentration is reduced during solar cell processing indicates that more oxygen precipitates are formed, which cannot be measured by means of an FTIR analysis.

In order to prove the presence of oxygen precipitates, the samples were polished and wet-chemically etched using the Sirtl etch [26]. Fig. 9(a) shows the PL image of sample C; the microscope pictures of small areas of the same sample can be seen in Figs. 9(b) and 9(c). Apart from dust particles and a scratch, no precipitates are present. Fig. 9(e) shows the PL image of sample B with ring defects. For this sample, the images of the optical microscope (Figs. 9f and 9g) reveal that in the outer region of the wafer, with high PL signal, no precipitates are present, while in the inner region, with low PL signal, lots of precipitates can be found. Therefore, the drop in lifetime and efficiency of group B can be attributed to the presence of oxygen precipitates.

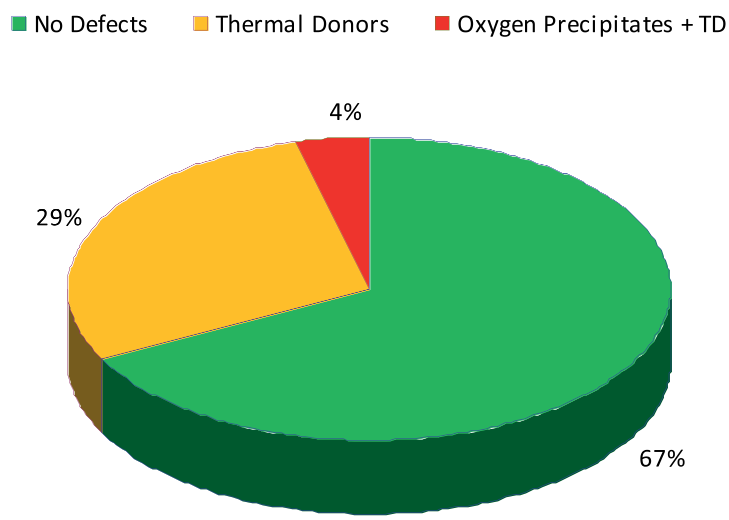


**Figure 10. Statistics of the defects in commercially available Cz-Si wafers used at Fraunhofer ISE since 2010. The classification is based on PL imaging performed on random samples of all incoming wafers. Only two-thirds of the Cz-Si wafers are defect free; 29% exhibit thermal donors and 4% severe oxygen precipitates.**

## Statistical evaluation

In order to estimate, in a more quantitative way, the practical relevance of the defect classes discussed above, the IQC results obtained at Fraunhofer ISE were evaluated statistically. Since September 2010 all incoming Cz-Si wafers have had to pass the IQC based on PL imaging. Between 1 and 5% of the samples are selected randomly from each wafer box, and PL measurements are carried out. Our statistics are currently based on PL measurements of 1529 wafers, representing approximately 40,000 wafers.

Fig. 10 shows that ring structures were found in 33% of the investigated Cz-Si samples. Most of these ring structures could be identified as being related to harmless thermal donors, which vanish after high-temperature treatments. However, in 4% of the samples with ring structures in the as-cut state, the critical lifetime-limiting ring defects could be activated. These particular samples cannot be used for solar cell production, as the oxygen precipitates limit the solar cell efficiency to a low level. Although these statistics do not claim to be representative or precise, they strongly suggest that the observed phenomenon is highly relevant in terms of material yield.

## Conclusion

This study has shown that commercially available Cz-Si materials labelled as 'high quality' may be affected by oxygen precipitates, which may reduce solar cell efficiency by 4% (absolute). Nucleation centres for oxygen precipitates have already been formed during crystallization; they strongly depend on the temperature cycles applied and may grow during high-temperature steps in the solar cell process, irrespective of the wafer doping. The critical defects appear throughout the production process as dark concentric rings in PL images.

Detection of oxygen precipitates in the as-cut state during incoming inspection is rather difficult, as the presence of harmless thermal donors can form similar patterns. Up till now, wafers that form efficiency-limiting oxygen precipitates during emitter diffusion could be detected with PL imaging in incoming inspections only if the presence of thermal donors could be excluded. If thermal donors cannot be excluded, reliable quality control after emitter diffusion is only possible using lifetime measurements or PL imaging.

Use of these results has allowed an incoming quality control based on PL imaging to be developed and introduced in the PV-TEC research line at Fraunhofer ISE. Two years of statistics have revealed that approximately 33% of all Cz-Si wafers show ring defects caused by thermal donors, and 4% form critical defects related to oxygen precipitates, demonstrating the relevance of the phenomenon in terms of material yield.

## Acknowledgements

We thank our colleagues at Fraunhofer ISE for their fruitful discussions and support in solar cell processing. This work was partially supported by the Fraunhofer Society under the framework of the ABICS-LUM project.

## References

[1] Fuyuki, T. et al. 2005, "Photographic surveying of minority carrier diffusion length in polycrystalline silicon solar cells by electroluminescence", *Appl. Phys. Lett.*, Vol. 86, p. 262108/1.

[2] Trupke, T. et al. 2006, "Photoluminescence imaging of silicon wafers", *Appl. Phys. Lett.,* Vol. 89, p. 44107.

[3] Chunduri, S.K. 2011, "Making the invisible visible: A market survey on luminescence imaging systems and cameras", *Photon Inter.* (January), p. 158.

[4] Nagel, H. 2010, "Luminescence imaging – A key metrology for crystalline silicon PV", *Proc. 12th Worksh. Cryst. Si. Sol. Cell Mater. & Process.*, Breckenridge, Colorado, USA, p. 40.

[5] Trupke, T., Nyhus, J. & Haunschild, J. 2011, "Luminescence imaging for inline characterisation in silicon photovoltaics", *physica status solidi (RRL)*, Vol. 5, p. 131.

[6] Haunschild, J. et al. 2010, "Quality control of as-cut multicrystalline silicon wafers using photoluminescence imaging for solar cell production", *Solar Energy Mater. & Solar Cells*, Vol. 94, p. 2007.

[7] Bothe, K. et al. 2010, "Determining the bulk lifetime of unpassivated multicrystalline silicon wafers", *Proc. 25th EU PVSEC*, Valencia, Spain, p. 204.

[8] Sinton, R. et al. 2010, "The effects of sub-bandgap light on QSSPC measurement of lifetime and trap density: What is the cause of trapping?", *Proc. 25th EU PVSEC*, Valencia, Spain, p. 1073.

[9] McMillan, W., Trupke, T. & Weber, J.W. 2010, "In-line monitoring of electrical wafer quality using photoluminescence imaging", *Proc. 25th EU PVSEC*, Valencia, Spain, p. 1346.

[10] Demant, M. et al. 2010, "Analysis of luminescence images applying pattern recognition techniques", *Proc. 25th EU PVSEC*, Valencia, Spain, p. 1078.

[11] Lawerenz, A. et al. 2010, "Photoluminescence lifetime imaging using LED arrays as excitation source", *Proc. 25th EU PVSEC*, Valencia, Spain, p. 2486.

[12] Haunschild, J. et al. 2011, "Detecting efficiency-limiting defects in Czochralski-grown silicon wafers in solar cell production using photoluminescence imaging", *physica status solidi (RRL)*, Vol. 5, p. 199.

[13] Cousins, P.J. et al. 2010, "Generation 3: Improved performance at lower cost", *Proc. 35th IEEE PVSC*, Honolulu, Hawaii, USA, p. 000275.

[14] Rein, S. et al. 2001, "Electrical and thermal properties of the metastable defect in boron-doped Czochralski silicon (Cz-Si)", *Proc. 17th EU PVSEC*, Munich, Germany, p. 1555.

[15] Schmidt, J. & Bothe, K. 2004, "Structure and transformation of the metastable boron- and oxygen-related defect center in crystalline silicon", *Physical Review B*, Vol. 69, p. 0241071.

[16] Haunschild, J. et al. 2011, "Quality control of Czochralski grown silicon wafers in solar cell production using photoluminescence imaging", *Proc. 26th EU PVSEC*, Hamburg, Germany, p. 1025.

[17] Marsden, K. et al. 1996, "Determination of the criteria for nucleation of ring-OSF from small as-grown precipitates in Cz-Si crsytals", *Mater. Sci. & Eng. B*, Vol. 36, p. 16.

[18] Porrini, M. et al. 2000, "Influence of Czochralski silicon crystal growth on wafer quality: An extensive investigation using traditional and new characterization techniques", *Mater. Sci. & Eng. B*, Vol. 37, p. 139.

[19] Voronkov, V.V. & Falster, R. 1999, "Grown-in microdefects, residual vacancies and oxygen precipitation bands in Czochralski silicon", *J. Cryst. Growth*, Vol. 204, p. 462.

[20] Meilwes, N. et al. 1994, "Thermal donors in silicon: An investigation of their structure with electron nuclear double resonance", *Semicond. Sci. Technol.*, Vol. 9, p. 1623.

[21] Wagner, P. & Hage, J. 1989, "Thermal double donors in silicon", *Appl. Phys. A*, Vol. 49, p. 123.

[22] De Kock, A.J.R., Roksnoer, P.J. & Boonen, P.G.T. 1975, "Formation and elimination of growth striations in dislocation-free silicon crystals", *J. Cryst. Growth*, Vol. 28, p. 125.

[23] Föll, H. 1975, "Formation and nature of swirl defects in silicon", *Appl. Phys. A*, Vol. 8, p. 319.

[24] Chen, L. et al. 2011, "Effect of oxygen precipitation on the performance of Czochralski silicon solar cells", *Solar Energy Mater. & Solar Cells*, Vol. 95, p. 3148.

[25] Glatthaar, M. et al. 2010, "Spatially resolved determination of dark saturation current and series resistance of silicon solar cells", *physica status solidi (RRL)*, Vol. 4, p. 13.

[26] Sirtl, E. & Adler, A. 1961, "Chromsäure-Flußsäure als spezifisches System zur Ätzgrubenentwicklung auf Silizium", *Z. Metallkde.*, Vol. 52, p. 529.

## About the Authors

**Jonas Haunschild** leads the luminescence imaging team at Fraunhofer ISE. He studied physics at the Philipp University of Marburg and received his diploma degree in 2007. He has been with ISE since 2008 and recently completed his Ph.D. on luminescence-based methods for quality control in industrial solar cell production.

**Juliane Broisch** is a Ph.D. student in the in-line measurement techniques and quality assurance group at Fraunhofer ISE. She studied physics at the Albert Ludwig University of Freiburg and received her diploma degree in 2010.

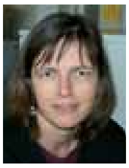

**Isolde E. Reis** is a member of the luminescence imaging team at Fraunhofer ISE. She received her diploma degree in 1984 in crystallography from the Albert Ludwig University of Freiburg, and was awarded a Ph.D. in 1988 for her work on the recrystallization of polycrystalline Si layers.

**Stefan Rein** is the head of the in-line measurement techniques and quality assurance group at Fraunhofer ISE, which focuses on metrology, production control, solar cell simulation and new silicon materials. He received his diploma degree in physics in 1998 from the Albert Ludwig University of Freiburg, and his Ph.D. degree in 2004 for work carried out at Fraunhofer ISE on lifetime spectroscopy for defect characterization of silicon for photovoltaic applications.

## Enquiries

Fraunhofer Institute for Solar Energy Systems (ISE)
Department PV Production Technology and Quality Assurance (PTQ)
Emmy-Noether-Straße 2
79110 Freiburg
Germany

Tel: +49 (0) 761 4588 5563
Fax: +49 (0) 761 4588 9250
Email: Jonas.Haunschild@ise.fraunhofer.de

# Diamond wire sawing: State of the art and perspectives

**Fabrice Coustier** & **Jean-Daniel Penot**, CEA-INES, LMPS, Le Bourget-du-Lac, & **Gérald Sanchez** & **Michel Ly**, Thermocompact, Pringy, France

ABSTRACT
The purpose of this paper is to give an overview of the use and potential of diamond wire for the silicon-shaping process in the PV industry. The current market and future prospects for helping to meet the goals of 2020's roadmap of thinner wafers and reduced $/W are described.

## Introduction

In PV silicon wafer production, a silicon ingot is transformed into wafers by means of three successive sawing stages: squaring, cropping and wafering (see Fig. 1). The first stage consists of cutting a crystallized silicon ingot into several bricks (generally 156mm × 156mm × 250mm). During that step, the external slabs which are contaminated by the crucible and the coating of the crucible are also removed. A few centimetres of silicon are then taken off the top and bottom of these bricks by the cropping operation in order to eliminate the lowest purity silicon. Finally, wafers are obtained from the slicing operation (also called wafering) of the cropped brick by using multiple loops of a single wire.

The actual PV silicon-shaping market consists mainly of an optimized slurry-based process that started about 30 years ago, when multi-wire saws slowly began to replace inner diameter (ID) saws in the industry, and at which time wafer thicknessess went below 500µm. This sawing process consists of the association/coupling of a thin steel wire and a slurry composed of a mixture of micrometre-sized abrasive grains (typically 10µm) and a lubricant fluid. The lubricant fluid was initially made of mineral oil, but nowadays polyethylene glycol (PEG) is used. A slurry layer of 15–20µm is carried by the wire, which is slowly pushed through the silicon bricks. The multiple indentations of the abrasive grains (generally SiC) on the material create a sawing effect by abrasive wear. In the slicing equipment, the 130µm-diameter steel wire is wound around polyurethane wire-guides with a typical groove pitch of 340µm, therefore currently producing 180µm-thick wafers.

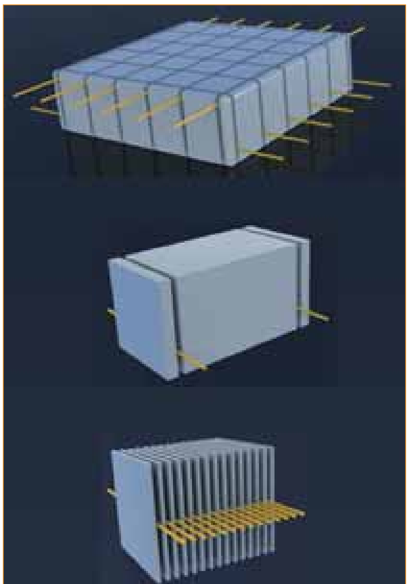

Figure 1. Successive cutting stages of the silicon (top down): squaring, cropping and wafering.

If this slurry-based technology is now well proven, its potential improvements tend to be limited. The wafer production cost reduction, which needs to be significant in the coming years, will probably be achieved by the arrival of a disruptive technology. Recently, the possible use of diamond wire created a lot of buzz with the promise of a satisfactory compromise between cost and performance, since, for example, the cutting speed is at least twice that of the steel wire and conventional slurry solution. Such wire has already been used by early supporters, mainly on squarers, as the necessary length of wire used during a cut does not exceed 500m and the associated risk of breaking it does not incur too great a financial loss.

> "Cutting with diamond wire is not an easy task and a lot of obstacles have to be overcome before this technology is widely accepted"

Nevertheless, cutting with diamond wire is not an easy task and a lot of obstacles have to be overcome before this technology is widely accepted. A change in silicon sawing technology appears to be imminent, so the purpose of this work is to give an overview of the silicon-shaping activity in the PV industry. The focus will be on the development of diamond wire technology potential and will take into account recent developments such as the crystallization of mono-like ingots.

## Advantages, challenges and roadmap

In the wafering operation, because the price of diamond wire per km is more than a hundred times more expensive than steel wire, a wire break can compromise the cost of ownership (COO) of the whole slicing operation and diamond wire adoption. On the other hand, as the volume of production of diamond wire increases, and other industries such as sapphire for LED applications and PV squaring operations with diamond wire ramp up, the price of diamond wire will consistently go down. In addition, any other improvement of the COO is always welcome for promoting quick adoption. For example, recycling a part or the totality of silicon kerf obtained during diamond wire slicing of silicon could dramatically change the picture.

Since more than 40% of the total cost of a finished module is the cost of the wafer itself [1], a substantial amount of money can be saved on PV systems by optimizing the wafering process. For several reasons, indications are that without the arrival of a disruptive technology such as diamond wire this will not be possible on the scale that groups of industrials (e.g. SEMI PV Group) have planned for the horizon of 2020 [2].

The first – and probably most important – expense item to reduce is the amount of silicon used per wafer. That is why one of the PV market goals is to slowly but surely reduce the wafer thickness as well as the kerf loss over time (silicon wasted during cutting). ITRPV Roadmap wafers [2] shows that in order to get to the $1/W grid parity goal in 2020, the wafer thickness should be reduced from 180µm to 100µm, and the kerf loss of currently 150–160µm should also be reduced to about 100µm (see Fig. 2).

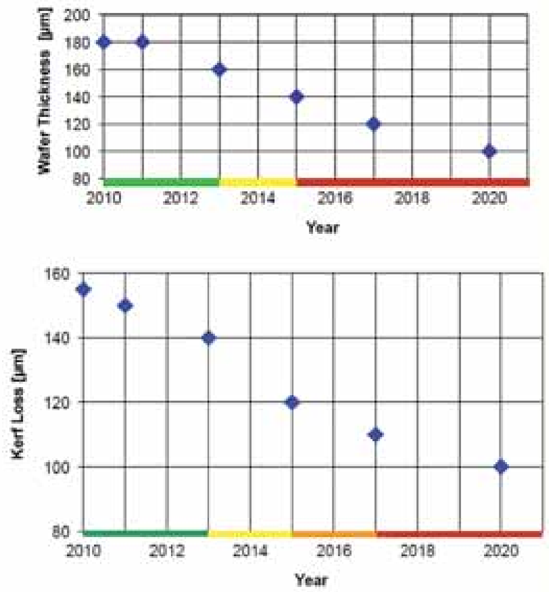


Figure 2. Roadmap of wafer thickness and kerf loss reduction.

*Credit: Images reproduced with permission from the ITRPV Roadmap [2].*

Today, world leaders in wafering technology use about 100m of 120µm (or 130µm) steel wire in order to obtain a single wafer. Almost no diameter reduction is observed during cutting (only 2–3µm) since the wire acts only as the carrier of the slurry which does the actual cutting. Nevertheless it is still a challenge for the wire to undergo further reductions in diameter without the risk of compromising the cut when 3000 to 5000 wafers are cut at a time. As regards kerf loss, a reduction to 100µm would necessitate wire of diameter 75 to 80µm that is capable of cutting more than 5000 to 8500 wafers of thickness 100µm on equipment similar to today's. Once again, that does not seem to be achievable without major changes. This is why all the interest in diamond wire has arisen and appears to make sense.

With 60% of the wafering market being for multicrystalline silicon wafers [3], which corresponds to 70% of the crystalline market, the production cost of a single wafer is pretty much as low as it can get, especially with the current downturn in the economy that has created stockpiles of consumables which in turn has led to suppliers decreasing their selling price dramatically. Today's total available market (TAM) for consumables for the squaring operation is around $7 million, and around $800 million for the whole wafering operation (discussed later). Taking into account that the individual costs for the steel wire, SiC, PEG, recycling operation of slurry and all surrounding consumables for the wafering operation have all been largely optimized, and independent of the equipment used, the cutting operation costs around $0.5 per wafer as shown in Fig. 3. That is the reason why opportunities to economize significantly on the current cost of slurry process consumables seem to be limited.

On the other hand, assuming that the use of diamond wire allows cutting at twice the speed of the slurry process on the same or equivalent equipment cost basis as today, the corresponding part of the capex will decrease proportionally. Additionally, even though today the cost of the slurry and diamond processes might

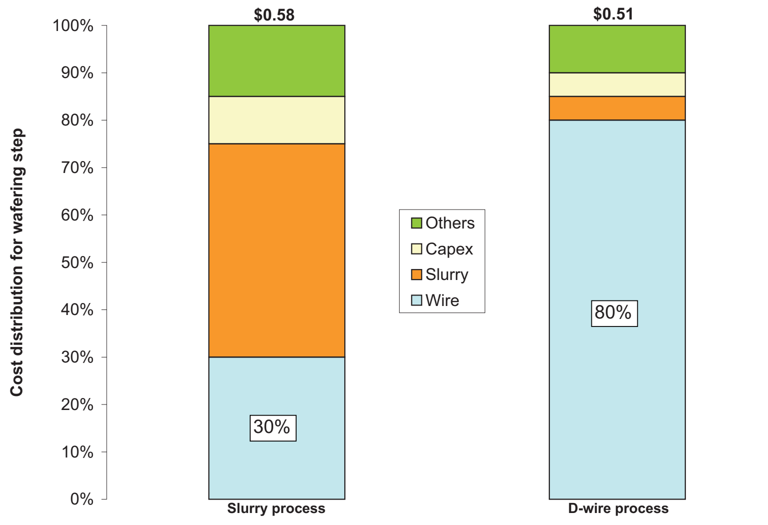


Figure 3. Cost distribution for the wafering step.

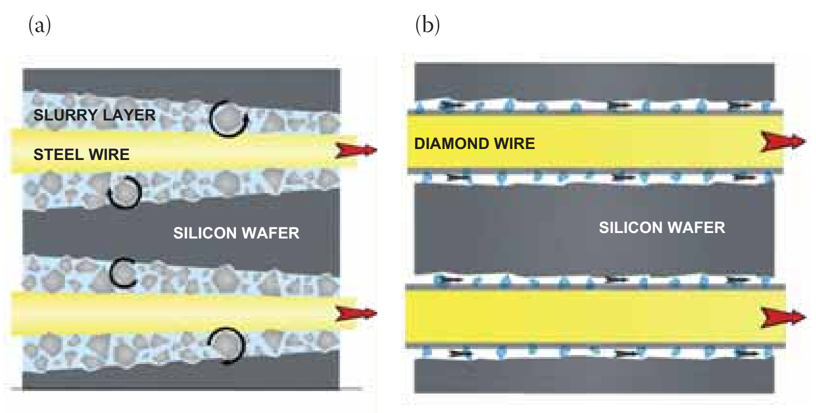


Figure 4. Wafer sawing process with (a) slurry and (b) diamond.

be comparable when in competition with each other, the removal of slurry preparation and recycling while moving towards diamond wire will eventually reduce the cost of the overall slicing operation as the cost of diamond wire falls. Moreover, as shown in Fig. 4, the better total thickness variation (TTV) observed using diamond wire will definitely be needed when the wafer thicknesses approach 100µm. Despite all of its advantages, diamond wire sawing is not without complications; the process will be discussed next.

## Towards diamond wire

Diamond wire has long been used for cutting hard substances such as sapphire, SiC and other materials and has proved to perform better than slurry (by cutting twice as fast) and to be cost effective once the process has been optimized. But cutting multicrystalline silicon is not the same as cutting hard, homogeneous, single crystals such as the ones just mentioned above. In fact, the first tests in late 1990 and early 2000 of cutting silicon ingots using the same diamond wire used in the sapphire industry were a disaster: the steel wire surface entirely covered with diamonds quickly became clogged by silicon kerf and did not cut anymore, and consequently rapidly led to wire breakage. Today's diamond wires sold for the PV industry no longer have their entire surface covered with diamonds (< 10% coverage), and the cleaning of the diamond wire is essential for maintaining its cutting effectiveness and ensuring a satisfactory lifetime.

For several years, companies such as Diamond Wire Technology have sold equipment that is capable of cutting silicon rods for use as seeds in Siemens reactors, and many companies today offer the possibility of cutting silicon ingots or supply silicon cropping equipment using diamond wire. The leading equipment manufacturers all have squaring equipment for Gen 5 ingots that today is able to cut with diamond wire. But with the arrival of 350µm-diameter structured wire on slurry squarers that can achieve cutting speeds of up to 2mm/minute, the difference in COO in favour of diamond wire that appeared obvious when the 'traditional' 250µm structured wire used for years was cutting at 1mm/minute maximum is not so obvious anymore. The difference between squaring and cropping of the ingots vs. wafering also needs to be made clear. For wafering, kerf loss is critical, but for cropping and squaring, it is not so much of an issue. It is certain that in the coming years all new PV fabs will go with diamond wire squarers, even if the wire diameter is a bit larger than today, simply for the amazing potential for high cutting speeds and for avoiding the hassle of slurry preparation.

Regarding the wafering operation with diamond wire, everyone is now becoming curious to know whether or not it will slowly replace its longtime competitor – steel wire and slurry – and if so, when that will happen. Apart from silicon not being as high on the hardness scale as sapphire and SiC (materials traditionally cut with diamond wire), monocrystalline ingots with only one crystal orientation are fairly similar to those materials in terms of cutting properties. As a matter of fact, almost the whole Japanese market for monocrystalline cells now uses wafers that have been cut with diamond wire. Furthermore, during the 2011 PVSEC conference, Norsun announced that it was in the process of switching its whole

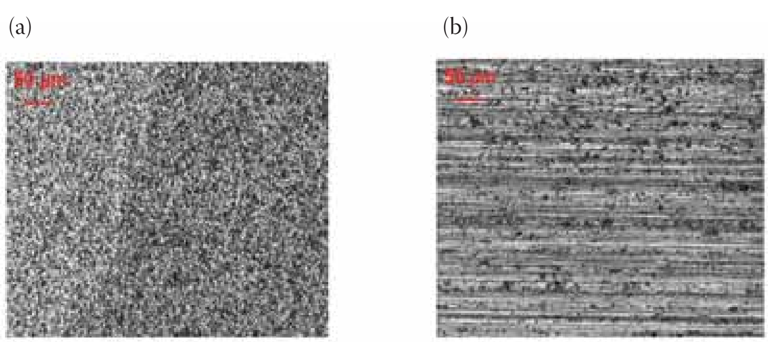


Figure 5. As-cut wafer surface with (a) slurry process, and (b) diamond process.

| | Diamond wire process | |
|---|---|---|
| | Pluses | Minuses |
| Wire | Price: potential to decrease (by 2 or 3) is high<br>Diameter: high reduction potential | Price: currently high (~$150-200/km)<br>Very few manufacturers of good-quality wire |
| Cutting performance | Twice as fast<br>Better TTV<br>Increased productivity | Difficulties in cutting mc-Si (heterogeneous)<br>Vibrations management<br>Wire breakage risk |
| Water-based coolant | Ease of use<br>Cheaper<br>Opens possibilities for recycling kerf<br>Cooling properties | Silicon deposit on equipment<br>Reaction of Si with water: H2 risk<br>Vibrations management |
| PEG-based coolant | Dampening effect of PEG on vibrations<br>Recycling of PEG already exists | Price<br>Need to remove PEG to recycle kerf |
| Equipment | Initial capex reduction (by ~2)<br>Potential reduction in the size of equipment<br>Cooling power much lower than with slurry<br>Less power required to drive wire<br>Reduction in price of equipment | New equipment needed<br>or retrofitting of existing equipment |
| Consumables | Reduction in quantity of consumables | Long-term contracts for SiC recycling will delay adoption<br>Wire: the strategic consumable |
| Conclusion | Thinner wafers with better TTV<br>Maturing market should reduce COO over years | |

**Table 1. Summary of the pluses and minuses of the diamond wire process.**

plant of monocrystalline wafers to using diamond wire technology.

Cutting multicrystalline silicon wafers with diamond wire, however, is a challenge. The inhomogeneity of the material, the different orientation of the grains and the precipitates located in the grain boundaries make it a lot more difficult to cut than monocrystalline silicon. That does not mean it is impossible, but today's industry leaders in equipment and diamond wire technology have announced that twice as much wire is necessary for cutting a multicrystalline wafer as a monocrystalline wafer (about 2m per wafer instead of 1m), without a guarantee that in the long term the COO will be much better in the event of too many wire breakages.

## Mechanisms during cutting and their consequences on as-cut wafers

In both the slurry and the diamond methods, the wire sawing effect is due to the physical phenomenon of abrasive wear during the sliding of one body on another. Nevertheless, two radically different mechanisms of abrasion can be distinguished as shown in Fig. 4.

Sawing with slurry involves free abrasive particles capable of having distinct movements from those of either the wire or the silicon. It has been precisely described in the past that the so-called three-body abrasion mode involved in slurry sawing embraces the fact that the role of the steel wire is only to carry the slurry to the silicon. The abrasion itself is done by multiple indentations of SiC grains on the surface of the silicon [4]. On the other hand, in diamond sawing the abrasive diamond particles stuck to the wire realize a two-body abrasion which can be represented by multiple scratches. This mechanical difference between free and bind abrasive particles has an impact on the wafer or surface created by sawing.

> "The total thickness variation (TTV) of wafers cut with diamond wire is better than with slurry and ranges from approximately 7 to 15μm."

A first difference concerns the wafer thickness shape. Since everyone in the industry is now cutting in a one-way mode in which the wire is carried through in a single direction at about 15m/s, the slurry layer around the steel wire of about 15μm on one side of a silicon brick decreases as it passes through a silicon brick, therefore resulting in tapered wafers with a standard TTV of around 15 to 20μm (Fig. 4a). Moreover, independent of the method of cutting using either a back-and-forth (or pilgrim) mode or a one-way mode, the 'squishing' effect observed with slurry while passing through silicon does not exist with diamond wire. The TTV of wafers cut with diamond wire is better than with slurry and ranges from approximately 7 to 15μm.

The abrasion mechanism involved also has an influence (on a smaller scale) on the surface roughness. These differences are evident in Fig. 5, which shows two examples of surface conditions – after slurry sawing and after diamond sawing.

In Fig. 5(a), the slurry as-cut wafer reveals the multiple indentations of SiC on silicon; cross-section imaging shows that about 5–6μm of subsurface damage (SSD) is due to that abrasion mode. Diamond wire composed of diamonds surrounded by a nickel layer deposited onto a steel wire does not yield the same final surface characteristics. The abrasion mode in this case is a two-body mode whereby the diamonds remove the silicon by plastic deformation in front of the diamond grain [5]. In this case, the surface of an as-cut wafer appears as shown in Fig. 5(b): the silicon removal creates lines on the surface. Cross-section imaging indicates only about 2–3μm of SSD resulting from the different abrasion mode.

## Performance of diamond wire

Even though everyone using diamond wire today in the PV industry has not necessarily fully understood and optimized the procedure compared to the slurry process that has been in use for decades, diamond wire has demonstrated its potential to cut a lot faster than steel wire and slurry in the future. As described in the following paragraphs, the potential for wafering, especially on monocrystalline or mono-like silicon ingots, is obvious. It has

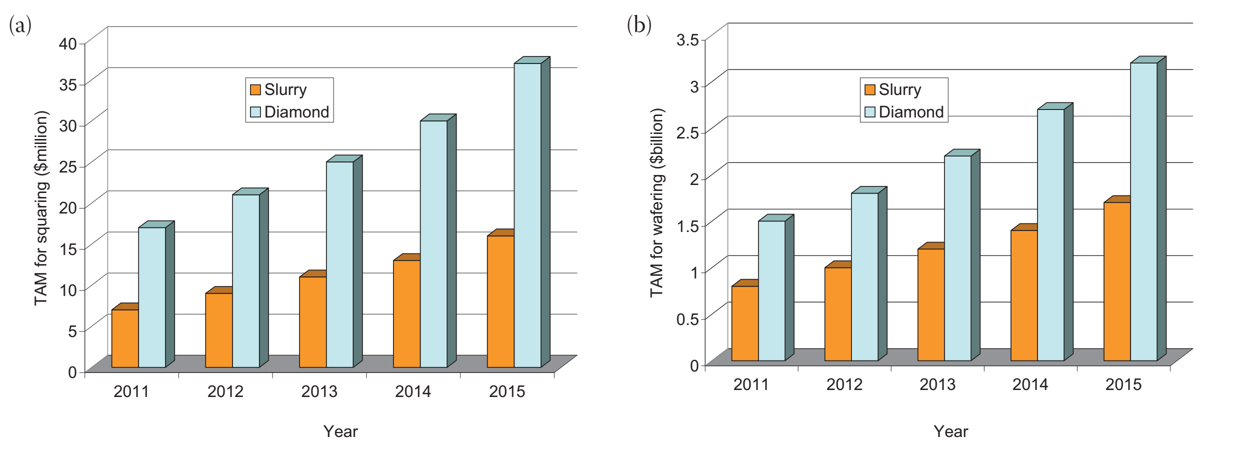


**Figure 6. TAM of consumables for (a) squaring and (b) wafering operations.**

already been mentioned that it is possible to cut monocrystalline wafers with a table speed of at least twice that of slurry. This has a significant impact on what form the silicon-shaping industry will take in the coming years. Table 1 summarizes the pluses and minuses of diamond wire compared to slurry.

The main assets of diamond sawing appear to be its capacity to cut at more than double the speed of the slurry method, increasing de facto equipment productivity and reducing the length of wire required. This technology also allows numerous potential improvements: a better TTV, the possibility of recycling Si powder, a reduction in wire diameter and a reduction of the number of consumables.

The adoption of diamond wire means that most of the difficulties from the saw and the slurry management are transferred to higher demands on wire characteristics. Probably the most important of these are a stronger mechanical resistance and a good diamond particle insertion inside the external coating. The latter requirement is one that is far from easy to meet, since diamond wire has a more complex structure than steel wire. This fact is accentuated if the wire diameter is further reduced. Because of these difficulties, the diamond wire manufacturers are limited to only the very competent and well-known ones (ASAHI, DWT) and the market prices are kept high. Furthermore, the difficulty in producing a defect-free wire over a length of many kilometres explains why diamond wire is currently only used in short versions – for squaring and cropping – and less frequently for wafering.

Equipment and processes also have to be developed or improved in order to allow diamond wire sawing to conquer the PV market. For example, it must be mentioned that there is a pressing need to limit wire vibration so that thinner wafers and a better surface finish can be obtained, and that a reliable process is necessary for cutting heterogeneous material such as multicrystalline silicon. Despite its drawbacks, the diamond wire process seems to be the future of silicon shaping in the PV industry, including the wafering stage.

## Different strategies

Even though it is becoming more and more apparent that within the next five years diamond wire technology is going to make significant progress, in the current PV context, in which competition is extreme in terms of cost reduction and in which becoming one of the industry leaders is everyone's goal, there is no global strategy for the industry. Diamond wire manufacturers are all trying to match the very few leaders such as Asahi Diamonds, Diamond Wire Technology and a few others in terms of quality, when lowering the price is essential in order to entice clients to switch from one solution (steel wire + slurry) to the other (diamond wire).

At the same time, compared to the old industry scenario in which the four main consumable costs were each absorbing a proportion of the cost (PEG, SiC, wire, slurry recycling), moving to diamond wire implies that the wire suddenly takes almost the whole consumable cost for itself. Knowing this, the previous providers of consumables are all trying to delay the arrival of the new diamond wire process. Assuming that the whole market used a single kind of wire (steel for slurry or diamond), the TAM for consumables for wafering with diamond wire was as much as \$1.5 billion in 2011 and could be as much as \$3.2 billion in 2015 as seen in Fig. 6(b).

Wafers manufacturers are all trying to be one of the first to cut with diamond wire at a lower cost than cutting with slurry, while equipment manufacturers do not have the same strategy. When Meyer Burger Group clearly set its roadmap when buying DWT in 2009, all the other companies such as AMAT, TOYO and NTC did not get specifically involved in the diamond wire manufacturing activity. AMAT, for example, is taking advantage of its joint patent with Arcelor Mittal [6] on structured wire to currently promote its thick version for squarers and a new, thin version for wafering to make the most of the well-proven slurry-based technology.

As part of reflecting on how to improve the wafer cost in the PV industry, there is also another approach: thinking 'out of the box' and not cutting silicon at all. Companies like Sharp have been working on making wafers by directly dipping a porous substrate into melted silicon and have demonstrated an efficiency of 14.8% [7]. The company 1366 Technologies recently announced that it was in the process of industrializing its direct wafer technology [8]. SiGen announced that it had sold two industrial-scale prototypes of ion implantation for manufacturing 85µm-thick monocrystalline wafers, having earlier achieved a record 20µm thickness [9]. RGS Development B.V. in the Netherlands is developing an industrial process for making direct wafers on substrates [10], while the idea of making kerf-less wafers has been given up by other companies such as Schott solar with their edge-defined film-fed growth (EFG), Evergreen with their string ribbon technologies and Astropower with their moulded wafers technology. Despite these efforts on kerf-less solutions, none of them seems to be ready to replace silicon shaping in the short term. It appears that none of these techniques combines cost, quality and productivity, although not all the necessary information on which to base such a statement is yet readily available.

## Alignment of two disruptive technologies

Sometimes two things happen at the same time and make something that seemed far-fetched suddenly appear plausible. This could be what is happening in the PV industry today. As everyone knows, two subjects created a lot of buzz last year: mono-like ingots and diamond wire. Without being clearly linked to each other, they could actually make many things happen at the same time. Mono-like ingots are created by using seeds of monocrystalline silicon deposited at the bottom of a crucible in order to melt standard solar-grade feedstock on the top part – and only the top part – of the seeds. The standard crystallization process follows to obtain a mono-like Gen 5 ingot. Depending on the process control, the ingot can be partially mono in the centre with some multi on the sides, or almost fully monocrystalline.

"Despite the technical challenges, including the manufacturing of stronger wires of thinner diameter and the capability of cutting inhomogeneous materials such as multicrystalline silicon, diamond wire certainly seems to be a potential solution for replacing the slurry process."

Teams have been working on the mono-like ingot process for many years in different parts of the world; at our laboratory [11–13] an active development of the process is now underway to produce Gen 5 mono-like ingots in an industrial-scale furnace in order to obtain the best quality. On the silicon-shaping activity front, since it is known that diamond wire cuts monocrystalline ingots more easily than multicrystalline ones, the structural, chemical and mechanical properties of the wafers are being investigated in order to develop the best cutting process using diamond wire. This is the goal of a current collaboration with Thermocompact, a French manufacturer of electrical discharge machining (EDM) wire that is moving towards saw wire manufacturing.

## Conclusions

PV roadmaps are guiding the industry towards improving the wafering processes, mostly by reducing the amount of silicon used to produce each wafer. As the slurry process reaches its limits, diamond wire appears to be a possible alternative to continue in that direction with the arrival of a disruptive technology. Despite the technical challenges, including the manufacturing of stronger wires of thinner diameter and the capability of cutting inhomogeneous materials such as multicrystalline silicon, diamond wire certainly seems to be a potential solution for replacing the slurry process. Such a step would, however, involve significant changes in the silicon-shaping market, mostly through the transfer of the cost of the equipment to the cost of the main consumable, that is the diamond wire. Nevertheless, the change should reduce the overall COO. Even though, of all the emerging kerf-less technologies, none yet seems ready to capture a significant part of the market, this developing technology is definitely one long-term strategy to keep an eye on.


## Acknowledgements

The authors would like to thank the SEMI PV Group for the use their figures, as well as J. Champliaud and G. Fortin for their contribution to Figs. 1 and 4.


## References


[1] Aberle, A. 2009, "Silicon wafer solar cells", presentation of the Solar Energy Research Institute of Singapore (SERIS) and the National University of Singapore (NUS).

[2] SEMI PV Group Europe 2011, "International technology roadmap for photovoltaic (ITRVP.net): Results 2010", 2nd edn (March) [available online at http://www.itrvp.net].

[3] GT Advanced Technologies 2011, announcement of Confluence Solar acquisition (August 25).

[4] Möller, H.J. 2004, "Basic mechanisms and models of multi-wire sawing", *Adv. Eng. Mater.*, Vol. 6, No. 7.

[5] Watanabe, N. et al. 2010, "Characterization of polycrystalline silicon wafers for solar cells sliced with novel fixed-abrasive wire", *Prog. Photovolt: Res. Appl.*, Vol. 18, pp. 485–490.

[6] Vaubourg, J.-P. 2004, "Monofilament metal saw wire", Patent No. LU 91126.

[7] Takakura, T. et al. 2008, "Effect of rapid thermal process for CDS silicon solar cells", *Proc. 23rd EU PVSEC*, Valencia, Spain.

[8] 1366 Technologies 2012 [website: http://www.1366tech.com/technology/direct-wafer/].

[9] Podewils, C. 2009, "A proton axe for thin silicon", *Photon Inter.* (April), p. 116.

[10] Schönecker, A. et al. 2008, "Compatibility of the RGS silicon wafer with industrial type solar cell processing", *Proc. Conf. Optoelec. & Microelec. Mater. & Devices*, Sydney, Australia.

[11] Stoddard, N. et al. 2008, "Casting single crystal silicon: Novel defect profiles from BP Solar's mono wafers", *Solid State Phenom.*, Vol. 131, pp. 1–8.

[12] Matter, P. 2011, "A new hybrid multi/mono cell technology", *Proc. 6th PV Prod. Equip. Conf. (c-Si)*, Berlin, Germany.

[13] Jouini, A. et al. 2011, "Improved multicrystalline silicon ingot crystal quality through seed growth for high efficiency solar cells", *Prog. Photovolt: Res. Appl.* [forthcoming].


## About the Authors


**Fabrice Coustier** joined CEA-INES in 2010 and is currently head of the silicon-shaping activity in the Laboratory for Materials and Processes for Solar Energy. He has been working in the silicon-shaping field since 2002, focusing on squaring and wafering. Before joining INES, Fabrice worked at AMAT Switzerland and Photowatt, and carried out a programme of research at the University of Minnesota, Minneapolis, USA.

**Jean-Daniel Penot** has been with CEA-INES since 2011 and is currently a scientist in silicon shaping. He obtained his Ph.D. in materials from microelectronics, after receiving a master of science and an engineer diploma in physics.

**Gérald Sanchez** received a Ph.D. from MIT, Boston, USA. Since 2003 he has been the head of R&D within the Thermo Technologies Group at Thermocompact.

**Michel Ly** has been the head of R&D for EDM wires at Thermocompact since 1999. He received a Ph.D. from the École des Mines de Paris, France.

## Enquiries

Fabrice Coustier
CEA-INES RDI – LMPS
Savoie Technolac BP332
50 Avenue du Lac Léman
73377 Le Bourget-du-Lac
France

Tel: +33 4 79 60 14 49
Email: fabrice.coustier@cea.fr
Website: http://www.ines-solaire.org

# Cell Processing

Page 67
News

Page 70
Product Reviews

Page 73
**Firing stability of $SiN_y/SiN_x$ and $Al_2O_3/SiN_x$ stacks for the rear-surface passivation of industrial-type crystalline silicon solar cells**

Sebastian Gatz et al., ISFH, Emmerthal & LUH, Hanover, Germany

Page 81
**Industrial n-type solar cells: Towards 20% efficiency**

Ingrid Romijn, ECN Solar Energy, Petten, The Netherlands & Lang Fang, Yingli Solar, Baoding, China, & Ard Vlooswijk, Tempress Systems BV, Vaassen, The Netherlands

Page 91
**TCAD for PV: A fast method for accurately modelling metal impurity evolution during solar cell processing**

Douglas M. Powell et al., MIT, Cambridge, Massachusetts, USA & Instituto de Energía Solar, Universidad Politécnica de Madrid, Madrid, Spain



## Bondholders of Q-Cells to take 95% ownership of the company

A debt-to-equity swap deal between Q-Cells and its bondholders has been agreed in principle, a situation that will result in the company's being majority owned (95%) by the bondholders. In return, Q-Cells would be virtually debt-free and retain the €304 million of liquidity the company had at the end of 2011 to continue to restructure and continue operations. Q-Cells will also sell further non-core assets that could raise €200 million, which would be given back to the 2012, 2014 and 2015 bondholders on an equal basis.

The implementation of the agreement requires the approval of the bondholders, the shareholders of Q-Cells SE and the involved authorities. An extraordinary general meeting has already been scheduled. The company noted that subject to approval the implementation of the planned financial restructuring would take place in the second half of 2012.


A debt-to-equity swap deal between Q-Cells and its bondholders has in principle been agreed.

**Cell Production News Focus**

### Researchers use nanomaterials-based technology to increase PV cell efficiency

Researchers from the University at Buffalo, Army Research Laboratory and Air Force Office of Scientific Research have developed a new, nanomaterials-based technology that has the potential to increase the efficiency of PV cells up to 45%. The researchers have also teamed up to found OPtoElectronic Nanodevices to commercialize this technology and are now seeking funding from private investors and federal programs. Through UB's office of science, technology transfer and economic outreach, the team has filed provisional patent applications to protect their technology.

The researchers have shown that embedding charged quantum dots into solar cells can improve electrical output by enabling the cells to harvest infrared light and thereby increasing the lifetime of photoelectrons. The technology can be applied to many different PV structures.

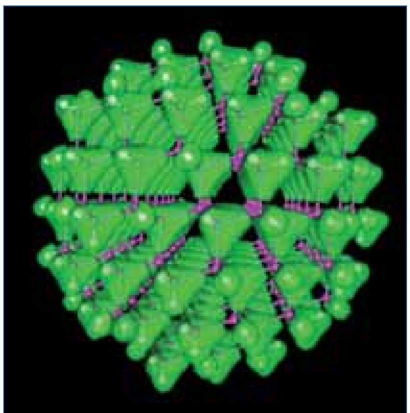

Source: Nanotechnology Foothill College

Embedding charged quantum dots into solar cells can improve electrical output by enabling the cells to harvest infrared light.

### JA Solar hits 18.5% efficiencies in volume production with Maple solar cell technology

JA Solar Holdings revealed that its Maple solar cells had reached an 18.5% conversion efficiency level in large volume production, with the average conversion efficiency for the Maple cells in mass production being recorded at 18%. The new record for JA Solar is noted as being higher than the industry's standard average conversion efficiency for multicrystalline solar cells of nearly 16.8%.

JA Solar's Maple solar cells are said to include silicon crystals that are broader, flatter and have fewer grain boundaries than standard multicrystalline silicon. The company advised that by using an original process technology, it has been able to reach the conversion efficiency rates with its Maple cells that are more typically seen in monocrystalline solar cells, while still holding the cost advantage of multicrystalline technology.

### Gintech Energy producing 'quasi-mono'-based solar cells

Cell efficiencies of higher than 18% using quasi-mono wafers have been claimed by Taiwan-based cell producer, Gintech Energy. The company also said its optimized pattern design and process recipe has achieved cell efficiencies of 19% for its Douro Series monocrystalline solar cells and more than17% for its multicrystalline solar cells.

The quasi-mono-based solar cells will be sold under its Solar Hybrid brand and employ a front alkaline textured surface with SiNx anti-reflecting coating with a back aluminium surface field. The cells can be used in modules to develop 255W/300W modules made of 60/72 cells.

Source: Gintech

Gintech's standard cells have been calibrated by Fraunhofer ISE.

**Business News Focus**

### Start-up company Nines Photovoltaics raises €750,000 to build processing tool

Irish PV equipment start-up Nines Photovoltaics has raised €750,000 to further develop and build its dry etching

Source: Nines Photovoltaics

The dry etch tool is to be validated at the Fraunhofer ISE.

silicon wafer tool. The Dublin, Ireland-based firm started operations in 2010 and has been collaborating with the Fraunhofer ISE, with plans for the tool to be validated at its pilot production line. The company has raised over €2.5 million, including €1.2 million through FP7 European Funding, which was announced in June 2011. The new funding will also be used to recruit additional staff, according to the company.

## Singulus to provide turnkey c-Si cell line to Lithuanian firm

Lithuania-based CD and DVD disc manufacturer BOD Group is entering the c-Si solar cell manufacturing market, using a complete line of equipment being provided by Singulus Technologies. The delivery of the line is scheduled to take place in early 2013; financial details were not disclosed. Singulus said that it would be supplying its own technology for the texturing step, the anti-reflective coating and wet-chemical phosphorous glass cleaning steps as well as the automated wafer handling systems.


*Source: Singulus*

**Singulus plans to deliver the line to the Lithuanian firm in early 2013.**

## Cost cutting pervades Applied Materials' solar division as orders drop by 62%

Overcapacity within the PV industry hit Applied Materials sales and orders in its financial first quarter, leading to further cost reductions within its Energy and Environmental Solutions division. New orders in the segment were down 62% to only US$33 million, while sales of US$207 million were down 34% on the prior quarter. The segment had a non-GAAP operating loss of US$17 million and a GAAP operating loss of US$23 million. Overall, Applied generated orders of US$2.01 billion and net sales of US$2.19 billion, exceeding guidance.

However, management were not confident in predicting when an upturn in equipment sales would occur, though they said they were surprised at the strong end-user demand for PV seen in the fourth quarter of 2011.

*Source: Applied Materials*

**Overcapacity within the PV industry hit Applied Materials sales and orders in its financial first quarter.**

## Amtech revenues fall by 59%; guides lower sales in FYQ2'12

In line with previous guidance, PV equipment supplier Amtech posted net revenue of US$24.7 million for its financial year first quarter of 2012, a decline of 59% compared to the previous quarter. The company reported minimal order cancellations but noted shipment push-outs as PV manufacturers tackle severe overcapacity.

Revenue for FY2Q12 was guided down to be in the range of US$20–US$22 million. Amtech's total orders in the first quarter of fiscal 2012 were US$11.1 million (US$3.1 million solar segment), down 34% compared to total orders of US$16.8 million (US$4.7 million solar segment) in the preceding quarter due primarily to overcapacity in the solar sector.

## Roth & Rau posts 2011 revenue of €208 million; plans faster restructuring and job losses

Roth & Rau has been forced to implement further company-wide restructuring to reduce its global headcount. Preliminary sales for 2011 reached €208 million, down from €285 million in 2010. The company reported new orders net of cancellations


*Source: photovoltaic-production.com*

**Only 12 companies will remain within the Group, down from the current 26. In Germany, the complexity of the group structure is to be further reduced by merging companies.**

amounted to €153 million, compared to €537 million in the prior year. Order backlog at the end of 2011 stood at €141 million, compared to €336.5 million in the prior year period.

Although the equipment supplier had undertaking a range of restructuring projects during 2011, management noted that due to the circumstances, further restructuring efforts would be implemented and at a faster pace.

## IMS Research: PV manufacturing equipment replacement cycle a US$25 billion revenue opportunity

IMS Research believes a PV manufacturing equipment replacement cycle could be the only bright spot in the near-term as suppliers face a lean capital investment year due to overcapacity and industry consolidation. The market research firm said that over the next four years, a 20GW-sized, US$25 billion sales opportunity exists for the upgrade or replacement of existing manufacturing capacity to remain competitive.

*Source: Aleo Solar*

**IMS Research said that over the next four years it had identified a 20GW-sized, US$25 billion sales opportunity.**

In contrast, NPD Solarbuzz analyst Finlay Colville believes the next wave of capital spending and technology upgrades will be limited until end-user demand for PV systems reaches around 30GW, as this would trigger tier 1 capacity expansions and higher cell/module efficiencies.

## NSP's solar cell sales up in January

Taiwan-based crystalline solar cell producer Neo Solar Power (NSP) reported January 2012 monthly sales of approximately US$22 million (NT$850 million), up from NT$663 million in December.

Taiwan-based crystalline solar cell producer, Neo Solar Power (NSP), said in early January it would allocate resources to establish a systems business unit focused on commercial and utility-scale PV markets. NSP is following other manufacturers such as MEMC

Source: Solar Panels Group

**Neo Solar Power (NSP) said in early January it would allocate resources to establish a systems business unit focused on commercial and utility-scale PV markets.**

and SunPower into the downstream market. NSP had previously noted that ASPs, sales and shipments decreased sharply in December 2011.

## Emcore to action one-for-four reverse stock split

Loss-making CPV solar cell manufacturer Emcore has approved a one-for-four reverse stock split. This implies that the number of issued and outstanding shares in the company would be reduced by approximately 94 million to approximately 23.5 million. The market value of the total number of shares would remain the same.

Emcore posted revenue in 2011 of US$200.9 million, a 5% increase compared to the prior year. Revenue for its photovoltaics segment was US$75.3 million, which represents an 8% increase compared to the prior year.

However, the company continued to make losses. Emcore posted a consolidated net loss of US$34.2 million in 2011, a US$10.5 million increase on the previous year. As of September 30, 2011, cash, cash equivalents, and restricted cash totalled approximately US$16.1 million.

Source: Emcore

**Emcore has approved a one-for-four reverse stock split.**

Typically, reverse stock splits are undertaken by companies to avoid being delisted should shares be trading below the US$1.0 Nasdaq rule, or to make shares look more valuable on reduced outstanding floating shares.

# Product Reviews

**Vitronic**

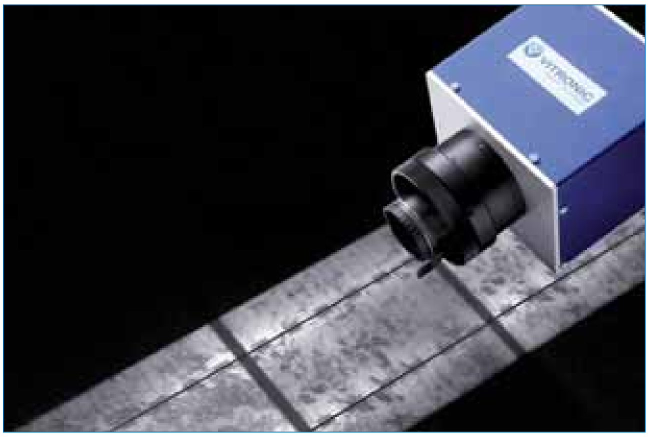

### New inspection system from Vitronic provides cell defect management

**Product Outline:** Vitronic's 'VINSPECsolar' electroluminescence inspection system is designed to detect defects within solar cells that could influence electrical performance of the solar module.

**Problem:** In module production, cells, strings, matrices all the way to modules are subjected to mechanical and thermal stresses. Missing electrical connections or wrong wiring can also occur during soldering. In addition, the solar cells used can display quality deviations depending on where they were purchased.

**Solution:** The VINSPECsolar electroluminescence inspection system detects inactive areas, cracks and grid line interruptions. The inspections can be conducted on the solar cell string and solar cell matrix before or after lamination as well as on the finished module. This makes it possible for the module manufacturer to intervene and implement improvements before lamination, thereby optimizing the module's performance. A classification of the modules, based on the electroluminescence inspection, takes place after lamination and the images are saved as proof of the quality.

**Applications:** Detecting inactive areas, cracks, weak active cells, cracks affecting electrical performance, micro-cracks and grid-line interruptions.

**Platform:** An automated image assessment, using specially-developed software methods, takes place in order to then display the defect areas on a monitor. The image is displayed on monitors of e.g. 46" in size and can also be made available to reworking stations. The frequency of the individual defect characteristics is recorded and evaluated using the integrated statistics function.

**Availability:** January 2012 onwards.

# Product Reviews



## BTU

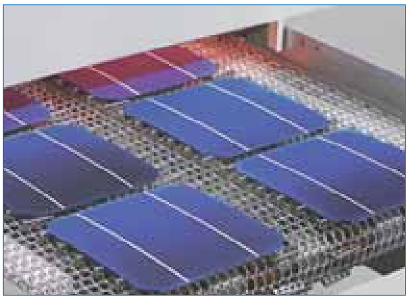

### Tritan HV90 from BTU features 3,600 wafers per hour throughput

**Product Outline:** BTU International's 'Tritan' HV90 dual-lane metallization firing system features increased throughput at 3,600 wafers per hour, with an edge belt, VOC abatement and a single zone spike with less than three seconds' spike time. BTU claims that by switching to the dual-lane system, cell manufacturers can expect a 35% increase in capital efficiency, coupled with unparalleled performance in lane-to-lane matching.

**Problem:** Key concerns include yield, repeatability and overall uniformity, amongst others.

**Solution:** The Tritan HV90 Metallization Firing furnace, featuring BTU's TriSpeed technology, allows users to take advantage of improved ramp rates up to 200°C per second while not compromising the drying and cooling sections of the profile. The three-belt system gives revolutionary control of profile development. The system is specifically optimized for paste drying, organics burn-out and contact firing in the 750–950°C range to achieve high-efficiency solar cells through rapid thermal processing. The system boasts a yield better than 99.99%.

**Applications:** Solar cell metallization thermal processing.

**Platform:** The process chamber is designed to provide access from both top and bottom of the conveyor for easy maintenance and serviceability, combined with extended lamp life and minimizes downtime. The drying section features stainless steel lining for easy cleaning. The furnace can be integrated with all mainstream printing/testing equipment.

**Availability:** Currently available.

## centrotherm

### c.FIRE fast-firing furnace from centrotherm offers compact footprint

**Product Outline:** centrotherm has introduced a new fast-firing furnace tool, c.FIRE, for metallization of front and rear contacts of solar cells. It is suited for all common sorts of metallization paste and comes with an integrated and versatile dryer. Also included is a compact footprint and maintenance systems in order to reduce the operating costs for solar cell producers.

**Problem:** Solar cell manufacturers target improved and stable cell performance and narrow distributions of conversion efficiency. Furthermore, the efficient use of limited floor space is of highest importance. Thus, a small and compact high-throughput manufacturing tool with precise process control and a robust design is essential.

**Solution:** centrotherm's c.FIRE is a single- and dual-lane furnace with a length of 11,000mm. The furnace consists of a powerful and flexible hot air paste dryer, an updated firing section and a re-engineered, shortened cooling zone. The system comes with energy efficient VOC handling (condenser).

**Applications:** c.FIRE is used for firing of front-side contact while alloying aluminium backside contact. It handles over-compensation of n+ layer and gettering of metallic impurities and drying of metallization pastes (front- and backside).

**Platform:** The c.FIRE dual-lane configuration is capable of a throughput of up to 3,500 wafers per hour in a modular design. The platform complies with European standards and regulations. In order to improve ease of inspection and maintenance, c.FIRE provides quick and convenient access through glass swing doors.

**Availability:** Currently available.

## Stäubli

### Stäubli offers TP80 four-axis fast pick and place machine

**Product Outline:** Stäubli Robotics has launched the TP80 fast Picker, an ultrafast four-axis new technology of high-speed pickers delivering speeds of more than 200 picks per minute and more flexibility at a lower cost, according to the company.

**Problem:** Delta parallel robots (one rotational and three translational (x, y, z) movements) are used widely in wafer/cell handling and sorting applications. Stäubli Robotics claims that an ultrafast four-axis robotic picker is more agile and lightweight and able to offer extremely fast cycle times and high precision with homogenous repeatability.

**Solution:** The TP80 is claimed to be more agile and lightweight than competitor delta robots, offering extremely fast cycle times while maintaining high precision with homogenous repeatability. A simple base or wall mounting is said to eliminate the need for a large, costly gantry, further enhancing the robot's cost effectiveness and ease of integration. The TP80 fast Picker is also extremely rigid, and competitively priced offering an economical alternative for numerous standard applications without sacrificing quality, durability or performance.

**Applications:** Typical applications include high-speed pick and place, assembly, material handling, packaging and machine tending.

**Platform:** Standard features include a maximum payload of 1kg, 800mm reach and a Z-axis stroke of 100mm. Additional features include very high rigidity, repeatability of +/- 0.05mm at IP65 Protection Class when equipped with bellows.

**Availability:** January 2012 onwards.

# Firing stability of $SiN_y/SiN_x$ and $Al_2O_3/SiN_x$ stacks for the rear-surface passivation of industrial-type crystalline silicon solar cells

**Sebastian Gatz**[1], **Jan Schmidt**[1,2], **Boris Veith**[1], **Thorsten Dullweber**[1] & **Rolf Brendel**[1,2]
[1]Institute for Solar Energy Research Hamelin (ISFH), Emmerthal; [2]Institute of Solid-State Physics, Leibniz University of Hanover (LUH), Hanover, Germany

## ABSTRACT
In the photovoltaics industry, contacts to crystalline silicon are typically formed by the firing of screen-printed metal pastes. However, the stability of dielectric surface passivation layers during the high-temperature contact formation has turned out to be a major challenge for some of the best passivating layers, such as intrinsic amorphous silicon. Capping of well-passivating dielectric layers by hydrogen-rich silicon nitride ($SiN_x$), however, has been demonstrated to improve the thermal stability, an effect which can be attributed to the atomic hydrogen (H) diffusing out to the interface during firing, and passivating dangling bonds. This paper presents the results of investigations into the influence of two different dielectric passivation stacks on the firing stability, namely $SiN_y/SiN_x$ ($y < x$) and $Al_2O_3/SiN_x$ stacks. Excellent firing stability was demonstrated for both stack systems. Effective surface recombination velocities of < 10cm/s were measured after a conventional co firing process on 1.5Ωcm *p*-type float-zone silicon wafers for both passivation schemes. On the solar cell level, however, better results were obtained using the $Al_2O_3/SiN_x$ stack, where an efficiency of 19.6% was achieved for a large-area screen-printed solar cell fabricated on conventional Czochralski-grown silicon.

## Introduction

Industrial crystalline sillicon solar cells typically feature a full-area aluminium (Al) back-surface field (BSF) at the rear. This provides an ohmic contact and a moderate rear-surface passivation, with effective rear-surface recombination velocities $S_{rear}$ ranging from 400 to 600cm/s on 2–4Ωcm *p*-type silicon. In order to increase cell efficiency, the passivation quality and the internal reflectivity at the rear need to be improved. These two requirements are fulfilled in the passivated emitter and rear solar cell (PERC) concept [1], which is schematically shown in Fig. 1(a).

> "In order to increase cell efficiency, the passivation quality and the internal reflectivity at the rear need to be improved."

In the PERC approach, screen-printed Al paste is deposited on the complete rear surface on top of locally opened dielectric rear-surface passivation layers. During a co-firing step in an industrial infrared beltline furnace, not only is a local BSF formed in the opened areas, but also the homogeneous phosphorous-doped emitter at the front is contacted by a screen-printed silver (Ag) paste. A thermally grown silicon dioxide layer exhibits an excellent firing-stable surface passivation. However, the low-throughput furnace process is disadvantageous for industrial applications. The described PERC process imposes some additional requirements on the passivation system at the rear:

- Thermal stability of surface passivation in order to withstand the high-temperature co-firing step
- High optical reflectivity in the infrared wavelength range
- No parasitic shunting at the rear contacts [2]

The one-dimensional device simulation [3] depicted in Fig. 1(b) shows that the effective surface recombination velocity in the passivated regions $S_{pass}$ has a strong impact on the solar cell efficiency $\eta$. The surface recombination velocity in the metallized regions $S_{met}$ is around 600cm/s [4]. In order to improve the conversion efficiency of about 18.5% for conventional solar cells with a full-area Al-BSF, it is essential to provide a passivation featuring

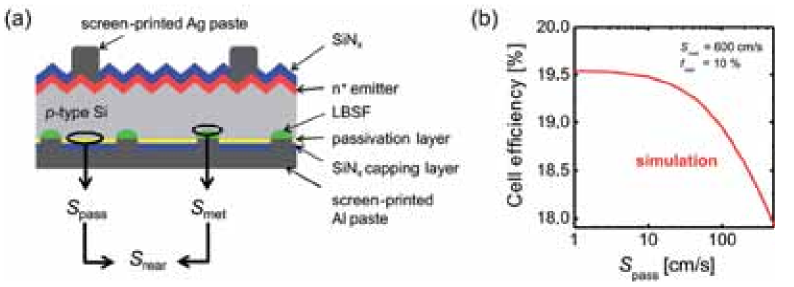


**Figure 1. (a) Schematic of a PERC solar cell applying screen-printed Ag front and Al rear contacts with local openings in the passivation stack. The electrical quality of the rear is characterized by the effective surface recombination velocity $S_{rear}$, which is influenced by the surface recombination velocities in the dielectric passivated areas $S_{pass}$ and in the metallized contact areas $S_{met}$. (b) PC1D simulation of the energy conversion efficiency as a function of $S_{pass}$ for a PERC solar cell on boron-doped Cz-silicon with a resistivity of 2.1Ωcm.**

$S_{pass}$ values below 100cm/s. However, the simulation reveals a saturation of the possible conversion efficiency at around 19.5% for $S_{pass}$ values under 20cm/s.

Because of the high throughput, the plasma-enhanced chemical vapour deposition (PECVD) technique for the surface passivation offers the possibility of reducing costs. For silicon nitride ($SiN_x$) layers, the surface passivation quality and firing stability are highly dependent on the composition and therefore on the refractive index $n$ of the dielectric [5,6]. A value of $n \approx 2.5$ results in low effective surface recombination velocities $S_{pass}$ for the as-deposited state, whereas a layer with $n \approx 2.05$ performs best after a firing step in the temperature range of 800 to 900°C [7]. The latter configuration is used, for example, with conventional screen-printed solar cells for passivating the phosphorus-diffused emitter at the front [6]. The passivation of these $SiN_x$ films, deposited in an $NH_3$-rich gas mixture, relies mainly on the field-effect passivation provided by a high density of fixed positive charges in the insulating $SiN_x$ films [8]. Additionally, the surfaces are passivated by atomic hydrogen (H) released from the precursor gases during the PECVD deposition. However, parasitic shunting between the back contacts and the inversion layer underneath the $SiN_x$ interface has been found to degrade the cell performance for *p*-type surfaces [2].

Intrinsic amorphous silicon (a-Si) films deposited on crystalline silicon exhibit only small, if any, charge densities and therefore do not cause parasitic shunting [9]. If the dangling bonds at the interface are saturated with hydrogen which is released during PECVD deposition, these a-Si films provide the same low $S_{pass}$ values as thermally grown $SiO_2$ [10–14]. But applying temperatures above 400°C severely deteriorates the passivation quality [15]. Depositing a $SiN_x$ capping layer with $n_{SiNx} \approx 2.05$ on top of the a-Si layer not only protects the a-Si layer from the Al rear metallization but also improves the thermal stability of the surface passivation [14,16,17]. However, the a-Si/$SiN_x$ stacks were shown to be stable only for firing temperatures $T \leq 750$°C. When standard firing temperatures between 800 and 900°C are applied, the surface passivation severely deteriorates. In this paper, it is shown that the addition of small amounts of nitrogen to the a-Si layer, resulting in $SiN_y/SiN_x$ stacks with $y < x$, improves the firing stability of the stacks significantly.

Another dielectric layer which provides an excellent level of surface passivation is aluminium oxide ($Al_2O_3$). With laboratory PERC cells, $Al_2O_3$ has been demonstrated to prevent any parasitic shunting because of its high negative fixed charge density that is responsible for the excellent field-effect passivation [18]. During firing, however, the high level of surface passivation provided by single $Al_2O_3$ layers deteriorates, an effect which is attributed to a release of interfacial hydrogen. It has recently been shown that the firing stability is significantly improved for $Al_2O_3/SiN_x$ stacks compared to single layers of $Al_2O_3$ [19,20]. In the present paper, both types of industrially-relevant passivation stacks – $SiN_y/SiN_x$ and $Al_2O_3/SiN_x$ – are directly compared on the basis of lifetime as well as solar cell results.

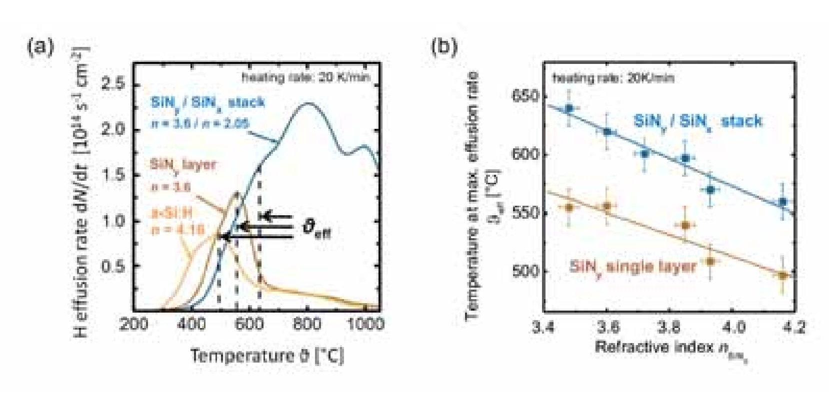


**Figure 2. (a) H effusion rate as a function of the measured temperature. The characteristic effusion temperatures $\vartheta_{eff}$ are related to the respective maximal H effusion rate from the passivating film. (b) Effusion temperatures $\vartheta_{eff}$ from the $SiN_y$ passivation layer increase with decreasing $n_{SiNy}$ for both $SiN_y$ single and $SiN_y/SiN_x$ stack layers. The increase in $\vartheta_{eff}$ using a $SiN_x$ capping layer indicates the further reduction of H effusion. The dashed lines are guides for the eye. (Data are taken from Gatz et al. [24].)**

## $SiN_y/SiN_x$ passivation stacks

The influence of $SiN_y/SiN_x$ passivation stacks on the firing stability with a silicon-rich $SiN_y$ passivation layer and a nitrogen-rich $SiN_x$ capping layer is investigated. The main idea is to increase the thermal stability of the surface passivation by supplying minor amounts of $NH_3$ during the a-Si deposition in order to reduce hydrogen effusion during a conventional screen-printing firing process. Moreover, it is known that the positive charge density, responsible for the parasitic shunting, is substantially reduced if the nitrogen content of the amorphous film is low [21,22].

In $SiN_y$, hydrogen is bonded in an amorphous silicon nitride network. Thermally stimulated hydrogen diffuses out of the PECVD layers, and is therefore no longer available for passivating the silicon surface. This was shown by hydrogen effusion experiments [23], which revealed information about the hydrogen content and the thermal stability of hydrogen bonds. During effusion our samples are annealed in vacuum with a heating rate of 20K/min. Hydrogen atoms and molecules that diffuse out of the PECVD layers are detected in real time by means of a mass spectrograph. For an a-Si single layer, a hydrogen effusion peak at a characteristic temperature ($\vartheta_{eff}$) is expected, which is a measure of the thermal stability of the hydrogen in the a- Si layer.

Fig. 2(a) shows measured effusion rates for various passivation layers. The hydrogen effusion rate of an a-Si single layer starts to increase at temperatures of about 300°C and reveals a peak at $\vartheta_{eff}$, the characteristic effusion temperature, equal to 495°C. For the $SiN_y$ single layer with $n = 3.6$ the temperature at which hydrogen effusion starts and the value of $\vartheta_{eff}$ have both increased. When a 100nm-thick $SiN_x$ capping layer is deposited on top of the $SiN_y$ layer, the bend in the curve of the effusion rate at $\vartheta_{eff} \approx 630$°C can be attributed to the hydrogen diffusing out of the $SiN_y$ passivation layer. Effusion peaks at temperatures of approximately 800°C and 1000°C are found to be typical for the $SiN_x$ capping layer.

Fig. 2(b) shows $\vartheta_{eff}$ for single and double passivation layers as a function of the real part of the refractive index $n$ of the 10nm-thick passivation layers. $\vartheta_{eff}$ decreases continuously from 550°C for $SiN_y$ single layers ($n = 3.48$) to 495°C for an a-Si single layer ($n = 4.16$). The diffusing out of hydrogen is reduced because of the presence of nitrogen. It is concluded from FTIR measurements that this is due to the larger bonding strength of hydrogen with an increasing concentration of Si-N back bonds (as demonstrated by Gatz et al. [24]). In addition, Fig. 2(b) shows that, if a $SiN_x$ capping layer is applied, the peak temperature increases by 60 to 90°C for all $SiN_y$ layers. A reduced hydrogen effusion rate due to a $SiN_x$ capping layer has already been reported in the literature [25].

The following discussion will focus on carrier lifetime investigations of $SiN_y/SiN_x$ passivated crystalline Si surfaces. The effective lifetime $\tau_{eff}$ of symmetrically passivated *p*-type FZ Si

wafers is measured by means of the quasi-steady-state photoconductance (QSSPC) method [26,27]. If the total measured recombination rate is attributed to the interface, the upper limit for the effective surface recombination velocity can be estimated from the equation

$$S_{pass} = \frac{W}{2 \cdot \tau_{eff}} \quad (1)$$

where $\tau_{eff}$ is effective lifetime measured by QSSPC and $W$ is the wafer thickness.

The effective surface recombination velocity $S_{pass}$ before and after firing in an infrared conveyor-belt furnace for $SiN_y/SiN_x$ double layers is shown in Fig. 3. $S_{pass}$ in the as-deposited state decreases slightly with increasing refractive index from about 22cm/s ($n$ = 3.14) to 8cm/s ($n$ = 4.16). The firing step alters the $S_{pass}$ dependence significantly. A minimum of $S_{pass}$ occurs for $n$ in the range of $n$ = 3.4 to 3.8 with the minimum upper limit $S_{eff}$ = (10±2)cm/s for stacks with $n$ = 3.6. After firing, as the refractive index increases further towards $n_{a\text{-}Si}$ = 4.16, $S_{pass}$ increases significantly due to the reduced bonding strength of H in the $SiN_y$ film, as indicated by our FTIR and H effusion results. With optimization of the process gas composition, $S_{pass}$ remains below 10cm/s at relevant injection densities of the solar cell between $\Delta n = 10^{13}cm^{-3}$ and $\Delta n = 10^{15}cm^{-3}$ (as has been shown by Gatz et al. [24]).

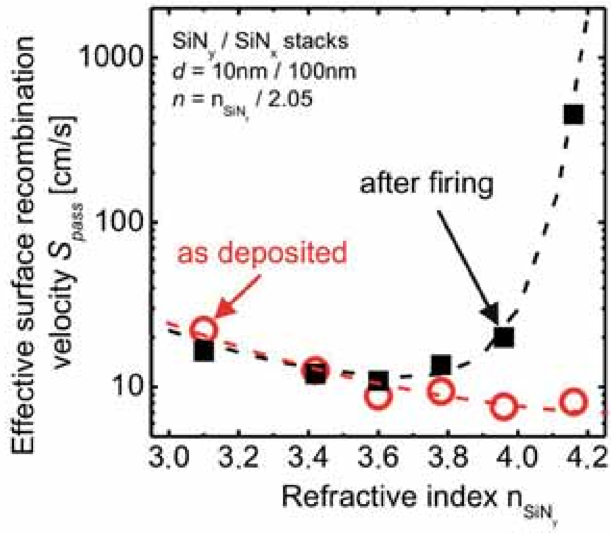


**Figure 3. Effective surface recombination velocity $S_{pass}$ at $\Delta n = 10^{15}cm^{-3}$ before and after a firing step as a function of the passivation layer's refractive index $n$ for $SiN_y/SiN_x$ stacked layers. The dashed lines are guides for the eye. (Data are taken from Gatz et al. [24].)**

## $Al_2O_3/SiN_x$ passivation stacks

Fig. 4 shows the effective surface recombination velocity $S_{pass}$, at a fixed injection density of $10^{15}cm^{-3}$ after firing in a belt furnace, as a function of the $Al_2O_3$ layer thickness. The $Al_2O_3$ layers were deposited by two variants of atomic layer deposition (ALD): (a) plasma-assisted ALD (PA-ALD), and (b) thermal ALD.

> "Both PA-ALD-$Al_2O_3$ and thermal ALD-$Al_2O_3$ stacks are well suited to application to high-efficiency screen-printed PERC solar cells."

For PA-ALD-$Al_2O_3$ single layers of thicknesses < 20nm, a pronounced degradation of the effective surface recombination velocity $S_{pass}$ after firing is observed, whereas $Al_2O_3/SiN_x$ stacks with thin $Al_2O_3$ layers < 20nm show a negligible increase of $S_{pass}$; there is even an improvement for ultrathin layers ≤ 4nm. For layers of thickness ≥ 20nm, no significant difference is detectable between single layers and $Al_2O_3/SiN_x$ stacks. Both PA-ALD-$Al_2O_3$ (Fig. 4a) and thermal ALD-$Al_2O_3$ (Fig. 4b) layers provide approximately the same excellent passivation level, with just slightly lower effective surface recombination velocities for the PA-ALD-$Al_2O_3/SiN_x$ stacks. It is noteworthy that both stack systems with $Al_2O_3$ layers of thicknesses between 4 and 10nm provide lifetimes between 1 and 3ms after firing, corresponding to surface recombination velocities below 10cm/s over a very broad injection range ($10^{13}$–$10^{15}cm^{-3}$). Hence, both stacks are well suited to application to high-efficiency screen-printed PERC solar cells.

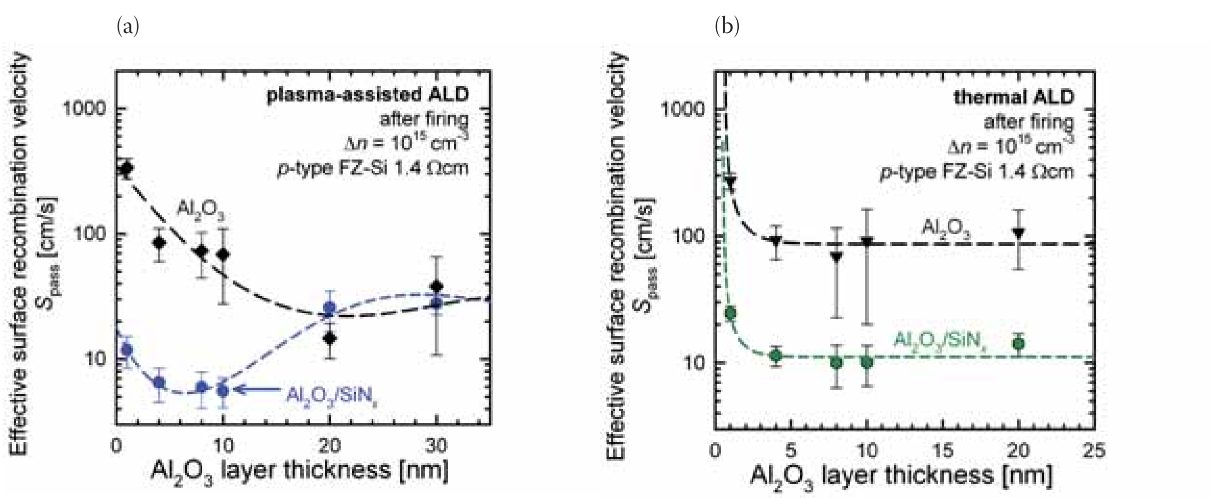


**Figure 4. Effective surface recombination velocity as a function of $Al_2O_3$ layer thickness after firing, for single layers of $Al_2O_3$ compared with $Al_2O_3/SiN_x$ stacks. The results are shown for $Al_2O_3$ layers deposited by (a) plasma-assisted ALD, and (b) thermal ALD. The samples received no anneal before firing. The dashed lines are guides for the eye.**

## Solar cell results

The processing sequence of our screen-printed PERC solar cells is described in Dullweber et al. [28]. Table 1 shows representative measured cell parameters of PERC solar cells with $SiN_y/SiN_x$ (cell type A), plasma-assisted ALD-$Al_2O_3/SiN_x$ (cell type B) and $SiO_2/SiN_x$ (cell type C) rear-surface passivation stacks after the permanent deactivation of the boron-oxygen-related recombination centres [29,30].

> "At the solar cell level, $Al_2O_3/SiN_x$ clearly outperforms $SiN_y/SiN_x$."

PERC solar cells of types B and C achieve conversion efficiencies of 19.6% and 19.4% [31] compared to 18.3% for cell type A [24]. This difference is related to the open-circuit voltage $V_{oc}$ of 633mV and short-circuit current density $J_{sc}$ of 37.1mA/cm² of the $SiN_y/SiN_x$ passivated solar cell, and is mainly attributed to significant improvements in $V_{oc}$ of up to 664mV and in $J_{sc}$ of up to 38.6mA/cm². Part of the improvement of cells B and C compared to cell A, however, is due to an improved front-side metallization. The fill factor *FF* does not depend on the passivation, but is strongly related to the metallization fraction at the rear and therefore to the pitch of the rear contacts [32].

| Cell type | Area [cm²] | Rear-surface passivation | Pitch [mm] | $V_{oc}$ [mV] | $J_{sc}$ [mA/cm²] | *FF* [%] | $\eta$ [%] |
|---|---|---|---|---|---|---|---|
| A | 141 | $SiN_y/SiN_x$ | 1 | 633 | 37.1 | 77.8 | 18.3* |
| B | 233 | $Al_2O_3/SiN_x$ | 1.2 | 645 | 38.6 | 78.5 | 19.6** |
| C | 149 | $SiO_2/SiN_x$ | 2 | 664 | 38.5 | 75.8 | 19.4** |

* in-house measurements at ISFH
** independently confirmed by FhG-ISE CalLab

**Table 1. Parameters of solar cells using *p*-type boron-doped Cz-silicon (2.1Ωcm), measured under standard test conditions.**

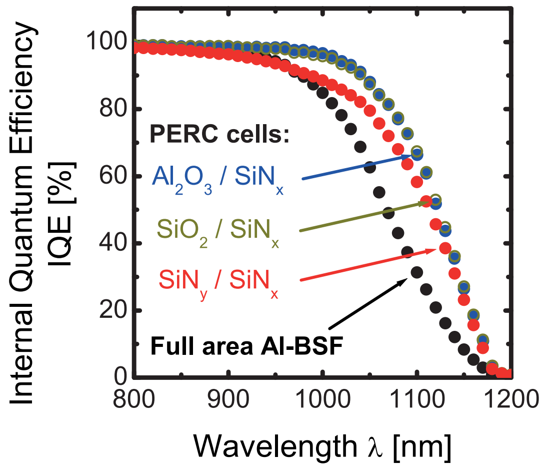


**Figure 5. Comparison of measured IQE of the PERC solar cells with $Al_2O_3/SiN_x$, $SiO_2/SiN_x$ and $SiN_y/SiN_x$ rear-surface passivation stacks and a reference cell with a full-area Al-BSF.**

**Figure 6. Contact formation of screen-printed solar cells in a conveyor-belt furnace at ISFH.**

Fig. 5 shows the measured internal quantum efficiency (IQE) data for the PERC solar cells, as well as for a conventional solar cell featuring a full-area Al-BSF. The effective rear-surface recombination velocity $S_{rear}$ of each solar cell is extracted, along with reflectance data (not shown here), in the wavelength region between 850nm and 1000nm. For cells of types B and C, the analysis leads to $S_{rear}$ < 100cm/s [31]. Assuming $S_{met}$ = 600cm/s for the metallized regions, then $S_{rear}$ < 100cm/s corresponds to $S_{pass}$ < 20cm/s in the passivated areas [4]; that confirms the lifetime measurement results for $Al_2O_3/SiN_x$ (see Fig. 4) and also previous measurement results for $SiO_2/SiN_x$ passivation stacks [33].

A solar cell of type A with $SiN_y/SiN_x$ rear-surface passivation shows an $S_{rear}$ of (400±100)cm/s. This value is slightly smaller than the $S_{rear}$ of about (550±100) cm/s for the solar cell with full-area Al-BSF, indicating that there is only a slightly improved surface passivation quality with the $SiN_y/SiN_x$ stack. However, if it is assumed that $S_{met}$ = 600cm/s for local Al contacts, then $S_{rear}$ = 400cm/s corresponds to $S_{pass}$ ≈ 300cm/s in the passivated areas [4]. That value clearly exceeds the $S_{pass}$ < 10cm/s obtained from lifetime measurements. The physical reason for this discrepancy is currently under detailed investigation at ISFH.

## Conclusions

As industrially-relevant alternatives to passivation by high-temperature-grown silicon oxide, two different low-temperature passivation schemes have been investigated for rear-surface passivation of screen-printed PERC solar cells: $SiN_y/SiN_x$ (y < x) and $Al_2O_3/SiN_x$ stacks. Both stack layers exhibit an excellent surface passivation quality before and after firing in an industrial conveyor-belt furnace, as demonstrated by effective surface recombination velocities $S_{pass}$ < 10cm/s. However, at the solar cell level, $Al_2O_3/SiN_x$ clearly outperforms $SiN_y/SiN_x$. When the optimized ISFH screen-printed PERC process is used, energy conversion efficiencies of up to 19.6% are obtained for large-area solar cells with conventional Cz-Si wafers.

## References


[1] Blakers, A.W. et al. 1989, "22.8% efficient silicon solar cell", *Appl. Phys. Lett.*, Vol. 55, pp. 1363–1365.

[2] Dauwe, S. et al. 2002, "Experimental evidence of parasitic shunting in silicon nitride rear surface passivated solar cells", *Prog. Photovolt: Res. Appl.*, Vol. 10, No. 4, pp. 271–278.

[3] Clugston, D.A. & Basore, P.A. 1997, "Pc1d version 5: 32-bit solar cell modeling on personal computers", *Proc. 26th IEEE PVSC*, Anaheim, California, USA, pp. 207–210.

[4] Gatz, S. et al. 2011, "Analysis of local Al-doped back surface fields for high-efficiency screen-printed solar cells", *Energy Procedia*, Vol. 8, pp. 318–323.

[5] Lauinger, T., Aberle, A.G. & Hezel, R. 1997, "Comparison of direct and remote PECVD silicon nitride films for low-temperature surface passivation of *p*-type crystalline silicon", *Proc. 14th EU PVSEC*, Barcelona, Spain, pp. 853–856.

[6] Upadhyaya, A., Sheoran, M. & Rohatgi, A. 2005, "Study of direct PECVD $SiN_x$-induced surface emitter and bulk defect passivation in p-type silicon solar cells", *Proc. 31st IEEE PVSC*, Lake Buena Vista, Florida, USA, pp. 1273–1276.

[7] Lenkeit, B. et al. 2001, "Excellent thermal stability of remote PECVD silicon nitride films for screen-printed bifacial silicon solar cells", *Solar Energy Mater. & Solar Cells*, Vol. 65, pp. 317–323.

[8] Hezel, R. & Jäger, K. 2989, "Low-temperature surface passivation of silicon for solar cells", *J. Electrochem. Soc.*, Vol. 136, pp. 518–523.

[9] Dauwe, S., Schmidt, J. & Hezel, R. 2002, "Very low surface recombination velocities on *p*- and *n*-type silicon wafers passivated with hydrogenated amorphous silicon films", *Proc. 29th IEEE PVSC*, New Orleans, Louisiana, USA, pp. 1246–1249.

[10] Plagwitz, H. et al. 2006, "A low-temperature passivation method for diffused phosphorus-as well as boron-emitters", *Proc. 21st EU PVSEC*, Dresden, Germany, pp. 688–691.

[11] Lauinger, T. et al. 1996, "Record low surface recombination velocities on 1 Ω cm *p*-silicon using remote plasma silicon nitride passivation", *Appl. Phys. Lett.*, Vol. 68, pp. 1232–1234.

[12] Schmidt, J. et al. 2004, "Recent progress in the surface passivation of silicon solar cells using silicon nitride", *Proc. 19th EU PVSEC*, Paris, France, pp. 391–396.

[13] Altermatt, P.P. et al. 2006, "The surface recombination velocity at boron-doped emitters: Comparison between various passivation techniques", *Proc. 21st EU PVSEC*, Dresden, Germany, pp. 647–650.

[14] Plagwitz, H. 2007, "Surface passivation of crystalline silicon solar cells by amorphous silicon films", Ph.D. thesis, Dept. Mathematics and Physics, Gottfried Wilhelm Leibniz Universität Hannover, Germany.

[15] Hofmann, M. et al. 2009, "Recent developments in rear-surface passivation at Fraunhofer ISE", *Solar Energy Mater. & Solar Cells*, Vol. 93, pp. 1074–1078.

[16] Ulyashin, A. et al. 2007, "Optical and passivation properties of double layer a-Si:H/$SiN_x$ anti-reflective coatings for silicon solar cells", *Proc. 22nd EU PVSEC*, Milan, Italy, pp. 1690–1693.

[17] Gatz, S. et al. 2008, "Thermal stability of amorphous silicon/silicon nitride stacks for passivating crystalline silicon solar cells", *Appl. Phys. Lett.*, Vol. 93, p. 173502.

[18] Schmidt, J. et al. 2008, "Surface passivation of high efficiency silicon solar cells by atomic-layer-deposited $Al_2O_3$", *Prog. Photovolt: Res. Appl.*, Vol. 16, pp. 461–466.

[19] Schmidt, J., Veith, B. & Brendel, R. 2009, "Effective surface passivation of crystalline silicon using ultrathin $Al_2O_3$ films and $Al_2O_3/SiN_x$ stacks", *physica status solidi* (RRL), Vol. 3, pp. 287–289.

[20] Veith, B. et al. 2011, "Comparison of the thermal stability of single $Al_2O_3$ layers and $Al_2O_3/SiN_x$ stacks for the surface passivation of silicon", *Energy Procedia*, Vol. 8, pp. 397–312.

[21] Mäckel, H. & Lüdemann, R. 2002, "Detailed study of the composition of hydrogenated $SiN_x$ layers for high-quality silicon surface passivation", *J. Appl. Phys.*, Vol. 92, pp. 2602–2609.

[22] Dauwe, S. 2004, "Low-temperature surface passivation of crystalline silicon and its application to the rear side of solar cells", Ph.D. thesis, Dept. Physics, Gottfried Wilhelm Leibniz Universität Hannover, Germany.

[23] Beyer, W. 2003, "Diffusion and evolution of hydrogen in hydrogenated amorphous and microcrystalline silicon", *Solar Energy Mater. & Solar Cells*, Vol. 78, pp. 235–267.

[24] Gatz, S. et al. 2012, "Firing stability of $SiN_y/SiN_x$ stacks for the surface passivation of crystalline silicon solar

STRAMAMPS
DER Sondermaschinenbauer

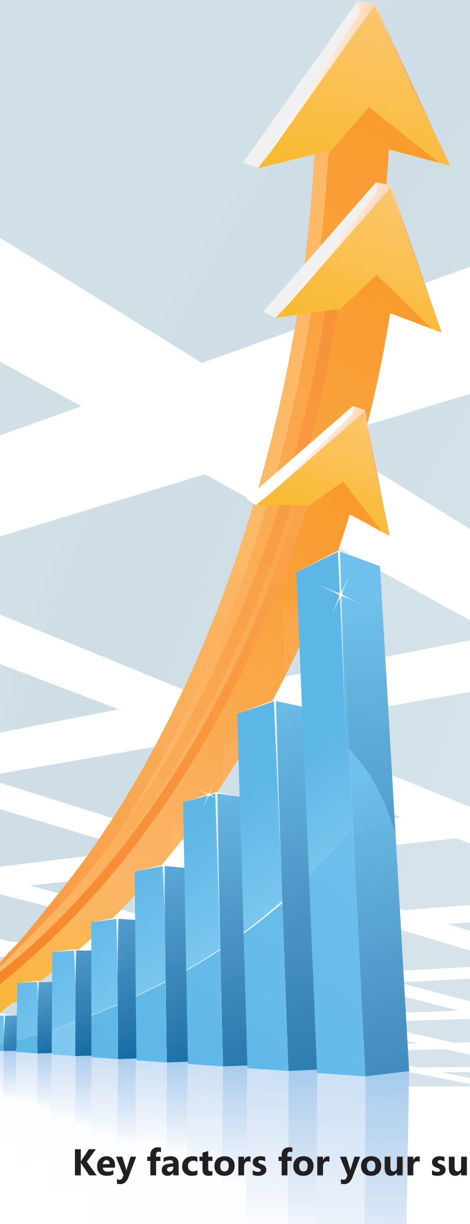

# Sun simulator ProMoSim®*evo³* maximizes the value of your PV cells and modules

**ProMoSim®*evo³*** is the state-of-the-art test system for photo-voltaic cells as well as solar modules. The large-surface, multi-coloured LED array offers short pulsed flash and continuous light.

Testing solar cells with LED technology

## Key factors for your success

- **Highly accurate efficiency measurement**
  Precise Pmpp selection due to minimum non-uniformity (<0.4%) and excellent spectral match (+/- 10%).
- **Simulating real sun light**
  Class A+A+A+ simulator offering steady state mode in addition to flash mode. Intensity variation and programmable spectra allow for additional tests e.g. darkfield measurements at multi junction cells.
- **Very high throughput**
  No recharging necessary. Therefore extremely short repetition rate of <0.5 sec and short flash rate. Immediate and stable light, no shutter or trigger limits needed.
- **Very long LED life time**
  LED arrays last more than 50.000.000 flashes without degradation effects, continuously keeping long term temporal instability of irradiance below 0.5%, thus providing a constant and reliable spectrum.

**Strama-MPS** Maschinenbau GmbH & Co. KG
Ittlinger Straße 195 · 94315 Straubing
Tel.: +49 9421 739-0
Fax: +49 9421 739-247
solar@strama-mps.de
www.strama-mps.de

**Moving the limits together. Constantly.**

cells", *Solar Energy Mater. & Solar Cells*, Vol. 96, pp. 180–185.
[25] Seiffe, J. et al. 2011, "Surface passivation of crystalline silicon by plasma-enhanced chemical vapor deposition double layers of silicon-rich silicon oxynitride and silicon nitride", *J. Appl. Phys.*, Vol. 109, p. 034105.
[26] Sinton, R.A. & Cuevas, A. 1996, "Contactless determination of current–voltage characteristics and minority-carrier lifetimes in semiconductors from quasi-steady-state photoconductance data", *Appl. Phys. Lett.*, Vol. 69, pp. 2510–2512.
[27] Nagel, H., Berge, C. & Aberle, A.G. 1999, "Generalized analysis of quasi-steady-state and quasi-transient measurements of carrier lifetimes in semiconductors", *J. Appl. Phys.*, Vol. 86, pp. 6218–6221.
[28] Dullweber, T. et al. 2011, "Towards 20% efficient large-area screen-printed rear-passivated silicon solar cells", *Prog. Photovolt.*, DOI:10.1002/pip.1198.
[29] Herguth, A. et al. 2006, "Avoiding boron-oxygen related degradation in highly boron doped Cz silicon", *Proc. 21st EU PVSEC*, Dresden, Germany, pp. 530–537.
[30] Lim, B., Bothe, K. & Schmidt, J. 2008, "Deactivation of the boron–oxygen recombination center in silicon by illumination at elevated temperature", *physica status solidi* (RRL), Vol. 2, pp. 93–95.
[31] Gatz, S. et al. 2011, "19.4%-efficient large-area fully screen-printed silicon solar cells", *physica status solidi* (RRL), Vol. 5, No. 4, pp. 147–149.
[32] Gatz, S., Dullweber, T. & Brendel, R. 2011, "Evaluation of series resistance losses in screen-printed solar cells with local rear contacts", *IEEE J. Photovoltaics*, Vol. 1, pp. 37–42.
[33] Schmidt, J., Kerr, M. & Cuevas, A. 2001, "Surface passivation of silicon solar cells using plasma-enhanced chemical-vapour-deposited SiN films and thin thermal SiO2/plasma SiN stacks", *Semicond. Sci. Technol.*, Vol. 16 (2001), pp. 164–170.

## About the Authors

**Sebastian Gatz** studied physics at universities in Regensburg and Dublin, and received his physics diploma from the Technical University of Munich in 2006. Since 2007 Sebastian has been a Ph.D. candidate at ISFH, where he is carrying out research on front- and rear-surface passivated screen-printed solar cells in the solar cell production processes group of Dr. Dullweber.

**Jan Schmidt** is head of the PV department at ISFH and professor of physics at LUH. He received his Ph.D. degree from LUH in 1998. Dr. Schmidt's current research interests include the analysis and manipulation of defects in silicon materials and the development of novel characterization techniques, as well as the development and evaluation of novel surface passivation methods for silicon solar cells.

**Boris Veith** studied physics at LUH and received his diploma degree in 2010. His thesis topic was a passivation method for silicon solar cells using aluminium oxide. Boris is currently employed as a scientist in the materials research group at ISFH, where he is involved with evaluating novel surface passivation methods for silicon solar cells.

**Thorsten Dullweber** leads the ISFH solar cell production processes research group, which focuses on process and efficiency improvements of industrial-type silicon solar cells. In particular, current research work includes the optimization of screen-printing processes, dielectric rear-surface passivation and high-rate aluminium evaporation.

**Rolf Brendel** is the scientific director of ISFH. He received his Ph.D. in materials science, specializing in infrared spectroscopy, from the University of Erlangen. Dr. Brendel's current research focuses on the physics and technology of crystalline silicon solar cells. Since 2004 he has been a full professor at the Institute of Solid-State Physics at LUH.

## Enquiries

S. Gatz
Institute for Solar Energy Research Hamelin (ISFH)
Am Ohrberg 1
D–31860 Emmerthal
Germany

Tel: + 49 5151 999 314
Fax: + 49 5151 999 400
Email: s.gatz@isfh.de

# Industrial n-type solar cells: Towards 20% efficiency

**Ingrid Romijn**, ECN Solar Energy, Petten, The Netherlands, **Lang Fang**, Yingli Solar, Baoding, China, & **Ard Vlooswijk**, Tempress Systems BV, Vaassen, The Netherlands

ABSTRACT

This paper presents examples of recent process developments at ECN in silicon solar cells on n-type monocrystalline base material. For all PV manufacturers, the challenge is to increase module efficiencies while maintaining low production cost. An effective way to move to higher and more stable efficiencies, using low-cost industrial-type processing, is n-type solar cell technology. The solar cell considered in this paper is the n-pasha cell – a bifacial solar cell with homogeneous diffusions and screen-printed metallization. The n-pasha cell is currently produced on an industrial scale by Yingli Solar; in 2011 a maximum solar cell conversion efficiency of 19.97% was obtained using this cell concept on 239cm² n-type Cz at the ECN laboratory. The focus of the paper will be increasing efficiency by optimization of the cell process, in particular the front-side metallization, and by improvements to the rear-surface passivation. These two steps have contributed to an increase in efficiency of 0.8%, allowing cell efficiencies of 20% to be reached.

## n-type silicon solar cells

More than 85% of the solar cells currently produced worldwide make use of crystalline silicon, and most are based on p-type wafers [1]. The most common multi- and monocrystalline solar cells used in the majority (~90%) of PV modules are made by applying a phosphorous-diffused emitter and an aluminium back-surface field to a p-type wafer. Efficiencies obtained are of the order of 17% and 18%, respectively, for multicrystalline and monocrystalline p-type wafers. Sunpower and Sanyo use n-type wafers as base material for their high-efficiency cells: interdigitated back-contacted (IBC) cells in the case of Sunpower [2], and heterojunction with intrinsic thin (HIT) layer cells in the case of Sanyo [3]. Efficiencies above 23% have been reported with both cell types [4]. Yingli Solar also took high-efficiency cells based on n-type wafers into mass production in 2010, under the type name 'PANDA' and average efficiencies of about 18.9% were achieved in their production in 2011 [5].

The use of n-type material has several advantages over the use of p-type. First, there is no boron dopant in n-type material; hence formation of boron–oxygen (B–O) complexes will be negligible [6]. B–O complexes are formed upon exposure to light in p-Cz material that is relatively rich in oxygen, and degrade the bulk lifetime of the material. This severely limits the efficiencies that can be obtained with these wafers [7,8]. Second, n-type material has been found to be much less sensitive to transition metal impurities such as, for example, Fe [9]. This could give the n-type material a higher tolerance for variations in the feedstock purity [10].

Manufacturing solar cells based on n-type wafers poses some additional challenges compared to the processing of p-type material. For n-type cells, boron emitter diffusion requires higher temperatures than phosphorous emitter diffusions common to p-type cells. Furthermore, in 'standard' p-type cells, the $p^+$ back-surface field (BSF) is formed by alloying the aluminium back side, while in n-type cells the $n^+$ BSF is usually a phosphorous diffusion. Formation of good emitter and BSF for n-type cells is therefore a challenge. In addition, the conventional method of passivating the emitter by silicon nitride ($SiN_x$) is less effective on the $p^+$ boron emitter [11]. Several methods have recently become available to passivate boron emitters effectively at relatively low temperatures. One that has received considerable attention is the application of an $Al_2O_3$ layer by atomic layer deposition (ALD). This layer introduces fixed negative charges at the $Al_2O_3$/Si interface [12,13]. ECN has developed a simple wet chemical process followed by a plasma-enhanced chemical vapour deposition (PECVD) that forms a $SiO_x/SiN_x$ passivation stack on the boron emitter, having similar passivation performance to passivation by $Al_2O_3$ layers [14,15].

"The n-pasha cell has an open rear side and is therefore a bifacial cell, which produces additional power output when incorporated into a module with a transparent rear side."

## ECN's n-pasha cell concept

Fig. 1 shows the basic configuration of the n-pasha (**p**assivated **a**ll **s**ides **H**-p**a**ttern) solar cell. The n-pasha cell has an open rear side and is therefore a bifacial cell, which produces additional power output when incorporated into a module with a transparent rear side [15]. The bifacial characteristic distinguishes it both from conventional (full aluminium back side) p-type solar cells and from high-efficiency passivated emitter and rear contact (PERC) n-type or p-type cells. Bifacial cells benefit from enhanced internal reflection, which is better for a dielectric rear coating than for a full aluminium alloy at the rear. Both the front and rear sides of n-pasha cells feature H-grid metallization patterns; Yingli's PANDA cells are also based on this structure.

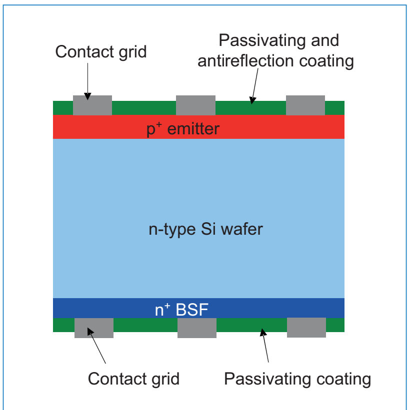


**Figure 1. Cross section of the ECN n-pasha cell, featuring an n-type Cz Si wafer with a boron $p^+$ emitter and phosphorous $n^+$ BSF. Yingli's PANDA cells are also based on this structure.**

The n-pasha cells are fabricated on 6-inch semi-square n-type Cz wafers. The first processing step is to texture the wafers with random pyramids using alkaline etching. The boron emitter and phosphorous BSF are formed using an industrial tube furnace from Tempress

[16]. A 60Ω/sq emitter is made using $BBr_3$ as a precursor. The BSF is made using $POCl_3$ as a precursor and provides additional lateral conductivity at the rear side. This results in a good fill factor (*FF*) despite the open-rear-side metallization, even for cells processed on high-resistivity (~8Ωcm) base material.

The front and rear sides are both coated with $SiN_x$ layers for passivation and antireflective purposes. The metallization is applied to both sides using screen printing, and the contacts on the emitter and BSF are formed during a single co-firing step. The front and rear metallization can be directly soldered, so no additional metallization step is necessary to allow interconnection into a module. The open rear side also ensures that there will be no bending of the cells when (very) thin wafers are used, as is the case for the full aluminium BSF on p-type cells. All processing steps used for the n-pasha cell are compatible with production on an industrial scale.

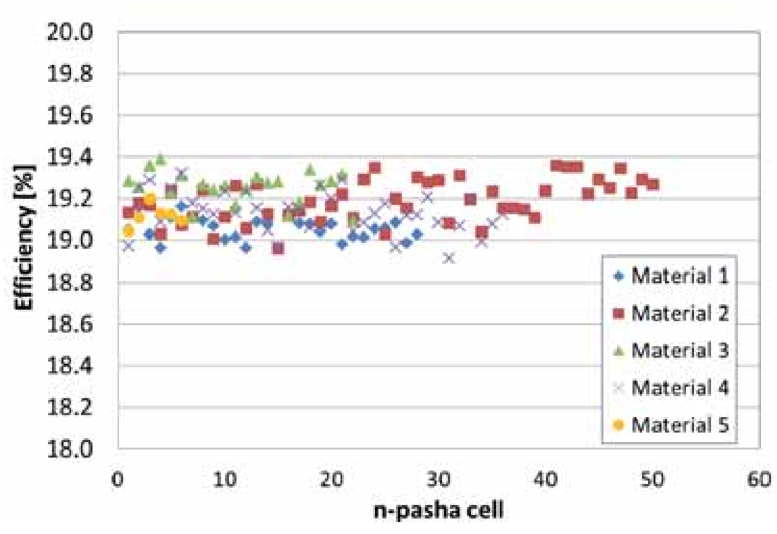


**Figure 2. Efficiency distribution of n-pasha cells on Cz material from five different suppliers, with resistivity of the base material ranging from 1.5 to 10Ωcm. The index of the cells in each group is indicated on the x-axis. Efficiencies vary between 19.0 and 19.4%, indicating that high-efficiency n-pasha cells can be made with wafers from a variety of commercial material suppliers.**

## Industrialization of n-pasha

For industrialization, a cell concept needs to be applicable to material from different suppliers. At ECN several batches of standard n-pasha cells were processed from n-type Cz wafers from different commercial wafer producers. The base resistivity of the materials ranged from 1.5 to 10Ωcm. The efficiency distribution of n-pasha cells on material from five different wafer suppliers is shown in Fig. 2. The efficiencies obtained range from 19.0 to 19.4%, indicating that high-efficiency n-pasha cells can be made, with the efficiency being largely independent of the base material.

The n-pasha cell process has been developed in ECN's pilot line. In June 2009, ECN, Amtech Systems and Yingli Green Energy announced a three-party research agreement, to further develop and industrialize the n-type open-rear-side cell. The best independently confirmed (by ISE CalLab) efficiency of n-pasha cells processed in the Yingli cell line is 19.5% (on 239cm²) [5].

## Efficiency improvements to n-pasha cells

During the early stages of development of the n-pasha concept at ECN, attention was mostly focused on optimizing the front and rear sides, i.e. the boron diffusion and the front- and rear-surface passivation [15,17,18]. In this paper the results of two recent efficiency enhancements for n-pasha cells will be presented. The first one is stencil printing of the front-side metallization (an option generically available to p-type as well as n-type solar cells); and the second is improved phosphorous BSF (specific to n-pasha cells).

### Front-side metallization

Over the past years ECN has developed a two-step stencil-printing metallization [19]. By using a single-layer stencil and a high aspect ratio paste, the deposition of very high, fine lines has been demonstrated (see Fig. 3). However, the completely open nature of the fingers in the stencil requires a two-step process in which fingers are stencilled and busbars are printed separately.

Applying the two-step process to the n-pasha cells, 55μm-wide fingers with an aspect ratio of over 0.5 (height/width) have been achieved, as can be seen in Fig. 3. The metal coverage and therefore shading of the front surface can be reduced from approximately 7.5% to 5.5%, i.e. by around 2%. The line definition is also much better using stencil printing (see Fig. 4).

A change of equipment is not required, but the metallization paste has to be optimized for stencil printing. The reduced metallization coverage will result in an increase in short-circuit current ($I_{sc}$) due to a larger active area of the solar cell, as well as a rise in open-circuit voltage ($V_{oc}$) due to the smaller contact area. The smaller contact area reduces the contribution of contact recombination to $J_{0front}$, resulting in an overall reduction of dark saturation current. The smaller contact area may result in a higher resistive loss due to contact resistance, but in our experience the area-specific contact resistance of

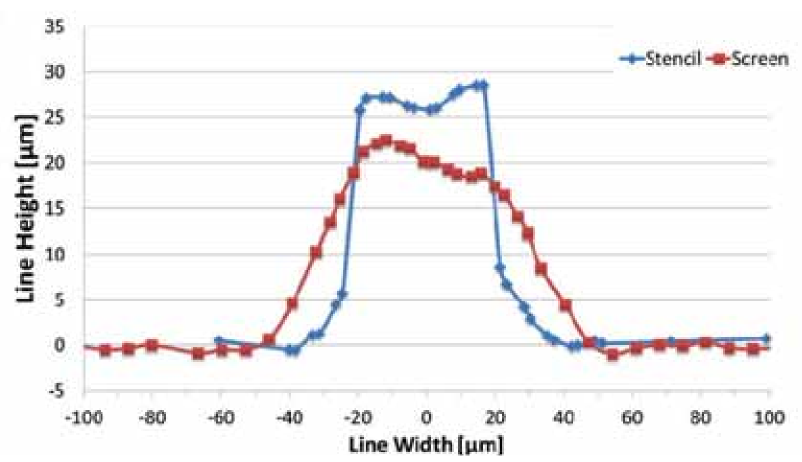


**Figure 3. Measured cross sections of two metal fingers: deposited using screen printing (red) and deposited using stencilling (blue).**

stencil-printed fine lines is slightly better than for screen-printed normal lines.

Several tests of stencil-printed front grids for n-pasha cells have been performed in order to investigate optimized pastes and tune the stencil parameters. The averaged $I_{sc}$ and $V_{oc}$ results from the most recent experiment between a group with a standard screen-printed and a stencil-printed front-side print are shown in Fig. 5. Because of the reduced metal coverage, the *FF* is reduced by approximately 0.5% relative for the stencil print due to increased line resistance (see Table 1). However, this is more than compensated for by the gain in $I_{sc}$ and $V_{oc}$, giving rise to an increase in efficiency of around 0.4% absolute.

"The resulting gain in efficiency using a stencil print is around 2% relative, which equates to an increase of almost 0.4% absolute for a 19% n-pasha cell."

The relative gains in $I_{sc}$ and $V_{oc}$ and relative losses in *FF* for stencil print vs. screen print are summarized in Table 1 from three different experiments. The resulting gain in efficiency using a stencil print is around 2% relative, which equates to an increase of almost 0.4% absolute for a 19% n-pasha cell. An additional attractive feature of stencil printing is that the silver consumption can be reduced by 10 to 20% compared to (single print) screen printing.

### Rear-surface passivation

The surface recombination of the non-metallized area on the rear surface depends on two factors: the surface doping concentration determined by the BSF diffusion, and the surface passivation by the deposited dielectric layer. The two are interrelated: a higher surface doping concentration typically results in higher recombination velocities at the interface with the dielectric layer. Moreover, Auger recombination takes place in the doped layer, which is proportional to the square of the doping concentration (in the appropriate low-level injection regime). Free carrier absorption also occurs in the doped layer, which will increase as doping increases. Generally, a lower surface doping concentration will result in higher $J_{sc}$ and $V_{oc}$.

Two further constraints on the doping profile are: 1) the requirement for good contact resistance with the rear metallization; and 2) the requirement for sufficient lateral conductance between the metal fingers to ensure a high *FF*. An industrial optimization of all these effects is being pursued: as a first step, the phosphorous BSF profile has been optimized.

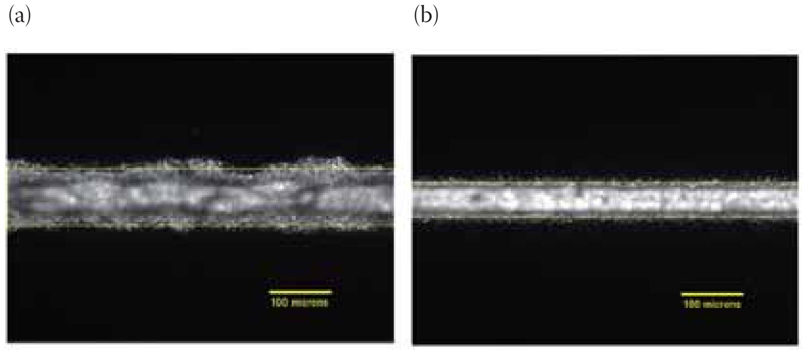


Figure 4. Microscope picture of (a) a screen-printed finger, and (b) a stencil-printed finger.

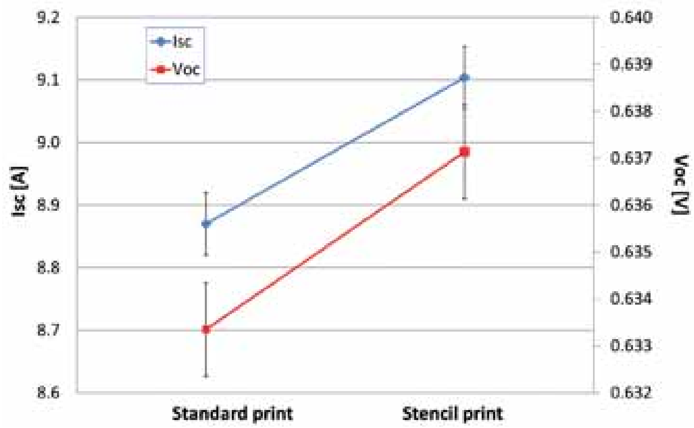


Figure 5. Averaged $I_{sc}$ and $V_{oc}$ values for groups of cells with a standard screen-printed front side and a stencilled front side.

| | $I_{sc}$ (%) | $V_{oc}$ (%) | *FF* (%) | $\eta$ (%) |
|---|---|---|---|---|
| Experiment 1 | 1.5 | 0.6 | –0.4 | 1.9 |
| Experiment 2 | 2.6 | 0.5 | –0.9 | 2.2 |
| Experiment 3 | 2.2 | 0.4 | –0.3 | 2.3 |

Table 1. Relative changes in *I-V* characteristics for stencil print vs. screen print from three experiments.

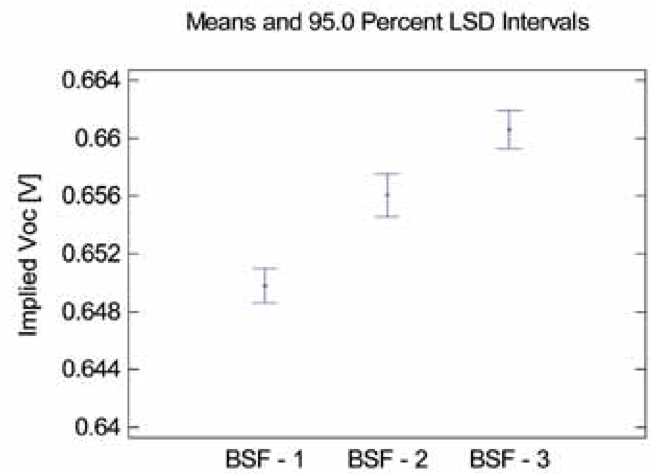


Figure 6. Implied $V_{oc}$ values of cells for three different BSF profiles with increasing $R_{sheet}$.

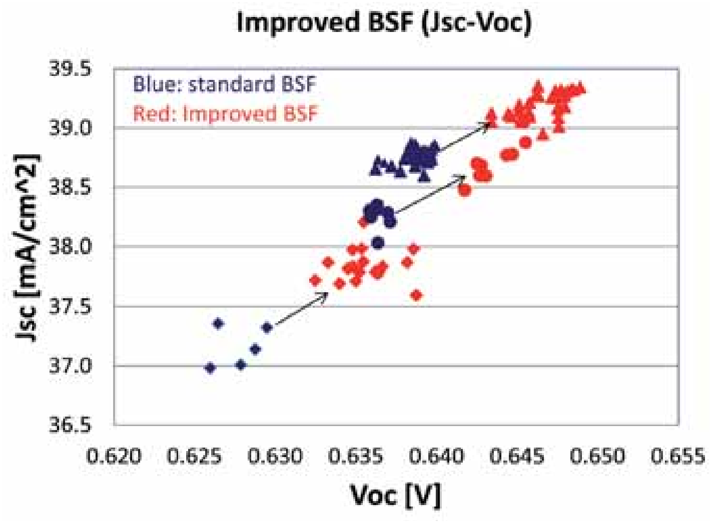


Figure 7. Current and voltage gains observed for experiment runs using a variety of base materials (represented by different symbols). The colours depict the type of BSF: blue for standard (BSF-1 in Fig. 6) and red for improved (BSF-3 in Fig. 6). The arrows are a guide for the eye to indicate the improvement within an experiment.

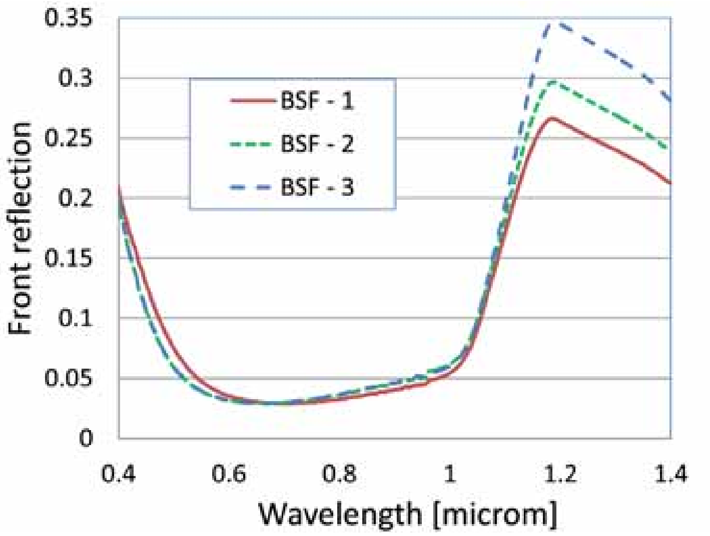


Figure 8. Front reflection measurements of cells with three different BSF profiles. Above 1000nm, the increase in reflection is clear, indicating a decrease in free-carrier absorption and an increase in internal rear reflection. This results in an increase in $J_{sc}$.

| | $I_{sc}$ [A] | $J_{sc}$ [mA/cm$^2$] | $V_{oc}$ [V] | $FF$ [-] | $\eta$ [%] |
|---|---|---|---|---|---|
| Group 1 (standard) | | | | | |
| avg | 9.26 | 38.7 | 0.640 | 0.784 | 19.4 |
| max | 9.27 | 38.8 | 0.640 | 0.787 | 19.5 |
| Group 2 (improved) | | | | | |
| avg | 9.38 | 39.2 | 0.648 | 0.780 | 19.8 |
| max | 9.40 | 39.3 | 0.649 | 0.783 | 20.0 |

Table 2. *I-V* results for a reference group and a group with improved rear surface. Both groups had a stencilled front metal grid.

Fig. 6 shows the implied $V_{oc}$ values of cells without metallization for three different phosphorus BSF doping profiles with increasing sheet resistivity $R_{sheet}$ (lower doping). The rest of the processing is the same. For BSF profile 3, a gain of implied $V_{oc}$ of more than 15mV is observed over the standard BSF profile 1.

On the cell level, the best BSF doping profile from the test was compared to the standard BSF profile. Fig. 7 shows the $J_{sc}$ and $V_{oc}$ data of the different experiment runs (again executed on n-type Cz from different suppliers). For each run (distinguished by different symbols), a standard group (blue) and a group with an improved rear surface (red) were processed. The gain in $J_{sc}$•$V_{oc}$ is around 3% relative, which was clearly reproducible for each run and independent of the material properties.

For each of the experiments, a gain of 8 to 10mV was observed for the cells with improved BSF profile; this increase in $V_{oc}$ can be explained by the improved rear-surface passivation. The difference in $V_{oc}$ improvements between cells with metallization (~8–10mV) and without metallization (15mV) can be explained by the contact recombination below the rear metal contacts. To optimize the rear surface further, reducing the metal fraction is clearly one option. Another possibility is improving the surface passivation itself by changing or adjusting the deposited dielectric layer.

In Fig. 7 an increase in $J_{sc}$ is observed for the improved BSF. This is partly due to improved rear-surface passivation, but also results from the reduction in free-carrier absorption. The measured front reflection of cells with three different BSF profiles is shown in Fig. 8: BSF-2 and BSF-3 show enhanced reflection above 1000nm. For the improved phosphorous profiles of BSF-2 and BSF-3, the free-carrier absorption is reduced and therefore more light is reflected from the rear, causing an increase in $J_{sc}$.

The *I-V* measurement results for one of the experiments aimed at improving BSF diffusion are shown in Table 2. In this experiment both groups had an improved front-side metallization using the stencil print as described earlier. This resulted in an average efficiency of 19.4% (19.5% maximum) for group 1 with a standard BSF. Group 2, with an improved rear surface, yielded significantly improved voltage $V_{oc}$ and current $J_{sc}$. Even though the *FF* is somewhat lower, an overall efficiency gain of 0.4% absolute is realized, leading to an average efficiency of 19.8%. A maximum efficiency of 20%, measured in-house, has been achieved.

As the cell is bifacial, the internal quantum efficiency (IQE) can be determined for both front and rear sides. The IQE graphs from the front side (Fig. 9a) show that the long wavelength response has improved, while with rear-side illumination (Fig. 9b) both long and short wavelength responses have improved. This is a clear indication of reduced rear-surface recombination and improved rear internal reflection, as was also confirmed by PC1D fits on these measurements.


bundle of energy loves regeneration
Innovative solutions from BASF ensure that solar panels remain full of energy even if the sun doesn't shine for brief periods. Our solutions and expertise cover the entire solar cell production process from wafer cutting to module framing. Sunlight can be efficiently turned into energy. At BASF, we create chemistry.
solar-cells@basf.com
BASF
The Chemical Company

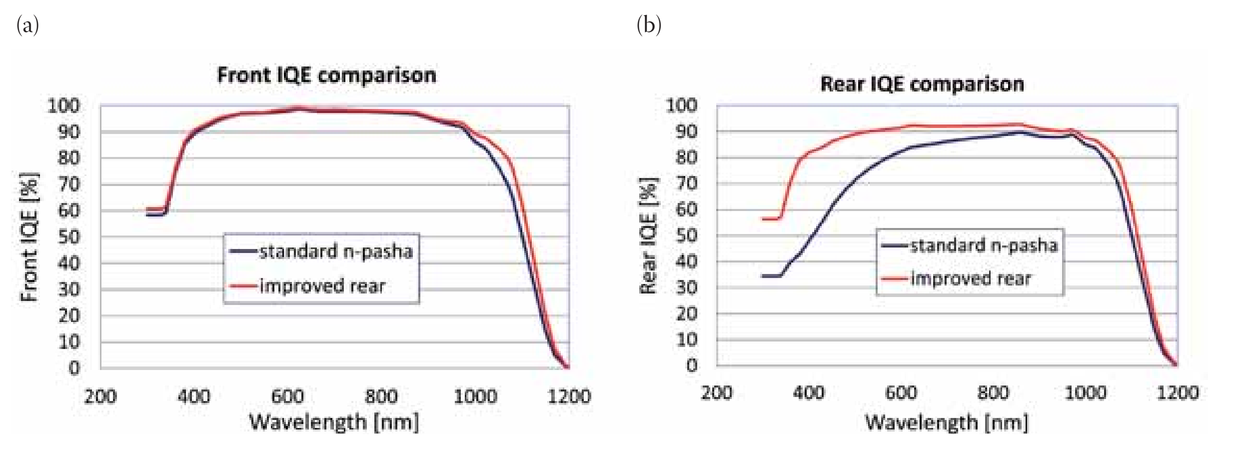


**Figure 9. (a) Internal quantum efficiency (IQE) measured from (a) the front, and (b) the rear. The difference for cells with an improved rear surface is clear in both graphs.**

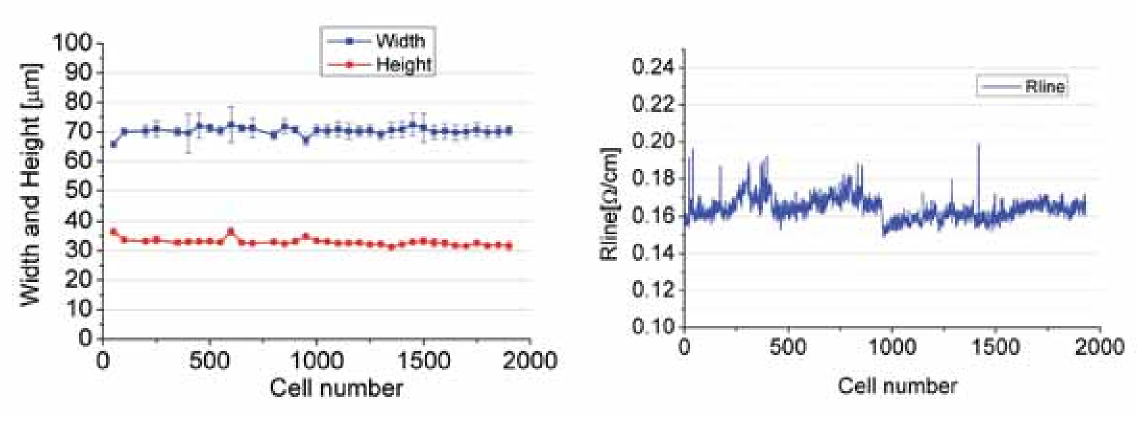


**Figure 10. Line resistance and line width and height of the stencilled fingers as a function of cell number for 2000 industrially processed solar cells.**

A two-dimensional model is currently being built to simulate the *I-V* and IQE characteristics of n-pasha cells, on the basis of input parameters such as diffusion profiles, surface recombination velocities and bulk lifetime. Use of this model will allow the current n-pasha cells to be accurately simulated, as well as providing insight into how the efficiency might be improved even further.

## Industrial application of the new process steps

In order to test the industrial application of the two-step stencil printing concept, a limited endurance test was conducted in a production environment. The standard two-step stencil process as presented by Heurtault et al. [19] was selected for this test.

| Width [µm] | Height [µm] | $R_{line}$ [mΩ/cm] |
|---|---|---|
| 70.4±1.3 | 32.9±1.1 | 164±11 |

**Table 3. Average geometrical and electrical results for stencilled fingers.**

Approximately 2000 cells were printed using one stencil, and one screen was used to print the busbars. Testing was done in two subsequent runs; the stencil was cleaned after the first half of the test and reused in the next. Line resistance was monitored for all cells, and line width and height for every 50 cells, with width and height values being averaged from nine measurement points per cell. The results are shown in Fig. 10 and Table 3.

Throughout the test, the geometry of the lines remained within specifications, with a very low standard deviation; the line resistance was stable, staying below 200mΩ/cm. The stencil did not show any signs of wear or tear and kept its integrity during the entire test. This first trial is promising as regards the robustness of the stencil process, but a more extensive test will be necessary to quantify the lifetime of the stencil and the print quality on longer runs.

The improved BSF has not yet been tested on very large quantities of cells. However, as can be seen from Fig. 7, the process has yielded quite stable results on different selections of materials, with similar increases in $J_{sc}$ and $V_{oc}$ in all cases.

## Further improvements

The next steps towards achieving efficiencies higher than 20% for n-type pasha cells will involve:

- Decreasing the rear-surface metallization. This will not only improve the efficiency by decreasing the drop in $V_{oc}$ from the implied $V_{oc}$ values, but also improve the cost of ownership by decreasing silver consumption.
- Optimizing rear-side passivation layers, which is expected to further increase the benefit in $J_{sc}$ and $V_{oc}$ from the tuned BSF.
- Improving the emitter profile and optimizing further the front-surface passivation. With better rear-surface and reduced front-side metallization, improvements to the front side will have a beneficial impact on efficiency.
- Investigating a different cell architecture. One way to further reduce the front metal coverage, and thereby improve $I_{sc}$ and $V_{oc}$ without *FF* loss, is to use a metal-wrap-through (MWT) cell concept [20]. Another advantage of this

cell concept is the smaller losses in *FF* when the cells are interconnected into a module. Yingli and ECN have published results of their ongoing development in this area [21,22].

Cell Processing

"Combining the use of stencilled fingers and an optimized BSF diffusion has made it possible to achieve an efficiency of 20% for n-pasha cells manufactured using industrial processes."

## Conclusions

This paper has presented two improved processes that have been recently tested on ECN's n-pasha cell concept. By using stencilled fingers, the front-side metallization has been reduced by 2%, resulting in an improvement of around 0.4% absolute in efficiency. Furthermore, the BSF diffusion has been optimized in terms of passivation and optics, also resulting in a gain of 0.4% absolute in efficiency. Combining the use of stencilled fingers and an optimized BSF diffusion has made it possible to achieve an efficiency of 20% for n-pasha cells manufactured using industrial processes.

The two-step stencil process has been successfully tested on a large number of cells in a production environment. The performance remained stable, and the stencil did not show any signs of wear, demonstrating its industrial applicability.


## Acknowledgements

T. Burgers, B. Geerligs, K. Tool, A. Carr, A. Gutjahr, D. Saynova, B. Heurtault, J. Anker, M. Koppes, X. Jingfeng, L. Gaofei, X. Zhuo, W. Hongfang, H. Zhiyan and P. Venema are gratefully acknowledged for their contributions to this paper.


## References


[1] Hirshman, W.P. 2009, "Little smiles on long faces (cell production 2008: survey)", *Photon Inter.* (March), pp. 170–206.

[2] Sunpower [details online at http://us.sunpowercorp.com].

[3] Sanyo [details online at http://www.sanyo.com/solar].

[4] Cousins, P.J. et al. 2011, "Generation 3: Improved performance at lower cost", *Proc. 35th IEEE PVSC*, Honolulu, Hawaii, USA, pp. 275–278.

[5] Burgers A.R. et al. 2011, "19.5% efficient n-type Si solar cells made in production", *Proc. 26th EU PVSEC*, Hamburg, Germany.

[6] Saitoh, T. et al. 2000, "Suppression of light-induced degradation of minority carrier lifetimes in low-resistivity Cz-silicon wafers and solar cells", *Proc. 16th EU PVSEC*, Glasgow, UK, pp. 1206–1209.

[7] Das, A. & Rohatgi, A. 2011, "The impact of cell design on light induced degradation in p-type silicon solar cells", *Proc. 37th IEEE PVSC*, Seattle, Washington, USA.

[8] Schmidt, J. & Hezel, R. 2002, "Light-induced degradation in Cz silicon solar cells: Fundamental understanding and strategies for its avoidance", *Proc. 12th Worksh. Cryst. Si. Sol. Cell Mater. & Process.*, Golden, Colorado, USA.

[9] Macdonald, D. & Geerligs, L.J. 2004, "Recombination activity of interstitial iron and other transition metal point defects in p- and n-type crystalline silicon", *Appl. Phys. Lett.*, Vol. 85, pp. 4061–4063.

[10] Cuevas., A. et al. 2002, "Millisecond minority carrier lifetimes in n-type multicrystalline silicon", *Appl. Phys. Lett.*, Vol. 81, pp. 4952–4954.

[11] Altermatt, P.P. et al. 2006, "The surface recombination velocity at boron-doped emitters: Comparison between various passivation techniques", *Proc. 21st EU PVSEC*, Dresden, Germany, pp. 647–650.

[12] Hoex, B. et al. 2007, "Excellent passivation of highly doped p-type Si surfaces by the negative-charge-dielectric $Al_2O_3$", *Appl. Phys. Lett.*, Vol. 91, p. 112107.

[13] Hoex, B. et al. 2008, "On the c-Si surface passivation mechanism by the negative-charge-dielectric $Al_2O_3$", *J. Appl. Phys.*, Vol. 104, p. 113703.

[14] Mihailetchi, V.D. et al. 2008, "Nitric acid pretreatment for the passivation of boron emitters for n-type base silicon solar cells", *Appl. Phys. Lett.*, Vol. 92, p. 63510.

[15] Mihailetchi, V.D. et al. 2010, "Screen-printed n-type silicon solar cells for industrial application", *Proc. 25th EU PVSEC*, Valencia, Spain, pp. 1446–1448.

[16] Komatsu, Y. et al. 2009, "Homogeneous p+ emitter diffused using boron tribromide for record 16.4% screen-printed large area n-type mc-Si solar cell", *Solar Energy Mater. & Solar Cells*, Vol. 93, pp. 750–752.

[17] Naber, R.C.G. 2009, "ECN n-type silicon solar cell technology: An industrial process that yields 18.5%", *Proc. 34th IEEE PVSC*, Philadelphia, Pennsylvania, USA.

[18] Weeber A.W. 2009, "Status of n-type solar cells for low-cost industrial production", *Proc. 24th EU PVSEC*, Hamburg, Germany.

[19] Heurtault, B. & Hoonstra, J. 2010, "Towards industrial application of stencil printing for crystalline silicon solar cells", *Proc. 25th EU PVSEC*, Valencia, Spain.

[20] Weeber, A.W. 2006, "17% cell efficiencies on large back-contacted multi-crystalline silicon solar cells", *Proc. 21st EU PVSEC*, Dresden, Germany.

[21] Guillevin, N. et al. 2010, "High efficiency n-type metal wrap through Si solar cells for low-cost industrial production", *Proc. 25th EU PVSEC*, Valencia, Spain, pp. 1429–1431.

[22] Guillevin, N. et al. 2011, "Development towards 20% efficient n-type Si MWT solar cells for low-cost industrial production", *Proc. 26th EU PVSEC*, Hamburg, Germany.


## Enquiries


ECN Solar Energy
P.O. Box 1
NL-1755 ZG Petten
The Netherlands
Tel: +31 224 56 4959
Fax: +31 224 56 8214
Email: romijn@ecn.nl

Yingli Solar
3399 Chaoyang North Street
Baoding
China

Tempress Systems BV
Radeweg 31
8171 Vaassen
The Netherlands

# TCAD for PV: A fast method for accurately modelling metal impurity evolution during solar cell processing



**Douglas M. Powell**[1], **David P. Fenning**[1], **Jasmin Hofstetter**[1], **Jean-François Lelièvre**[2], **Carlos del Cañizo**[2] & **Tonio Buonassisi**[1]
[1]Massachusetts Institute of Technology, Cambridge, Massachusetts, USA; [2]Instituto de Energía Solar, Universidad Politécnica de Madrid, Madrid, Spain

## ABSTRACT
Coupled device and process simulation tools, collectively known as technology computer-aided design (TCAD), have been used in the integrated circuit industry for over 30 years. These tools allow researchers to quickly converge on optimized device designs and manufacturing processes with minimal experimental expenditures. The PV industry has been slower to adopt these tools, but is quickly developing competency in using them. This paper introduces a predictive defect engineering paradigm and simulation tool, while demonstrating its effectiveness at increasing the performance and throughput of current industrial processes. The impurity-to-efficiency (I2E) simulator is a coupled process and device simulation tool that links wafer material purity, processing parameters and cell design to device performance. The tool has been validated with experimental data and used successfully with partners in industry. The simulator has also been deployed in a free web-accessible applet, which is available for use by the industrial and academic communities.

## Introduction: why simulate metal impurities?

Computer simulation has transformed industries by allowing rapid, low-cost design iterations during product development. The photovoltaic industry has benefited from device simulators for over 25 years: some early examples include PC1D [1,2], AMPS-1D [3,4], and SCAPS [5,6]. These tools, especially PC1D, continue to have a large influence on the photovoltaics industry. While existing device simulators achieve their intended purpose, an integrated approach that considers the interdependency of processing and performance is superior. Technology computer-aided design (TCAD) tools provide these integrated capabilities. Initial codes were written over 30 years ago and tailored to specific applications in the semiconductor industry [7,8]. The PV industry has lagged behind the integrated circuit industry in the application of process modelling, but interest has recently increased with the availability of commercial packages targeting photovoltaics [9,10]. However, care must be taken when adapting existing tools, designed for the integrated circuit industry, to the PV industry, because of the inherently higher defect densities present in solar-grade silicon material.

The optimization of the time-temperature profile of phosphorus diffusion gettering (PDG) (Fig. 1) presents a useful application of process modelling [11]. In the as-grown wafer, many metal impurities are distributed inhomogeneously as interstitial point defects, found throughout the wafer, and metal-silicide precipitates, found mainly at structural defects such as dislocations and grain boundaries [12,13]. During the high-temperature plateau and cool-down of PDG, most interstitial metals – e.g. Cu, Fe and Cr – diffuse and segregate to the phosphorus-rich layer, because these species have a higher effective solubility in the *n*-type region than in the *p*-type bulk [14,15]. This decreases the bulk interstitial concentration below the solubility limit at the process temperature, causing metal precipitates to dissolve. The newly dissolved interstitial atoms can then diffuse to the emitter, driving further precipitate dissolution. By the end of the process, PDG generally reduces both total and interstitial metal concentrations and thereby increases cell performance. But the effectiveness of the gettering step critically depends on the time-temperature profile, and in particular on the cool-down rate, because the segregation coefficient, the ratio of the bulk and emitter solubilities, and the diffusivity of metal point defects are strong functions of temperature.

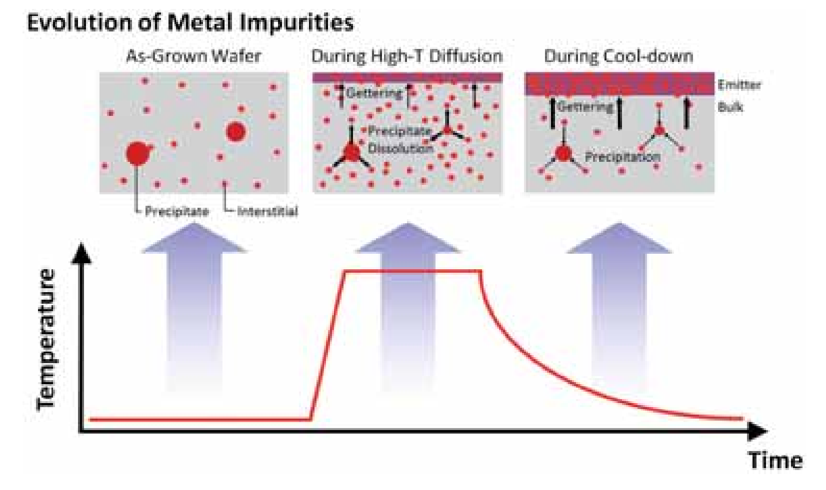


**Figure 1. Interplay between point defects and precipitates before phosphorus diffusion gettering, during diffusion and during cool-down.**

The PDG process must be optimized to address both the total concentration and the distribution of metal impurities for maximum improvement of minority carrier lifetime [14,16–18]. For example, total as-grown iron concentration is a better predictor of lifetime after gettering than the interstitial as-grown concentration (Fig. 2) [19]. Iron is of particular interest in silicon solar cells because it is typically the performance-limiting defect in as-grown materials [17,20]. Additionally, the concentration

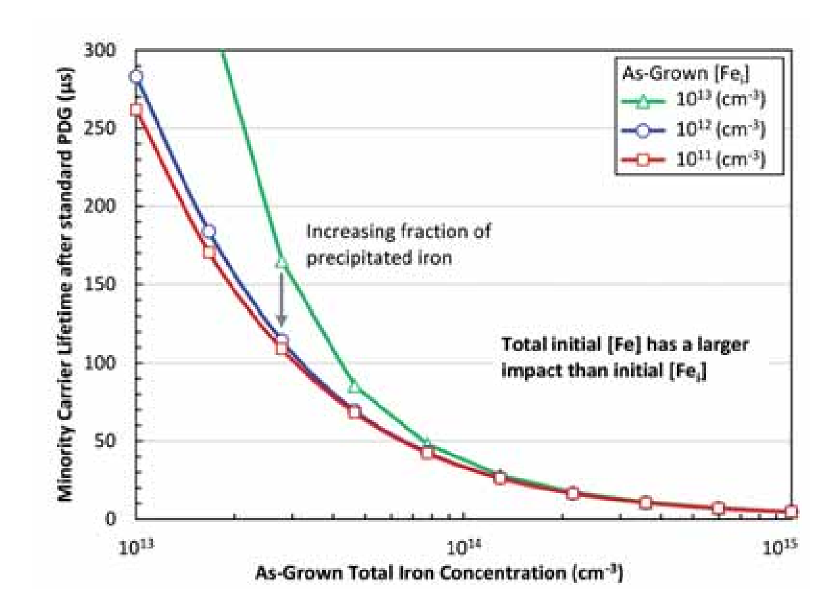


**Figure 2. After standard PDG, the bulk lifetime is affected primarily by the as-grown total iron concentration and secondarily by the as-grown interstitial iron concentration. Lifetime calculated with I2E simulation of standard PDG.**

of total iron, especially in cast silicon materials, can be orders of magnitude higher than the interstitial iron concentration [21]. The concentration of interstitial iron can be measured with relative ease by flash or thermal dissociation of Fe-B pairs and subsequent re-measurement of the minority carrier lifetime [22]. The total iron concentration, however, including both dissolved and precipitated iron, is more difficult (and costly) to measure, because metal concentrations are often at or below the detection limits of readily available mass-spectroscopy methods.

In a material with high total iron concentrations, for example wafers extracted from the top or borders of an ingot, large metal-silicide precipitates cannot be completely dissolved in many gettering processes, and act as recombination-active defects and sources of interstitials during subsequent high-temperature processing [23,24]. Additionally, standard gettering processes are less effective in multicrystalline silicon (mc-Si) than in monocrystalline silicon (mono-Si), as dislocations and grain boundaries impede the effective extraction of metal impurities in mc-Si material [25–27]. This contributes to the relatively low efficiencies of mc-Si devices compared to mono-Si [28].

The impurity-to-efficiency (I2E) simulator – a coupled device and process TCAD tool – has been developed to address the challenges of optimizing the time-temperature profile of solar cell processing to specific distributions and concentrations of iron in as-grown wafers [29]. This paper presents a description of the I2E simulator, a demonstration of the effectiveness of predictive defect engineering in industrial applications, and a discussion of the online implementation of the tool.

“The impurity-to-efficiency (I2E) simulator – a coupled device and process TCAD tool – has been developed to address the challenges of optimizing the time-temperature profile of solar cell processing to specific distributions and concentrations of iron in as-grown wafers.”

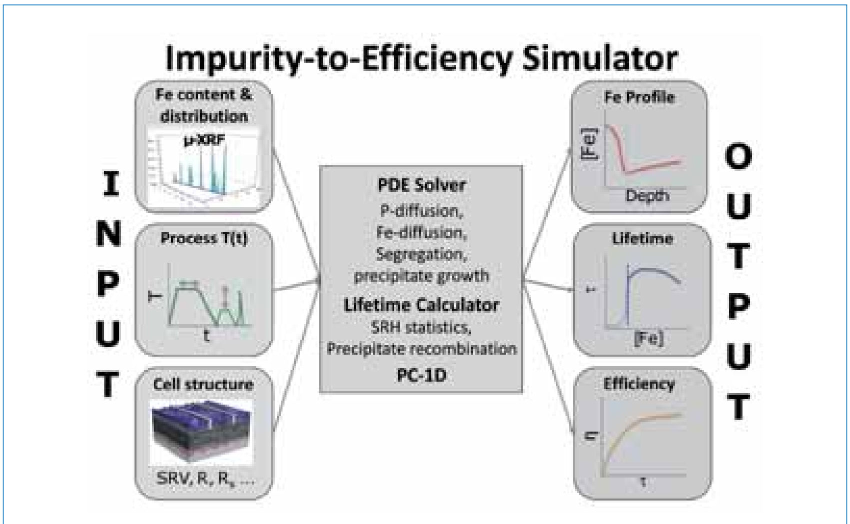


**Figure 3. The I2E simulator predicts the impact of as-grown iron impurities on final solar cell performance as a function of device processing conditions and cell architecture.**

## Method: predictive defect engineering

The I2E simulation tool has been developed to predict the impact of as-grown iron impurities on final solar cell performance as a function of device processing conditions and cell architecture (Fig. 3) [29]. The I2E simulator operates in 1D to capture the essential physics of iron interstitial gettering and precipitate dissolution with minimum computational expense, and is a compactly packaged deployment of previous simulation efforts [24,30–34]. The simulator consists of three components:

- A kinetic model for the diffusion and segregation of iron point defects, as well as iron-silicide precipitate dissolution and growth, during high-temperature solar cell processing.
- Minority carrier lifetime calculator as a function of both interstitial and precipitated iron concentration using a Shockley-Read-Hall recombination model for the iron interstitial concentration and an effective surface recombination value at iron-silicide precipitate and silicon interfaces.
- The industry standard 1D device simulator, PC1D, to determine device performance as a function of the device architecture, the calculated charge carrier lifetimes and the calculated phosphorus emitter profile [1,2].

The kinetic simulator requires the solution of three coupled non-linear partial differential equations [29]. The system of

equations contains steep concentration gradients and fast-moving fronts which are unstable with many numerical methods [35,36]. A solution algorithm was developed that can reliably solve the system of equations and supports the complete dissolution of precipitates. The algorithm generates an optimized spatial mesh distribution for the device. Execution times for practical problems range from 30 seconds to 30 minutes and depend strongly on the resolution of the mesh and complexity of the time-temperature profile. The simulator has been validated through comparisons with experimental data for gettering in mono-Si and mc-Si wafers [29].

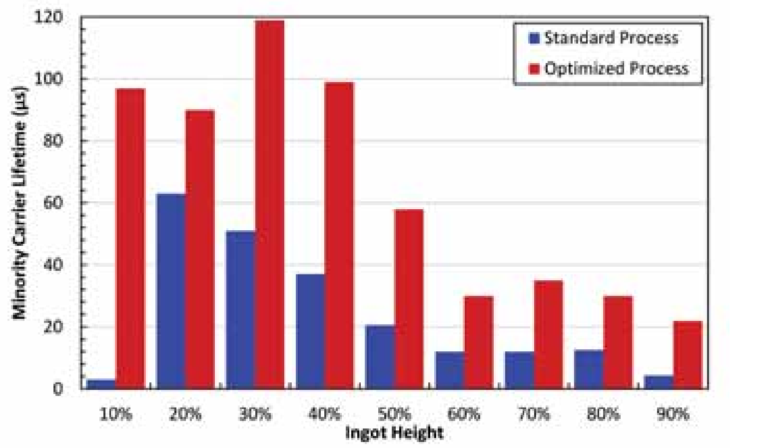


**Figure 4. Industrial application: increased ingot yield and material quality through process tailoring to specific impurity levels [38].**

## Results: improvements guided by predictive defect engineering

The I2E simulator has been successfully employed to optimize cell processing conditions with academic and industrial partners. The success described below demonstrates the potential of predictive defect engineering and the significant performance improvements that can be realized through tailoring processing conditions to specific material qualities.

### Process tailoring to specific impurity levels

Approximately half of the wafers produced by ingot casting contain some portion of so-called 'red zones' – regions of low minority carrier lifetime from high residual iron concentrations [37]. A few centimetres of 'red zone' material near the crucible wall are removed from the ingot prior to brick and wafer sawing, as the lifetime typically fails to improve during standard solar cell processing. A low-temperature anneal (LTA) was applied following phosphorus diffusion, to improve the gettering of residual iron. Results of the standard and optimized processes are shown in Fig. 4. Optimized phosphorus diffusion not only improved the minority carrier lifetime over the entire ingot, but also increased the lifetime of the bottom 10% of the ingot to an acceptable value, resulting in a yield increase. In the future, predictive simulation may be employed to optimize solar cell processing for different regions of the ingot, which have specific distributions and concentrations of iron [19].

### P-diffusion co-optimization of bulk lifetime and throughput

Cell manufacturers must optimize their manufacturing lines for both device performance and throughput, while accounting for varying impurity levels. Simulations were conducted for an industrial partner to optimize the hold temperature, plateau time and cooling time of a PDG gettering step for both bulk minority carrier lifetime and throughput. Many researchers have found that extending PDG, by slow cooling or LTA, can improve lifetime by reducing the concentration of interstitial iron [39–44]. More recently, it has been shown that a shorter anneal at lower temperatures can achieve much of the lifetime improvement of extended LTAs by forcing segregation of iron to the external gettering layer [45]. Learning from these previous efforts, in the current study the balance between extending the high-temperature hold time and/or the cooling time was investigated.

I2E simulations were performed to co-optimize lifetime and throughput (Fig. 5). The initial total iron concentration was $3 \cdot 10^{13}$ atoms/$cm^3$, with 10% of the iron present as Fe-B pairs [46] and the remainder homogeneously distributed as 20nm-radius precipitates [23,47]. First, the standard process of our industrial partner was simulated. Next, attempts were made to shorten the standard process while maintaining the existing hold temperature. Although the total process time was reduced in these cases, the lifetime provided was insufficient for acceptable device performance. Finally, an I2E optimized process was suggested that provided a sufficient bulk minority carrier lifetime for our industrial partner, while doubling throughput.

### Reduction in interstitial iron concentration after contact co-firing

To date, significant efforts have been made to optimize the time-temperature profile of PDG to reduce the impact of lifetime-limiting impurities in mc-Si material. In contrast, little attention has been paid to optimizing the time-temperature profile of contact firing in order to control metal impurities, despite it being the final high-temperature step of the solar cell fabrication process and the last opportunity to manipulate the metal impurity distribution. Contact firing is usually carried out at peak temperatures between 800°C and 900°C, and is therefore

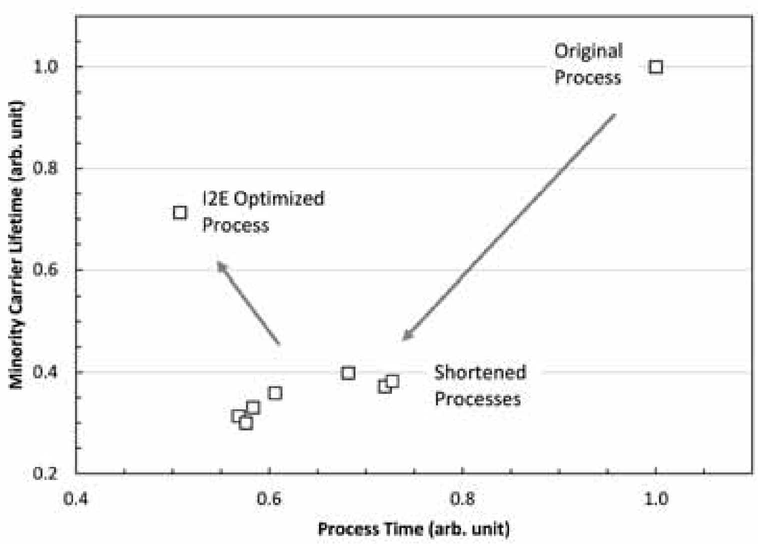


**Figure 5. Industrial application: P-diffusion co-optimization of bulk lifetime and throughput.**


Surprisingly Versatile
Multifunctional tool for everyman
Multifunctional tool for solar-experts
Laser Scribing with 355 to 1064 nm, Nanoseconds to Picoseconds
LPKF Presto – the all-rounder for superior laboratory-scale solar module structuring.
Transform your ideas into near-series quality thin-film modules: quickly, efficiently and flexibly.
www.lpkf-solarquipment.com
SNEC Shanghai: May 16 – 18 2012, Hall E3, Booth 808/809
LPKF SolarQuipment GmbH Mittelbergstraße 17 98527 Suhl, Germany Phone +49 (0) 3681-8924-0 info.solar@lpkf.com
LPKF
SolarQuipment


THE
WET PROCESSING
COMPANY
RENA
New RENA WaSep unit separates 3,000 - 6,000 wafers/hour
The latest generation RENA WaSep separates up to 6,000 wafers/h (double unit) with a breakage rate < 0.5 %. The world's only production proven wet wafer separation system.
More at www.rena.com

likely to produce the partial dissolution of metal precipitates, which can offset the reduction in concentration of dissolved impurities achieved during PDG [41,48].

The dissolution and gettering of iron during the co-firing step (Fig. 6) was examined with the I2E simulation tool [49]. First, a standard time-temperature profile of the co-firing step was simulated for a typical iron concentration and distribution in a P-diffused mc-Si wafer. Simulations were carried out for two different peak temperatures, 800°C and 900°C, followed by a rapid cool-down to room temperature. Simulations predict that, after firing at $T_{peak}$ = 800°C, the interstitial iron concentration remains constant (see blue bars in Fig. 6). After firing at $T_{peak}$ = 900°C, however, an increased interstitial iron concentration is predicted, indicating that the dissolution of iron precipitates increases at a higher temperature.

> "Experimental results confirm that a standard firing step can lead to material degradation, whereas material performance can be maintained or even enhanced during an extended firing step optimized with I2E."

Second, I2E simulations were performed to optimize the cool-down profile of the firing step to allow for effective gettering of $Fe_i$ atoms to the P-diffused layer. Simulation results suggest that an *extended* firing step, including an additional low-temperature plateau of less than 2 minutes, results in a lower interstitial iron concentration than the standard firing step for both peak temperatures (see red bars in Fig. 6). For $T_{peak}$ = 800°C, an extended firing step can even result in further reduced interstitial iron concentrations after standard PDG.

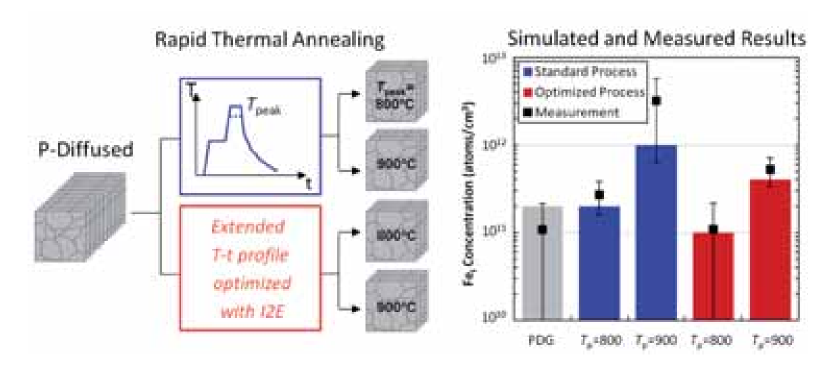


**Figure 6. Industrial application: reduction in iron precipitate dissolution during contact co-firing [49].**

Simulated trends are confirmed by experimental results, shown as black dots in Fig. 6. Several sets of *p*-type mc-Si wafers were P-diffused using a standard process, then divided into four groups and subjected to peak temperatures of 800°C or 900°C while following a standard firing or extended firing profile in a rapid thermal annealing (RTA) furnace. Interstitial iron concentrations and electron lifetimes were measured on P-diffused and fired wafers [49]. Experimental results confirm that a standard firing step can lead to material degradation, whereas material performance can be maintained or even enhanced during an extended firing step optimized with I2E.

## Discussion: online tool implementation

The simulator has been deployed in a free web-accessible applet [50], which is available for use by the industrial and academic communities. The applet's user interface, shown in Fig. 7, allows users to configure simulations and interpret output data. Required inputs to the tool include the time-temperature profile used during cell fabrication, the as-grown total and interstitial iron concentrations in the wafer, and the average precipitate radius. Impurity concentrations can be estimated from the ingot location of the wafer, or measured using a combination of Fe-B dissociation and mass-spectrometry methods such as ICP-MS [51]. Precipitate radius can be estimated as described in the literature [18,23]. Though only needed to simulate device performance, cell architecture is defined by a PC1D parameter (.prm) file.

The applet communicates with a dedicated high-performance server (maintained by the MIT Photovoltaic Research Laboratory in Cambridge) that carries out all calculations all input and output files after results are printed to the user. The applet was initially made available to a user group of approximately 80 individuals. Over 1300 simulations have now been performed during the first three months of operation, with users concentrated in North America, Europe and Asia.

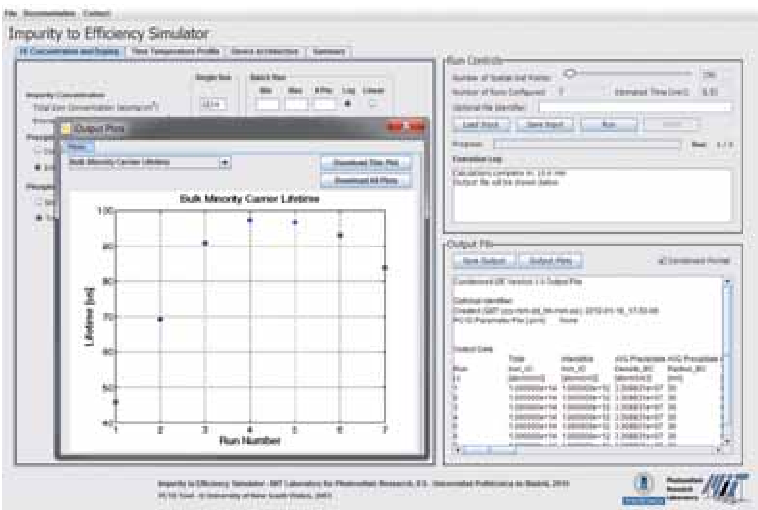


**Figure 7. I2E simulator screenshot after calculations are complete: a plot of the results is shown, as well as an output text file.**

## Conclusions

The effectiveness of predictive defect engineering while using the I2E simulation tool has been demonstrated. This tool has benefited the photovoltaic community by providing the information necessary for understanding the interplay between material purity, processing parameters, cell design and device performance. Through the work carried out on this project, it has been concluded that significant performance and throughput improvements can be realized by tailoring processing conditions to specific material qualities. Additionally, the I2E tool allows a rapid optimization of existing processes and the identification and evaluation of new approaches with minimal expenditures. Readers are encouraged to explore problems of interest with the online implementation of the tool.

## Acknowledgements

This work was supported by the U.S. Department of Energy (Contract No. DE-FG36-09GO1900), the MIT Deshpande Center, the MIT-Spain/La Cambra de Barcelona Seed Fund and the Spanish Ministerio de Ciencia e Innovación (through Thincells Project No. TEC2008-06798-C03-02). The authors thank N. Stoddard and R. Sidhu, who collaborated in the study leading to the results presented in Fig. 4. In addition, D.M. Powell acknowledges the support of the Department of Defense through the NDSEG fellowship programme, and D.P. Fenning acknowledges the support of the NSF Graduate Research Fellowship.

Cell Processing

## References

[1] Clugston, D.A. & Basore, P.A. 1997, "PC1D version 5: 32-bit solar cell modeling on personal computer", *Proc. 26th IEEE PVSC*, Anaheim, California, USA, pp. 207–210.

[2] Basore, P.A. 1990, "Numerical modeling of textured silicon solar cells using PC-1D", *IEEE Trans. Electron. Dev.*, Vol. 37, No. 2, pp. 337–343.

[3] Zhu, H. et al. 1999, "Applications of AMPS-1D for solar cell simulation", *Proc. AIP Conf.*, Vol. 462, No. 1, pp. 309–314.

[4] Fonash, S.J. et al. 1997, "A manual for AMPS-1D for Windows 95/NT".

[5] Burgelman, M., Nollet, P. & Degrave, S. 2000, "Modelling polycrystalline semiconductor solar cells", *Thin Solid Films*, Vol. 361–362, pp. 527–532.

[6] Niemegeers, A. & Burgelman, M. 1996, "Numerical modelling of AC-characteristics of CdTe and CIS solar cells", *Proc. 25th IEEE PVSC*, Washington DC, USA, pp. 901–904.

[7] Antoniadis, D.A., Hansen, S.E. & Dutton, R.W. 1978, "Supreme II – A program for IC process modeling and simulation", Technical Report No. 5019-2, Stanford Electronics Laboratory.

[8] Ananthasuresh, G.K. (ed.) 2003, *Optimal Synthesis Methods for MEMS*. Norwell, MA: Kluwer Academic.

[9] Cowen, N.E.B. & Ahn, C. 2011, "TCAD in the semiconductor industry and its advantages for solar cell manufacturing", *PVI*, 12th edn, pp. 72–80.

[10] Michael, S. & Michalopoulos, P. 2002, "Application of the SILVACO/ATLAS software package in modeling and optimization of state-of-the-art photovoltaic devices", *Proc. 45th Midwest Symp. Circ. & Syst.*, Washington DC, USA, 651–654.

[11] Goetzberger, A. & Shockley, W. 1960, "Metal precipitates in silicon p-n junctions", *J. Appl. Phys.*, Vol. 31, pp. 1821–1824.

[12] Bertoni, M.I. et al. 2011, "Nanoprobe X-ray fluorescence characterization of defects in large-area solar cells", *Energy & Env. Sci.*, Vol. 4, No. 10, pp. 4252–4257.

[13] Liu, A., Fan, Y.-C. & Macdonald, D. 2011, "Interstitial iron concentrations across multicrystalline silicon wafers via photoluminescence imaging", *Prog. Photovolt: Res. Appl.*, Vol. 19, No. 6, pp. 649–657.

[14] Kang, J. 1989, "Gettering in silicon", *J. Appl. Phys.*, Vol. 65, No. 8, p. 2974.

[15] Gilles, D., Schröter, W. & Bergholz, W. 1990, "Impact of the electronic structure on the solubility and diffusion of 3d transition elements in silicon", *Physical Review B*, Vol. 41, No. 9, pp. 5770–5782.

[16] Hopkins, R.H. & Rohatgi, A. 1986, "Impurity effects in silicon for high efficiency solar cells", *J. Cryst. Growth*, Vol. 75, pp. 67–79.

[17] Coletti, G. et al. 2011, "Impact of metal contamination in silicon solar cells", *Adv. Functional Mater.*, Vol. 21, pp. 879–890.

[18] Buonassisi, T. et al. 2005, "Engineering metal-impurity nanodefects for low-cost solar cells", *Nature Mater.*, Vol. 4, pp. 676–679.

[19] Hofstetter, J. et al. 2011, "Towards the tailoring of P diffusion gettering to as-grown silicon material properties", *Solid State Phenom.*, Vol. 178–179, pp. 158–165.

[20] Sopori, B.L. 1987, "Crystal defects in RTR ribbons: Their characteristics and influence on the ribbon cell performance", *J. Cryst. Growth*, Vol. 82, pp. 228–236.

[21] Macdonald, D. et al. 2005, "Transition-metal profiles in a multicrystalline silicon ingot", *J. Appl. Phys.*, Vol. 97, p. 033523.

[22] Zoth, G. & Bergholz, W. 1990, "A fast, preparation-free method to detect iron in silicon", *J. Appl. Phys.*, Vol. 67, No. 11, pp. 6764–6771.

[23] Fenning, D.P. et al. 2011, "Iron distribution in silicon after solar cell processing: Synchrotron analysis and predictive modeling", *Appl. Phys. Lett.*, Vol. 98, No. 16, p. 162103.

[24] Schon, J. et al. 2011, "Understanding the distribution of iron in multicrystalline silicon after emitter formation: Theoretical model and experiments", *J. Appl. Phys.*, Vol. 109, No. 6, p. 063717.

[25] Sopori, B.L., Jastrzebski, L. & Tan, T. 1996, "A comparison of gettering in single- and multicrystalline silicon for solar cells", *Proc. 25th IEEE PVSC*, Washington DC, USA, pp. 625–628.

[26] Bentzen, A. et al. 2006, "Gettering of transition metal impurities during phosphorus emitter diffusion in multicrystalline silicon solar cell processing", *J. Appl. Phys.*, Vol. 99, p. 093509.

[27] Istratov, A.A. et al. 2003, "Metal content of multicrystalline silicon for solar cells and its impact on minority carrier diffusion length", *J. Appl. Phys.*, Vol. 94, No. 10, pp. 6552–6559.

[28] Green, M.A. et al. 2011, "Solar cell efficiency tables (Version 38)", *Prog. Photovolt: Res. Appl.*, Vol. 19, No. 5, pp. 565–572.

[29] Hofstetter, J. et al. 2011, "Impurity-to-efficiency simulator: predictive simulation of silicon solar cell performance based on iron content and distribution", *Prog. Photovolt: Res. Appl.*, Vol. 19, No. 4, pp. 487–497.

[30] Haarahiltunen, A. et al. 2005, "Modeling of heterogeneous precipitation of iron in silicon", *Appl. Phys. Lett.*, Vol. 87, No. 15, p. 151908.

[31] Smith, A.L., Dunham, S.T. & Kimerling, L.C. 1999, "Transition metal defect behavior and Si density of states in the processing temperature regime", *Physica B: Condensed Matter*, Vol. 273–274, pp. 358–362.

[32] Cañizo, C. del & Luque, A. 2000, "A comprehensive model for the gettering of lifetime-killing impurities in silicon", *J. Electrochem. Soc.*, Vol. 147, No. 7, pp. 2685–2692.

[33] Plekhanov, P.S. et al. 1999, "Modeling of gettering of precipitated impurities from Si for carrier lifetime improvement in solar cell applications", *J. Appl. Phys.*, Vol. 86, No. 5, pp. 2453–2458.

[34] Hieslmair, H. et al. 1998, "Analysis of iron precipitation in silicon as a basis for gettering simulations", *J. Electrochem. Soc.*, Vol. 145, No. 12, pp. 4259–4264.

[35] Vande Wouwer, A., Saucez, P. & Schiesser, W.E. 2003, "Simulation of distributed parameter systems using a Matlab-based method of lines toolbox: Chemical engineering applications", *Ind. Eng. Chem. Res.*, Vol. 43, No. 14, pp. 3469–3477.

[36] Ames, W.F. 1992, *Numerical Methods for Partial Differential Equations*. Boston, MA: Academic Press.

[37] Nærland, T.U., Arnberg, L. & Holt, A. 2009, "Origin of the low carrier lifetime edge zone in multicrystalline PV silicon", *Prog. Photovolt: Res. Appl.*, Vol. 17, No. 5, pp. 289–296.

[38] Stoddard, N. & Sidhu, R. 2010, "Gettering of impurities in cast monocrystalline silicon", *Proc. MRS Spring Meeting*, San Francisco, California, USA.

[39] Manshanden, P. & Geerligs, L.J. 2006, "Improved phosphorus gettering of multicrystalline silicon", *Solar Energy*

*Mater. & Solar Cells*, Vol. 90, pp. 998–1012.

[40] Pickett, M.D. & Buonassisi, T. 2008, "Iron point defect reduction in multicrystalline silicon solar cells", *Appl. Phys. Lett.*, Vol. 92, p. 122103.

[41] Tan, J. et al. 2007, "Optimised gettering and hydrogenation of multi-crystalline silicon wafers for use in solar cells", *Proc. 22nd EU PVSEC*, Milan, Italy.

[42] Hofstetter, J. et al. 2010, "Study of internal versus external gettering of iron during slow cooling processes for silicon solar cell fabrication", *Solid State Phenom.*, Vol. 156–158, pp. 387–393.

[43] Härkönen, J. et al. 2003, "Recovery of minority carrier lifetime in low-cost multicrystalline silicon", *Solar Energy Mater. & Solar Cells*, Vol. 73, pp. 125–130.

[44] Rinio, M. et al. 2011, "Improvement of multicrystalline silicon solar cells by a low temperature anneal after emitter diffusion", *Prog. Photovolt: Res. Appl.*, Vol. 19, No. 2, pp. 165–169.

[45] Hofstetter, J. et al. 2011, "Enhanced iron gettering by short, optimized low-temperature annealing after phosphorus emitter diffusion for industrial silicon solar cell processing", *physica status solidi (c)*, Vol. 8, No. 3, pp. 759–762.

[46] Coletti, G. et al. 2008, "Effect of iron in silicon feedstock on p- and n-type multicrystalline silicon solar cells", *J. Appl. Phys.*, Vol. 104, p. 104913.

[47] Buonassisi, T. et al. 2005, "Synchrotron-based investigations of the nature and impact of iron contamination in multicrystalline silicon solar cell materials", *J. Appl. Phys.*, Vol. 97, p. 074901.

[48] Schön, J. et al. 2010, "2D modelling of the iron concentration from crystallization to final firing of mc silicon solar cells", *Proc. 25th EU PVSEC*, Valencia, Spain.

[49] Lelièvre, J.-F. et al. 2011, "Dissolution and gettering of iron during contact co-firing", *Energy Procedia*, Vol. 8, pp. 257–262.

[50] Buonassisi Group 2012, Impurity-to-Efficiency Simulator [available online at http://pv-i2e.mit.edu].

[51] Gray, A.L. 1985, "The ICP as an ion source—origins, achievements and prospects", *Spectrochim. Acta, Part B*, Vol. 40, No. 10–12, pp. 1525–1537.

## About the Authors

**Douglas M. Powell** received a B.S.M.E. from Ohio State University in 2008. After spending some time at GE Wind as a customer value engineer, Douglas is now working towards a Ph.D. in mechanical engineering at MIT. His current research focuses on structural defects in silicon and c-Si PV manufacturing.

**David P. Fenning** received a B.S. in mechanical engineering from Stanford University in 2008. He is currently studying for a Ph.D. in mechanical engineering at MIT after receiving his M.S. in 2010. David's research interests include impurity kinetics in silicon, defect characterization in semiconductors, and alternative device architectures for improved solar cell efficiency.

**Jasmin Hofstetter** received a degree in physics from Freie Universität Berlin in Germany in 2006 and completed her Ph.D. in photovoltaic solar energy at Universidad Politécnica de Madrid in Spain. Dr. Hofstetter is currently working as a postdoctoral fellow at MIT, where she is studying the kinetics of metallic impurities and structural defects in silicon, and their interaction during solar cell processing.

**Jean-François Lelièvre** is an engineer in materials and nanotechnologies (INSA of Rennes) and received his Ph.D. degree in 2007 (INSA of Lyon). After a 2-year postdoctoral appointment at the Instituto de Energía Solar in Madrid, Dr. Lelièvre joined CENTESIL, where he now researches silicon crystallization.

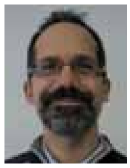

**Carlos del Cañizo** is an engineer in telecommunications. He received his Ph.D. degree in 2000 and is currently the head of the Instituto de Energía Solar at the Universidad Politécnica de Madrid. Prof. del Cañizo has been involved in the fabrication and characterization of silicon solar cells since 1994, and also works in the area of silicon ultrapurification.

**Tonio Buonassisi** heads the Photovoltaic Research Laboratory at MIT, which combines crystal growth, processing, characterization, defect simulation and cost-performance modelling to engineer naturally abundant and manufacturable materials into cost-effective, high-performance devices. Prof. Buonassisi's research interests include silicon (thin kerfless absorbers, laser processing, advanced manufacturing), thin films (Earth-abundant chalcogenides and oxides) and high-efficiency concepts.

## Enquiries

D. M. Powell
Massachusetts Institute of Technology
Laboratory for Photovoltaic Research
Cambridge, MA 02139
USA

Email: i2e_simulator@mit.edu
Website: http://pv-i2e.mit.edu/

# Thin Film

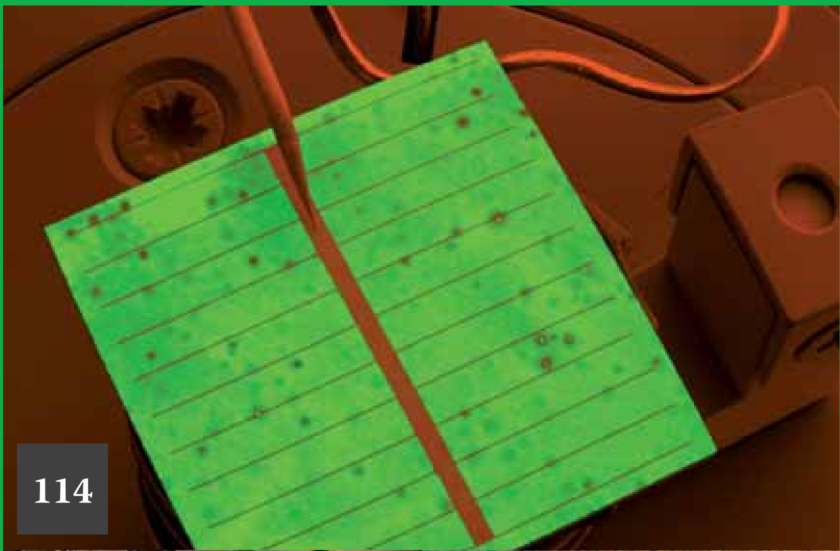





**Page 102**
**News**

**Page 106**
**Product Reviews**

**Page 107**
**Crystalline silicon thin foils: Where crystalline quality meets thin-film processing**

Frédéric Dross, Kris Baert & Jef Poortmans, imec, Leuven, Belgium

**Page 114**
**Si nanorod-based thin-film solar cells on glass: A potentially low-cost and high-efficiency all-inorganic approach**

Silke Christiansen & Michael Kiometzis, Max Planck Institute for the Science of Light (MPL), Erlangen, and Institute of Photonic Technology (IPHT), Jena, Germany

# News

## Largest-ever OPV module created at NREL's labs

The National Renewable Energy Laboratory (NREL) has, in collaboration with New Energy Technologies, produced its largest-area OPV module ever at 170cm$^2$. The companies' engineers have worked together on developing New Energy's SolarWindow technology that allows the generation of electricity on see-through glass windows.

New Energy's SolarWindow module is said to be more than 14 times larger in area than OPV devices previously fabricated by NREL. This achievement represents an important step in the commercialization of BIPV technologies, with researchers having already investigated and made use of a high-speed/large-area solution-coating process, allowing for rapid scale-up to larger glass surface areas.

Dr. Scott Hammond, New Energy's principal scientist, worked with NREL's researchers at lab scale to develop the solution-processable coating technique in order to deposit see-through electricity-generating coatings on to glass surfaces. The coatings consist mainly of polymers that are designed and produced by means of organic synthesis and then applied to glass.


Source: New Energy Technologies

**Dr. Scott Hammond, principal scientist, works on development of the SolarWindow module.**

News

**R & D News Focus**

## UCLA researchers reach 10.6% efficiency for tandem polymer solar cells

The *Nature Photonics* journal has reported that researchers at the UCLA Henry Samueli School of Engineering and Applied Science and UCLA's California Nanosystems Institute (CNSI) have significantly enhanced polymer solar cells' performance. They have used a device with a new 'tandem' structure that combines multiple cells with different absorption bands. The device had a certified power-conversion efficiency of 8.62% and set a world record in July 2011.


Source: University of California, Los Angeles

**Researchers at the UCLA Henry Samueli School of Engineering and Applied Science and UCLA's California Nanosystems Institute (CNSI) have significantly enhanced polymer solar cells' performance.**

In the effort to convert sunlight into electricity, PV solar cells that use conductive organic polymers for light absorption and conversion have shown great potential. Organic polymers can be produced in high volumes at low cost, resulting in PV devices that are cheap, lightweight and flexible.

This study opens up a new direction for polymer chemists to pursue designs of new materials for tandem polymer solar cells. Furthermore, it indicates an important step towards the commercialization of polymer solar cells.

## €14 million SUNFLOWER initiative to boost OPV in Europe

An EU-funded project has been launched to encourage the development of new organic photovoltaic cells. The SUstainable Novel FLexible Organic Watts Efficiently Reliable program aims to develop a new generation of cheap, efficient and long lasting printed-plastic cells. With a budget of €14.2 million, the four-year initiative is to be led by the Swiss Centre for Electronics and Microtechnology.


Source: DuPont

**The SUNFLOWER project will develop new organic PV cells.**

Through the use of tandem cells and dedicated light management systems, the project partners hope to increase the efficiency of existing OPV cells, whilst reducing the cost of the flexible solar cells with roll-to-roll atmospheric printing processes.

Amongst SUNFLOWER's other 16 consortium members are industrial organizations such as BASF, AFGA and DuPont Teijin Films, as well as academic and research institutions like Glasgow and Linköping universities.

Source: Singulus

**Singulus Technologies CIGS thin film tool.**

## Singulus to raise €60 million to pursue thin-film opportunities

As part of its previously publicized aims to become a key supplier of thin-film equipment to the PV industry, Singulus Technologies is planning a bond issue to raise €60 million. The funds were said to be needed to support larger projects in its solar division, including the expansion of partnerships with thin-film producers and new product offerings. The company also said it would use funds for the next-gen of equipment for Blu-ray disc production.

## Nanosolar secures US$20 million in funding to realize expansion plans

Investors Mohr Davidow Ventures and OnPoint Technologies, alongside aeris CAPITAL, have pumped US$20 million into thin-film company, Nanosolar, to aid expansion. At the beginning of this year, there was a great deal of media speculation surrounding the company's ability to produce a competitive product amid management changes. Nanosolar declares the last six months to be a success with the completion of a number of projects to strengthen its position in the market.

## Abound Solar plans CdTe thin-film modules with 12%-plus efficiency

Although new conversion efficiencies have yet to be ratified by the US Department

### First project in Japan to use NexPower 160W modules starts construction

Having already announced that it will ship approximately 12MW of its a-Si thin-film modules for use in Japan-based projects this year, NexPower Technology Corporation has said that the first project in Kansai, Japan has started construction. The 200kW power system is the first to use its 160W modules in the country, according to the company. NexPower's Japanese distributor is Marubun Corporation. The Kansai project is expected to be completed and grid-connected in the first half of 2012.

### MBJ Solutions installs electroluminescence inspection systems in Centrosolar production lines

MBJ Solutions has completed installation of its electroluminescence inspection systems into the production lines of Centrosolar Sonnenstromfabrik. The new equipment inspects 100% of Centrosolar's module production to ensure any anomalies not visible to the naked eye will be detected.

The inspection is retro-fitted into the existing flasher systems and integrates seamlessly into the final production step. MBJ claims the flexible setup of the inspection system allows a fast and easy installation. The flasher integrated EL system provides an immediate feedback and provides valuable information for optimization of the production process.

### Eight19 operates pay-as-you-go off-grid PV system in four countries

Through collaboration with international charitable organization WorldVenture, South Sudan is now the fourth country in which Eight19's pay-as-you-go off-grid PV system is in operation. The plan is to deploy 1,000 units in the first half of 2012 in South Sudan and a total of 3,000 units of its small flexible OPV modules in Kenya, Zambia and Malawi. The IndiGo units contain a battery, a solar panel, lights and a phone charging device.

### Solar Frontier helps power Mt. Komekura solar plant in Japan

Solar Frontier provided 10MW of its CIS thin-film solar modules to power the Mt. Komekura Solar Power Plant in Yamanashi Prefecture, Japan, which started operations on January 27. Shigeaki Kameda, president of Solar Frontier, was in attendance for the plant's opening celebration.

The facility is being hailed as one of the largest solar plants in Japan. It is operated by both Yamanashi Prefecture and Tokyo Electric Power and expected to produce nearly 12 million kWh of electricity per year.

### Singulus nabs order for CIGS/CIS thin-film solar cell production processing technology

Singulus Technologies has advised that it has received a new order for its processing machine used in the production of CIGS/CIS thin-film solar cells. The order came from an undisclosed international thin-film solar manufacturer and will be used for the set-up of a pilot production of CIGS/CIS modules. Singulus noted that upon successful commissioning by the thin-film solar manufacturer, the company plans to expand its module production, hence the order placed with Singulus. Further details, including a delivery date, were not available.

### NexPower extends Japanese portfolio with 12MW of module shipments

Taiwan-based NexPower Technology has announced that it will ship approximately 12MW of its a-Si thin-film modules for use in Japan-based projects. The company plans for these shipments to be spread across three promotional channels: local distributions, EPCs and construction developers.

of Energy's National Renewable Energy Lab (NREL), Abound Solar would seem to have caught up with CdTe thin-film leader, First Solar. It may have an enormous task to close the gap on manufacturing metrics, but aperture area efficiencies of 12.2%, generating modules with 82.8W specification on existing production equipment is a good start. First Solar reached volume production of modules with an average efficiency of 11.7% in 2011.

Abound Solar expects to begin mass production of 82W modules in the second half of 2012 and 85W modules in the first half of 2013. However, First Solar has already reiterated it expects to reach production efficiencies of 12.7% in the fourth quarter of 2012.

### Polyera claims 9.1% power conversion efficiency on its OPV cell

According to Polyera, Newport Corporation's PV cell lab has confirmed that Polyera's polymer/fullerene OPV cell has achieved a 9.1% power conversion efficiency with an inverted bulk heterojunction architecture using ActivInk PV 2000 semiconductor material. The company said its active layer materials are able to be deposited using a wider range of film thickness without lower cell efficiency, which is said to improve yields and simplify manufacturing.

## Business News Focus

### Ceres Technologies purchases CIGS technology assets from Veeco

Ceres Technologies advised that it had bought technology and product assets from the CIGS system business that was operated by Veeco Instruments. The CIGS product line is expected to add to Ceres's products and services for the renewable energy sector with production-ready CIGS deposition tool sets, including machines for molybdenum back contact, CIGS absorber layer and transparent conductive oxide (TCO) layers.

Ceres noted that the current product offering allows for roll-to-roll deposition on stainless steel substrates at 0.3m, 0.6m and 1.0m widths, while its production-scale CIGS glass process tool is under development. Under the technology purchase, Ceres additionally received the right to manufacture, support and further develop the CIGS equipment technology that Veeco previously sold.

### Solyndra's manufacturing plant for sale

The Bankruptcy Court overseeing Solyndra's insolvency has assigned Jones Lang LaSalle to undertake the sale of its manufacturing plant in Fremont, California. The 450,000-square-foot manufacturing facility was said to be designed to exceed California seismic standards and can be operating immediately following a seismic event, though not at the levels created by the current solar industry shakeout.

### Heliatek and Reckli announce new concrete BIPV technology

Heliatek's OPV panels will be used in Reckli's concrete walls to create a new solution in BIPV without compromising on aesthetics. Heliatek claims the flexibility

Source: Heliatek

**Heliatek's modules are available in various colours and dimensions so they can be integrated unobtrusively into the overall design.**

of its panels allows them to be fully integrated into the concrete walls whilst maintaining efficiency.

Heliatek states that its panels can resist temperatures of up to 80°C and can still perform efficiently even in low light conditions with a yield advantage of 10–20%, compared to conventional solar panels. The companies have said the new solar-concrete façade will offer numerous advantages. The solar cells are applied to a thin, flexible and lightweight plastic film with a weight of 0.5kg per square metre. By comparison, conventional solar panels weigh an average of between 10kg and 15kg per square metre. Furthermore, the modules are available in various colours and dimensions so they can be integrated unobtrusively into the overall design. The solar cells are then deposited by Heliatek at low temperatures in a roll-to-roll process on a plastic sheet.

## Exelon and First Solar defer change of ownership of AVSR PV project

Exelon and First Solar have extended their deadline for initial funding of the DOE loan for the 230MW Antelope Valley Solar Ranch One (AVSR) project, in northern Los Angeles County, California. A revised construction permit has been approved but the delay could mean First Solar has to repurchase the project from customer Exelon from February 24, 2012, as federal loan and loan guarantees would not be released in time of contract clauses kicking-in.

The new deadline for initial funding of the DOE loan has been moved to April 6, 2012 to allow the expected time for the initial funding to be in place. The extended deadline means the risk of First Solar repurchasing the project has diminished. Construction of AVSR has not been affected.

Source: First Solar

**Exelon and First Solar have extended their deadline for initial funding of the DOE loan for the 230MW Antelope Valley Solar Ranch One (AVSR) project.**

# Product Review

**ULVAC Technologies**

### Ulvac UNECS-2000 spectroscopic ellipsometer designed for R&D

**Product Outline:** ULVAC Technologies has introduced the UNECS-2000 spectroscopic ellipsometer for the high-speed measurement of film thickness and optical constants of thin films in R&D applications.

**Problem:** Spectroscopic ellipsometers can analyze multi-layer films or other complex structured thin films by measuring the polarized light condition of thin films in certain wavelength bands. These methods require either mechanical or electrical control of complex optical systems. This is why developing more compact and faster ellipsometers has been difficult.

**Solution:** The compact UNECS-2000 spectroscopic ellipsometer eliminates the need for conventional methods that mechanically or electrically control polarization devices. It takes advantage of the spectrums obtained from the polarization interference occurring between two high-order phase shifters to instantaneously capture the wavelength distribution of the sample's spectroscopic polarization parameters. The motor stage can handle samples up to 200mm in diameter. Using parallel measurement, the thickness of up to six individual film layers are measurable at the same time.

**Applications:** Transparent or semi-transparent films on the substrates up to 200mm in diameter.

**Platform:** UNECS-2000 is based on spectroscopic ellipsometry by utilizing high-order retarders.

**Availability:** Currently available.

# Crystalline silicon thin foils: Where crystalline quality meets thin-film processing

**Frédéric Dross**, **Kris Baert** & **Jef Poortmans**, imec, Leuven, Belgium

ABSTRACT

Today, c-Si photovoltaic technologies dominate the market, accounting for more than 85% of market share in 2010. A large scientific community made up of academic as well as industrial stakeholders strives to find solutions to improve device efficiencies and to drive down costs. One of the important cost elements of a module is the c-Si wafer itself. This paper discusses the fabrication of a carpet of c-Si foils on glass, either by layer transfer of an epitaxially-grown layer or by bonding of a very thin wafer, and processing this c-Si thin-foil device into a photovoltaic module. This could constitute an advantageous meet-in-the-middle strategy that benefits not only from c-Si material quality but also from thin-film processing developments.

## The best of both worlds

Despite a drastic decrease in silicon feedstock prices, and because of even more aggressive cuts in processing costs, it is estimated that the solar wafer today accounts for ~30–40% of the module cost [1]. Reducing the solar wafer thickness, therefore, carries a very strong leverage factor in cutting down costs. Understandably, therefore, the International Technology Roadmap predicts that the thickness of solar wafers will decrease from ~180µm today to ~100µm in 2020 [2]. But the same publication warns the reader that the technological solution to the processing of wafers thinner than 150µm remains to be found. Any attempt by PV manufacturers to reduce the thickness below 150µm has so far resulted in an increase in breakage of the devices during processing, reducing the production yield and therefore annihilating all potential cost reduction offered by thinner wafers.

“Any attempt by PV manufacturers to reduce the thickness below 150µm has so far resulted in an increase in breakage.”

Meanwhile, the thin-film PV development community has no issues with handling. Module and cell fabrication are non-dissociable since the device is grown directly on the module glass. The challenge of this community is elsewhere: device efficiencies remain lower than for crystalline Si modules. Lower module efficiency immediately translates into an increase in balance-of-system cost, jeopardizing the competitiveness of thin-film systems. In addition to the continuous and aggressive decrease in module production costs, increasing conversion efficiency is perceived today as a strategic way for thin-film PV to improve the chance of catching up with the moving target established by the mainstream technology.

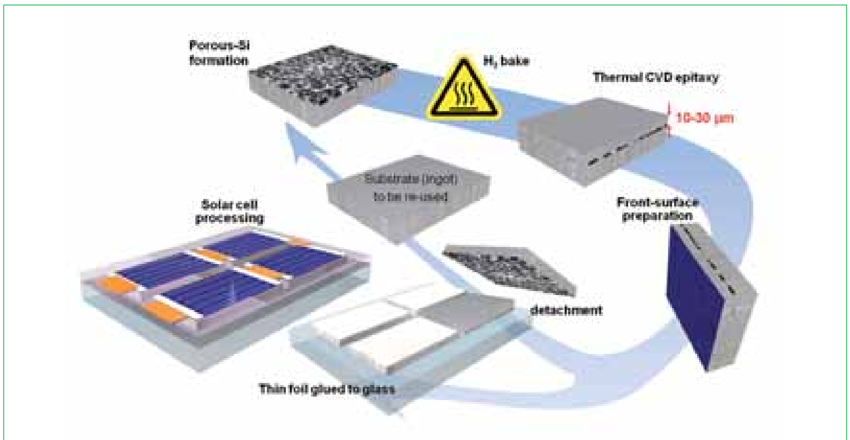


**Figure 1. Schematic of the process proposed for creating an epitaxially-grown crystalline silicon foil on glass.**

The concept described in this article targets a balanced meet-in-the-middle strategy. The intention is to take the best of both worlds: the quality and efficiencies of crystalline silicon devices on the one hand, and low material consumption and parallel and module-level processing of thin-film PV solutions on the other [3]. A c-Si PV device concept compatible with thicknesses below 50µm is proposed; a device concept inspired by thin-film technologies and compatible with efficiencies exceeding 18% is also proposed. These two concepts are in fact only one, consisting of the fabrication of a thin foil of c-Si on glass, followed by its processing, at the module level, into a highly-efficient PV device. The next section describes how the silicon foil can be fabricated on glass, and explains the possibilities offered by the thin-film community for processing it into a PV device. The question of the efficiency potential is finally raised in the last section.

## A crystalline Si foil on glass

The first question that needs to be asked is how to deposit a good-quality c-Si on glass [4]. Direct deposition, in a thin-film-like approach, of a layer of crystalline silicon results in poor electronic properties. It has therefore been proposed to epitaxially grow a monocrystalline Si layer on a monocrystalline seed-substrate and transfer this material to a foreign substrate [5–7]. The method implies the use of a sacrificial weak layer, which can either be an oxide layer [8,9], or be achieved by light-ion implantation [10], or more often by porosification of the parent substrate before growth [6]. In the latter case, as depicted in Fig. 1, a high-quality wafer is first anodized to create a superficial layer of porous Si (PSi); a chemical vapour deposition (CVD) process deposits a relatively thick (several tens of microns) active layer epitaxially on the wafer, which replicates the initial crystallographic quality of the wafer; the active layer is then detached from the parent wafer and bonded to a foreign sub/superstrate, while the parent wafer is reused. The bonding can be realized with, for instance, a silicone material, specifically tuned to buffer the stress due to the difference in thermal coefficient of expansion between the Si layer and the glass.

The foil quality is of utmost importance and strongly depends on the morphology of the porous layer. The weak layer therefore usually consists of a double layer of high and low porosity [11,12]. The high-porosity layer is tuned to approximately 40–70% porosity to allow easy detachment. The low-porosity layer (15–25%) seeds the epitaxial growth. A high-temperature (>900°C) annealing step is required to close the Si surface before growth. The growth of the active layer provides an elegant way of creating the p-n junction of the device (and potentially also surface fields) directly by epitaxy. This potentially reduces the number of process steps, and facilitates the implementation of advanced emitter profiles [13]. Solar cell efficiencies of up to 19.1% were recently obtained on free-standing foils fabricated on a PSi weak layer, showing the high-material-quality potential of the method [14,15].

In the concept we are proposing the front-surface treatment (texturization, surface passivation, antireflective coating deposition) is performed just before bonding while the foil is still attached to the mother substrate, and the rear side is processed on glass. The thin foil is thus constantly mechanically supported during the process. The porous layer should therefore be strong enough to withstand front-side processing, but weak enough to allow easy detachment after bonding [12].

Standard (180µm-thick) wire-sawn silicon wafers are, in principle, compatible with the process described in this paper. They can be bonded in a carpet-like fashion on a glass plate, creating a layer of crystalline silicon material, which can be further processed into a solar module. Nonetheless, because of the very high contribution of the silicon material to the cost of solar modules today, and since the concept described does not suffer from handling issues during processing, it is desirable to consider much thinner wafers. Multiple-wire saw technology is unlikely to be able to produce wafers thinner than 80–100µm [2,16]. In addition, the kerf (saw cut) has dimensions comparable to the wafer thickness, leading to an intrinsic kerf loss of 40–50%, and up to 70% for wafers < 100µm thick [2,17]. Therefore, in order to get the full benefit of this concept, alternative kerf-free wafering techniques that conserve the material quality have to be developed.

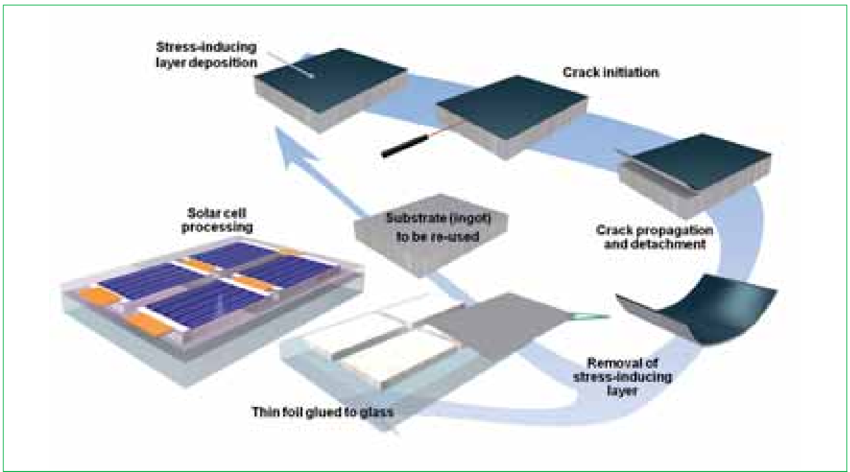


**Figure 2. Schematic of the SLiM-Cut process for the kerf-free fabrication of a c-Si thin foil.**

Several technologies have already been proposed [18], ranging from light-ion implantation [19] and laser wafer-cutting [20], to electrochemical cutting [21] and the stress-induced lift-off method [22]. The stress-induced lift-off (or SLiM-Cut) technique is a kerf-free method investigated at imec, and makes use of a thermomechanically induced crack propagation [22]. A schematic of the process is shown in Fig. 2. A layer of material with a coefficient of thermal expansion (CTE) significantly different from silicon is bonded, at an elevated temperature, on top of a bare silicon substrate. Upon cooling, the stress-inducing layer tends to shrink more than the silicon, giving rise to a stress field inside the silicon substrate. When this stress is higher than the tensile strength of silicon, a fracture occurs, with a spall-off of a thin silicon layer. Under given conditions (material geometries, mechanical properties, process conditions), this fracture can be controlled in terms of depth and direction. The SLiM-Cut development targets a smooth crack path, propagating at a depth of ~50µm, parallel to the original surface.

A proof-of-concept solar cell was fabricated using this material and achieved an efficiency of 10.0% with no intentional texturing and no rear-surface passivation [22]. A crucial requirement for using this material in the c-Si thin-foil concept is the conservation, in the fabricated foil, of the minority-carrier lifetime of the parent substrate. When using metallic stress-inducing layers and a high-temperature process, a complex metallurgic process takes place which explains the excellent adhesion and the thermal stress transferred to the substrate [23]. This process, nonetheless, introduces (metal-decorated) defects, which reduce the minority-carrier lifetime of the sample [24]. From the results of numerical modelling, imec has identified and successfully implemented a polymer material for inducing the stress [25]. The process is metal-free and the temperature remains below 150°C, reducing the chance of contamination and crystal dislocation formation. The material quality is currently being investigated.

## Processing a solar cell on glass

The carpet of silicon foils, obtained either by epitaxy or by a kerf-free wafering method, is then processed at the module level, using the module glass as a mechanical superstrate during processing. For this part of the process, thin-film technologies can be an extensive source of inspiration: light-trapping strategies can be similarly applied, doped layers can be deposited to create rectifying junctions, laser processing can be used for isolation or patterning purposes, large-area metal deposition can be adapted to the needs of the device, etc. The synergies that can be envisaged between thin-film technologies and c-Si thin-foil processing will now be discussed.

Probably the biggest drawback of crystalline silicon for PV application is its low absorption coefficient. Si is an indirect-band-gap semiconductor with, therefore, a smooth absorption edge, leading to only moderate absorption in the near-IR region (600–1200nm). Sunny-side light trapping can be, to a large extent, copied from bulk c-Si technologies. In the case of an epitaxial c-Si thin foil grown on a weak seed layer, the weak layer can be tailored to withstand front-side texturing (e.g. alkaline-based) and antireflection-coating deposition (e.g. PECVD $SiN_x$) [12] – the two main elements in wafer-based light-trapping strategies. Since it has been proved that a two-sided texture can improve the absorption in the active layer, light-management elements can also be placed on the rear [26]. The thin-film community might provide here some elements for solutions [27,28].

In thin-film technologies, the different polarities forming the p-n junction are not diffused, but deposited sequentially. The translation of this principle to the c-Si thin-foil concept implies depositing a material of polarity opposite to the c-Si material to form the junction. One obvious candidate material is a hydrogenated a-Si (a-Si:H) emitter (so-called 'heterojunction'), standardly deposited by PECVD at temperatures below 220°C, compatible with glass. Heterojunction emitters consist of an ultrathin (a few nm) intrinsic a-Si layer, followed by a thin (a few 10nm) doped a-Si layer. This solar cell structure has a high efficiency potential: device efficiencies of up to 23% [29,30,31], and world-record $V_{oc}$s of up to 744mV on 80µm devices have been reported [32]. Since the sunny side is bonded to the glass superstrate, the cell technology will provide both contacts on the rear side. The targeted concept is known as heterojunction-interdigitated back contact (HJ-IBC) and carries all the advantages (and potential) of a back-contact technology [33]. Lately, HJ-IBC technology has been a relatively active field of investigation within several institutes, and the most efficient device, reaching 20.2% efficiency, was recently demonstrated by ISFH and HZB [31]. In the case of an epitaxially-grown active layer, in-situ junction formation for at least one polarity is possible. The epitaxial stack on top of the weak porous-Si layer can consist of, for instance, an emitter, a base of opposite doping type, and a front-surface field.

The common approach nowadays for interconnections of cells in wafer-based technologies involves the build-up of strings of cells already interconnected with Cu-based ribbons. The full strings are then 'gently' grabbed and positioned on the module glass before lamination. The technology is robust and enables module manufacturers to guarantee a lifetime of more than 25 years in the field. Nonetheless, it has the disadvantages of being sequential and barely compatible with very thin cells.

Interconnection of thin-film PV devices is performed directly at the module level. Transparent conductive oxides and/or metals are usually deposited by large-area physical vapour deposition (PVD). The metallization of thin-film c-Si cells mimics the thin-film PV approach based on large-area PVD interconnections: thanks to parallel processing, the complexity and number of steps is reduced [34]. In addition to the parallel-processing possibilities, PVD deposition leads to processing temperatures that are well below 200°C, and is contactless. Moreover, the cells are metallized when already bonded to the final glass superstrate, which alleviates the handling bottleneck of today's technology. Last, but certainly not least, reliability issues are fundamental elements to be mastered before deploying a new module technology involving in particular a novel metallization scheme. They are currently being investigated at imec for this module-level interconnection concept [34,35].

One possible drawback of the concept is the limitation in 'binning' possibilities. In today's mainstream technology, the finished cells are sorted into different classes, and assembled in modules according to their performance. The concept presented here must rely on deposition processes with a particularly high uniformity across the large-area deposition chamber. The risk of mis-processing moves from wafer-to-wafer reproducibility (with binning possibilities) to within-module uniformity.

> "Since the sunny side is bonded to the glass superstrate, the cell technology will provide both contacts on the rear side."

## Evaluation of the efficiency potential

A possible implementation of thin-film-like technologies for c-Si thin-foil devices has been discussed in the previous section. The technology development still faces several challenges, but a careful analysis shows no obvious show-stopper. The most relevant question today is the estimation of the efficiency potential of the technology: in order to justify the technology development and to trigger the paradigm shift, the efficiency potential of the concept has to be (at least) as high as the one achieved with wafer-based crystalline silicon technologies, i.e. above 20%. An assessment of the efficiency potential of the concept is currently being carried out at imec; recent developments are presented next.

High-quality n-type 4-inch FZ 170µm-thick wafers were bonded to a quartz superstrate and a significant part of the process was carried out after the c-Si layer was bonded. Among the different possibilities for creating the c-Si layer, a mimicking of the layer-transfer approach based on epitaxial growth of the active layer was chosen. A schematic of the resulting structure is presented in Fig. 3.

The front side of the bulk wafers was processed free-standing, just like an epitaxial layer would be processed before bonding, while still attached to the mother substrate, as explained previously. Random pyramid texturization was followed by high-temperature passivation, and application of a silicon nitride anti-reflective coating. In addition, the rear-surface diffusion of a p-type emitter was included. Before being bonded, the pre-processed wafer was therefore equivalent to an epitaxial foil based on n-type material, for which the p-type emitter had been epitaxially grown in situ, and the front surface had been processed after epitaxial growth while the thin foil was still mechanically supported by the mother seed-substrate.

The pre-processed wafer was then bonded to a piece of quartz. The chosen bonding material was a silicone developed by Dow Corning for solar cell encapsulation. The rear side of the process occurred on glass, taking into account the processing constraints of glass and encapsulant, such as temperatures below 200°C. The rear-side emitter was patterned (by photolithography), the n+ a-Si back-surface field was deposited by PECVD, and the metallic contact was made by e-beam evaporation.

Table 1 presents the best and average solar cell parameters obtained with the process described above. The best 2cm × 2cm (4cm² aperture area) device achieves an efficiency of 18.3%. This proves that processing the rear side of a solar cell on glass is compatible with efficiencies exceeding 18%.

A somewhat similar study was carried out by the IPE group in Stuttgart [15], who achieved an efficiency of 16.9% with a front-and-rear-contacted epitaxial foil

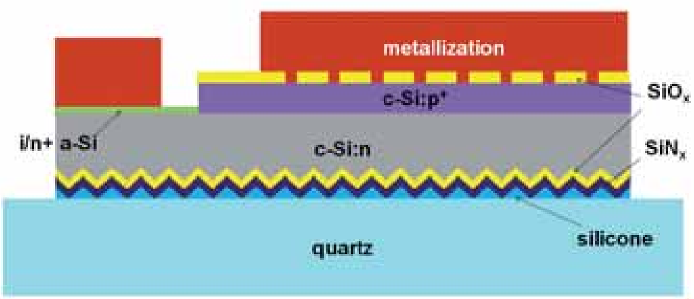


Figure 3. Schematic of the fabricated solar cell device.

having a rear surface partly processed on glass. These results give a lower limit of the potential efficiency of the concept. A careful identification of the sources of losses [36] has led us to believe that the upper efficiency limit has not yet been reached. In fact, the device carries no intrinsic element that drastically reduces its efficiency potential compared to a standard IBC solar cell. The upper limit of the efficiency potential has to be determined in state-of-the-art, free-standing IBC devices reaching efficiencies higher than 23% [37,38,39], and in similar devices based on heterojunctions (and therefore potentially compatible with the constraints of processing on glass), currently achieving efficiencies exceeding 20% [31].



"Starting from pre-processed free-standing monocrystalline wafers bonded to glass, the rear side was processed at a low temperature into an interdigitated contact pattern, and an efficiency exceeding was 18% obtained."

| | $J_{sc}$ [mA/cm$^2$] | $V_{oc}$ [mV] | *FF* [%] | Efficiency [%] | No. of cells |
|---|---|---|---|---|---|
| Average | 36.10 ± 1.42 | 648 ± 7 | 72.0 ± 2.9 | 16.8 ± 1.1 | 16 |
| Best cell | 37.23 | 652 | 75.2 | 18.3 | 1 |

**Table 1. Average and best characteristics of the solar cell devices processed on glass.**

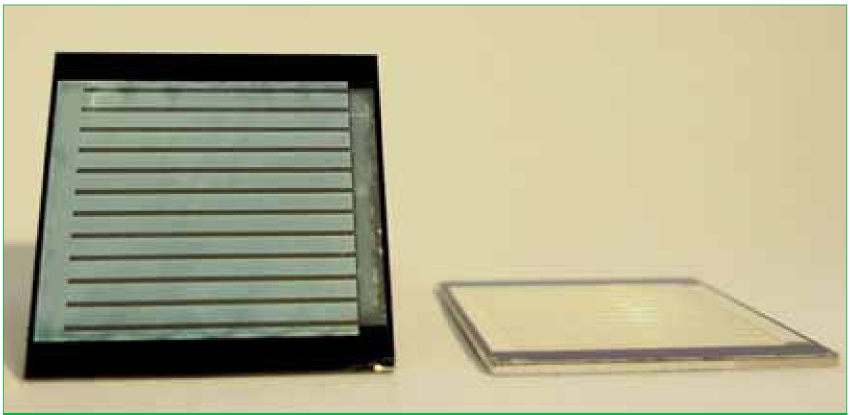

**Figure 4. Picture of the fabricated solar cell device.**

## Conclusion

Today, manufacturers of c-Si wafer-based solar cells cannot reduce the thickness of the starting material, mainly because of mechanical issues. Meanwhile, thin-film producers have absolutely no handling issues, but cannot catch up with the rapidly improving efficiencies of c-Si technologies. Fabricating a carpet of c-Si foils on glass, either by layer transfer of an epitaxially-grown layer or by bonding of a very thin wafer, and processing this c-Si thin-foil device into a photovoltaic module could constitute an advantageous meet-in-the-middle strategy that benefits not only from c-Si material quality but also from thin-film processing developments. How such a device could be envisaged has been discussed; a proof-of-concept and a preliminary estimation of the efficiency potential of the concept have also been presented. Starting from pre-processed free-standing monocrystalline wafers bonded to glass, the rear side was processed at a low temperature into an interdigitated contact pattern, and an efficiency exceeding 18% was obtained.

### Acknowledgements

The work was carried out by a team of engineers, researchers and research managers. The complete list of contributors is as follows: F. Dross, M. Aleman, T. Bearda, M. Debucquoy, J. Deckers, V. Depauw, O. El Daif, I. Gordon, J. Govaerts, S. Granata, R. Labie, X. Loozen, R. Martini, A. Masolin, M. Meuris, B. O'Sullivan, B. J. Pawlak, N. Posthuma, Y. Qiu, J. Robbelein, S. Singh, C. Trompoukis, J. Vaes, D. Van Gestel, A. Vanleenhove, K. Van Nieuwenhuysen, K. Baert and J. Poortmans, all from imec; P. Verlinden from Amrock Pty Ltd. and C. Boulord and G. Beaucarne, from Dow Corning. This work was made possible thanks to the financial support of the European Commission and the IWT. The author would also like to thank A. de Kergommeaux for fruitful discussions and for the production of the 3D figures. Finally, the contribution of the partners of the imec industrial affiliation program is gratefully acknowledged.

### References

[1] Hanwha SolarOne report [available online at http://investors.solarfun-power.com/releasedetail.cfm?ReleaseID=625835].

[2] International Technology Roadmap [see http://www.itrpv.net/].

[3] Dross, F. et al. 2012 [forthcoming], "Crystalline thin-foil silicon solar cells: Where crystalline quality meets thin-film processing", *Prog. Photovolt: Res. Appl.*, DOI: 10.1002/(ISSN)1099-159X.

[4] Gordon, I. et al. 2011, "Three novel ways of making thin-film crystalline-silicon layers on glass for solar cell applications", *Solar Energy Mater. & Solar Cells*, Vol. 95, pp. 1–6 [available online at http://linkinghub.elsevier.com/retrieve/pii/S0927024810006744].

[5] Brendel, R. 2001, "Review of layer transfer processes for crystalline thin-film silicon solar cells", *Jpn. J. Appl. Phys.*, Vol. 40, No. 55, pp. 4431–4439.

[6] Solanki, C.S. et al. 2004, "Porous silicon layer transfer processes for solar cells", *Solar Energy Mater. & Solar Cells*, Vol. 83, No. 1, pp. 101–113.

[7] Brendel, R. 2004, "Thin-film crystalline silicon mini-modules using porous Si for layer transfer," *Solar Energy*, Vol. 77, pp. 969–982.

[8] Hebling, C. et al. 1997, "High-efficiency (19.2%) silicon thin-film solar cells with interdigitated emitter and base front-contacts", *Proc. 14th EU PVSEC*, Barcelona, Spain, pp. 2318–2321.

[9] Weber, K.J. et al. 1997, "Lift-off of silicon epitaxial layers for solar cell applications", *Proc. 26th IEEE PVSC*, Anaheim, California, USA.

[10] DeJule, R. 1998, "Bringing SDI Wafer Technology to the Mainstream", *Semi. Internat.*, No. 40.

[11] Van Hoeymissen, J. et al. 2010, "The use of porous silicon layers in thin-film silicon solar cells", *physica status solidi A*, Vol. 208, No. 6, pp. 1433–1439.

[12] Van Nieuwenhuysen, K. et al. 2012, to be presented at the 27th EU PVSEC, Frankfurt, Germany.

[13] Van Nieuwenhuysen, K. et al. 2008, "Epitaxially grown emitters for thin film crystalline silicon solar cells", *Thin Solid Films*, Vol. 517, pp. 383–384.

[14] Petermann, J.H. et al. 2011, "19%-efficient and 43 mm-thick crystalline Si solar cell from layer transfer using porous silicon", *Prog. Photovolt: Res. Appl.*

[15] Reuter, M. et al. 2009, "50 µm thin solar cells with 17.0% efficiency", *Solar Energy Mater. & Solar Cells*, Vol. 93, pp. 704–706.
[16] Jetschny, M. 2007, "Sawing of silicon wafers", *Symp. Mech. Issues in Manufac.*, Halle, Germany.
[17] Beesley, J.G. & Schönholzer, U. 2007, "Slicing 80 micrometer wafers – process parameters in the lower dimensions", *Proc. 22nd EU PVSEC*, Milan, Italy.
[18] Henley, F. 2010, "Kerf-free wafering: technology overview and challenges for thin PV manufacturing", *Proc. 35th IEEE PVSC*, Honolulu, Hawaii, USA.
[19] Henley, F. et al. 2008, "Direct film transfer (DFT) for kerf-free silicon wafering", *Proc. 23rd EU PVSEC*, Valencia, Spain.
[20] Hopman, S. et al. 2008, "First results of wafering with laser chemical processing", *Proc. 24th EU PVSEC*, Hamburg, Germany.
[21] Lee, C.-L. et al. 2011, "Electrochemical method for slicing Si blocks into wafers using platinum wire electrodes", *Solar Energy Mater. & Solar Cells*, Vol. 95, pp. 716–720.
[22] Dross, F. et al. 2007, "Stress-induced large-area lift-off of crystalline Si films", *Appl. Phys. A*, Vol. 89, No. 1, pp. 149–152.
[23] Vaes, J. et al. 2010, "SLiM-Cut thin silicon wafering with enhanced crack and stress control", *Proc. SPIE Conf.*, San Diego, USA.
[24] Masolin, A. et al. 2011, "Evidence and characterization of crystallographic defect and material quality after SLiM-Cut process", *Proc. MRS Spr. Meet.: Symp. C*, San Francisco, USA.
[25] Martini, R. et al. 2012, to be presented at the siliconPV conference, Leuven, Belgium.
[26] Green, M. 1995, *Silicon Solar Cells: Advanced principles and practice*. Sydney, Australia: Center for Photovoltaic Devices and Systems, pp. 97–111.
[27] Zeman, M. et al. 2010, "Advanced light trapping in thin film silicon solar cells", *Proc. 25th EU PVSEC*, Valencia, Spain.
[28] El Daif, O. et al. 2010, "Absorbing one-dimensional planar photonic crystal for amorphous silicon solar cell", *Optics Expr.*, Vol. 18, pp. A293–A299.
[29] Tsunomura, Y. et al. 2009, "Twenty-two percent efficiency HIT solarcell", *Solar Energy Mater. & Solar Cells*, Vol. 93, No. 6–7, pp. 670–673 [available online at http://linkinghub.elsevier.com/retrieve/pii/S0927024808000834].
[30] Kanno, H. 2008, "Over 22% efficient HIT solar cell", *Proc. 23rd EU PVSEC*, Valencia, Spain, pp. 1136–1139.
[31] Mingirulli, N. et al. 2011, "Efficient interdigitated back-contacted silicon heterojunction solar cells", *physica status solidi (RRL)*, Vol. 5, pp. 159–161.
[32] Shimokawa, R., Yamanaka, M. & Sakata, I. 2007, "Very low temperature epitaxial growth of silicon films for solar cells", *Jpn. J. Appl. Phys.*, Vol. 46, No. 12, pp. 7612–7618.
[33] Kerschaver, E.V. & Beaucarne, G. 2006, "Back-contact solar cells: A review", *Prog. Photovolt: Res. Appl.*, Vol. 14, pp. 107–123.
[34] Govaerts, J. et al. 2011, "Progress in i-module: Towards improved performance, reliability and module-level fabrication technologies for back-contact PV modules based on ultra-thin silicon solar cells", *Proc. 26th EU PVSEC*, Hamburg, Germany.
[35] Govaerts, J. et al. 2011, "The i-module approach: Towards improved performance and reliability of photovoltaic modules", *Proc EMPC.*, Brighton, UK.
[36] Dross, F. et al. 2012, to be presented at the 27th EU PVSEC, Frankfurt, Germany.
[37] Cousins, P.J. et al. 2010, "Generation 3: Improved performance at lower cost", *Proc. 35th IEEE PVSC*, Honolulu, USA, pp. 000275–000278.
[38] Posthuma, N. et al. 2012, to be presented at the 27th EU PVSEC, Frankfurt, Germany.
[39] Aleman, M. et al. 2012, to be presented at the siliconPV conference, Leuven, Belgium.

## About the Author

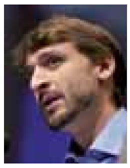

**Frédéric Dross** received his Ph.D. from the École Nationale Supérieure des Télécommunications, Paris, France, in 2004. He joined imec in 2005 as a research engineer, working on back-contact solar cell technologies, and was later promoted to team leader. Dr. Dross has been a principal researcher at imec since January 2011, with research interests encompassing c-Si thin-film and thin-foil solar cells (including fabrication of Si material and solar cell processing on glass), epitaxy-based solar cells, novel solar cell concepts such as all-Si tandem cells, and novel module concepts.

**Kris Baert** obtained his Ph.D. on PECVD of thin-film c-Si from the Katholieke Universiteit Leuven in Leuven, Belgium, in 1990. In 1992 he joined imec, where he managed research and development in various areas of MEMS and integrated microsystems. Since 2008 Kris has been Programme Manager of solar cells in the SOLO department.

**Jef Poortmans** received his degree in electronic engineering from the Katholieke Universiteit Leuven in Leuven, Belgium, in 1985 and his Ph.D. degree on strained SiGe-layers in June 1993. In 1998 he initiated activity on organic solar cells at imec which was complemented in 2000 by study of III-V solar cells. Jef currently holds the titles of Program Director of the Strategic Programme SOLAR+ and Director of the Department of Solar and Organic Technologies at imec.

## Enquiries

Frédéric Dross
imec
Kapeldreef 75
B-3001 Leuven
Belgium

Tel: +32 16 28 13 79
Email: frederic.dross@imec.be

Thin Film

# Si nanorod-based thin-film solar cells on glass: A potentially low-cost and high-efficiency all-inorganic approach

**Silke Christiansen** & **Michael Kiometzis**, Max Planck Institute for the Science of Light (MPL), Erlangen, and Institute of Photonic Technology (IPHT), Jena, Germany

ABSTRACT
Advances in nanofabrication for enhancing the efficiency of optical devices, such as solar cells and photo-detectors, via nanostructuring have attracted a great deal of interest. A photoconversion strategy employing nanorods (NRs) has emerged as a powerful way of overcoming the limitations of planar wafer-based or thin-film solar cells. But there is also a broad spectrum of challenges to be tackled when it comes to putting into practice cost-effective NR solar cell concepts. ROD-SOL is a 10-partner, 'nanotechnology for energy' project with end-users, equipment manufacturers and institutes from six countries forming the consortium. The aim of the project is to provide the photovoltaic market with a highly efficient (> 10%), potentially low-cost, thin-film solar cell concept on glass, based on silicon nanorods. This paper presents the project's achievements and discusses what the future might hold for nanotech-based solar energy production.

## Introduction

The ROD-SOL project [1] was created to realize thin-film NR-based solar cell concepts utilizing different bottom-up and top-down NR fabrication techniques that are scalable and cost-effective. This collaborative project was comprehensive in that every aspect of the development chain – such as device simulation and realization, material characterization, and testing and benchmarking – was covered by one of the scientific or industrial partners. The benchmark included the estimation and comparison of potential manufacturing costs of the ROD-SOL cells, which in any case fall well within the range of known production costs associated with thin-film PV turnkey production lines.

Probably the most significant result of ROD-SOL is the realization of a semiconductor-insulator-semiconductor (SIS) solar cell concept based on Si NRs, no more than 2μm in length, currently exhibiting a non-optimized efficiency of ~10%. To achieve this, an $Al_2O_3$ insulating layer acts as a tunnelling barrier for minority charge carriers. A top-down approach via metal-assisted wet-chemical etching (WCE) is utilized to realize NRs in an n-doped Si(100) wafer and in multicrystalline Si thin films on glass. The ordered NRs are realized through patterning using nanosphere lithography (NSL). The resulting NR arrays exhibit an absorbance greater than 90%. Atomic layer deposition (ALD) then allows for a suitable application of the tunnelling barrier and a transparent conducting oxide (TCO) layer, which is then contacted with a screen-printed gold contact grid.

## Lowering the cost of solar energy

The sun is our only universal source of energy, and photovoltaics (PV) allows for a broad range of applications on all scales to exploit solar energy. However, more than 90% of today's solar cells are made from bulk silicon wafers, which are expensive because of production costs, even though silicon itself is an abundant resource. In recent years increased demand has further inflated the price of solar-grade silicon. With the price of silicon accounting for at least one-third of the total price of the cell, this still makes solar energy roughly four times as expensive as energy derived from fossil fuels.

> "The most likely candidates for solving the problem of poor efficiency are nanomaterial-based approaches, often termed 'third-generation PV'."

An obvious way to lower the cost of solar energy is therefore to reduce the amount of silicon used, and thus thin-film solar cells are expected to dominate future markets. By using thin-film technology, the thickness of the silicon can be reduced from 200–300μm to 0.2–5μm – but at a price. First, the absorption length of visible light in silicon is about 200μm. Consequently, effective light trapping needs to be in place when silicon layers of only a few micrometres in thickness are used. Second, the quality of thin-film silicon on alternative substrates, for example glass, is usually limited by a large density of extended lattice defects, such as grain boundaries and dislocations, which means that high efficiencies can no longer be achieved. The efficiency of this thin-film material is poor (usually less than 10%), largely due to carrier recombination at grain boundaries that follow from the material's inherently small grains.

The most likely candidates for solving the problem of poor efficiency are nanomaterial-based approaches, often termed 'third-generation PV'. The nanocomponents under consideration are not limited to a silicon base: they can be organic or inorganic in nature, or a hybrid of the two. However, silicon is still favoured for solar cell production, despite the free path length of visible light in silicon of ~200μm, since it is non-toxic and abundant on earth. Furthermore, the properties of silicon are well understood and its processing is highly controlled as a result of decades of microelectronics research.

## Nanomaterials-based solar power: the science of 'third-generation PV'

When Green [2] coined the term 'third-generation PV' almost 15 years ago to describe all alternative approaches to classical Si photovoltaics, it was meant as a call for new strategies to overcome the Shockley-Queisser limit and to broaden the applicability of PV as a source of renewable energy. Nanostructuring solar cells is one such strategy, as it is based on two pronounced light-trapping effects. First, resonance phenomena having geometric dimensions of the same order of magnitude as the wavelength of visible light become established, thus significantly enhancing the absorption of light within the active NR regions. Second, an array of NRs is essentially a rough surface, which again supports the enhancement

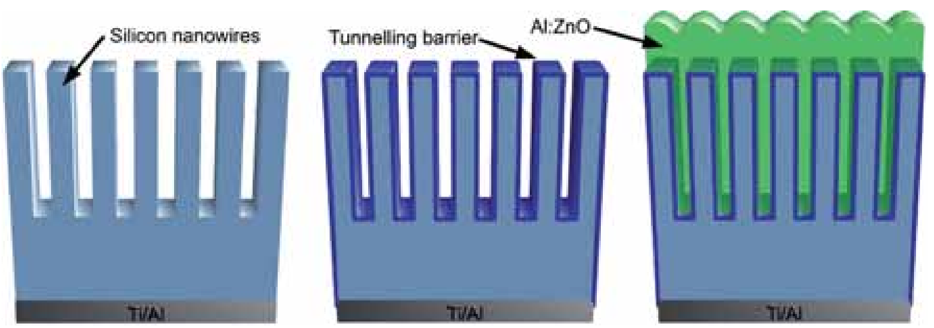


**Figure 1. Schematic of a semiconductor-insulator-semiconductor (SIS) solar cell concept based on Si NRs. The $Al_2O_3$ insulating layer (dark blue) acts as a tunnelling barrier for minority charge carriers. A TCO layer of Al-doped ZnO (green) serves as the degenerately doped second semiconductor.**

of absorption due to multiple scattering and final absorption within the NR layer. Furthermore, an NR geometry almost automatically increases the defect tolerance of the utilized semiconductor layers, eases the facile strain relaxation and allows the decoupling of the charge separation path from the photon path. Altogether this not only opens up the field for a broad range of manufacturing technologies, but also facilitates the development of new approaches regarding multijunction solar cells, which offer the potential of achieving efficiencies higher than 60%, thus overcoming the Shockley-Queisser limit.

## Next generation PV and ROD-SOL

The ROD-SOL project exploits the strongly absorbing Si NRs as absorbers in a 3D solar cell architecture. The most promising cell concept is shown in Fig. 1 and is based on a semiconductor-insulator-semiconductor (SIS) cell configuration with Si NRs no longer than 10µm, with an $Al_2O_3$ insulating layer acting as a tunnelling barrier for minority charge carriers. A TCO layer of Al-doped ZnO serves as the degenerately doped second semiconductor. A barrier layer and TCO are deposited by ALD, a chemically self-limited and therefore suitable deposition process that permits wrapping a layer around even NRs with high aspect ratios.

A top-down approach was utilized in ROD-SOL in order to realize the NRs via metal-assisted WCE in an n-doped Si(100)-wafer (for initial trials) and ultimately in multicrystalline Si layers on glass substrates. The latter were obtained from crystallizing amorphous Si (a-Si) starting layers using furnace anneals, lasers or electron beams as sources of energy for the crystallization, either with the a-Si layer in its solid phase or liquefying it prior to re-crystallization. The NRs were initially created by a random self-aligned etching process shown in Figs. 2(a) and (c).

The WCE approach is based on a self-organized two-step process: step one is creating Ag-nanoparticles on the Si layer or wafer surface; step two is performing metal-enhanced oxidation of the Si, combined with removal of the resulting Si oxide using hydrofluoric acid (HF) [3]. In the first step, the samples are immersed in an aqueous solution of 0.02M silver nitrate ($AgNO_3$) and 5M HF in a volume ratio of 1:1. In the second step, an etchant of 5M HF and 30% $H_2O_2$ in a 10:1 volume ratio is applied. Due to the nature of the etching process, the Si NRs are aligned in the <100> crystal orientation and therefore reside perpendicular or oblique to the substrate surface for Si grains of different orientation. Finally, the samples are washed in concentrated (65%) nitric acid ($HNO_3$) for several minutes to remove residual Ag nanoparticles from the Si NR surfaces.

With this self-aligned process, the control over NR dimensions is very limited. Even so, it was possible to realize a large area cell with ~10% efficiency as shown in Fig. 3. So far, this has been achieved with a cell size between 1.2cm × 1.2cm and 6cm × 6cm (Fig. 3a). The layer sequence of the SIS cell from Fig. 1 is obtained by ALD and the Al-doped ZnO (AZO) TCO layer is shown in the scanning electron micrograph in Fig. 2.

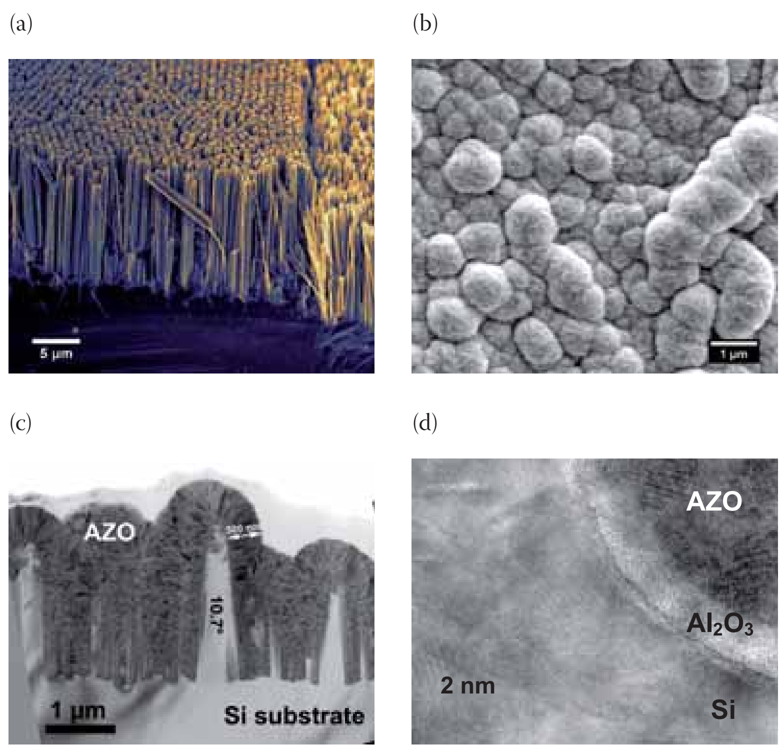


**Figure 2. Scanning electron micrographs: (a) WCE Si NRs in a Si(100) wafer; (b) WCE NRs with $Al_2O_3$ barrier layer and degenerately doped AZO layer viewed from the top at an angle (both layers deposited by ALD). Transmission electron micrographs: (c) an SIS cell based on the concept of WCE Si NRs in Fig. 1; (d) high-resolution image of the interfacial region between the Si NRs, $Al_2O_3$ barrier layer (amorphous) and degenerately doped AZO layer (nanocrystalline).**

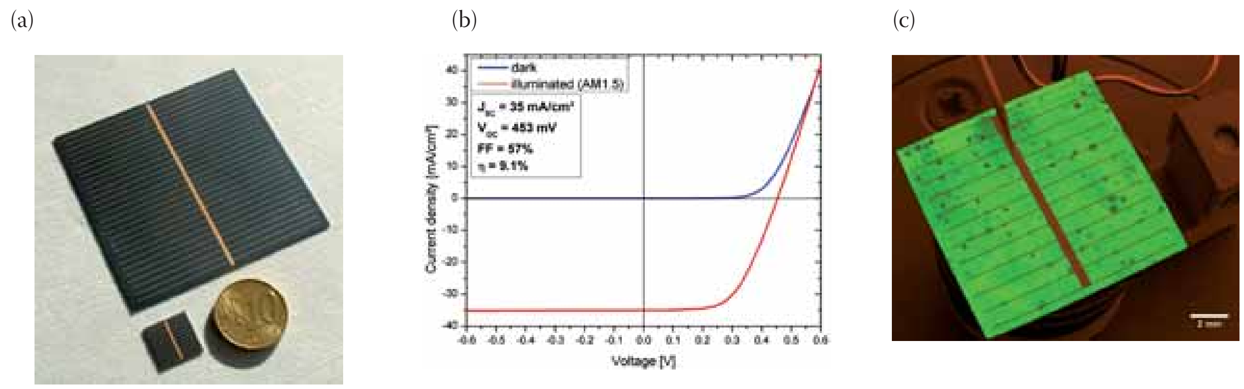


**Figure 3. SIS cells based on WCE Si NRs: (a) prototypes with a screen-printed gold grid; (b) dark and illuminated (AM1.5) *I-V* curves of the same cell with an 11Å-thick $Al_2O_3$ tunnelling barrier layer and an AZO front-contact layer; (c) electron-beam-induced current measurements for the same SIS cell. The homogeneous green contrast indicates the generated photocurrent. The dark spots show areas that are not intact and thus only a lower effective photocurrent can be measured. These defective areas will be reduced substantially when structured etching of NRs is applied.**

The same type of cell, but with better control of the optical and interfacial properties of the NRs, can be realized by structured etching of Si wafers or multicrystalline Si layers. The control over NR dimensions is accomplished by nanosphere lithography (NSL) as shown in the scanning electron micrographs in Fig. 4. Polystyrene spheres (yellow) of the desired diameters are densely packed on a Si-wafer or Si-layer surface in a Langmuir trough. Thus, a hexagonal densely packed sphere layer is realized, which then serves as a shadow mask for the deposition of a metal layer (e.g. sputtered gold shown in Fig. 4a). This lacy metal layer (blue) locally enhances the metal-assisted WCE of NRs (Fig. 4b), or the spheres themselves serve as an etching mask, such as in a dry-etching process as shown in Fig. 4(c).

"A thin-film solar cell based on Si NR with an efficiency above 15% is at hand and a 20% cell concept can also be aimed for."

All in all, the well-separated optically and electrically controlled Si NRs that are produced from lithography-assisted etching permit a much wider range of optimization options, so that a thin-film solar cell based on Si NR with an efficiency above 15% is at hand and a 20% cell concept can also be aimed for.

## Issues and problems to be solved

To achieve the highest efficiencies possible with a certain cell concept, a solar cell, being an optoelectronic device, needs optimization in terms of the most efficient optical absorption as well as of band structure engineering (given by the optimal location of the charge-separating junction within the nanocomposite material). In view of this, the proposed SIS cell concept deserves further optimization to meet its full potential. Preliminary simulations and modelling have indicated where improvements could lead.

The optimal organization of the Si NR ensembles can be derived from numerical finite-element modelling (FEM) to solve Maxwell's equations. For the purposes of optimization of solar light conversion, the scattering and absorption behaviour of the NR ensembles was studied. It was subsequently learned that a decreasing reflection occurs with increasing NR length (when the period of the NR ensemble is kept fixed). Furthermore, longer NRs act as a waveguide, leading the wave deep into the NR and permitting absorption even in the bulk Si underneath and between NRs. Comprehensive modelling shows that absorption (of green light, for example)

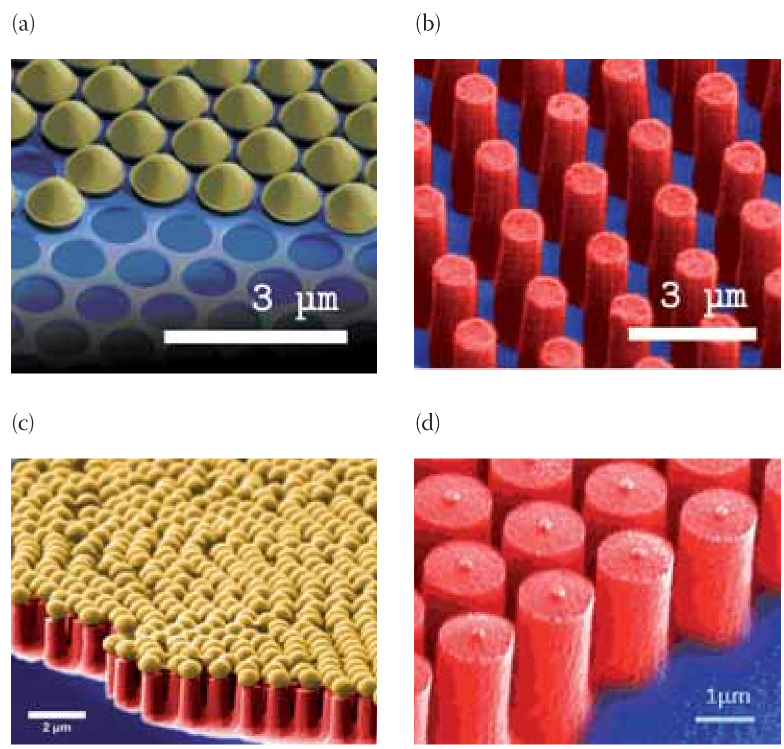


**Figure 4. Scanning electron micrographs: (a) NSL assembly of polystyrene spheres (yellow), serving as a shadow mask for gold layer (light blue) deposition; (b) the lacy gold layer serves as an etching enhancer of the Si in a WCE process, thus leaving Si NRs (red) behind; (c) nanospheres (yellow) serving directly as a mask for dry etching (reactive ion etching with Bosch process) of Si wafers or layers; (d) the resulting Si NRs (red) produced by the etching process.**

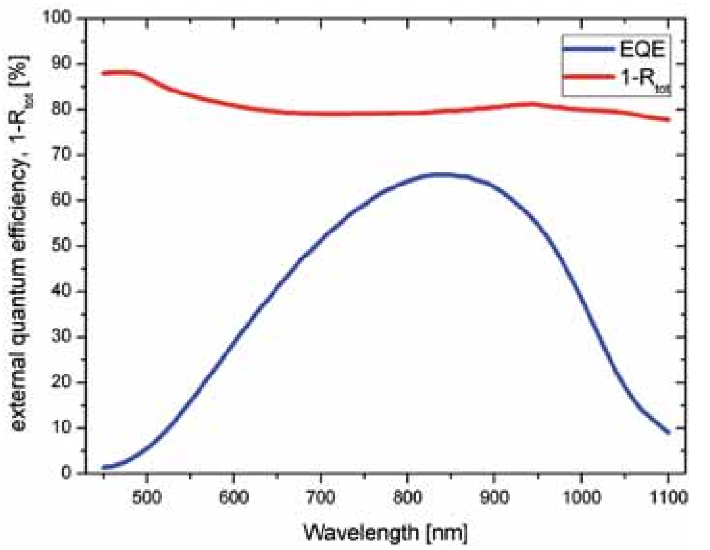


**Figure 5. Comparison of the absorbed photon flux (1 – $R_{tot}$), where $R_{tot}$ is a total reflection, and the external quantum efficiency EQE. The EQE describes the ratio between the extracted electron-hole pairs and the incident photons.**

occurs essentially in the top 10µm of the NR ensemble. A significantly longer absorption distance is needed to gain similar absorption in flat silicon. The difference in reflection between the 2µm- and 20µm-long NR ensembles is 10%.

A comparison of the absorption profiles can be used to establish a basic rule for designing the electrical structure of the NR solar cell. In case of NRs of length 2–10µm, the SIS configuration is preferred, since significant absorption occurs in the entire NR. For longer NRs, a different cell concept using an axial p-n junction would be advantageous. A smooth effective reflection below 20% could be obtained by optimizing the diameters and lengths of the NRs.

In all cases, the NR surface should be well passivated, and strong repellent fields should be present at the glass-Si heterointerface. Further optimization of the back-contact area is required here, just as the ALD layers need optimizing to fulfil different property requirements, comprising a proper tunnelling barrier and passivation of the surface states of the NRs. The *I-V* curves of the SIS cells show a tail ranging from 0.6–0.9V, indicating a non-ideal back contact. It is in this contact area that the major source of improvement of the cells is seen. This assessment is supported by the *I-V* curves showing that our SIS cell has a poor fill factor (FF ~68%), again pointing to non-ideal collection properties and thus non-ideal contacts. However, the good news is that the SIS cell consequently has good collection properties and a good electrical structure, and both $V_{oc}$ and $I_{sc}$ can be enhanced by improving the FF.

From additional external quantum efficiency (EQE) measurements and optical absorption measurements (given by the measured total reflection $R_{tot}$ according to [1 – $R_{tot}$]) presented in Fig. 5, it can be concluded that, for an improvement of the SIS solar cell efficiency, the following steps could be beneficial:

1. To improve the short-circuit current ($I_{sc}$), a thicker absorber region (taller NRs of the order of 10µm) and/or better back contact with an optical reflector should be used.

2. To improve the open circuit voltage ($V_{oc}$), a back-contact surface field that repels holes, and thus lowers the recombination losses, should be applied.

3. To improve both $I_{sc}$ and $V_{oc}$, a thinner contact layer that absorbs less light essentially of the low-wavelength type should be created.

Fig. 5 shows an example of EQE and absorption (1 – $R_{tot}$) measurements. The absorption does not precisely represent the absorption in the SIS solar cell, but rather the total incident flux that is reduced by the amount of reflected light. But, because the contacts of the SIS solar cell are completely transparent, the non-reflected light is absorbed in the SIS solar cell and/or in the silver back contact.

The difference between the (1 – $R_{tot}$) and the EQE curves therefore comprises the generated (but not collected) carriers, i.e. the recombined carriers, and the photon flux that did not contribute to carrier generation, but on the contrary is absorbed in the back contact. Since the EQE shape from 900nm to 1200nm represents a characteristic band-gap cut-off of the absorption in Si, it is assumed that the EQE maximum at 900nm represents to a large extent the absorbed photon flux rather than recombination losses. Therefore, the difference between EQE and (1 – $R_{tot}$) at 900nm could be largely attributed to the photon flux that was absorbed in the back contact. Part of this loss could also be attributed to the back-contact recombination.

> "If a module efficiency of 15% can be achieved with Si NRs, the costs of ROD-SOL energy production on an industrial scale will compare well to those of current state-of the-art thin-film production lines."

A significant loss of the generated carriers may be observed in the low and middle wavelength region of the absorbed spectra. These losses can be attributed to the non-ideal position of the junction, where the n-type AZO layer might be too thick and thus absorb too large a portion of the low-wavelength photons.

## Outlook

NR-based solar cell architectures have a long way to go yet in terms of research and optimization. Despite the encouraging results of the project so far in achieving ~10% efficiency with ~2µm long, still random Si NRs (without having yet implemented known ways to improve the cell), there are still tremendous challenges ahead for a successful commercialization of the ROD-SOL technologies.

That said, an exploitation strategy for ROD-SOL solar cells based on NRs has been developed by industry partners BISOL, PICOSUN and AIXTRON. Cost structure calculations show good potential for high-efficiency, low-cost ROD-SOL cell production. Another partner, IHS iSuppli, has developed cost models of three turnkey thin-film lines for manufacturing solar modules, taking into account ROD-SOL manufacturing requirements.

It should be recognized that, if a module efficiency of 15% can be achieved with Si NRs (which does not seem out of reach), the costs of ROD-SOL energy production on an industrial scale will compare well to those of current state-of the-art thin-film production lines. In order to reduce costs, monolithic integration instead of wafer-based concepts will be investigated, along with ways of avoiding vacuum and high-temperature processes, as well as the use of ordered NR ensembles to take advantage of the superior control of physical properties and device parameters. In addition, extensive electrical and optical modelling will yield deeper insight into the transport properties of NRs, and optimization of the technology, though a laborious task, seems straightforward at this stage.


## Acknowledgement

The authors acknowledge the EU Seventh Framework Programme (FP7-NMP-227497) for funding the ROD-SOL project and would like to express their gratitude to all partners for their support in ensuring its success. For contributing results, discussions and much enthusiasm in the development of the novel solar cell concept, the authors thank their co-workers B. Hoffmann, V. Sivakov, S. Schmitt, C. Tessarek, F. Talkenberg, S. Srivastava, M. Bashouti, M. Pietsch, G. Sarau, A. Bochmann and F. Schechtel. The authors would also like to thank M. Hadjipanayi from the Department of Electrical and Computer Engineering, Cyprus University, Nicosia, Cyprus, for the EQE measurements.


## References


[1] ROD-SOL project 01/2009–12/2011, "All-inorganic nanorod-based thin-film solar cells on glass" [details online at www.rodsol.eu].

[2] Green, M.A. 2003, *Third Generation Photovoltaics: Ultra-high efficiency at low cost*. Berlin: Springer-Verlag.

[3] Sivakov, V. et al. 2011, "Wet - chemically etched silicon nanowire architectures: Formation and properties", in Hashim, A. (ed.), *Nanowires – Fundamental Research*. InTech (Open Access Publisher), pp. 45–80.


## About the Authors


**Silke Christiansen** received her M.S. and Ph.D. degrees in materials science from the University of Erlangen-Nuremberg, Germany. Since 2003 she has managed a department for semiconductor nanostructures, first at the Max Planck Institute for Microstructure Physics in Halle, Germany, and more recently at IPHT in Jena, Germany. Since January 2010 Dr. Christiansen has managed a scientific research and technology development unit at MPL in Erlangen, while retaining her IPHT appointment. Prior to this she was a research staff member at the IBM corporate research facility in Yorktown Heights, USA, as well as at Columbia University in New York. She has more than 240 peer-reviewed publications and is the holder of five patents.

**Michael Kiometzis** received his Ph.D. in theoretical physics from Freie Universität, Berlin, in 1996. After spending several years as an IT manager in the private and public sectors, he returned to scientific work as a member of the team on the RODSOL project, for which he carried out numerical simulations and modelling.


## Enquiries


PD Dr. Silke Christiansen
Project Coordinator
Tel: +49 9131 6877 550
Email: silke.christiansen@mpl.mpg.de
Website: www.rodsol.eu

Max Planck Institute for the Science of Light (MPL)
Günther Scharowsky-Str 1
D-91058 Erlangen
Germany

Institute of Photonic Technology (IPHT)
Albert-Einsteinstr. 9
D-07745 Jena
Germany

# PV Modules


Page 121
News

Page 125
Product Reviews

Page 126
EL imaging and infrared thermography of PV modules

Shokufeh Zamini et al., AIT, Vienna, Austria

Page 136
LCA of modules: A multicrystalline silicon case study

Trond Westgaard, REC, Sandvika, Norway, & Carol Olson & Ton Veltkamp, ECN, Petten, The Netherlands

Page 141
Studying the lifetime of crystalline PV modules by interpreting the acceleration test data with statistical reliability models

Sreenivasa Murty Dasari et al., TATA BP Solar India Ltd, Bangalore, India

Page 148
A novel glue-membrane integrated backsheet for PV modules

Wenjin Xia et al.,Jolywood (Suzhou) Sunwatt Co., Ltd. & Shanghai Jiaotong University, Shanghai, P. R. China




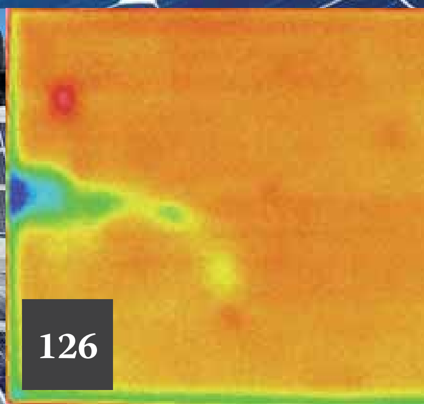

# News



## Suntech receives multiple accolades from IMS Research, MIT Technology Review and EuPD Research

The last 12 months have been quite successful for Suntech, even amid the chaos surrounding Suntech's response to accusations by US companies of impeding US growth. On a shipment basis, Suntech Power has retained its position as the 'Number 1' module manufacturer in the world for 2011, according to the latest report from IMS Research. In retaining the top position, Suntech shipped over 2GW of modules last year – the first in the PV industry to do so. The company also consistently out-shipped rivals in each quarter of 2011.

The company was also classed as one of the world's 50 most innovative companies by the MIT Technology Review. The annual list comprises 50 of the world's most innovative companies and Suntech has been nominated in the energy and materials category. Editors look for companies that have demonstrated original, valuable technology to market and significantly influencing their competitors.

EuPD Research recently gave Suntech 'Top Brand PV' label after an independent survey of installers and end-customers, making it the first Chinese module manufacturer to be given the title. The company also teamed up with researchers from Swinburne University of Technology to develop the world's most efficient broadband nanoplasmonic solar cells.

Two Suntech innovations that achieved large-scale production in 2011 are its Pluto cell processing technology and its SuperPoly silicon processing technology. Suntech's Pluto cell processing technology, developed in collaboration with the University of New South Wales, features a proprietary front-surface metallization process that creates grid contacts thinner than 30 microns wide, about a quarter the size of traditional screen-printed cells. These ultra-thin metal lines – made primarily of copper instead of silver – reduce shading on the cell surface, allowing the cells to absorb more sunlight and generate more electricity.


**Suntech's Pluto technology, developed in collaboration with the University of New South Wales, has been installed in this project in Sydney, Australia.**


**Suntech shipped over 2GW of modules last year – the first in the PV industry to do so.**

## EuPD awards Sharp 'Top Brand PV' honour for Germany

Sharp has been awarded the 'Top Brand PV' by EuPD Research for its presence in Germany. The award was granted after EuPD examined several factors, including brand awareness and distribution depth, with brand perception among customers one of the leading factors for determining the seal. The award is granted to leading PV manufacturers that have passed an appropriate quality model.

*Source: Sharp*

**Sharp's PV modules have been awarded the 'Top Brand PV' by EuPD Research.**

"This award shows that our brand is firmly anchored in the minds of our customers here in Germany. We are particularly pleased that our partners – the installers and distributors – recommend our products in consultations. This demonstrates the confidence we enjoy from the intermediaries", said Peter Thiele, executive vice president of Sharp Energy Solutions Europe.

## Competitive pricing leads to Chinese tier 2 crystalline PV module prices dropping to US$0.96/W

According to IMS Research's latest PV module pricing report, the average cost of Chinese tier 2 crystalline PV modules dropped to US$0.96 per watt in January, representing an annualized price decline shift to 22%, after exceeding 50% in December. The report cites reduced incentive levels in the major PV markets at the end of last year as having had the biggest effect on the prices.

The IMS report noted that competitive pricing from Chinese tier 2 manufacturers has continued into this year and led to the average crystalline PV module price from these suppliers to fall twice as quickly as the total market in January. The report acknowledged that while other spot prices had been recently been offered below the US$0.96/W price, this marks the first time that the global average price has dipped below the industry milestone.

Prices as low as US$0.80/W were recorded for Chinese tier 2 module suppliers last month; these prices were found most often in connection with large orders from German distributors.

## AU Optronics to trade under BenQ Solar's name

Solar solutions provider AU Optronics has announced it will now trade under the name BenQ Solar in order to enhance its global presence on the solar market through a "global operation, local delivery" business strategy. Its solar modules have achieved a 22.5% efficiency rate.

BenQ Solar will be launching AUO's alternating current generating solar solution: AC Unison. It includes a microinverter integrated with the solar module and equipped with a monitoring system. AUO will also have access to BenQ Solar's established distribution channels in North America, Europe and Asia.

## German Federal Cartel Office approves LDK Solar's majority ownership of Sunways

LDK Solar's bid to acquire Sunways has passed approval by the German Federal Cartel Office and Federal Financial Supervisory Authority (BaFin). LDK Solar had previously supplied wafers to Sunways and later in 2010 had secured production for branded Sunways modules. LDK gains access to Sunways' range of PV inverters as part of the takeover.

A voluntary public takeover offer for all outstanding shares in Sunways at €1.90 per share was offered by LDK in early January 2012, valued at approximately €22 million. The entire transaction is expected to be completed in the first quarter of 2012.

## JA Solar inks MOU with Intertek as it signs up to participate in data satellite program

JA Solar Holdings and Intertek advised that they had signed a strategic cooperation MOU aiming to build cooperation in the fields of quality, safety and ecology. Additionally, JA Solar announced that it would be taking part in Intertek's "Satellite Program," a data acceptance program that integrates speed, flexibility, cost effectiveness and certification marks, while issuing test reports to customers based on accepting internal laboratory test data from qualified customers. JA Solar noted that by taking part in the program it looks to improve its product operating cycle and strengthen its product quality.

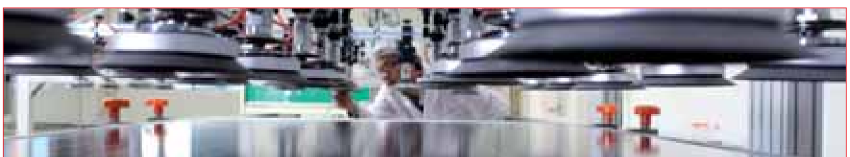

*Source: JA Solar*

**JA Solar is looking to improve its product operating cycle and strengthen its product quality.**



## Ecoprogetti's LED light sourced sun simulator receives triple class A rating

Ecoprogetti's sun simulator, ECOSUN10L, has received a triple class 'A' rating under EN60904-9 and IEC 60904-09 specifications, undertaken by TÜV intercert. The specialist equipment manufacturer said the system, which uses LEDs as its light source, was the first module LED simulator to work in triple class A. It is suitable for testing both standard crystalline modules and thin-film and back-contact solar cell modules.

*Source: Ecoprogetti*

**Ecoprogetti's ECOSUN10L sun simulator has received a triple class 'A' rating under EN60904-9 and IEC 60904-09 specifications.**

Ecoprogetti also noted that the impulse duration of the simulator could be extended to more than five seconds, while maintaining an A-class radiation stability. This feature is said to exclude the phenomenon of capacitive effects making the unit usable on next-generation high-efficiency cells and low-loss junction boxes.

## JinkoSolar opens PV module testing lab in China and receives UL WTDP certificate

JinkoSolar Holdings has opened a PV module testing lab in Jiangxi, China, which has been awarded the Underwriters Laboratories (UL) Witness Testing Data Program (WTDP) certificate. The company worked with UL to obtain

SOMONT
CELL CONNECTING

# NEW SOMONT PRODUCTS

## Profitable cell connecting


### SOMONT CERTUS TWO

Cost effective cell connection for cutting-edge PV modules

- Speed: 1300 cells/h
  Real output
- Low breakage rates
  < 0.2%
- Minimum Cost of Ownership
- Well-proven Somont Soft Touch Soldering Technique
- Modular concept
- New user-friendly vision and HMI


### SOMONT CONSOL

Material testing and qualification under production conditions

- Cost effective: No loss of production time or output
- Recipe simulation and proofing under real stringer conditions
- Suitable for different types of material and testing objectives
- High quality soldering results
- Faster validation of materials possible
- Essential for module, cell, ribbon, paste, flux manufacturers and laboratories

### SOMONT CONFORCE

Peel force tester for standardised verification of cell/ribbon connection

- High accuracy:
  ±0,125 N, 500 data/s
- Force standardisation – allows comparison of results with different ribbon widths
- Flexible measurement options:
  Force vs. distance or force vs. time
- Test reports as CSV data or PDF
- Easy to operate
- Results displayed during testing

A member of Meyer Burger Group

Visit us at
**SNEC PV POWER EXPO**
Shanghai New International Expo Center
May 16-18, 2012
Hall E3, Booth no. 660

Somont GmbH / Im Brunnenfeld 8 / 79224 Umkirch / Germany
Phone +49 7665 9809 7000 / www.somont.com

## 8minutenergy Renewables secures 25-year 200MW module supply deal with SDG&E

As part of its utility-scale project pipeline in Imperial Valley, California, 8minutenergy Renewables has signed a 25-year contract to sell 200MW (AC) of modules from the planned Mount Signal Solar project to San Diego Gas & Electric (SDG&E). The Mount Signal Solar project is expected to begin supply to SDG&E in mid-2013 and has an 18-month construction time, employing 450 direct jobs and more than 500 indirect jobs in Imperial County. The contract is pending approval from the California Public Utilities Commission.

## SunPower supplies Phoenix Sky Harbor International Airport with 5.4MW of E20 panels

SunPower has installed 5.4MW of its E20 solar panels on three rooftop locations at Phoenix Sky Harbour International Airport. The system is expected to generate the equivalent of 51% of the electricity demand at the airport's rental car centre, two East Economy parking garages and toll plaza, saving US$4.7 million over the next 20 years. The installation was constructed in two months.

## Canadian Solar's modules used on Denmark's largest rooftop installation

A 605kW rooftop system in the Danish city of Virum has employed 2,800 of Canadian Solar's modules. Currently holding the title of Demark's largest rooftop installation, it was constructed by German firm, SRU Solar, on two roofs of an office complex in collaboration with Danish energy company Greengo Energy.

## NRG Solar receives delivery of 13.2MW module supply from Solar Frontier

NRG Solar, a subsidiary of NRG Energy, advised that its December 2011 module supply agreement with Solar Frontier had been shipped and delivered recently. Per the module supply agreement, Solar Frontier provided NRG Energy with 13.2MW of its CIS thin-film solar modules.

This is the first agreement between Solar Frontier and NRG Solar. The companies advised that the modules purchased are not being allocated for any specific project and noted that this is the first purchase of thin-film CIS technology by NRG Solar.

## JA Solar modules used for 23MW Chinese installation

Chinese module manufacturer JA Solar has announced that its PV modules have been used in a 23MW installation in Lingwu, Ningxia province. The utility-scale solar plant was developed by the Angli Group and state-owned power enterprise China Datang Corporation, and will qualify for the RMB 1.15/kWh feed-in tariff introduced last year.

The new project comes shortly after the construction of another MW-scale installation in Ningxia, which was completed by Canadian Solar in January of this year.

## China Sunergy signs 50MW contract with Bull PowerTech

China Sunergy has been selected by Bull PowerTech to provide 50MW of solar modules for projects in Europe. The shipment is expected to be fully completed by the end of 2012, although exact details are yet to be disclosed.

certification and will now be able to offer customers and third parties testing facilities, under the supervision of UL personnel, with an aim to ensure high quality and expedite the time to market.

Jinko's new lab can run over 16 different tests ranging from basic pressure and impact to hot spot, pre-decay and UV aging tests. All the tests conform to UL and IEC regulations with the factory being outfitted with state-of-the art equipment to ensure the testing is conducted in accordance with UL test standards and procedures.

UL provided technical guidance and oversight during the establishment of the laboratory. JinkoSolar notes that in the next two to three years, it hopes to reach a higher level of strategic partnership with UL under the Client Test Data Program (CTDP), under which JinkoSolar will be authorized by UL to conduct test programs independently.

## Emmvee modules receive TÜV Rheinland confirmation for Italian GSE

TÜV Rheinland has certified Emmvee modules as being compliant with the Italian Energy Agency's GSE guidelines. The TÜV Rheinland confirmation certifies that Emmvee modules are equipped with cells manufactured in Europe, primarily in Germany. The company notes that TÜV Rheinland will soon begin testing the origin of the cells in order to certify their manufacture and production sites.

## Seraphim solar modules receive Intertek salt corrosion certificate

Intertek has awarded Seraphim a salt mist corrosion certificate for all of its solar PV modules as dictated under the IEC 61701 standard. Seraphim's modules underwent – and passed – various salt, mist and corrosion tests, which resulted in the modules' receipt of the certification that they possess the ability to tolerate harsh natural environments. The company noted that the tests and resulting certificate confirms that the modules can be used in a coastal environment or regions with high levels of rain, fog and acidity while maintaining a high level of performance.

## Trina Solar's multicrystalline solar modules receive 'Made in EU' certification

Trina Solar has advised that ICIM, an independent Italian institute, has certified its multicrystalline solar modules, manufactured with European-sourced silicon wafers, as fulfilling GSE requirements and therefore as being eligible for a 10% FiT premium in Italy.

Certified Trina products include TSM-PC05, TSM-PC05.08, TSM-PC05.10, TSM-PC05.15, TSM-PC05.18 and TSM-PC14. The ICIM certification process included the inspection of two Trina factories and two tests of the final products with ICIM auditors checking the production of Trina's silicon wafer supplies in Europe and its production of modules with European-made silicon wafers. All of the certified products received Product Certification by ICIM, stating that they have been tested according to CEI/EN 61213 and CEI/EN 61730.

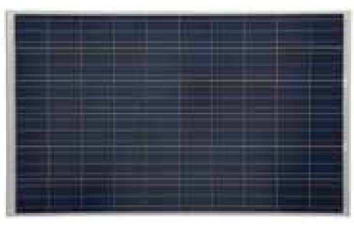

Source: Trina Solar

Trina Solar's TSM-PC05 module is among those that have been certified by ICIM.

# Product Reviews



## PSE

### PSE's mechanical load test stand for PV modules provides realistic results

**Product Outline:** PSE has introduced its new mechanical load test stand for the more realistic and comprehensive determination of mechanical stress from wind and snow loads.

**Problem:** Today's standards require the determination of the effects of wind and snow loads on PV modules. The load tests are normally performed at room temperature with the module mounted horizontally and the artificial force acting vertically to the module. As snow loads do not occur at room temperature and wind does not affect vertically on the modules, these tests do not simulate the real stresses which occur in the field.

**Solution:** PSE developed a test stand which is able to test both non-horizontal loads and loads at high and low temperature. The usage of high-tech components now offers the possibility to test loads of up to 10,000 Pa in a climate chamber from 80°C down to 40°C. The non-vertical application of force is realized through suction cup holders with angular adjustments.

**Applications:** All kinds of module testing according to IEC 61215 and IEC 61646 as well as solar thermal standards.

**Platform:** The standard size of the test stand is 2250mm × 1500mm with 24 pneumatic cylinders for an even load distribution. In order to shorten the set-up time, all cylinders can jointly be adjusted to different module sizes. PSE offers a variety of options for enhanced testing.

**Availability:** Currently available.

## Simrit

### Simrit's EPDM compound is UL 1703-certified

**Product Outline:** Simrit's latest ethylene propylene diene monomer (EPDM) rubber compound has garnered the Underwriters Laboratory (UL) 1703 certification and is applicable for o-rings used in sealing applications of PV connectors and junction boxes used in solar energy systems.

**Problem:** The extreme temperatures occurring in solar technology particularly affect seals. Depending on the application, the service life of a seal can be additionally compromised by the contacting media such as air, water and heat transfer medium.

**Solution:** The 70 EPDM 291 material developed by Simrit represents temperature-resistant solution for o-rings and moulded components that exhibit strong sealing properties in long-term use and is also ozone and UV resistant.

**Applications:** Simrit has developed a seal design especially for solar engineering applications with reliable sealing at temperatures of more than 200°C.

**Platform:** According to UL, manufacturers are able to achieve end-product certification more efficiently and cost effectively if the critical components that are used in PV modules are already tested and certified by the organization. UL has set minimum requirements for superstrates, substrates, encapsulants, adhesives, sealing materials and potting compounds used for fabricating PV modules or components based on the following criteria: flammability, resistance to ignition, thermal endurance and electrical properties.

**Availability:** Currently available.

## ViscoTec

### ViscoTec dosing pumps ensure high quality bonding and potting

**Product Outline:** ViscoTec offers specialized dosing solutions for all production steps that work with adhesives, sealants and metal pastes to increase process reliability, whilst lowering costs leading to production efficiency increase.

**Problem:** Since PV modules are exposed to extreme weather conditions and must accordingly satisfy stringent demands on quality, perfect dosing results during production are directly proportional to the long-term success of the manufacturer's business.

**Solution:** The most commonly used media for gluing module parts and casting connection sockets are two component adhesives and potting compounds with properties such as high viscosity and filler content, placing very high demands on dosing systems. The endless-piston principle of ViscoTec dosing pumps has been developed specifically for such applications. The dosing systems can be easily integrated into various processes and goes into reverse flow at the end of dosing, which breaks off the product thread or prevents any dripping.

**Applications:** Module frame and junction box assembly.

**Platform:** ViscoTec dosing pumps are rotating positive displacement pumps. Their operating principle can be compared with an endless piston that conveys the product from the suction side to the discharge side, building up a differential pressure in the process. At the core of every application is a volumetric conveying pump.

**Availability:** Currently available.

Fab & Facilities
Materials
Cell Processing
Thin Film
PV Modules
Power Generation
Market Watch

# Non-destructive techniques for quality control of photovoltaic modules: Electroluminescence imaging and infrared thermography

**Shokufeh Zamini**, **Rita Ebner**, **Gusztáv Újvári** & **Bernhard Kubicek**, Austrian Institute of Technology (AIT), Vienna, Austria


## ABSTRACT

Non-destructive methods for measuring photovoltaic modules are discussed in this paper, with the aim of comparing different quality-assurance methods for different module technologies (e.g. crystalline and thin-film technologies: a-Si, CdTe, CIS). For a complete quality control of PV modules, a combination of fast and non-destructive methods was investigated. In particular, camera-based measurements, such as electroluminescence (EL) and infrared (IR) technologies, offer excellent possibilities for determining production failures or defects in solar modules, which cannot be detected by means of standard power measurements. These methods are applied effectively in quality control and development support, and EL is already an important characterization tool in industry and research. Most short circuits reduce the voltage in their surrounding area and appear dark in EL images. However, as this failure is not always critical and apparent, short circuits are only precisely identifiable in combination with IR measurements. Therefore, to quickly detect at high resolution the most common defects in a PV module, a combination of EL and IR measurements is advisable.


## Introduction

Infrared (IR) and electroluminescence (EL) imaging are both non-destructive measurement techniques. These types of optical measurement provide fast, real-time and (in the case of EL imaging) high-resolution images with a two-dimensional distribution of the characteristic features of PV modules.

These methods have been introduced and used by several groups for determining a few physical parameters of solar cells, e.g. EL for measuring local effective diffusion length $l_{eff}$ [1], carrier collection length $l_c$ [2], local junction voltage [3] and series resistance [4,5]. The work presented in this paper, however, focuses on quality control and characterization using EL and IR imaging with conventional cameras; as an example, imaging is carried out before and after ageing. In addition, some rules for measuring with cameras are included in the presentation of this work.

> "The high resolution of EL images allows some defects to be determined more precisely than with IR images."

EL has proved to be a useful tool for investigating electrical inhomogeneities caused by intrinsic defects (e.g. grain boundaries, dislocations, shunts or other process failures) and extrinsic defects (e.g. cell cracks, TCO corrosion or interrupted contacts). IR measurements, on the other hand, allow the thermal behaviour of cells in a module and a number of defects (e.g. short circuits in solar cells, shunts, inactive cell parts, moisture, defective bypass diodes) to be determined.

## Theory

### IR thermography

IR measurements can be taken by using an external current or by applying light. During measurements in the dark, no light is applied to the module but an external current (less than or equal to the short-circuit current $I_{sc}$) is supplied in the forward direction [6]. In order to avoid thermal damage to thin-film modules it must be ensured that the $I_{sc}$ of the modules is not exceeded. During illuminated measurements, a current is generated by incident light (e.g. the sun), which can cause different emitted heat radiation.

For a more precise defect detection, illuminated thermography imaging is performed and comparisons are made for modules operated under different conditions, such as short circuit, open circuit and maximum power point (MPP). Several defects can be distinguished by varying the electrical load corresponding to certain states of the current–voltage characteristics.

Heating can be identified using an appropriate IR camera, and compared to electroluminescence measurements. In this work, thermography imaging was performed by means of a portable, uncooled IR camera, with the IR detector having a wavelength between 8 and 14μm.

### Electroluminescence (EL)

EL measurements take advantage of the radiative interband recombination of excited charge carriers in solar cells. For EL investigations the module is operated as a light-emitting diode and the emitted radiation due to recombination effects is detected with a sensitive Si-CCD camera. The wavelength window of the Si-CCD camera is 300 to 1000nm.

The solar cells are supplied with a defined external excitation current (less than or equal to $I_{sc}$) while the camera takes an image of the emitted photons. Damaged areas of a solar module appear dark or are less shiny than areas without defects. Electroluminescence imaging can be used to detect a number of defects in crystalline and thin-film solar cells [7]. The high resolution of EL images allows some defects to be determined more precisely than with IR images.

## Experiments

Different module technologies, such as crystalline (single and multicrystalline) and thin-film (CIS, a-Si, CdTe), were analyzed by electroluminescence and IR thermography under external bias and illumination. Additional characterization tools used were common characterization measurements (e.g. *I-V* measurements) and new improved evaluation processes.

### EL and IR measurements of a single crystalline module

In the EL image of the single crystalline (sc-Si) module shown in Fig. 1, the defects

appear as dark areas. Some cracks and dark cells of lower electrical activity are visible. The illuminated IR image of the sc-Si module in Fig. 2, under short-circuit current conditions, shows some hot cells. The darker cells in Fig. 1, where a bad cell quality was assumed, caused higher cell temperatures.

When the sc-Si module is operated at MPP (Fig. 3), some cells have lower temperatures than when under $I_{sc}$ conditions; this is caused by different $I_{sc}$ levels of the cells. Cell measurements before integrating the cells in the sc-Si module confirmed that the hottest cells are mainly those with high series resistances and/or low short-circuit currents.

It turned out that dark thermography measurements were not suitable for crystalline modules (Fig. 4). In the dark thermography image of crystalline modules, only fractured cells could be identified as very hot cells with an inactive part. Other defects could not be identified very clearly using this method.

## EL measurements of a multicrystalline (mc-Si) module before and after mechanical load

The EL imaging and the current–voltage measurements of a mc-Si module were carried out before and after a mechanical load analysis for loads of 1500Pa, 2400Pa, 4500Pa, 5400Pa, 6500Pa and 9000Pa. The module broke when subjected to a pressure of 9000Pa. The imaging and measurement results before and after the application of mechanical loads of 2400Pa and 6500Pa are shown in Figs. 5–7 and Table 1.

Besides some darker areas, caused by grain boundaries, in the EL image of Fig. 5, there are also some significant defects (e.g. cracks and finger failures) visible. After a load of 2400Pa (Fig. 6), the number of cracks (visible as darker cell areas) increased. After four mechanical load tests (Fig. 7), the number of cracks and broken cells increased further.

The results of the current–voltage measurements indicate a degradation of power of 7% as seen in Fig. 8. This power loss is mainly caused by the reduction of $U_{mp}$ and $I_{mp}$, which is dependent on the number of cracks, the consequently reduced available cell area and the increased series resistances.

Vertical and horizontal 'line scans' over the EL images of the mc-Si module, before and after applying the load tests, help to identify a defect increase per row or column. By averaging all EL pixel colours along an axis, average line scans can be calculated over the whole module. A decrease of EL radiation density with distance from the bus bars, especially in the projection along the long axis (x-direction, 9 cells), is evident in Figs. 5–7.

Fig. 9 shows a vertical line scan over the short axis (y-direction, 6 cells). It is

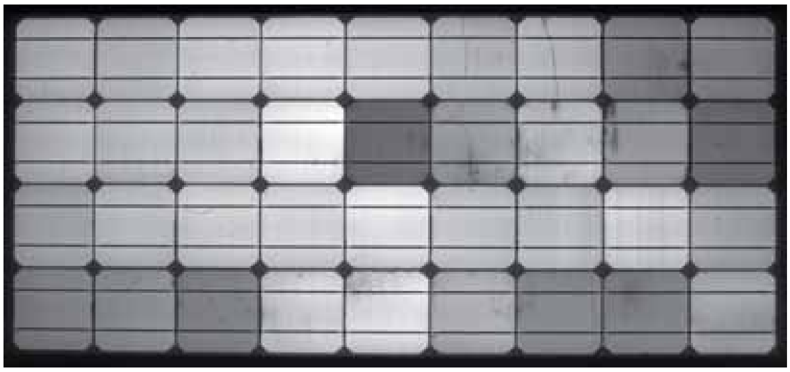

Figure 1. EL image of the sc-Si module.

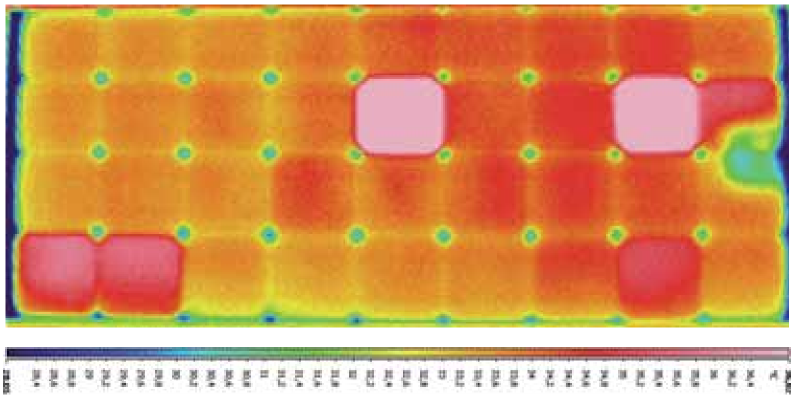

Figure 2. IR image of the $I_{sc}$-operated sc-Si module.

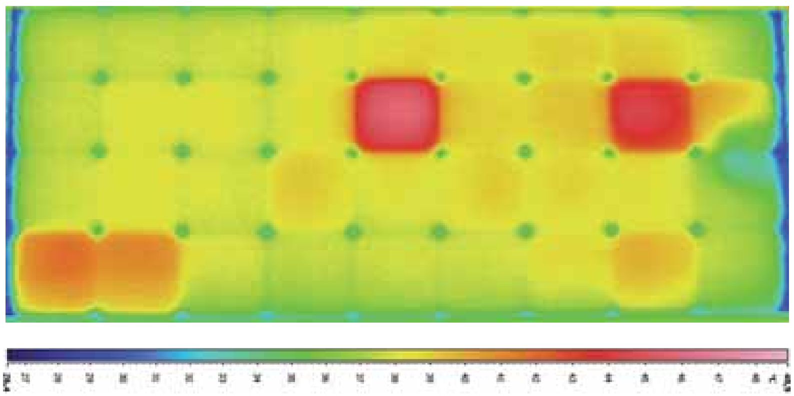

Figure 3. IR image of the MPP-operated sc-Si module.

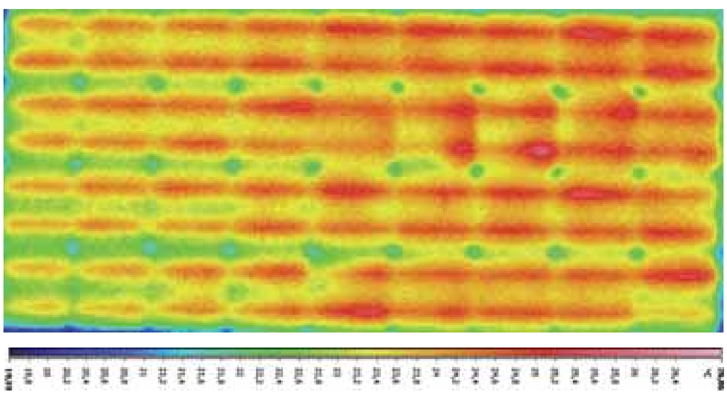

Figure 4. Dark IR image of the sc-Si module.

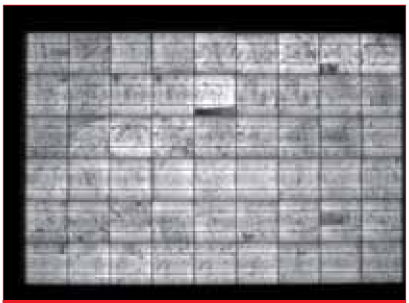
Figure 5. EL image – mc-Si module before the mechanical load test.

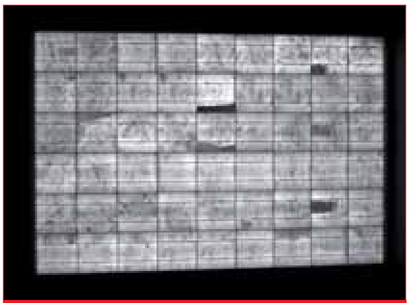
Figure 6. EL image – mc-Si module after the 2400Pa load test.

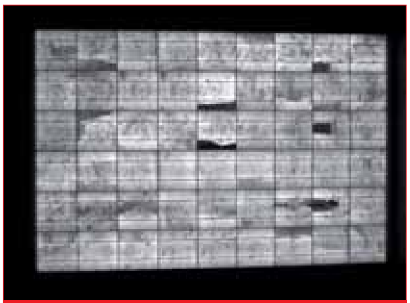
Figure 7. EL image – mc-Si module after the 6500Pa load test.

| | $U_{oc}$ [V] | $I_{sc}$ [A] | $U_{mp}$ [V] | $I_{mp}$ [A] | $P_{max}$ [W] | $FF$ [%] |
|---|---|---|---|---|---|---|
| Before load test | 33.43 | 8.54 | 26.71 | 7.93 | 211.68 | 74 |
| After 2400Pa load test | 33.38 | 8.55 | 26.51 | 7.79 | 206.61 | 72 |
| After 6500Pa load test | 33.34 | 8.54 | 26.14 | 7.23 | 196.18 | 69 |

$U_{oc}$ = open-circuit voltage; $I_{sc}$ = short-circuit current; $U_{mp}$ = voltage at $P_{max}$; $I_{mp}$ = current at $P_{max}$; $P_{max}$ = maximum power point; $FF$ = fill factor

Table 1. Current–voltage measurements before and after mechanical load tests.

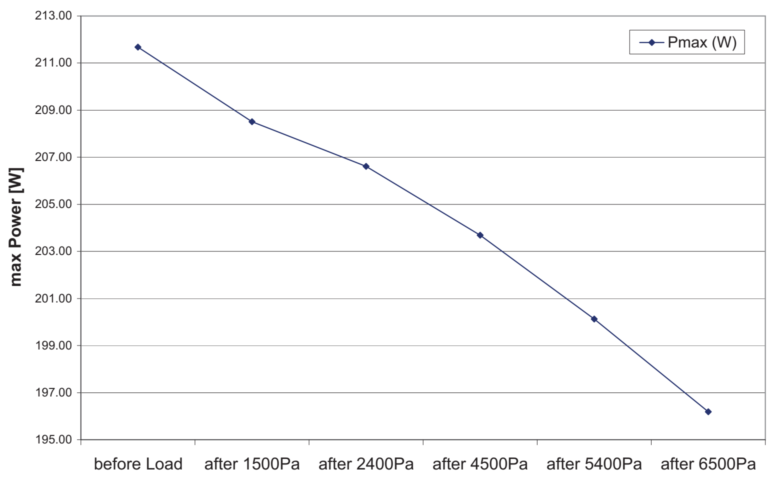

Figure 8. Power degradation.

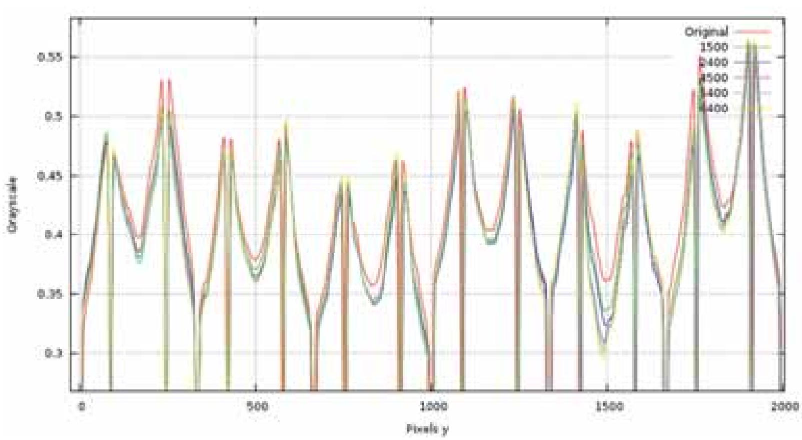

Figure 9. Vertical 'line scan': averaging of all pixel intensities along the module long axis. The busbars and borders of the six cells are visible, together with the developing effect of the load tests.

remarkable that the upper three cell rows (on the left of the figure) have relatively more damaged cell areas than the lower three cell rows (on the right), while an inhomogeneous current distribution between the two bus bars of a cell row is also observed. The individual asymmetries were, however, hardly affected by the load tests.

## Characterization of an a-Si module before and after ageing processes

An a-Si module was characterized before and after it was exposed to some ageing tests – preconditioning, light soaking and application of a reverse current. EL and IR imaging, as well as performance measurements, was carried out and the results compared.

In the EL image of the a-Si module before ageing (Fig. 10), there are no significant


Figure 10. EL image – a-Si module before ageing.

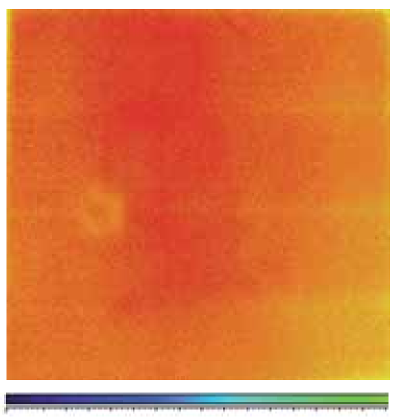
Figure 11. Dark IR image – a-Si module before ageing.

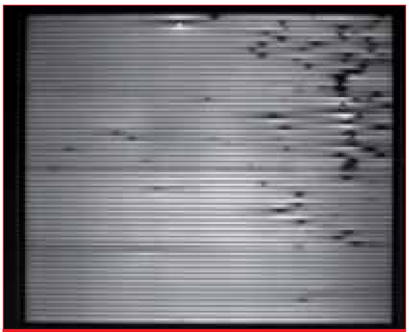

Figure 12. EL image – a-Si module after ageing.



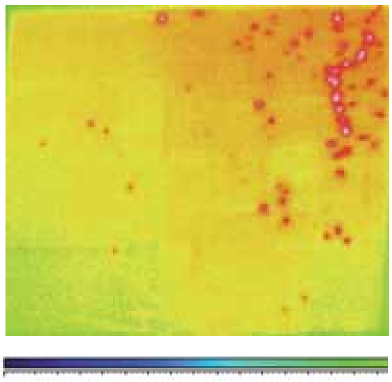

Figure 13. Dark IR image – a-Si module after ageing.

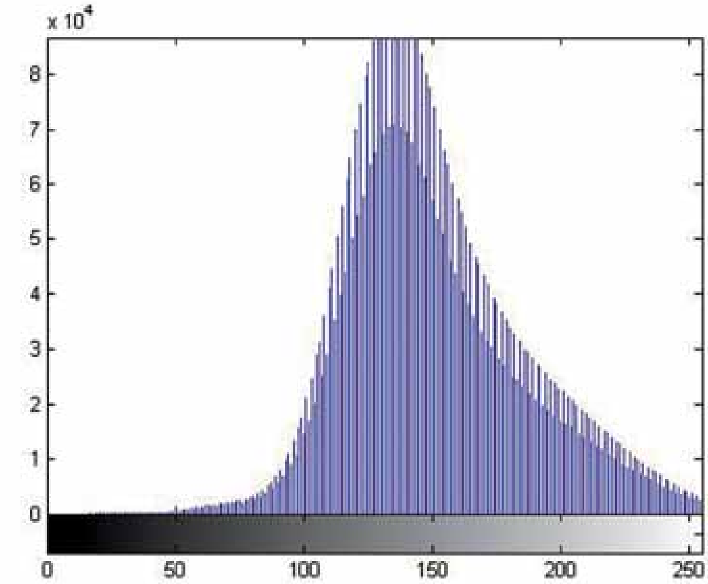



Figure 14. Frequency distribution of grey values before ageing.

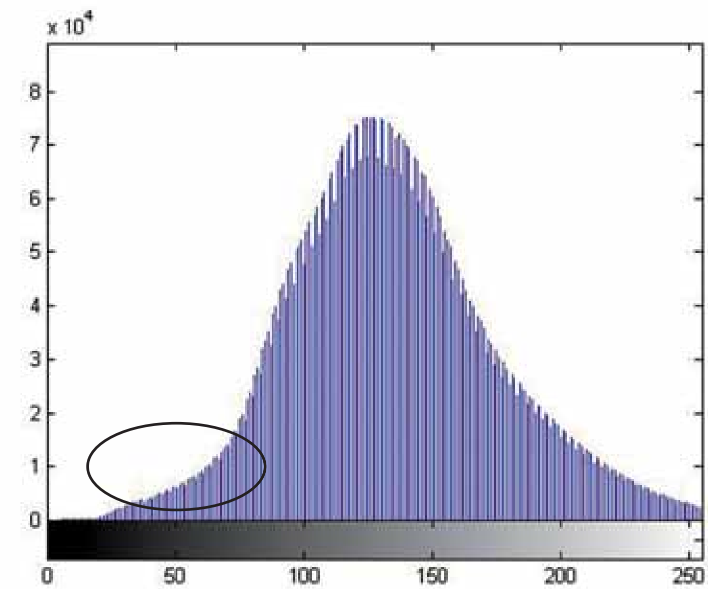



Figure 15. Frequency distribution of grey values after ageing.

| | $U_{oc}$ [V] | $I_{sc}$ [A] | $U_{mp}$ [V] | $I_{mp}$ [A] | $P_{max}$ [W] |
|---|---|---|---|---|---|
| Before ageing | 23.59 | 7.07 | 16.97 | 5.73 | 97.23 |
| After ageing | 22.98 | 5.19 | 16.60 | 4.13 | 68.52 |

Table 2. Current–voltage measurement results.

defects visible, apart from some darker areas. Likewise, there are hardly any defects identifiable in the IR image of the same module (Fig. 11): only the metallic junction box was visible as a cooler area in the image.

The EL image of the a-Si module after ageing (Fig. 12) mainly shows punctual shunts inside a cell or between the metal layers of two adjacent cells. In the EL image the punctual shunts in the cell area appear as black points; bright points appear in between two cells, where the current flows through the shunt to the Si-layer of the next cell. The bright points are caused by increased recombination of electron-hole pairs and/or increased thermal radiation in the surroundings of the shunt area [8]. The dark thermography image of the a-Si module (Fig. 13) shows almost the same defects as the EL image, but it is not always possible to identify their exact locations.

The EL image detected with the Si-CCD camera generally shows an intensity distribution (grey-scale image) of the luminescence radiation. A further evaluation process is the generation of a frequency distribution, specifically a histogram of the available grey values in the EL image. The increase in defects before and after electrical or mechanical loading of modules can be more accurately determined using this evaluation.

A comparison of the frequency distributions of the available grey values before and after ageing tests (Figs. 14 and 15) shows a shifting of the intensity distribution and a rise in the dark/defect areas (circled in Fig. 15). This evaluation process is very helpful in the case of modules for which no increase in defects is clearly observable.

Since not all defects have an influence on the power output of cells or modules, performance measurements were taken in addition to the EL and IR measurements. These measurements show a relation between the increase in defects within a cell or module and the measured power losses. The results of the current–voltage measurements before and after ageing are shown in Table 2. After ageing of an a-Si module (Fig. 12), there was a degradation in power of approximately 30%; this power loss was mainly caused by the reduction of the short-circuit current due to the reduced cell area.

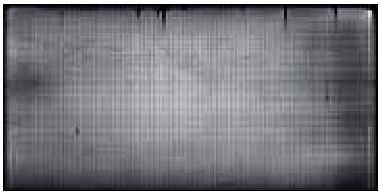

Figure 16. EL image – CdTe module (injected current = 1A).

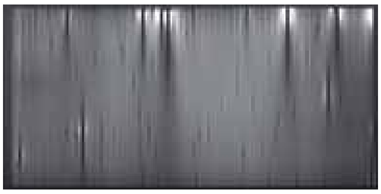

Figure 17. EL image – CdTe module (injected current = 0.1A).

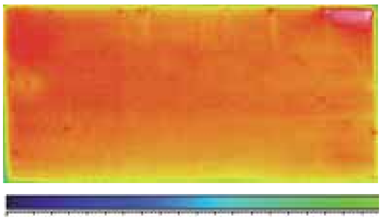

Figure 18. Dark IR image – CdTe module.

### Injection current-dependent EL measurements of a CdTe module

To determine the influence of defects (e.g. shunts), the EL behaviour of modules when different current densities are applied was investigated. When a low current density is applied, the conductivity of shunts is very high: the stronger the shunts, the lower the EL intensity in this area. Strong shunts can supress the EL intensity of a whole cell. When higher current densities are applied, the increase in conductivity of the p-n junction is relatively greater compared to the shunt conductivity, and shunts are less influential on the EL intensity distribution [9].

The EL images of a CdTe module, taken after applying different forward bias voltages, were compared. Fig. 16 shows the EL image of the CdTe module with an injected current of 1A ($I_{sc}$ of the module); Fig. 17 shows the EL image with an injected current of 0.1A. A comparison of the two EL images shows very clearly that effective shunts are visible as punctual defects and thus better detectable when high currents are injected. On the other hand, the EL intensity of the area around effective shunts is considerably increased when low currents are injected.

Most of the identified defects (mainly shunts) in the EL image of the CdTe module in Fig. 16 are also visible in the dark thermography image in Fig. 18. The hot spots identified in Fig. 18 can be attributed to areas with a low shunt resistance, where the current flows through the defect and creates a heat source.

### Comparison of EL and IR images of a CIS module

Fig. 19 shows the EL image of a CIS module: punctual areas of reduced EL intensity are caused by shunts. Since shunts are easier to locate at high current densities, the current applied was the $I_{sc}$ of the module. An illuminated thermography image (Fig. 20) of the CIS module operated under short-circuit conditions reveals some hot spots, but they are not as clear as in the dark thermography image (Fig. 21). With regard to thin-film technology, it transpired that dark thermography measurements generally supplied more detailed images than illuminated thermography measurements.

## Conclusions

It has been shown that EL is clearly an appropriate method for detecting micro-cracks, interrupted contacts or a number of process failures (e.g. shunts or defects in the antireflection layer). However, it was not possible to determine the influence of these defects on the cell/module power output. The IR measurements taken proved that, on the one hand, not all identified defects lead to an increase in temperature. On the other hand, cells/

Figure 19. EL image – CIS module.

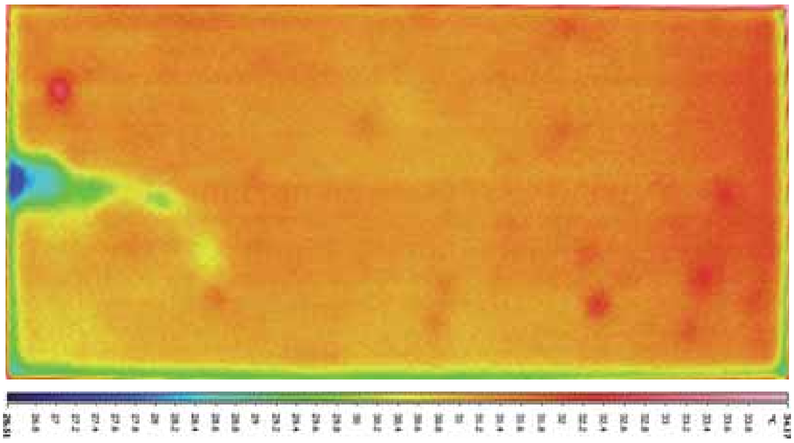

Figure 20. IR image – $I_{sc}$-operated CIS module.

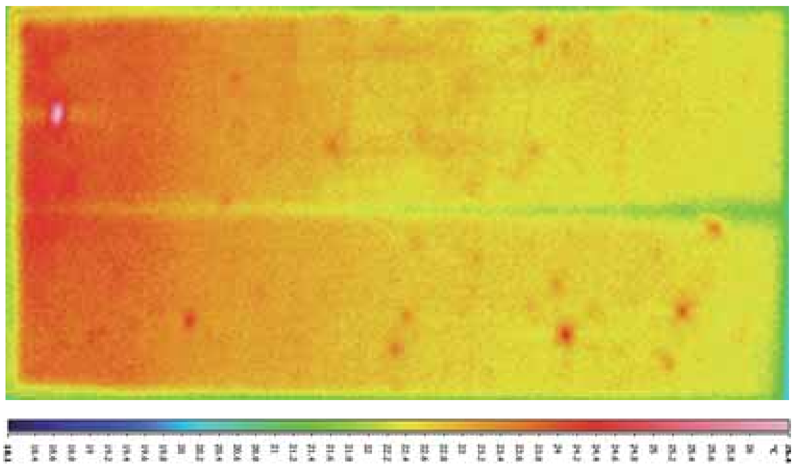

Figure 21. Dark IR image – CIS module.

modules with unremarkable EL images sometimes supply IR images with hot areas, which are caused by high power losses. Therefore, a combination of EL and IR techniques is necessary in order to identify as many defects as possible [8]. Short-circuit measurements of each cell in a module also give information about the cell's condition. In most cases the cell that produces the largest decrease in short-circuit current is also the hottest one (identified by IR measurements).

In the case of sun-illuminated thermography, varying the electrical load helps to distinguish several defects. If the voltage is increased from zero to that at MPP, some hot spots disappear because of the different $I_{sc}$ of the cells. The hot spots, which vanish if the voltage is increased towards $U_{oc}$, are caused by areas of increased series resistance [10].

It was easier to distinguish defects in crystalline modules than in thin-film modules. In the thermography images of thin-film modules the exact location of the defects could not always be identified and the large number of small spots made this determination difficult.

As regards IR thermography measurements, it turned out that illuminated thermography is more suited to crystalline modules, whereas dark thermography is a better tool for thin-film modules [11]. Compared to dark thermography images of crystalline modules, illuminated thermography images offer more detail and a better defect resolution; for thin-film modules the opposite is true.

"Compared to dark thermography images of crystalline modules, illuminated thermography images offer more detail and a better defect resolution; for thin-film modules the opposite is true."

A vitally important loss mechanism, mainly applicable to thin-film modules, is the loss due to localized shunts in the module. A typical thin-film module consists of a number of elongated cells connected in series and separated from each other by scribe lines. Shunt paths can be caused by imperfections in the scribing procedure, develop during the film growth process (e.g. penetration of the junction depletion layer) or occur when layers are too thin or not properly deposited. The existence of localized shunts, specifically hot spots, could also be proved in this case by means of EL and IR thermography measurements. Finally, it could be proved that the effectiveness of defects (e.g. very strong shunts) is identifiable by means of current-dependent EL measurements.

It was also noticed that the radiation of thin-film modules under forward bias was weaker than that of crystalline modules. It is therefore very important that, when taking EL measurements of thin-film modules, there is no reflection of any other light source on the module: the measurement room must be kept in complete darkness.

## Acknowledgement

This work was undertaken within the project IPOT, funded by the COMET programme line of the Austrian Research Promotion Agency.

## References

[1] Wuerfel, P. et al. 2007, "Diffusion lengths of silicon solar cells from luminescence images", *J. Appl. Phys.*, Vol. 101, p. 123110.

[2] Bothe, K. et al. 2007, "Combined quantitative analysis of electroluminescence images and LBIC mappings", *Proc. 22nd EU PVSEC*, Milan, Italy.

[3] Bothe, K. et al. 2006, "Electroluminescence imaging as an in-line characterisation tool for solar cell production", *Proc. 21st EU PVSEC*, Dresden, Germany, p. 597.
[4] Hinken, D. et al. 2007, "Series resistance imaging of solar cells by voltage dependent electroluminescence", *Appl. Phys. Lett.*, Vol. 91, p. 182104.
[5] Haunschild, J. et al. 2009, "Fast series resistance imaging for silicon solar cells using electroluminescence", *physica status solidi (RRL)*, Vol. 3, pp. 227–229.
[6] Hoyer, U. et al. 2009, "Analysis of PV modules by electroluminescence and IR thermography", *Proc. 24th EU PVSEC*, Hamburg, Germany.
[7] Ankner, M. et al. 2010, "Analyse von Fehlerbildern an Dünnschichtmodulen über das EL-Verfahren", *Proc. 25th PV Symp.*, Staffelstein, Germany.
[8] Ebner, R., Zamini, S. & Újvári, G. 2010, "Defect analysis of different photovoltaic modules using electroluminescene (EL) and infrared (IR)-thermography", *Proc. 25th EU PVSEC*, Valencia, Spain.
[9] Helbig, A. et al. 2009, "Electroluminescence analysis of Cu(In,Ga)$Se_2$ thin-film modules", *Proc. 24th EU PVSEC*, Hamburg, Germany.
[10] Ebner, R. et al. 2011, "Electroluminescence (EL) and infrared (IR) imaging of different module technologies", presented at the PV World Conf. & Expo, Tampa, Florida, USA.
[11] Ebner R. & Zamini, S. 2011 "Electroluminescene (EL) and infrared (IR) methods for characterising different thin-film module technologies", *Proc. 3rd Int. Conf. Thin-Film PV*, Munich, Germany.

## About the Authors

**Shokufeh Zamini** joined the Energy Department at AIT in 2006 and is currently responsible for research and analysis in the field of PV modules. She is in charge of several national and international research projects concerning the analysis and performance of PV devices. Since 2008 Dr. Zamini has been a lecturer for the IR-Thermography Laboratory at the University of Applied Sciences Technikum Vienna in Austria. She has been a member of the scientific committee of the OTTI-Thin-Film Forum since 2009.

**Rita Ebner** has been working as a scientist and project manager in the Energy Department at AIT since 2009. She specializes in photovoltaics and is responsible for national and international research projects in this field. Dr. Ebner was a lecturer at the college of renewable energies (TGM, Vienna) in 2003, and in charge of the research and development of a new generation of solar cells at KIOTO Photovoltaics GmbH (Carinthia) in 2007.

**Gusztáv Újvári** studied audio, video and telecommunications at the University of Applied Sciences Technikum Vienna from 2001 to 2005. He has been working as an engineer in the Energy Department at AIT since 2009, specializing in photovoltaic device testing, and hardware and software development. Before that, Gusztáv spent four years at Business Unit Monitoring, Energy and Drive Technologies in Vienna, where he gathered expertise in pattern recognition, simulation of partial discharge patterns and software development.

**Bernhard Kubicek** studied physics at AIT in the field of nuclear simulation. Since then he has been working for AIT, where he focuses on numerical fluid dynamics, simulation of electric discharges and nonlinear optimization, as well as image processing. Bernhard's most recent project concerned the automated processing of electroluminescence images.

## Enquiries

Austrian Institute of Technology (AIT)
Energy Department
Giefinggasse 2
1210 Vienna
Austria

# Life cycle analysis of modules: A multicrystalline silicon case study

**Trond Westgaard**, Renewable Energy Corporation, Sandvika, Norway, & **Carol Olson** & **Ton Veltkamp**, Energy Research Centre of the Netherlands, Petten, The Netherlands


## ABSTRACT

The improved performance and reduced manufacturing costs of photovoltaic (PV) modules that have been achieved in recent years have positioned this technology as an economically attractive renewable electric energy source. In order to verify that this also has a positive impact on energy payback time (EPBT) and carbon footprint, the Energy Research Centre of the Netherlands (ECN) has conducted a life cycle analysis (LCA) for REC Peak Energy-series PV modules produced by Renewable Energy Corporation (REC). The LCA study was based on a full set of actual production data obtained for the first quarter of 2011 from REC's manufacturing sites. Because REC is an integrated manufacturer, the LCA study includes internal data for the production steps from polysilicon production to module assembly, as well as for all materials and transportation associated with production. ECN used generic figures for installation, operations and recycling together with the REC data to assess the environmental impact indicators. For polysilicon produced in the USA, and for wafers, cells and modules produced in Singapore, an EPBT of 1.2 years was achieved, with a corresponding carbon footprint of 21g $CO_2$-eq/kWh for PV systems located in southern Europe (1700kWh/$m^2$ · year irradiation). For modules with wafers and cells produced in Norway, the corresponding values were 1.1 years and 18g $CO_2$-eq/kWh. A key contributor in achieving these values is REC's highly efficient fluidized bed reactor (FBR) process for the production of polysilicon.


## Background

Photovoltaic modules convert absorbed energy from sunlight directly into electricity. In this sense, PV technology represents an effective way of producing clean electric energy from a renewable source. PV power plants can produce electricity for decades with minimal energy consumption and without carbon dioxide emissions. However, there is direct energy consumption associated with the production and installation of PV systems, and there is indirect energy consumption associated with the materials that are used. This energy consumption leads to associated carbon dioxide emissions. A complete life cycle analysis (LCA), or life cycle assessment, also considers these factors during the operations period and in the dismantling and recycling phases of PV power plants.

The total energy consumption associated with PV system manufacturing is used to calculate the energy payback time (EPBT). This refers to the time a PV system has to operate after installation before it has produced the amount of electricity corresponding to the energy used to produce, install and finally recycle its components. The calculation is done for a typical installation at a specific location. The energy mix used for the supply of electricity to the grid has to be considered at production locations and at the location where the PV system is installed. The carbon footprint is calculated for the assumed lifetime of the installation.

In a recent article by van der Meulen [1], PV module customer awareness of PV's carbon footprint is discussed. Although the general impression is that module manufacturers are not yet active in documenting the carbon footprint, this is actually important for PV manufacturers. Documentation of low energy consumption and low carbon footprint is crucial for maintaining support from the public and regulators for PV as a technology that provides clean electricity. Some markets already have a strong awareness of environmental issues: an example of this is France, where there are regulations in place that provide incentives for commercial systems using PV modules from suppliers that document the modules' environmental impact.

An integrated manufacturer such as REC monitors consumption and emissions starting from polysilicon production, through wafer, cell and module manufacturing, and ending with the final recycling of the modules. The value chain is based on primary materials, which makes it possible to establish a reliable value for the environmental impact of the technology. A primary material is a material that is not a by-product of the production of other materials. (LCAs for other PV manufacturers that use, for example, discarded PV cells or secondary metals need to correctly represent the impacts of the primary activities, such as cell production or mining and refining of the associated primary metals.)

## LCA methodology

An LCA evaluates the environmental impact of a product (or service) from the first associated production phase to the recycling phase. The international standard ISO14040 describes the general principles and framework for LCAs. A set of more specific methodology guidelines on life cycle assessment of photovoltaic electricity has been published by the International Energy Agency [2]. These guidelines were used for the present LCA study. A complete data set for consumption factors and emissions has to be collected from the value chain under consideration. These data are then processed to obtain the LCA metrics. ECN uses the software SimaPro 7.2.4 [3] combined with the ecoinvent 2.2 database [4]. This database contains data associated with energy supply and data for externally supplied materials.

Since ECN uses the ecoinvent database, the ecoinvent methodology is used in order to maintain internal consistency. For example, when a PV module is recycled and aluminium from the module frame is going to recycling, no credits are obtained for the avoidance of the production of primary aluminium. The credits are obtained at the moment the aluminium is consumed in the manufacturing of the module (20% primary Al, 47% secondary Al from new scrap, 33% secondary Al from old scrap).

### Energy payback time

The *energy payback time* is the time needed for the PV system to generate the amount of electric energy that replaces the amount of primary energy required to produce it (Equation 1).

The energy input is calculated using the 'cumulative energy demand' (CED) method, which is the total life cycle primary energy consumption. In this study the CED 1.07 method is used as implemented in SimaPro. The efficiency of the electricity supply used in the calculation is 11.4$MJ_{primary}$/kWh (UCTE electricity mix).

Energy payback time is a metric that is easy to relate to, but it is important to note that it does not consider the system lifetime. Reliable PV systems with long lifetimes represent an important aspect of PV as a viable source of renewable energy.

## Carbon footprint

The *carbon footprint* is obtained from the LCA by considering all emissions that have an effect on climate change. It is quantified using the global warming potential (GWP) index. The Intergovernmental Panel on Climate Change (IPCC) has defined the GWP100a index as the relative effect of a greenhouse gas in terms of climate change over a fixed time period of 100 years and is expressed as carbon dioxide equivalents ($CO_2$-equivalents). ECN uses the IPCC2007 GWP100a method version 1.02 as it is implemented in SimaPro. Standardization of carbon footprinting is described by the SETAC Europe LCA Steering Committee [5]. The most relevant metric for renewable electricity sources is the total GWP of the PV system divided by the total electricity production of the system during its lifetime (Equation 2).

> "An LCA has to consider both the consumption of energy and materials involved in its production and the actual electricity production during its lifetime."

This metric allows the low carbon footprints of renewable electric energy sources to be compared to the carbon footprints of electricity produced in coal- or gas-fired power plants. A particularly favourable situation occurs when renewable energy, such as hydroelectricity, is used in the manufacture of PV products.

## System considered and collection of production data

Since a PV module is intended to produce electricity, an LCA has to consider both the consumption of energy and materials involved in its production and the actual electricity production during its lifetime. The PV system analyzed is a multicrystalline silicon photovoltaic system using REC Peak Energy-series modules of dimensions 1665mm × 991mm (area 1.65m$^2$). One module is made up of 6 × 10 solar cells of size 156mm × 156mm. The considered PV system is an on-roof installation in southern Europe (or a location with equivalent conditions), having an in-plane irradiation of 1700kWh/m$^2$ · year and a system performance ratio of 0.84. This performance ratio was demonstrated in tests performed in 2010 in San Luis Obispo, California, which is a location with conditions very close to the considered case. Tests performed by *Photon* magazine show a higher performance ratio for this module type, but these results do not include energy loss in the inverters [6]. A generic data set obtained by ECN is used for installation materials, inverters and end-of-life recycling of the PV modules. The lifetime of the system is assumed to be 30 years. During operation of the PV system, it is taken into account that the inverters will be replaced after 15 years of operation, which is considered realistic for present inverter technology.

The LCA is performed with actual production data for the first quarter of 2011 from REC manufacturing sites in the USA, Norway and Singapore. This ensures that real values for production output, yield factors and waste streams are considered. For each production site the energy mix associated with electricity consumption is the actual mix for the production site. REC's manufacturing sites use predominantly hydroelectricity and electricity generated from the combustion of natural gas. The transportation distances between the USA, Norway and Singapore were calculated using on-line logistics calculators for freight transport by sea and land, as it actually took place. Average transport distances were used for shipping of materials from European countries to Norway. Transport of module materials

$$\text{Energy payback time} = \frac{\text{Primary energy input}}{\text{Replaced primary energy relating to the electric energy output per year}}$$

**Equation 1.**

$$\text{Carbon footprint} = \frac{\text{Emissions (g } CO_2\text{-equivalents)}}{\text{Total electric energy production over lifetime (in kWh)}}$$

**Equation 2.**

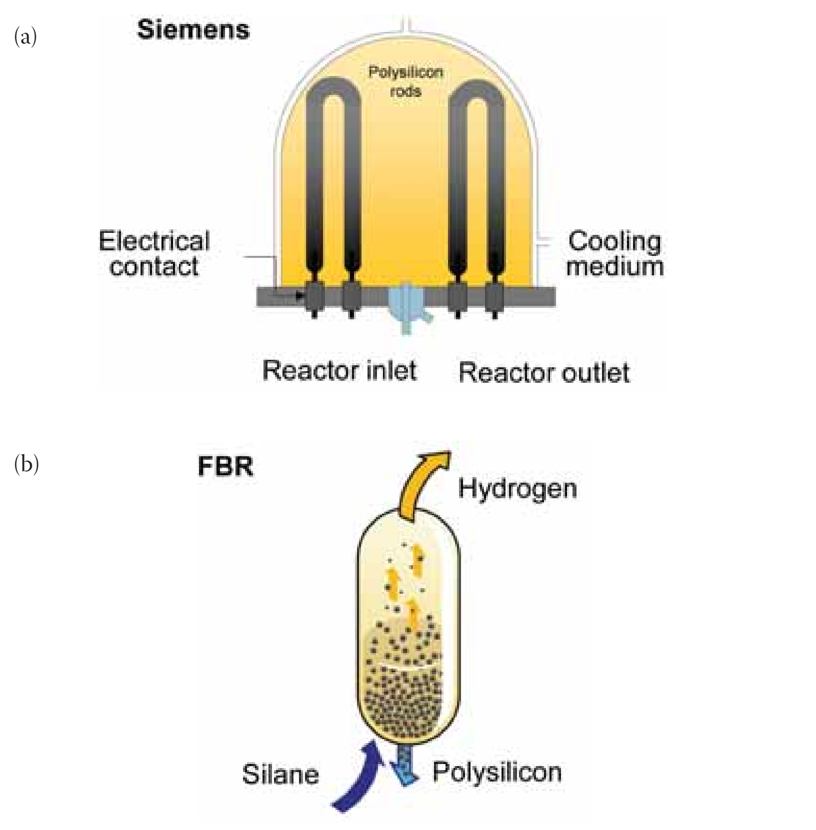


**Figure 1. Schematic of the principles of (a) a Siemens polysilicon reactor, and (b) a fluidized bed reactor (FBR) for polysilicon production.**

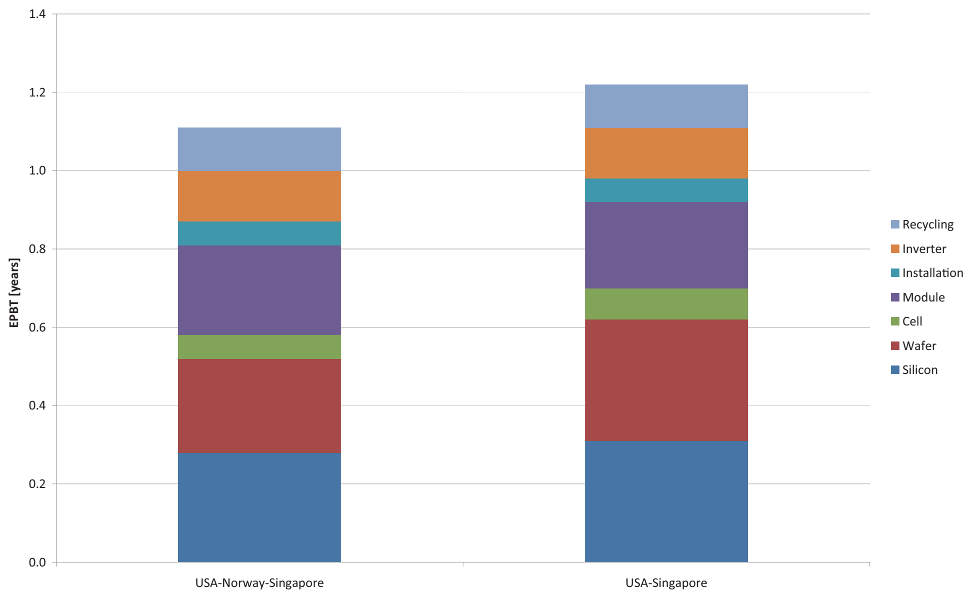


**Figure 2. Energy payback time (EPBT) of on-roof PV systems with REC modules installed at a location in southern Europe (1700kWh/m$^2$ · year irradiation).**

from Tokyo to Singapore was used as an average estimate of the transport of components from suppliers located in Southeast Asia to Singapore.

Data for polysilicon production were obtained from the manufacturing units in Moses Lake, Washington, USA. These units produce semiconductor-grade silane gas from metallurgical-grade silicon. The silane gas is converted into polysilicon in conventional Siemens-type reactors and in fluidized bed reactors (FBRs). The principles of these two processes are illustrated in Fig. 1. The direct energy consumption for the FBR process is approximately 80% lower than the classical Siemens process via the silane route. The electricity consumption reduction associated with the FBR process is even more distinct.

Multicrystalline silicon wafer production data are collected from the REC production sites in Herøya, Norway, and in Singapore. There are only minor differences in consumption data between these sites. However, the energy mix for electricity in Norway is mainly hydroelectricity, while electricity in Singapore is produced from natural gas. The granular form factor of FBR polysilicon enables up to 29% higher silicon charges in the ingot-casting process when blended with polysilicon from the Siemens process than when conventionally charged with polysilicon chunks. The LCA is based on the actual blend of FBR and Siemens polysilicon that was used by REC.

In the period considered in the LCA, REC produced solar cells in Narvik, Norway, and in Singapore. These sites also had equivalent consumption data, but with the same difference in electricity supply as for wafer production. PV modules were manufactured in REC's automated module assembly unit in Singapore.

## LCA results

The analysis is based on data from two production flows within REC. One is based on wafer and cell production at Norwegian locations, with module assembly in Singapore: a PV module from this value chain has a cumulative energy demand of 13.0MJ/$W_p$ and a carbon footprint of 570g $CO_2$-eq/$W_p$. The other production flow is for the integrated wafer, cell and module production at the Singapore site, with corresponding values for cumulative energy demand of 15.2MJ/$W_p$ and a carbon footprint of 726g $CO_2$-eq/$W_p$. Both production flows include polysilicon from the Moses Lake production facility. The major difference between these two production flows is that the first is based on electricity from a renewable source (hydroelectricity), while the second is based on electricity produced by the combustion of natural gas.

These LCA results are easier to relate to when the complete system is considered. Fig. 2 shows energy consumption related to energy production, reported as energy payback time. It is seen that the energy payback time including recycling is just above one year, and it can in fact be brought down below one year by using 100% FBR polysilicon. (In order to have optimal silicon charging of crucibles it is practical to run with a blend of polysilicon feedstock.) Polysilicon feedstock is an important (but not dominating) part of the energy consumption. Ingot casting and wafer production contribute to roughly the same extent. The results show a distinct advantage in using renewable electric energy for production of wafers (including ingot production) and cells over using electricity from natural gas. This advantage would be even larger if a comparison were made with potential production based on electricity from coal-fired power plants. Although the impact of cell production appears minor, high cell efficiencies reduce the impact of all other factors.

> "Polysilicon feedstock is an important (but not dominating) part of the energy consumption."

The same issues are reflected among the factors contributing to the carbon footprint shown in Fig. 3. The polysilicon feedstock contribution to the carbon footprint is relatively small compared to the total carbon footprint, which ranges from 18 to 21g $CO_2$-eq/kWh. The difference in relative impact between wafer production (including ingot production) in the two value chains is even more pronounced for carbon footprint than it is for energy consumption. It is also evident that the contributions from installation and recycling are important. Continued improvements in module efficiency are an effective way of further reducing these contributions.

## Conclusions and outlook

ECN and REC's LCA study of PV modules with multicrystalline silicon cells shows that both module production value chains – one based on hydroelectricity and the other on electricity generated from natural gas – result in systems with environmental impacts at the lowest end of the range

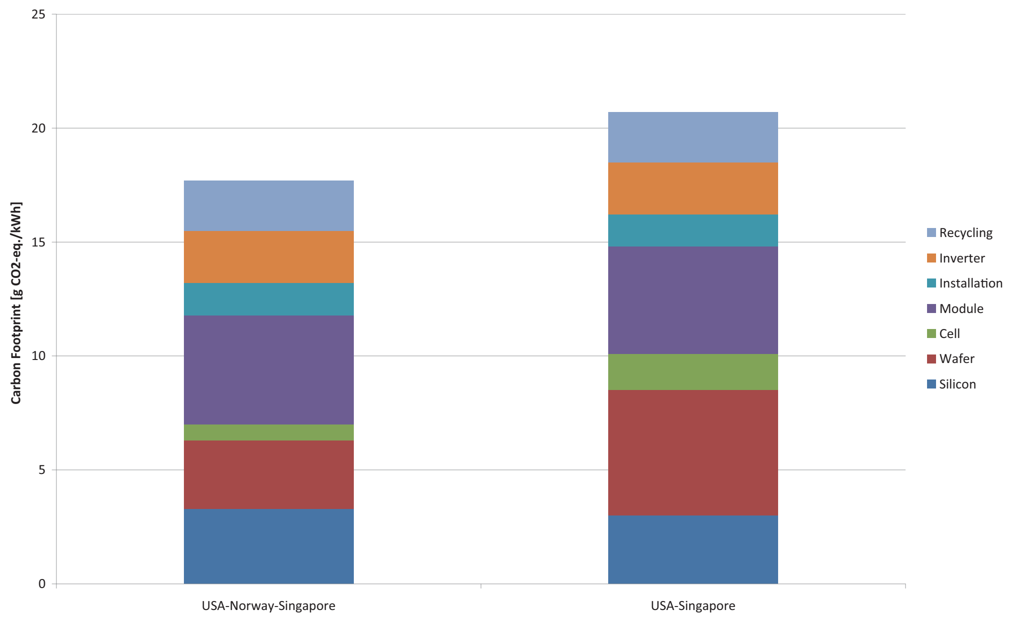


**Figure 3. Life cycle greenhouse gas emissions (carbon footprint) per kWh of electricity produced for REC PV systems installed at a location in southern Europe (1700kWh/m$^2$ · year irradiation, with system lifetime of 30 years).**

indicated in van der Meulen [1], with energy payback times just above one year and carbon footprints of approximately 20g $CO_2$-eq/kWh. There is a distinct advantage in using a renewable electricity source, but both value chains have enormous advantages over electricity from fossil fuel-based power plants. For reference, the carbon footprint of electricity from natural gas is 330–440g $CO_2$-eq/kWh, and electricity from coal-fired power plants has a considerably higher value of 670–1000g $CO_2$-eq/kWh [7,8].

Further reductions of the environmental impact are imminent: PV modules with higher conversion efficiency due to increases in cell efficiency will reduce the impacts of all factors along the value chain. The PV industry is also continuously striving to reduce energy consumption and therefore costs by using more efficient production methods.

## References


[1] van der Meulen, R. 2011, "True sustainability in the PV industry: The case for carbon footprint certification", *PVI*, 14th edition, pp. 20–26.

[2] IEA 2011, "Methodology guidelines on life cycle assessment of photovoltaic electricity", Report IEA-PVPS T12-03:2011 [available online at http://www.iea-pvps.org/fileadmin/dam/public/report/technical/rep12_10.pdf].

[3] SimaPro 7.2.4 software [details available online at http://www.pre.nl/simapro/].

[4] ecoinvent 2.2 database [details available online at http://www.ecoinvent.org/].

[5] SETAC Europe LCA Steering Committee 2008, "Standardization efforts to measure greenhouse gases and 'carbon footprinting' for products", *Int. J. Life Cycle Assess.*, Vol. 13, No. 2, pp. 87–88.

[6] Photon Laboratory 2011, "Photon Lab's outdoor module tests – October results", *Photon International* (December), pp. 152–155.

[7] EPIA 2011, "Fact sheet on the carbon footprint" [available online at http://www.epia.org/publications/sustainability-factsheets.html].

[8] IEA 2011, "$CO_2$ emissions from fuel combustion: Highlights" [available online at http://www.iea.org/co2highlights/co2highlights.pdf]. (Listed values partly include utilized residual heat.)


## About the Authors


**Trond Westgaard** holds a Dr. ing. degree in semiconductor physics from the Norwegian University of Science and Technology, Trondheim. He is currently Vice President of Technology at Renewable Energy Corporation ASA, based in Sandvika, Norway, where his primary tasks are development strategies and benchmarking of PV products. Before joining REC in 2008, Dr. Westgaard worked on development of silicon-based detectors and MEMS sensors.

**Carol Olson** received a Ph.D. in physics from Imperial College, London, in 2003. After joining ECN in 2006, she carried out research in the areas of thin-film photovoltaics and characterization of silicon solar cells. Currently, Dr. Olson is a project manager of projects relating to life cycle assessment of photovoltaic products and processing lines, as well as those relating to cost and sustainability of photovoltaics.

**Ton Veltkamp** obtained his Ph.D. in chemistry at the Free University of Amsterdam in 1989. He worked as a research scientist in environmental chemistry at ECN from 1989 to 1990, after which he managed various research laboratories at NRG and ECN, then later joined ECN Solar Energy as manager of the thin-film photovoltaics group. Since 2008, Dr Veltkamp has been the manager of the crystalline silicon photovoltaics manufacturing technology group at ECN, where he is responsible for the environmental assessment studies of photovoltaic technologies. He is a member of the EPIA sustainability working group and a member of the IEA-PVPS Task 12 working group that deals with PV environmental health and safety activities.


## Enquiries


Renewable Energy Corporation ASA
Kjørboveien 29
PO Box 594
NO-1302 Sandvika
Norway
Email: post@RECGroup.com

Energy Research Centre of the Netherlands
P.O. Box 1
1755 ZG Petten
The Netherlands

# Studying the lifetime of crystalline PV modules by interpreting the acceleration test data with statistical reliability models

**Sreenivasa Murty Dasari**, **K. V. Nagaraj**, **S. Saravanan**, **Prakash Suratkar** & **T. S. Keshav Prasad**, TATA BP Solar India Ltd, Bangalore, India

ABSTRACT

Crystalline silicon solar modules installed in the field are exposed to atmospheric conditions and experience stress, which induces a wear-out phenomenon in various parts of the modules and degrades performance over time. The performance eventually reaches a point where the output power falls below an acceptable level. Thermal cycling (TC) and damp heat (DH) are two important reliability tests for estimating infant failures related to materials and the manufacturing process, as well as providing the information on performance degradation with respect to time. In this study, modules composed of 156mm × 156mm multicrystalline silicon cells were subjected to TC and DH tests. By applying acceleration models, such as the Norris-Landzberg model for TC and the Hallberg-Peck model for DH, the minimum guaranteed life was calculated. The electrical and reliability results were interpreted and explained on the basis of the respective models.

## Introduction

Photovoltaic (PV) technology has the advantage of being able to generate power by means of solar panels that can receive solar radiation irrespective of other environmental factors such as humidity, temperature and rainfall. Crystalline PV technology is a primary solution for energy generation in remote areas where conventional power is not feasible, and also becomes an alternative solution to the on-grid power option when power demand exceeds conventional power generation capacity. Solar panels installed in the field experience adverse environmental effects and degraded power generation capacity year in, year out. In today's solar market, module manufacturers offer a warranty of a minimum of 25 years of power generation and workmanship, up to a limit of 80–85% power.

> "With continuous exposure to solar radiation, EVA reacts with ultraviolet radiation in the solar spectrum."

As for the industry standard, solar module manufacturers have to follow International Electrotechnical Commission (IEC) 61215 guidelines [1] and obtain certification of their products from authorized certification institutes. During certification tests, modules will be subjected to an accelerated stress test for factors such as temperature and humidity to understand the types of failures that can occur and their relation to the quality of the process and materials used in module manufacturing. If either the process or the materials change, the new modules are required to be re-certified by following the IEC retest guidelines [2]. The solar industry needs to adhere to stringent quality standards due to the 25-year product warranty.

There are two kinds of power degradation: light-induced degradation and wear-out degradation. *Light-induced degradation* is related to EVA and the performance of a solar cell with respect to time. With continuous exposure to solar radiation, EVA reacts with ultraviolet radiation in the solar spectrum and hence light transmission to the solar cell through EVA will be reduced [3]. The rate of current generation of the solar cell will decrease after exposure to radiation because boron in the silicon substrate reacts with oxygen contamination and forms recombination centres [4]. *Wear-out degradation* – mainly due to thermal, mechanical and humidity-related stress factors and maximum test failures – is related to thermal cycling (TC) and damp heat (DH) stresses only [5]. There are various studies of TC and DH failures [6–8] in terms of failure analysis. This paper presents the results of studies focusing on TC and DH tests for modules manufactured at Tata BP (TBP) and these results are interpreted to determine the equivalent lifetime using statistical models.

For this study, seven 60-cell modules of multicrystalline 156mm × 156mm cells,

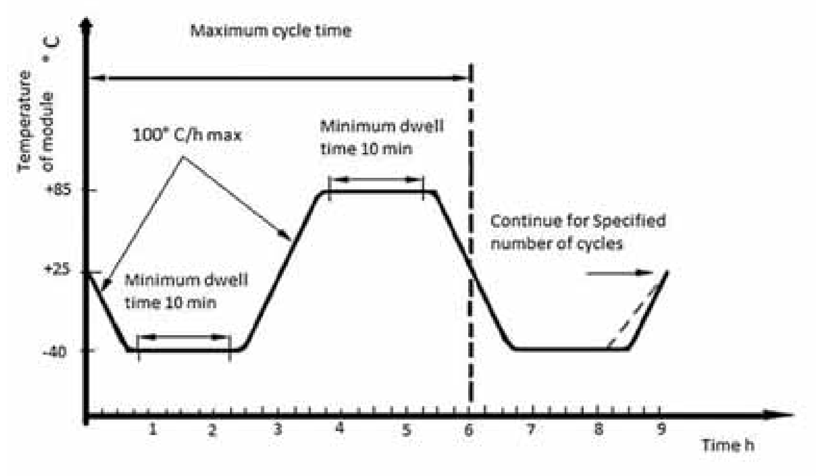


**Figure 1. Thermal cycling profile in accordance with IEC guidelines.**

manufactured by a standard process, were subjected to accelerated environmental tests. Four modules were subjected to the TC test for 500 hours, two modules were subjected to the DH test for 1140 hours and one module was used as a control sample. Test data were correlated with statistical models and the minimum guaranteed lifetime for the product was calculated. *IV* data measured at regular intervals during the TC test were converted to correspond to a real-time distribution.



"Since the environmental conditions are outside of human control, manufacturers should ensure that their modules are robust for any eventual conditions."

## Background

As mentioned previously, during their operation in the field, crystalline silicon solar modules are exposed to atmospheric conditions such as radiation, temperature and humidity. These conditions are not constant and vary from minimum to maximum values in a cyclic manner, causing a build-up of stress in all parts of the module. The wear-out mechanism induced by stress leads to degradation of module performance; the rate of degradation increases with time and eventually reaches a point where the module fails to achieve an acceptable level of performance. The amount of time from the day of installation until a module begins to perform below the acceptable level depends for the most part on two factors: 1) the module process and material quality, and 2) the environmental conditions of the location where the module is installed. Since the environmental conditions are outside of human control, manufacturers should ensure that their modules are robust for any eventual conditions.

In order to withstand the environmental conditions, PV manufacturers use acceleration tests. The accelerated ageing test in indoor chambers uses a mixture of environmental conditions such as pressure, radiation, moisture and temperature, all at higher values than nominal product operating conditions. This kind of reliability testing has been in use in the solar industry since the day of inception of PV products. Accelerated tests proposed by IEC 61215 for design qualification of crystalline PV modules replicate the environmental conditions over 25 years in a short period to find out the failures related to design flaws, material quality and the manufacturing process [9]. There are six types of test:

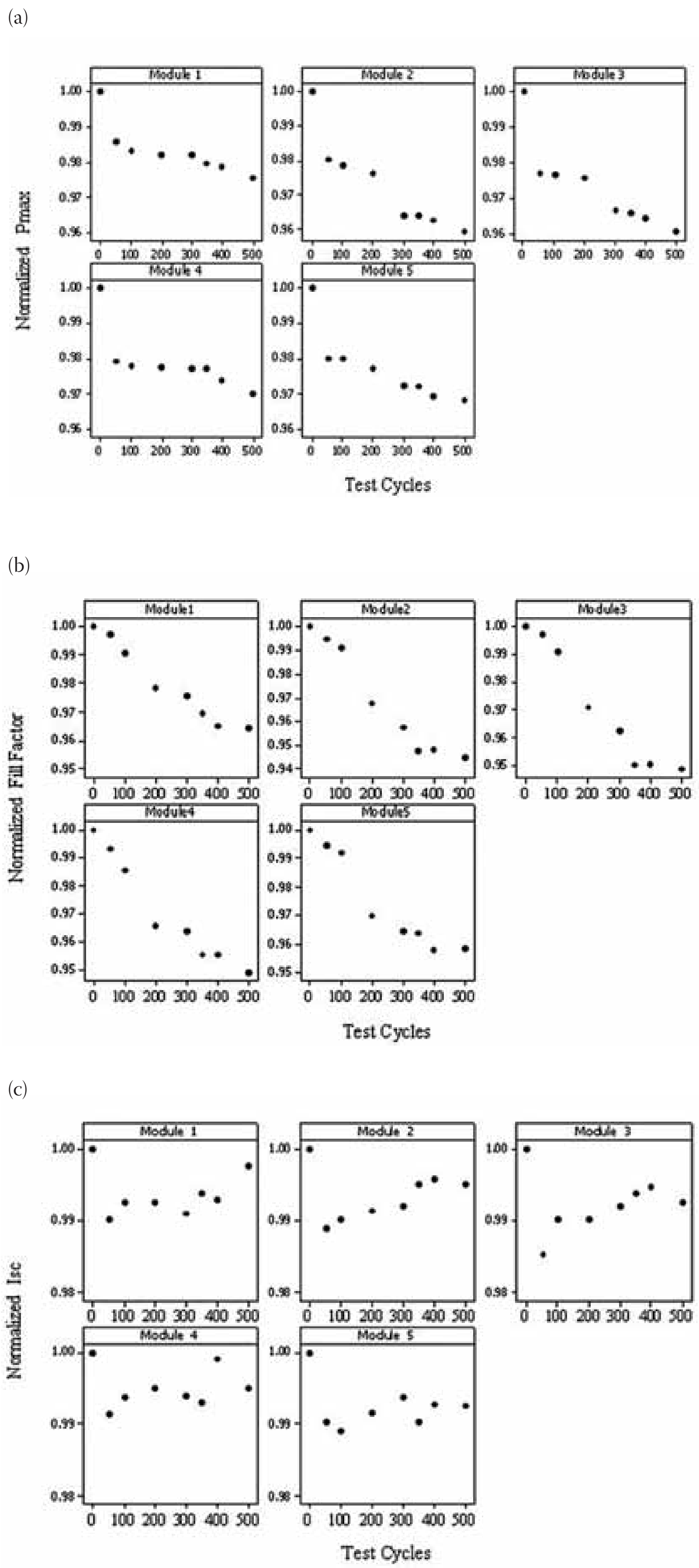


**Figure 2. Relative changes in the characteristics of test modules at various test cycles of thermal cycling: (a) power drop; (b) fill factor drop; (c) short-circuit current drop.**

- Electrical – insulation resistance and wet leakage current tests
- Performance – $P_{max}$, temperature coefficients and normal operating cell temperature (NOCT)
- Thermal – bypass diode and hot-spot tests
- Irradiance – outdoor exposure, UV exposure and light-soaking tests
- Environmental – TC, humidity, freeze and DH tests
- Mechanical – mechanical load and hail tests

Among the mentioned stress tests, the environmental ones are the most critical because according to a survey, most reports indicated that TC and DH failures were more numerous [10]. In this paper, TC studies and DH test results are correlated with a statistical model to estimate lifetime and reliability.

## Experimental details

p-type boron-doped multicrystalline 156mm wafers were converted into solar cells by using standard screen-print technology; modules were then fabricated with these cells. Wafer to module conversion was performed at in-house manufacturing facilities. The steps involved in the module manufacturing process were:

- Tabbing the inspected cells by using interconnect ribbon
- Stringing the tabbed cells
- Making the lay-up by using standard lamination materials
- Laminating
- Fixing the junction box
- Framing
- Testing and grading the module

The *IV* characteristics of these modules were determined using standard operating procedures.

Modules were constructed using the conventional process and tested in accordance with IEC 61215 guidelines for TC and DH in the well-known module reliability test lab. One module was conserved as a control sample in order to compare the performance of the modules after the acceleration tests. Four modules were kept for TC tests and two modules subjected to the DH test. To minimize measurement errors, the control module was measured each time before measuring the test modules.

## Acceleration models

A product is said to be aged when its characteristics (physical, mechanical, chemical, etc.) have changed as a result of the stress experienced in operation over a period of time and its performance or quality has degraded. Some products take longer to age, and it is difficult for product developers to collect failure and lifetime data for their products. The accelerated ageing test is a universally accepted method in industry for testing a product at higher stress levels under various conditions – such as temperature, radiation and humidity – than it normally encounters during its operation.

The accelerated test has two purposes: 1) to determine failures related to design and the manufacturing process, and 2) to estimate the useful lifespan of the product. Since the accelerated tests are carried out at higher levels of stress to evaluate the failure time, the test results cannot be interpreted directly for normal operating conditions. Appropriate acceleration models need to be used to convert the test results to normal operating conditions [11]. A linear time relationship will be assumed to use a transformation function

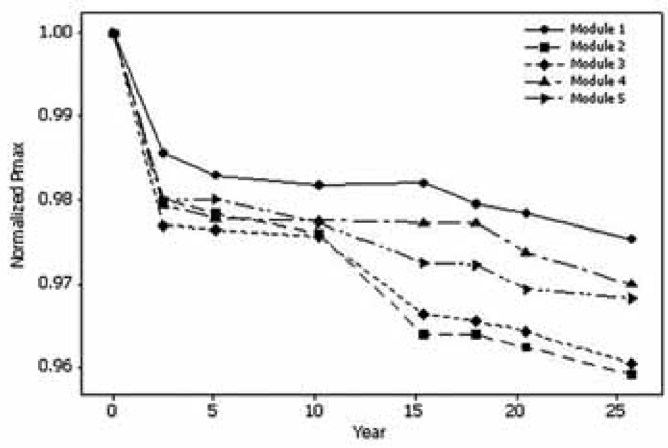


**Figure 3. Power drop with respect to the equivalent years calculated using the acceleration factor.**

for modelling acceleration results; the time to fail under normal operating conditions is therefore

$$T_o = A_f \, T_t \quad (1)$$

where $T_o$ is the minimum guaranteed lifetime, $A_f$ is the acceleration factor and $T_t$ is the time spent in the test.

### Thermal cycling

When a product is exposed to different temperature conditions, not all of its parts will expand or contract at the same rate in all directions because of a mismatch in the temperature coefficients of expansion and contraction of different materials. The stress built up due to this mismatch is called thermal stress. Crystalline PV modules are subjected to TC to characterize the level of damage in solder joints. The temperature coefficients of tin-copper interconnects (TCIs) ($17.5\times10^{-6}$/K), silver busbars ($18.9\times10^{-6}$/K) and silicon ($4.68\times10^{-6}$/K) are different, so the rates of expansion and contraction will be different when a module experiences cyclic changes in temperature. Due to this mismatch in temperature coefficients, the solder joints associated with TCIs, silver busbars and silicon will wear out and increase the series resistance.

> "The fill factor (*FF*) is strongly dependent on the series resistance and shunt resistance of the solar cell."

It is well known that the fill factor (*FF*) is strongly dependent on the series resistance and shunt resistance of the solar cell, and hence any increase in contact resistance will reduce the fill factor significantly. For the study reported on in this paper, TBP multicrystalline 156mm 230W modules were tested for TC using the temperature range defined by IEC 61215 and held for 500 cycles, since the stress level will be increased if held for longer (Fig. 1).

### Norris-Landzberg model (modified Coffin-Manson model)

The Coffin-Manson equation models the effects of thermally induced stress and follows an inverse power law relationship. In other words, as the magnitude of the induced stress increases, the number of cycles to failure decreases by a power of two. Norris-Landzberg modified the Coffin-Manson model by including time- and frequency-dependent anomalies [12,13]. The acceleration factor is calculated using the equation

$$A_{TC} = \left(\frac{\Delta T_L}{\Delta T_U}\right)^2 \left(\frac{F_U}{F_L}\right)^{1/3} \exp\left\{1414\left(\frac{1}{T_U} - \frac{1}{T_L}\right)\right\} \quad (2)$$

where $A_{TC}$ is the acceleration factor for the time duration (dimensionless), $\Delta T_L$ is thermal cycle temperature change in the accelerated lab environment, $\Delta T_U$ is the temperature change in the operating environment, $F_U$ is the frequency (cycles/day) of the thermal cycles in the operating environment, $F_L$ is the frequency (cycles/day) of the thermal cycles in the accelerated environment, $T_U$ is the maximum temperature in the operating environment and $T_L$ is the maximum temperature in the accelerated environment.

> "The temperature of the module starts to increase from 297K along with sun radiation."

The parameters for the acceleration tests conducted in this study are $\Delta T_L$ = 398K, $T_L$ = 358K and $F_L$ = 4 cycles/day. Based on field data of TBP modules installed in the southern part of India, the maximum operating temperature ($T_U$) is 328K. The minimum temperature experienced by modules in the field before and after peak radiation during a day is normally 297K, and hence the difference in operating temperatures ($\Delta T_U$) in a day is 304K. The temperature of the module starts to increase from 297K along with sun radiation and falls back down again to the nominal value when the sun sets. Assuming typical wind speeds and the cloudy behaviour of a particular tropical region, the estimated maximum number of thermal cycles ($F_U$) is four per day. The acceleration factor calculated for TC by substituting the given values and field conditions in Equation 2 is 37. The minimum guaranteed life is therefore equal

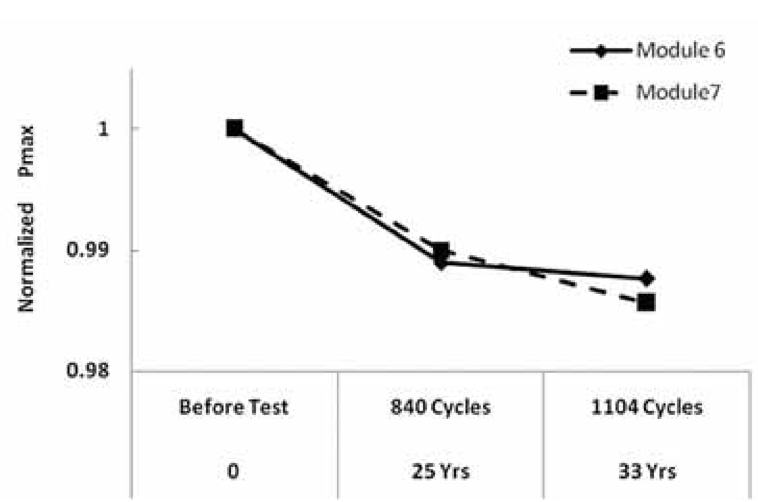


**Figure 4. Power drop of test modules at various test cycles of the damp heat test (85°C, 85% RH).**

to $A_{TC} \times T_t$ = acceleration factor × (number of cycles × 6 hours) = 37 × (500 × 6) hours = 25 years.

**Results and discussion**

Fig. 2 shows the relative change of maximum power $P_{max}$, fill factor $FF$ and short-circuit current $I_{sc}$ of test modules at various test cycles. Zero represents the results for an as-fabricated module, and the $IV$ measurements of modules were carried out at regular intervals to understand the relative drop with respect to the level of stress experienced. The observed drop in power is linear with respect to the number of cycles, and the initial drop of 50 cycles is larger than for subsequent intervals. This is because the short-circuit current dropped significantly compared to the fill factor in the first 50 cycles; the reason for this drop is not yet understood.

As the stress increases with the number of cycles, the fill factor decreases, since the solder joints of the TCI, silver and silicon wear out due to the mismatch in thermal expansion coefficients. By using Equation 1, a number of test cycles were converted into equivalent years by substituting the acceleration factor and time. The power drop with respect to time in years is shown in Fig. 3. It is interesting to note that the contribution of the degradation of the solder joints to power drop in the crystalline solar module during its operation in the field is a maximum of 4% over a 25-year period. The observed decrease in power after 500 cycles of the TC test is quite reasonable for 25 years and can give a manufacturer confidence in their process and material quality.

**Damp heat**

The ageing of a material can be explained using the collision theory of particles, according to which particles in a material are in continuous collision, and a collision with sufficient energy will break existing bonds and form new bonds. This in turn leads to a change in the properties of the material in terms of its physical, mechanical and chemical attributes. The sufficiency energy, also known as activation energy, which decides the success rate of collision, can be increased by changing the temperature. It is well known that at higher temperatures, particles will have higher energy states and have the activation energy necessary to make a collision successful; for every 10°C rise in temperature, the reaction rate doubles [14].

As discussed earlier, the maximum temperature of PV modules in the field is 328K, so the acceleration test is conducted at 358K to increase the rate of reaction. Along with maintaining this temperature, the humidity is also kept at 85% RH, which is higher than normal operating conditions. High humidity in combination with high temperature causes moisture to diffuse through joints and accelerates the corrosion in metal parts of the product [15]. The main objective of the DH test is to assess the lamination process by observing moisture ingress and related corrosion in metallic parts such as silver contact fingers, busbars and interconnect ribbons.

> “At higher temperatures, particles will have higher energy states and have the activation energy necessary to make a collision successful.”

**Hallberg-Peck model**

Arrhenius's equation was the first acceleration model developed for temperature-related stress modelling. This equation was subsequently modified by Hallberg and Peck to combine the effects of temperature and humidity [16] and is given by

$$A_{DH} = \left(\frac{RH_L}{RH_U}\right)^3 \exp\left\{\frac{E_a}{K}\left(\frac{1}{T_U} - \frac{1}{T_L}\right)\right\} \quad (3)$$

where $A_{DH}$ is the acceleration factor, $E_a$ is the activation energy (eV), K is Boltzmann's constant ($8.617 \times 10^{-5}$ Ev/Tk), $T_U$ is the operating temperature (K), $T_L$ is the acceleration test temperature (K), $RH_L$ is the acceleration test humidity and $RH_U$ is the operating humidity. The acceleration test was conducted at a temperature $T_L = 85 \pm 2°C$ with a relative humidity $RH_L = 85 \pm 5\%$ for 1000 hours. Based on field data, the nominal operating temperature and humidity is $T_U = 323K$ and $RH_U = 55\%$; the activation energy for EVA is taken to be 0.9eV [17]. The acceleration factor for the DH test was calculated by substituting the given parameters in Equation 3, yielding $A_{DH} = 87$. The minimum guaranteed life is therefore equal to $A_{DH} \times T_t = 87 \times 1000$ hours = 30 years.

### Results and discussion

Fig. 4 shows the power degradation with respect to the number of test cycles and equivalent years. As the purpose of the test is to verify the stress in a continuous fashion without any discontinuity, the modules were only taken out of the chamber after 840 cycles, which equates to 25 years. The modules were inspected visually and no defects or corrosion in metallic parts was found. If the lamination is irregular, moisture will penetrate in between the layers and react with the metallic parts as well as EVA. Moreover, moisture penetration at higher temperatures will lead to aluminium and back-sheet delamination of the cell back surface, resulting in a significant reduction in module power. For the modules tested, a power drop of 1.3% after 1104 cycles of DH stress testing confirms that the lamination process is optimum and also proves that the quality materials used in module making justify a 25-year warranty.

"The calculations based on reliability models confirmed that the IEC guidelines for acceleration testing are sufficient for providing a long-term warranty on the product."

## Conclusions

Multicrystalline solar modules were subjected to TC and DH tests in accordance with IEC 61215 guidelines; the resulting power drop was correlated to the lifetime calculated from acceleration models. It was clear from reliability calculations that modules made using the standard TBP manufacturing process are able to withstand environmental stresses such as temperature and humidity, as well as delivering the power within acceptable limits for 25 years. This study also confirmed that the power degradation noticed during reliability testing correlated with actual observed performance in the field. The calculations based on reliability models confirmed that the IEC guidelines for acceleration testing are sufficient for providing a long-term warranty on the product. As part of future research in this area, it is envisaged that a detailed understanding and relative analysis of module degradation at various stages of IEC testing could provide an opportunity for manufacturers to improve lifetime and performance.

### Acknowledgements

The authors would like to thank K. Subramanya, CEO, TATA BP Solar India Ltd, for support in carrying out this project. The authors are also indebted to the production and quality teams for their suggestions and feedback.

### References

[1] IEC 61215:2005 / IEC 61646:2008 (design qualification and type approval of PV modules).

[2] IECEE retest guidelines for IEC 61215:1993 Ed. 1.0 and IEC 61215:2005 Ed. 2.0 (crystalline silicon terrestrial PV modules – design qualification and type approval).

[3] Kempe, M.D. et al. 2006, "Ethylene-vinyl acetate potential problems for photovoltaic packaging", *Proc. IEEE 4th World Conf. PV Energy Conver.*, Waikoloa, Hawaii, USA.

[4] Osterwald, C.R. et al. 2002, "Degradation analysis of weathered crystalline-silicon PV modules", *Proc. 29th IEEE PVSC*, New Orleans, Louisiana, USA.

[5] TamizhMani, G. et al. 2008, "Failure analysis of design qualification testing: 2007 vs. 2005", *PVI*, 1st edn.

[6] Osterwald, C.R. 2008, "Terrestrial photovoltaic module accelerated test-to-failure protocol", Technical Report NREL/TP-520-42893.

[7] Hacke, P. et al. 2010, "Test-to-failure of crystalline silicon modules", *Proc. 35th IEEE PVSC*, Honolulu, Hawaii, USA.

[8] Hacke, P. et al. 2009, "Application of the NREL test-to-failure protocol for PV modules", *Proc. 19th Workshop Cryst. Si Solar Cells & Mod.: Mater. & Processes*, Vail, Colorado, USA.

[9] Arndt, R. & Puto, I.R. 2011, "Basic understanding of IEC standard testing for photovoltaic panels" in *IN Compliance Magazine: 2011 Annual Guide*. Hopedale, MA: Same Page Pub., p. 194–205.

[10] Wohlgemuth, J.H. 2003, "Long-term photovoltaic module reliability", NCPV & Solar Progr. Rev. Meeting, NREL/CD-520-33586, p. 179.

[11] Dodson, B. & Nolan, D. 1999, *Reliability Engineering Handbook*. Boca Raton, FL: CRC Press, pp. 221–250.

[12] Arnold, J. et al. 2008, "Reliability testing of Ni-modified SnCu and SAC305: Accelerated thermal cycling", *Proc. SMTAI*, Surface Mount Technol. Assoc., Edina, Minnesota, USA, p. 187.

[13] Weglinski, R. 2007, "Highly accelerated stress screening for air-cooled switching power supplies. Part 1: Understanding stress test methodology", TDI Power White Paper: TW0058.

[14] Wohlgemuth, J.H. et al. 2006, "Long-term reliability of photovoltaic modules", *Proc. IEEE 4th World Conf. PV Energy Conver.*, Waikoloa, Hawaii, USA.

[15] Hallberg, Ö. & Peck, D.S. 1991, "Recent humidity acceleration: A base for testing standards", *Quality & Rel. Eng. Internat.*, Vol. 7, pp. 169–180.

[16] Hulkoff, T. 2009, "Usage of highly accelerated stress test (HAST) in solar module ageing procedures", M.Sc. thesis, Chalmers University of Technology, Göteborg, Sweden.

[17] Kempe1, M.D. et al. 2006, "Ethylene-vinyl acetate potential problems for photovoltaic packaging", *Proc. IEEE 4th World Conf. PV Energy Conver.*, Waikoloa, Hawaii, USA.

### About the Authors

**Sreenivasa Murty Dasari** received his M.Tech. degree in optoelectronics from Cochin University of Science and Technology, India, in 2003. He has carried out work on laser plasma technology at the Indian Institute of Technology, Kanpur. Sreenivas is currently the deputy manager of the Department of Cell Technology and Process Engineering at TATA BP Solar India Ltd.

**K. V. Nagaraj** received his diploma in electronics from Bangalore University and is currently a manager in quality and reliability at TATA BP Solar India Ltd.

**S. Saravanan** received his Ph.D. in Physics from the Cochin University of Science and Technology, India, in 2005. He carried out research work on III-V nitride thin films for the Australian Defense Force Academy at the University of New South Wales, Australia, and on oxide films at the Indian Institute of Science, India. Dr. Saravanan is currently the deputy manager of the Department of

Cell Technology and Process Engineering, TATA BP Solar India Ltd.

**Prakash Suratkar** is head of the Technology and Process Engineering Department at TATA BP Solar India Ltd. Besides working on cell and module technology he worked at Infineon and, prior to that, spent almost 10 years at Lucent Technologies and Bell Labs. He has also worked on a broad range of microwave semiconductor device technologies. Prakash was a visiting research scholar at the University of Surrey, UK, specializing in the area of ion beam synthesis and metal semiconductor field transistors. He has over 20 years of experience in research and development of semiconductor devices.

**T. S. Keshav Prasad** received a distinction in mechanical engineering from Visweswarayya College, India, and has completed a master's degree in management, specializing in marketing and TQM. Having been associated with TATA BP Solar India Ltd since 1989, he is currently an executive vice president of projects, as well as an active leadership team member. Keshav also spent 5 years as a scientist at the renowned Indian Space Research Organization.

## Enquiries

Dr. S. Saravanan
Deputy Manager – Technology, Cell Technology
TATA BP Solar India Ltd
Plot No. 78, Electronics City
Hosur Road
Bangalore 560 100
India

Tel: +91 80 4070 2297
Email: saravanan.s@tatabp.com
Website: http://www.tatabpsolar.com

# A novel glue-membrane integrated backsheet for PV modules

**Wenjin Xia**[1], **Yuzheng Zhang**[1], **York Yu**[1], **Hong Liu**[2], **Wenzhong Shen**[2] & **Jianwei Lin**[1]
[1]Jolywood (Suzhou) Sunwatt Co., Ltd.; [2]Institute of Solar Energy, Shanghai Jiaotong University, Shanghai, P. R. China

## ABSTRACT

This paper presents a novel glue-membrane integrated backsheet specifically for PV modules, which has been designed and fabricated by utilizing a flow-tangent cast roll-to-roll coating process combined with a plasma technique. Polyethylene terephthalate (PET) is adopted as a substrate and is surface activated and etched by atmospheric plasma. Then a special coating formulation containing reactive fluoropolymers is applied to both sides of the PET, followed by thermal curing, resulting in a glue-membrane integrated coating layer with a polyurethane structure. Finally, a monolayer of silane molecules is grafted onto the surface via plasma-enhanced deposition to provide a medium level of surface energy, rendering excellent long-term adhesion to ethylene vinyl acetate (EVA). Scanning electron microscope (SEM) images have revealed that plasma etching and activation significantly improves compatibility between the PET and the coating layer, resulting in a tight and strong integration between the two. It has also been confirmed by SEM that the obtained novel backsheet integrates the glue layer and the membrane layer perfectly. There is no clear boundary between the two layers, distinguishing the novel backsheet from the conventional layer-by-layer laminated backsheet. The unique glue-membrane integrated structure has already been demonstrated by many practical applications under harsh environmental conditions to have significant advantages over other backsheets regarding delamination, blistering and discoloration. Furthermore, the novel backsheets showed excellent barrier properties (water vapour transmission rate, WVTR < $0.3g/m^2$.day), weatherability (85°C, 85% RH, 1000h), mechanical properties and electrical isolation properties. Because it is a promising photovoltaic material, the novel backsheet has already been widely used in China for PV module encapsulation and has obtained extensive praise from customers.

## Introduction

A PV module consists of many different materials ranging from silicon wafer PV cells to packaging materials, such as protective frontsheets, backsheets, sealants and encapsulants. These account for almost half of the cost of materials in thin-film PV modules and are associated with a significant percentage of the failures experienced in the field [1]. To survive in harsh operating environments, PV modules rely on packaging materials to provide the requisite durability. Generally, PV modules are embedded in soft EVA sheets and encapsulated by either glass/glass or glass/plastics technology. With increasing demand in terms of both quality and quantity, the glass/plastics encapsulation laminate structure has been increasingly promoted [2]. Replacing the glass backsheet with soft cover (polymeric) layers can eliminate glass breakage because of edge pinching and provide a more durable mechanical package. In addition, the lighter weight can result in easier installation and lower cost.

For PV modules a total lifetime of at least 25 years is intended. The modules are exposed to various stresses (e.g. UV radiation, temperature, atmospheric gases and pollutants, and diurnal and annual thermal cycles), which may decrease module stability and performance. Additional losses in performance may be caused by rain, dust, wind, hail, condensation and evaporation of water, and thermal expansion mismatches [3]. It is therefore necessary that the backsheets provide the following key functions:

- **Physical protection:** offer resistance to puncture and abrasion
- **Moisture protection:** minimize moisture and water vapour ingress
- **Electrical insulation:** isolate the cells and connections from the environment
- **Long-term protection:** demonstrate UV stability and moisture stability over the life of the module, protecting the absorber layer
- **Colour:** provide the colour that helps the modules blend into the environment
- **More power:** improve efficiency, possibly, through optimized internal reflection

To fulfil these requirements, multi-layer (layer-by-layer) laminated backsheets are normally used, while fluoropolymers such as polyvinyl fluoride (PVF) and polyvinylidene fluoride (PVDF) act as a protection layer against weathering influences, and polyester such as PET provides mechanical strength.

The most popular backsheet construction is a tri-laminate 'sandwich' of polyester film between two layers of Tedlar film (DuPont). This is commonly referred to as a Tedlar/polyester/Tedlar (TPT) structure. To date, multi-layer laminated backsheets have dominated the market because of their excellent strength, weather resistance, UV resistance and moisture-barrier properties. Nevertheless, PV module failures related to multi-layer laminated backsheets are frequently reported. These failures include adhesion loss of EVA as well as delamination. In several publications delamination has been described as an important failure mechanism of PV modules [4–6]. Delamination phenomena of PV modules comprise delamination within the backsheet material and delamination between EVA and backsheet. A lot of research about the delamination of PV modules focuses only on EVA/backsheet interfaces. During applications, adhesive bonds between encapsulants and substrate materials of PV modules can be weakened because of the non-stick property of fluoropolymers (low surface energy), leading to delamination failure and/or moisture ingress.

However, delamination within the backsheet material itself can contribute significantly to the initial failure of PV encapsulation and is attributable to the poor integration between layers, i.e. between substrate and fluoropolymer layers. This can allow water vapour to enter the encapsulation at the edge of a PV module, resulting in degradation and oxidation, as well as electrochemical corrosion of the semiconductor, and ultimately device failure. Therefore, there

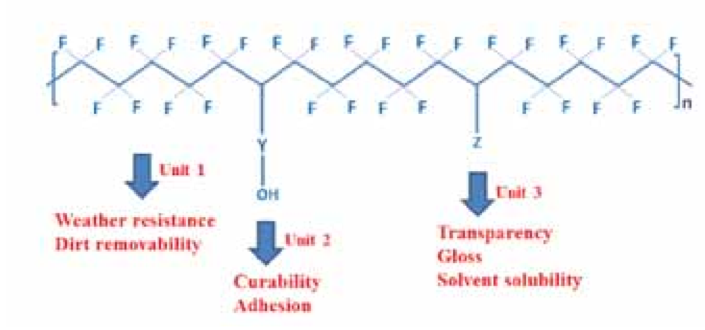


Figure 1. Chemical structure of the reactive fluoropolymer.

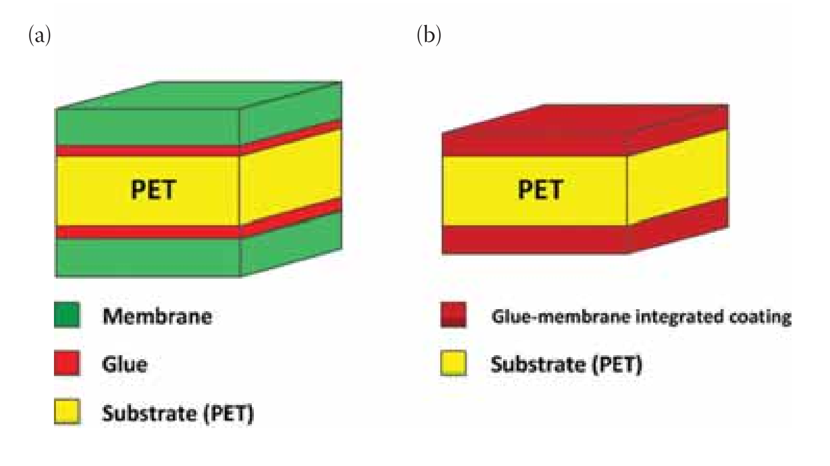


Figure 2. (a) Conventional layer-by-layer backsheet; (b) Glue-membrane integrated backsheet.

is still a strong need for the PV industry to develop a backsheet with excellent properties. This paper presents such a PV backsheet, coined 'glue-membrane integrated backsheet'. It has been extensively characterized and evaluated using many techniques and the test results confirm that it possesses excellent properties required by PV modules.

> "PET – a material utilized extensively in the food packaging industry – was used as a substrate: it is attractive for PV module packaging applications because of its good mechanical properties and low cost."

## Design and fabrication of the glue-membrane integrated backsheet

To fabricate a PV backsheet with excellent properties, an intelligent design of the backsheet construction is crucial. In our approach, PET – a material utilized extensively in the food packaging industry – was used as a substrate: it is attractive for PV module packaging applications because of its good mechanical properties and low cost. However, uncoated (unmodified) PET exhibits high water vapour permeability [7]. PET is also subject to various types of degradation during applications. The main degradations that can occur are hydrolytic and thermal oxidation, which will result in poor performance: therefore, PET cannot be used directly as a PV backsheet material. To coat/modify PET, a coating material has to be identified. Fluorine-containing polymers have been demonstrated to possess many properties that are desirable in coatings, for example excellent hydrophobicity and oleophobicity (stain resistance), low coefficients of friction, excellent chemical resistance and good weatherability [8–12]. Conventional fluoropolymer coatings, such as polytetrafluoroethylene (PTFE) and polyvinylidene fluoride (PVDF), besides their high cost, are generally difficult to process because they are chemically inert and not soluble in most of the organic solvents. After a long screening time, a reactive fluoropolymer was identified and used as a main coating component to fabricate the novel glue-membrane integrated PV backsheet. The chemical structure of this reactive fluoropolymer is shown in Fig. 1.



As shown in Fig. 1, the reactive fluoropolymer is a triblock copolymer with tetrafluoroethylene (TFE) as a main monomer. The TFE unit (monomer 1) provides the polymer with excellent weather resistance and dirt removability (anti-fouling) as well as barrier properties; monomer 2 (unit 2) contains the hydroxyl group (–OH) and therefore contributes curability and adhesion of the polymer; and monomer 3 (unit 3) consists of organic groups (mainly ester groups) and contributes solubility as well as transparency. The reactive fluoropolymer was used as the main ingredient, together with other components such as pigments and a cross-linking reagent, to create a special coating formulation. The coating formulation was applied to both sides of the PET substrate and then subsequently cured by thermal heating, resulting in a well-integrated coating layer on both sides of the PET.

In order to improve adhesion between the coating layer and the PET substrate, atmospheric plasma treatment was carried out prior to coating. It has been demonstrated that plasma treatment can increase the adhesion in the polymer-coating interfaces by positively affecting one or several of the following phenomena: cleaning by ablation of low molecular weight species, dehydrogenation, chain-scissioning combined with cross-linking, generation or incorporation of radicals and reactive species, and structural modifications of the surface topography [13]. The most important feature of the plasma treatment is that the surface properties, for example the chemical composition and topological structure of the materials, can be changed simultaneously without altering their intrinsic bulk properties.

After plasma treatment, the PET surface was etched and activated, resulting in a strong bonding between the coating layer and the substrate. This kind of strong bonding will definitely minimize, or even

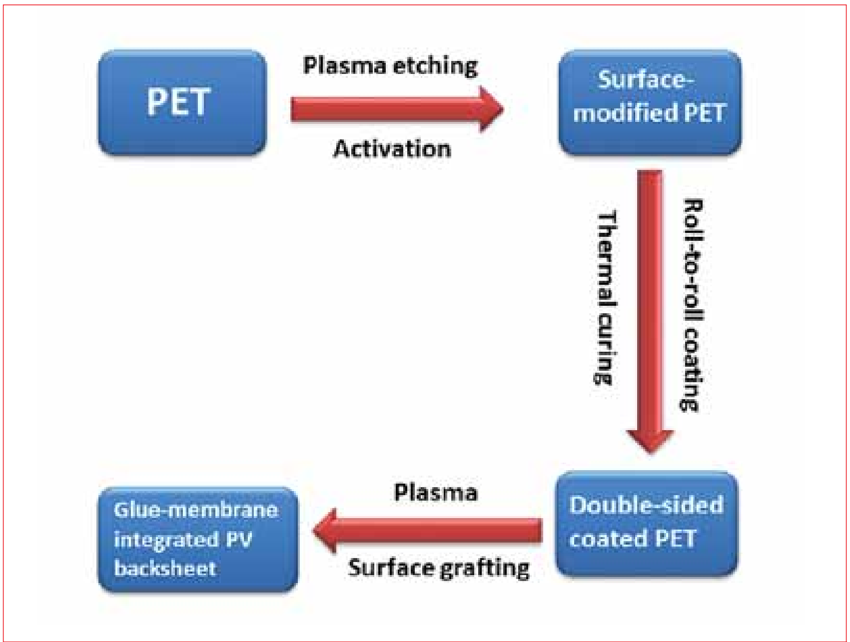


**Figure 3. Schematic process diagram of the fabrication of the glue-membrane integrated PV backsheet (FFC-JW30).**

| Item | Test method (standard) | Value |
|---|---|---|
| Total thickness of backsheet [μm] | Microscope | 305±11 |
| Coating thickness (air side) [μm] | Microscope | 30±3 |
| PET thickness [μm] | Microscope | 245±5 |
| Coating thickness (EVA side) [μm] | Microscope | 30±3 |
| Tensile strength (MD) [N/mm²] | ASTM D 882-2002 | ≥ 120 |
| Tensile strength (TD) [N/mm²] | ASTM D 882-2002 | ≥ 120 |
| Elongation (MD) [%] | ASTM D 882-2002 | ≥ 100 |
| Elongation (TD) [%] | ASTM D 882-2002 | ≥ 90 |
| Shrinkage 150°C × 30min (MD) [%] | ASTM D 1204-2002 | ≤ 1.0 |
| Shrinkage 150°C × 30min (TD) [%] | ASTM D 1204-2002 | ≤ 0.6 |
| Inter-layer adhesion [grade] | ASTM D 3359-2002 | 5B |
| Peeling strength with EVA (initial) [N/10mm] | GB/T 2790-1995 | ≥ 60 |
| Peeling strength with EVA (85°C, 85% RH, 1000h) [N/10mm] | GB/T 2790-1995 IEC 61215-2005,10.13 | ≥ 55 |
| Breakdown voltage [kV/mm] | ASTM D 149-1997 | ≥ 85 |
| Partial discharge [VDC] | IEC 60664-1-2007 IEC 61730-2-2004 | ≥ 1010 |
| Water vapour transmission rates (WVTR) [g/m².d] | ASTM F 1249-2006 | ≤ 0.3 |
| Weather resistance (85°C, 85% RH, 2000h) Peeling strength with EVA [N/10mm] | GB/T 13448-2006 IEC 61215-2005,10.13 | No delamination, no blistering, no yellowing ≥ 45 |
| Radiation exposure (QUVB, 4000h) [grade] | GB/T 16422.3-1997 | 4 |

MD=machine direction; TD=transverse direction

**Table 1. Properties of the FFC-JW30 backsheet.**

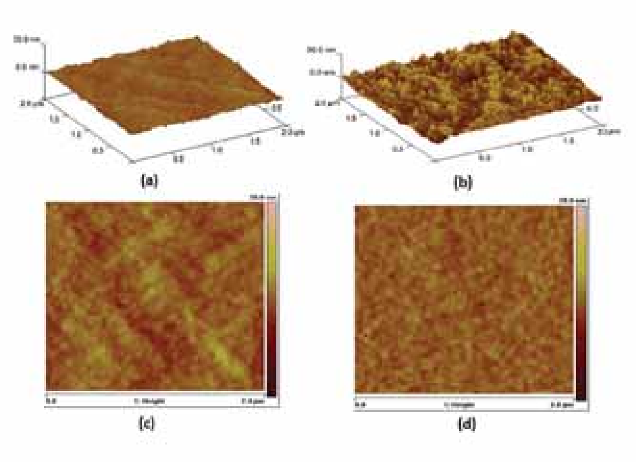


**Figure 4. Atomic force microscope (AFM) images of the backsheet: (a) and (c) before; (b) and (d) after plasma grafting of the silane monolayer.**

totally eliminate, delamination between the coating layer and the substrate during applications. It can be seen that no glue (adhesive) was used in the fabrication process, which distinguishes this approach from conventional layer-to-layer laminating methods. The coating layer is a glue-membrane integrated system which functions as both a glue and a membrane at the same time. From the polymer chemistry point of view, the coating layer is a kind of polyurethane (PU) because hexamethylene diisocyanate (HDI) was used as a curing agent.

During thermal curing, the isocyanate groups of HDI reacted with –OH groups of the reactive fluoropolymer to form a polymer network containing the urethane linkage. Generally, PU is a unique material that can offer the elasticity of rubber combined with the toughness and durability of metal. The fluorine-containing PU coating will possess the excellent barrier properties and long-term durability that are required by a PV backsheet. It should be emphasized here that a lot of active groups, such as hydroxyl groups and amino groups, were introduced during plasma treatment. These active groups also participate in the curing reaction, resulting in covalent chemical bonding between the coating layer and the substrate, namely the PET. The covalent bonding ensures the tight and dense integration of the coating layer and the substrate, which will minimize the delamination problem suffered by a conventional layer-by-layer laminated backsheet.

It has been widely accepted that a good backsheet must also exhibit excellent adhesion to the encapsulant material, which is typically a formulated EVA film. To achieve this, a surface

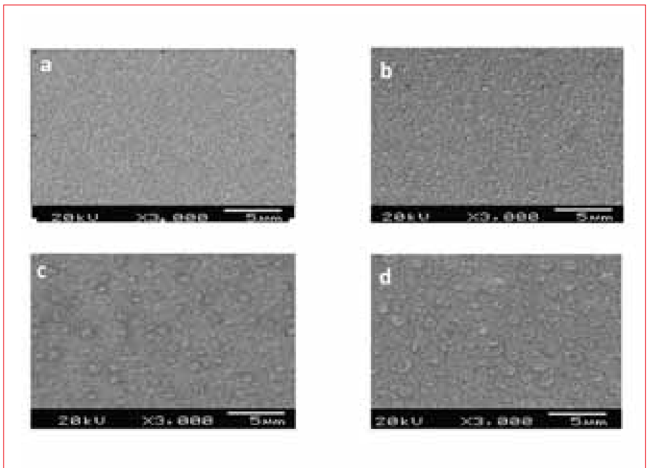


**Figure 5. SEM images of the PET surface: (a) before plasma treatment; (b)–(d) after having been treated for 3s, 5s and 10s, respectively.**

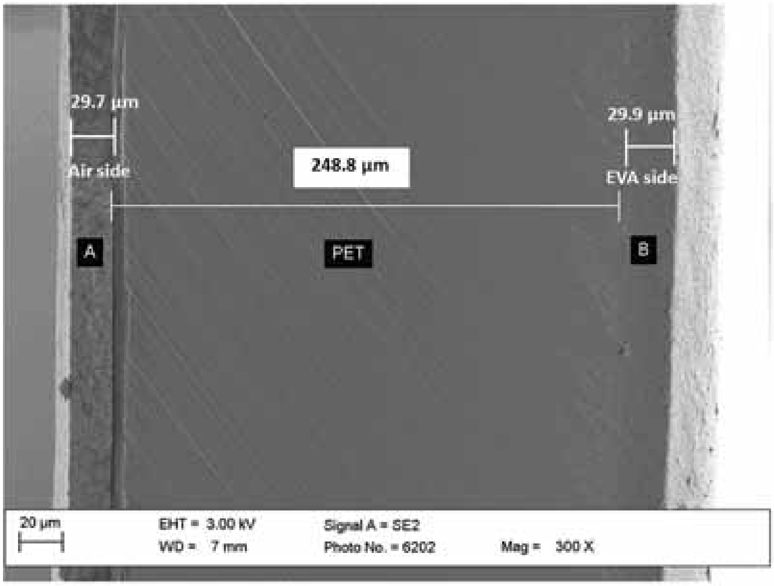


**Figure 6. SEM image of a cross section of an FFC-JW30 backsheet.**

modification of the coating layer is essential because fluorine-containing polymers normally have low surface energy, rendering them non-stick. The non-stick property of fluoropolymers is actually the main cause of the delamination problem in most conventional layer-by-layer laminated backsheets. To overcome this drawback of fluoropolymers, a monolayer of silane molecules was grafted onto the surface via plasma-enhanced deposition to give the surface a medium level of surface energy. The test results confirmed that the grafted silane molecules increased the surface energy to a medium level and significantly improved adhesion between the backsheet and the EVA film. Fig. 2 presents a schematical representation of the conventional and novel backsheets; the fabrication process of the novel glue-membrane backsheet (FFC-JW30) is shown in Fig. 3.

As mentioned above, the colour of the backsheet is sometimes a concern during practical applications. The right colour can not only help the modules blend into the environment but also meet the specific aesthetic requirements. In our approach, backsheets of different colours can readily be fabricated: it is only necessary to identify the right pigment and blend it with other components during the coating formulation. Currently, the three colours frequently used in our fabrication are white, black and blue, but other colours can easily be customized.

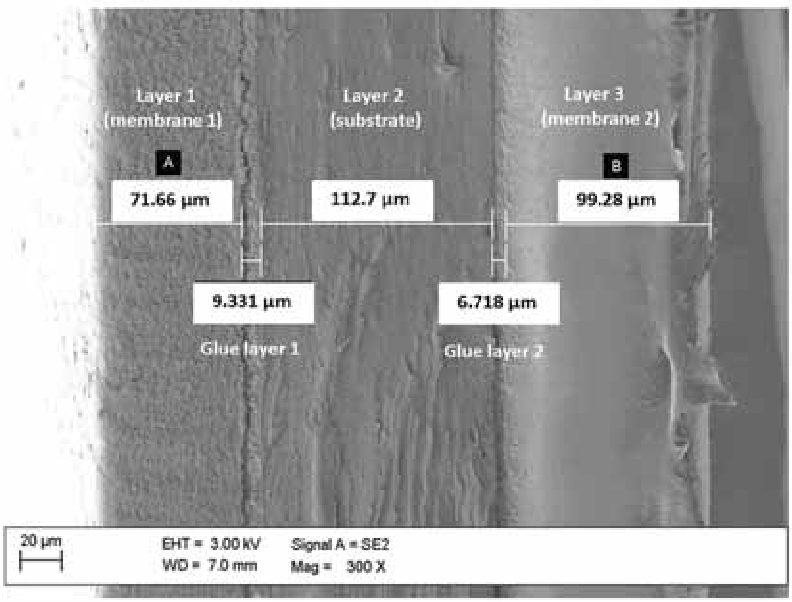


**Figure 7. SEM image of a cross section of a conventional layer-by-layer laminated backsheet.**

## Properties, surface characterizations and performance of the novel backsheet

Table 1 summarizes the basic properties of the glue-membrane integrated PV backsheet (FFC-JW30). For a good PV backsheet, the primary property of interest was adhesion, especially adhesion as a function of damp-heat exposure, peel strength and water vapour transmission rate (WVTR).

### Adhesion

It can be seen from Table 1 that FFC-JW30 with EVA showed excellent peel strength (≥ 60N/10mm), which was only slightly decreased (≥ 55N/10mm) after the damp-heat exposure test. The exposure test can simulate specific environmental conditions in order to investigate the properties of a backsheet in service. The samples were subjected to accelerated weathering in laboratory-controlled exposure chambers (damp heat, no light, 85°C, 85% RH). Relevant performance parameters were measured as a function of exposure time to evaluate how well the samples could withstand environmental stresses over time. The samples were allowed to dry out for several hours after damp-heat exposure prior to being tested, since testing too soon after exposure can result in catastrophic adhesive failure and therefore cannot provide an accurate evaluation.

"Fluoropolymers have poor adhesion properties and consequently the surface needs to be modified: a monolayer of short chain silane was grafted onto the surface by plasma-enhanced deposition."

A good backsheet should adhere well to the encapsulant before, during and after damp-heat exposure. In one of our tests, the initial peel strength with EVA was as high as 135N/cm; after 2000h damp-heat exposure, the peel strength was at 45N/cm, and was still at 31N/cm after 3000h. The excellent adhesion with EVA was attributed to plasma surface modification. As mentioned earlier, fluoropolymers have poor adhesion properties and consequently the surface needs to be modified: a monolayer of short chain silane was grafted onto the surface by plasma-enhanced deposition. The grafted silane monolayer significantly increases surface

| Samples/measured position (Fig. 6) | C [%] | O [%] | N [%] | F [%] | Si [%] | Cl [%] |
|---|---|---|---|---|---|---|
| A | 83.9±0.4 | 10.8±0.2 | 0.9±0.1 | 2.2±0.2 | 1.4±0.3 | 0.8±0.0 |
| B | 82.9±0.3 | 11.1±0.4 | 0.9±0.0 | 2.5±0.1 | 1.7±0.3 | 0.8±0.0 |
| Coating materials (before curing) | 76.0±0.2 | 16.2±0.1 | – | 7.8±0.2 | – | – |
| Uncoated PET | 73.6±0.5 | 24.7±0.3 | – | – | 0.5±0.0 | – |

**Table 2. Atomic composition of the surface of an FFC-JW30 backsheet.**



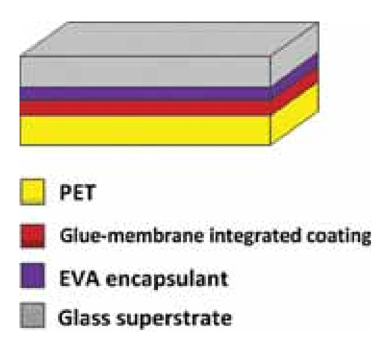


**Figure 8. A schematic representation of the test module used in the PCT. PV devices are normally located between the glass and the EVA.**

energy and the topological structure of the backsheet, resulting in excellent adhesion with EVA. Fig. 4 shows clearly the difference in topological structure of the backsheet before and after plasma grafting. It can also be seen that the surface becomes much rougher after plasma grafting. The rough surface facilitates good contact and compatibility between the backsheet and the EVA, leading to a strong adhesion between the two surfaces.

The inter-layer adhesion of the backsheet was evaluated in accordance with ASTM D3359-2002. A lattice pattern with 11 cuts in each direction was made in the coating film of the PET substrate; pressure-sensitive tape was applied over the lattice and then peeled off. The adhesion was evaluated by calculating the percentage of detached area at the intersections. Grade 5B was achieved, indicating that the edges of the cuts were completely smooth and none of the coating (the squares of the lattice) became detached. The inter-layer adhesion confirmed that the coating layers had extremely strong adhesion to the PET substrate; this favourable result was attributed to plasma etching and activation of the PET prior to coating.

It is well known that surface etching and activation by plasma pretreatment is an effective way to improve adhesion of the coating to the polymeric substrates [14]. Plasma treatment of a PET surface dramatically increases its wettability, which was confirmed by contact-angle measurement. The plasma-treated PET surface showed a lower contact angle compared with an untreated surface. In general, the lower the contact angle, the higher the surface energy. The increase of energy and decrease of contact angle usually correlates directly with improved adhesion since organic contaminants have been removed during the plasma treatment, and the free radicals and polar function groups are formed on the surface, allowing for a better interface between the surface and the typically polar fluid, i.e. the coating material.

Plasma treatment can also increase surface roughness. It can be seen from Fig. 5 that surface roughness increases as the duration of the plasma treatment increases. Fig. 5 also indicates that a relatively short treating time such as 3 to 10s is enough to significantly increase surface roughness. This is crucial for roll-to-roll fabrication because it allows a high rolling speed of, for example, between 15m/min and 30m/min to be used. The rough surface induced by plasma treatment will promote the diffusion of coating materials into the substrate, leading to better compatibility between them. Importantly, the active functional groups (such as hydroxyl and amino) on the rough surface obtained from plasma treatment will participate in a cross-linking reaction during thermal curing, resulting in a covalent chemical bonding between the coating layer and the PET substrate. SEM imaging of a cross section of the backsheet was used to investigate the well-integrated interfaces (Fig. 6).

Prior to SEM investigation, the sample was fast frozen in liquid nitrogen (–180°C) and then broken in order to keep the original structure of the interface. The cross section was coated with gold and the SEM images were then immediately recorded. Fig. 6 shows clearly the three-layer structure of the backsheet. The layer thicknesses of the air side (the side which contacts air), PET substrate and EVA side (the side which contacts the EVA) were 29.7µm, 248.8µm and 29.9µm, respectively. The coating layer thickness agrees quite well with the parameter setting of the coating process. As can be seen from Fig. 6, the interfaces between the three layers are unclear; in particular the interface between the EVA side and the PET almost disappears, indicating satisfactory integration between the coating layer and the PET substrate.

To evaluate the differences between the novel backsheet and the conventional one, the same SEM investigation was carried out on a conventional layer-by-layer laminated backsheet; the resulting SEM image is shown in Fig. 7. Surprisingly, the sandwich structure that people usually refer to as tri-laminate is actually composed of five layers: three polymer (membrane) layers and two glue (adhesive) layers. It can be seen that the interfaces between two of the layers are quite noticeable, indicating bad integration between them. The clear interfaces are normally the weak points of the backsheet and will lead to delamination during practical applications.

## Moisture barrier

In the PV industry, durability and maintaining performance over the lifetime of a module are crucial, and the encapsulant used will influence these key requirements. One major concern for durability is the corrosion of metallic components within a module because this can reduce the power output by increasing resistance at the electrical interconnects. Therefore, the backsheet material must prevent moisture ingress and this is the generally accepted mode of failure for devices that do not pass the IEEE qualification test [15]. High moisture transfer rates would result in more water being available for corrosion, leading to hydrolytic degradation of the PV device. Water permeation through a barrier film involves a multi-step process. The water vapour adsorbs at the high concentration side of the barrier surface, dissolves into the bulk, diffuses through the bulk, and desorbs from the low-concentration surface. Obviously, the surface should be water-repellent or hydrophobic in order to minimize moisture permeation. Fluorinated polymers can provide a surface with very low surface energy and demonstrate excellent hydrophobicity and oleophobicity [16,17].

The coating formulation applied to the PET substrate was a special material containing reactive fluoropolymers (Fig. 1) [18,19]. The fluorine element renders the coating layer hydrophobic. Surface analyses such as contact angle and XPS (X-ray photoelectron spectroscopy) were carried out to confirm the hydrophobicity and elemental compositions of the coating. The contact angle of the coated surface was as high as 92 degrees, which was approximately 20 degrees higher than that of uncoated PET. Uncoated PET normally has a very wide-ranging WVTR (between 3 and 20g/m$^2$.day), depending on its quality and grade. For PV applications, the typical value is around 4g/m$^2$.day (in our case). Table 1 shows clearly that the WVTR of the backsheet was less than 0.3g/m$^2$.day, which is more than 10 times lower than uncoated PET. The atomic percentage composition of the surface of the substrate (uncoated PET) and the backsheet was determined by XPS (Table 2).

Table 2 shows that there is a substantial incorporation of fluorine atoms in the backsheet surface, indicating that the reactive fluoropolymers were successfully coated on the PET substrate. Nitrogen atoms were also detected in the surface and this was attributed to the cross-linking reagent, i.e. curing agent (HDI). A tiny amount of silicon was detected on the uncoated PET surface and probably came from organic contamination during PET fabrication. However, a significant quantity of silicon atoms was detected on the surface of the backsheet, indicating that the plasma-enhanced grafting of the silane monolayer was successful. XPS is a surface chemical analysis technique that can be used to determine the quantitative amount of atoms as well as their in-depth distribution within the outermost ~10nm of a surface [20]. A large amount of fluorine was detected after plasma grafting of the silane monolayer, signifying that the thickness of the silane monolayer was less than 10nm. Table 2 also reveals that the atomic composition measured in the two different positions A and B on the backsheet surface was quite similar, which indicates that the coating was very homogeneous.

## Pressure cooker test (PCT)

It is interesting to see how well the novel PV backsheet retained its desired properties under PCT – a more severe exposure test (high pressure, high temperature and high humidity). The backsheet was vacuum laminated to EVA and a front glass superstrate to replicate the backsheet in a module construction (Fig. 8).

The test module was then subjected to accelerated weathering in a laboratory-controlled chamber, i.e. a pressure cooker (121°C, 2 atm, 100% RH). To investigate any changes at the interfaces of the laminates as a function of accelerated exposure, peel tests were conducted on strips of the samples in accordance with GB/T 2790-1995 and IEC 61215:2005(10.13). The coating was sometimes found to exhibit cracking during and/or after laminating. The cracking was attributed to a higher cross-linking degree of the coating. To totally avoid backsheet cracking and ensure good coating quality, a small batch (test batch) of coating formulation was always prepared and applied to the PET and then tested. In the test batch, the amount of cross-linking reagent had to be optimized to ensure a satisfactory coating that was flexible enough to prevent cracking. Once an optimized formulation was identified, it was then adopted to the roll-to-roll process.

During the peeling test, special attention was paid to the peel strength with EVA and to the delamination behaviour within the backsheet. Two EVAs from different suppliers were used in order to check the reproducibility of the test. To obtain a fair evaluation, several commercially available backsheets were used as references and treated and tested under the same conditions as the FFC-JW30 backsheet; the results for two of the commercial backsheets are summarized in Table 3.

As can be seen in Table 3, even the same backsheet shows different peeling strength with different EVAs used for lamination, indicating that the EVA properties might be slightly different. EVA is the copolymer of ethylene and vinyl acetate. The weight percentage of vinyl acetate might vary (usually from 10 to 40%) from manufacturer to manufacturer, and the cross-linking degree of EVA might also be different because of the manufacturing process. These differences have the potential to influence the peeling strength with backsheets. Generally, the FFC-JW30 backsheet showed high peeling strength with different EVAs. For example, the initial values of peeling strength were 82N/cm for EVA from Mitsui and 103N/cm for EVA from Hanwha (initial value data not shown in Table 3). After 24h, the values were slightly lower – 63.6N/cm and 81.3N/cm, respectively.

It is quite interesting to compare FFC-JW30 with S-4 and S-5. Both S-4 and S-5 showed higher peeling strength than FFC-JW30 after 24h exposure when EVA from Mitsui was used. However, when the exposure increased from 24 to 48h, the peeling strength of S-4 was dramatically reduced to 47.1N/cm, degrading by 65.4%. Similarly, the peeling strength of S-5 decreased to 38.7N/cm, degrading by 42.5%. In contrast, the peeling strength of FFC-JW30 with EVA degraded by only 27.5% when the exposure increased from 24 to 48h. The peeling strength of the FFC-JW30 with EVA was still at a higher level (43.4N/cm) than that of S-5 even after 60h exposure. However, S-4 became very brittle after 60h exposure, and no peeling strength could be measured.

Similar results were obtained when EVA from Hanwha was used. The FFC-JW30 showed higher peeling strength than all the reference samples after 24h, 48h and 60h exposures. No lamination was observed after the 48h exposure.

The PCT results confirmed that the bonds between the backsheet and the EVA would generally be weakened because of water ingress under harsh

| Samples | Manufacturing process | EVA used for test | | | | | | | | | | | |
|---|---|---|---|---|---|---|---|---|---|---|---|---|---|
| | | Mitsui Chemicals Tohcello, Inc | | | | | | Hanwha SolarOne | | | | | |
| | | Peeling strength [N/cm] | | | Interfaces | | | Peeling strength [N/cm] | | | Interfaces | | |
| | | 24h | 48h | 60h | 24h | 48h | 60h | 24h | 48h | 60h | 24h | 48h | 60h |
| S-1 | L-b-L | 37.5 | 31.5 | BT | NL | LM | BT | 48.1 | 22.8 | – | NL | LM | BT |
| S-2 | L-b-L | 56.9 | 34.3 | BT | NL | BK | BT | 47.3 | 42.1 | – | NL | BK | BT |
| S-3 | L-b-L | 47.4 | 35.7 | BT | NL | LM | BT | 45.2 | 39.3 | – | NL | LM | BT |
| S-4 | L-b-L | 136.1 | 47.1 | BT | NL | BK | BT | 50.8 | 37.8 | – | NL | BK | BT |
| S-5 | L-b-L | 67.3 | 38.7 | 33.2 | NL | NL | BK | 66.8 | 40.3 | 34.9 | NL | NL | BK |
| FFC-JW30 | G-M | 63.6 | 46.1 | 43.4 | NL | NL | BK | 81.3 | 56.1 | 50.2 | NL | NL | BK |

L-b-L=layer-by-layer laminated; BT=brittle; NL=no laminating; G-M=glue-membrane integrated; BK=broken; LM=laminated

**Table 3. PCT results (121°C, 2 atm, 100% RH) for backsheets laminated to EVA.**

exposure conditions. For a test module, the dominant path of moisture ingress is inwards from the edges and through the EVA due to the very large WVTR of EVA even at ambient temperature. When a sample module is placed in damp heat, the WVTR through the EVA is about 50 to 100 times higher than at room temperature, and water vapour more easily permeates the EVA. Water vapour rapidly diffuses throughout the EVA and reaches its equilibrium value at the glass/EVA interface, as well as the EVA/backsheet interface, as it progresses in from the edges.



> "For the FFC-JW30 backsheet, the reduction in peeling strength was approximately 25%, which is lower than most commercially available PV backsheets."

Investigations reported in the literature have shown that for most of the commercially available backsheets, there is a reduction in the peeling strength of at least 30% after 24h exposure [21]. For the FFC-JW30 backsheet, the reduction in peeling strength was approximately 25%, which is lower than most commercially available PV backsheets. The better performance of the FFC-JW30 under exposure conditions indicated that it was more difficult to destroy or weaken the bonding between the FFC-JW30 and the EVA, or there might be a different type of adhesive bonding or a reaction such as covalent chemical bonding taking place between the two. More detailed experiments and investigations are being carried out to understand the mechanism of adhesion between the backsheet and EVA. Ways to further improve the properties of the novel backsheet are also currently being pursued with our collaborators.

## Conclusions

A novel PV backsheet design, coined 'glue-membrane integrated backsheet', has been presented. This backsheet was fabricated by utilizing a flow-tangent cast roll-to-roll coating process combined with a plasma technique, and, unlike a conventional layer-by-layer lamination process, no glue (adhesive) was used in the fabrication. In this new approach, a special coating formulation containing reactive fluoropolymers was adopted as a coating material and applied to a PET substrate. This was followed by thermal curing to create the glue-membrane integrated backsheet. The fluoropolymer contributed all the necessary properties – weatherability, UV resistance, moisture barrier, durability and electrical insulation – required by a PV backsheet. The use of a plasma technique dramatically improves the surface properties of the PET substrate, resulting in better wettability and compatibility with coating materials, and eventually stronger adhesion between the coating layer and the substrate. After coating the PET substrate, a monolayer of silane molecules was grafted onto the surface via plasma-enhanced deposition in order to increase the adhesion between the backsheet and EVA.

The novel backsheet was extensively characterized and tested using different techniques, namely SEM, AFM, contact-angle measurement and XPS, and compared with other commercially available PV backsheets. A PCT experiment demonstrated that it was superior to most of the commercially available PV backsheets in terms of adhesion to EVA and delamination. The novel backsheet promises to be a suitable candidate as a replacement for the conventional layer-by-layer laminated backsheets currently used for PV module encapsulation.


## Acknowledgements

This work was carried out at Jolywood in cooperation with the Institute of Solar Energy, Shanghai Jiaotong University, Shanghai, China. The authors would like to acknowledge the support of the following foundations: 1) Program of Major Scientific and Technological Achievements Transfer and Breeding (Suzhou, China, SC0902); 2) Technology Support Program – Industrial Parts (Jiangsu Province, China, BE2009062); and 3) National Torch Program (2010GH030396). Special thanks go to Key Lab of Organosilicon Chemistry and Material Technology of the Ministry of Education, Hangzhou Normal University, Hangzhou, China, which carried out surface characterization and analysis.


## References


[1] Zweibel, K. 2000, "Thin film PV manufacturing: Materials costs and their optimization", *Solar Energy Mater. & Solar Cells.*, Vol. 63, pp. 375–386.

[2] Erler, B. et al. 2003, "Multi layer materials for the encapsulation of thin film modules", *Proc. 3rd World Conf. PV Energy Conver.*, Vol. 2, pp. 1896–1898.

[3] Czanderna, A.W. et al. 1995, "Encapsulation of PV modules using ethylene vinyl acetate copolymer as a pottant: A critical review", *Solar Energy Mater. & Solar Cells.*, Vol. 43, pp. 101–181.

[4] Pern, F.J. et al. 1996, "Factors that affect the EVA encapsulant discoloration rate upon accelerated exposure", *Solar Energy Mater. & Solar Cells.*, Vol. 41/42, pp. 587–615.

[5] Jorgensen, G. et al. 2003, "Materials testing for PV module encapsulation", Nat. Center for PV and Solar Prog. Review Meeting, Denver, USA. Reprint by National Renewable Energy Laboratory (NREL) (NREL/CP-520-33578) [available online at http://www.nrel.gov/publications/], pp. 1–4.

[6] Pern, F.J. et al. 2003, "Adhesion strength study of EVA encapsulants on glass substrates", Nat. Center for PV and Solar Prog. Review Meeting, Denver, USA. Reprint by National Renewable Energy Laboratory (NREL) (NREL/CP-520-33558) [available online at http://www.nrel.gov/publications/], pp. 1–4.

[7] Tropsha, Y.G. et al. 1997, "Activated rate theory treatment of oxygen and water transport through silicon oxide/poly (ethylene terephthalate) composite barrier structures", *J. Phys. Chem. B.*, Vol. 101, pp. 2259–2266.

[8] Anton, D. et al. 1998, "Surface-fluorinated coatings", *Adv. Mater.*, Vol. 10, pp. 1197–1205.

[9] Yoon, S.C. et al. 1986, "Surface structure of segmented poly(ether urethanes) and poly(ether urethane ureas) with various perfluoro chain extenders: An x-ray photoelectron spectroscopic investigation", *Macromolecules*, Vol. 19, pp. 1068–1079.

[10] Champan, T.M. et al. 1995, "Determination of low critical surface tensions of novel fluorinated poly(amide urethane) block copolymers: 2. Fluorinated soft-block backbone and side chains", *Macromolecules*, Vol. 28, pp. 2081–2085.

[11] Sun, F. et al. 1996, "Spontaneous polymer thin film assembly and organization using mutually immiscible side chains", *J. Am. Chem. Soc.*, Vol. 118, pp. 1856–1866.

[12] Winter, R. et al. 2002, " Perfluorinated polymer surfaces comprising $SF_5$-terminated long-chain perfluoroacrylate", *J. Fluorine Chem.*, Vol. 115, pp. 107–113.

[13] Rusu, I.A. et al. 2005, "Argon RF plasma treatment of PET films for silicon films adhesion improvement", *J. Optoelect. Adv. Mater.*, Vol. 7, pp. 2529–2534.

[14] Moosheimer, U. et al. 1999, "Plasma pretreatment of polymer films as a key issue for high barrier food packagings", *Surf. Coat. Technol.*, Vol. 116, pp. 812–819.

[15] Jorgensen, G.J. et al. 2001, "Electrical currents and adhesion of edge deleted regions of EVA-to-glass module packaging", *Proc. 2001 NCPC Rev. Meet.*, Lakewood, Colorado, USA,

pp. 137–138.
[16] Carr, C. et al. 1996, "Theoretical aspects of self-stratification", *Prog. Org. Coat.*, Vol. 28, pp. 161–171.
[17] Mason, R. et al. 2001, "Surface energy and surface composition of end-fluorinated polystyrene", *Adv. Colloid Interface Sci.*, Vol. 94, pp. 1–19.
[18] Lin, J.W. et al. 2009, "PV backsheet and manufacturing process", Patent Pub. No. EP 2333875 A1.
[19] Lin, J.W. et al. 2010, "Fluororesin membrane with high activity, preparation process thereof and solar cell", Patent Pub. No. CN 101814533 A.
[20] Tougaard, S. et al. 1998, "Accuracy of the non-destructive surface nanostructure quantification technique based on analysis of the XPS or AES peak shape", *Surf. Interf. Anal.*, Vol. 26, pp. 249–269.
[21] Barber, G.D. et al. 2002, "New barrier coating materials for PV module backsheets", *Proc. 29th IEEE PVSC*, New Orleans, Louisiana, USA, pp. 1541–1544.

## About the Authors

**Wenjin Xia** is the development and production manager at Jolywood. He is responsible for the knowledge transfer from research and development to industrialization. Wenjin received his bachelor's degree in chemical engineering in 2002 and worked as a process development engineer for various companies before joining Jolywood. His research interests include adhesives, coating formulations, fluoropolymers, polyurethane coating, membrane science and technology.

**Yuzheng Zhang** is the vice president of Jolywood. She is responsible for the purchase and quality control of raw materials used for backsheet fabrication, as well as for the QA of the product. Yuzheng received her bachelor's degree in 2007. Her research interests include the aluminium industry, adhesives and polymer materials.

**York Yu** is a senior technical advisor at Jolywood. He received his Ph.D. degree in polymer chemistry and physics in 1997 from the Institute of Polymer Chemistry, Nankai University, China, after which he did his postdoctoral research at Lund University, Sweden, where he investigated molecularly imprinted polymers. Dr. Yu's current research interests include polymer synthesis, characterization and application, and surface coating/modification via gas phase deposition techniques such as plasma-enhanced chemical vapour deposition (PECVD), molecular vapour deposition (MVD) and atomic layer deposition (ALD).

**Hong Liu** is a postdoctoral student at the Institute of Solar Energy, Shanghai Jiao Tong University. He received his Ph.D. degree in 2008 from Leibniz University of Hannover, Germany, where he investigated self-organization in a reaction-diffusion system in a surface catalytic process. Dr. Liu's current research interests include mechanisms and nanostructure formations of photovoltaic materials, dynamical and kinetic properties of non-equilibrium systems, and fabrication of nanostructures and their applications in solar cells, fuel cells, biological systems, etc.

**Wenzhong Shen** is the director and a professor of the Institute of Solar Energy, Shanghai Jiao Tong University. He received his Ph.D. degree in 1995 from the Shanghai Institute of Technical Physics, Chinese Academy of Sciences, and carried out his postdoctoral research in the USA, where he investigated nanowire arrays. Dr. Shen's current research interests include optical and electrical properties of semiconductors, semiconductor quantum electronic devices and solar cells.

**Jianwei Lin** is the founder and president of Jolywood. He received his master's degree from Macau University of Science and Technology (MUST), Taipa, Macau, in 2003. He has participated in the research, development and industrialization of PV backsheets at Jolywood from the beginning and is one of the patent inventors. His research interests include polymer films/membranes and their applications in the PV industry, adhesives and their applications in the building industry, plasma processing, and coating formulations, as well as surface coatings for the decoration industry.

## Enquiries

Jianwei Lin
Jolywood (Suzhou) Sunwatt Co., Ltd.
32 Qingnian Rd.,
Changkun Industrial Zone
Shajiabang Town
Changshu 215542, Jiangsu
China
Tel: +86-0512-52336611
Fax: +86-0512-52334515
Email: lin@jolywood.cn
Website: www.jolywood.cn

# Power Generation


Page 159
News

Page 165
Product Reviews

Page 169
Weighing the merits of solar power plants using CPV

Geoffrey S. Kinsey, Amonix, Seal Beach, California, USA

Page 178
Harmonized procedures for long-term energy yield measurements and performance evaluation of PV modules in outdoor conditions

Vincent Helmbrecht et al., DERlab e.V., Kassel, Germany; Sandia National Laboratories, Albuquerque, New Mexico, USA; CRES, Pikermi, Greece; ICCS-NTUA, Athens, Greece



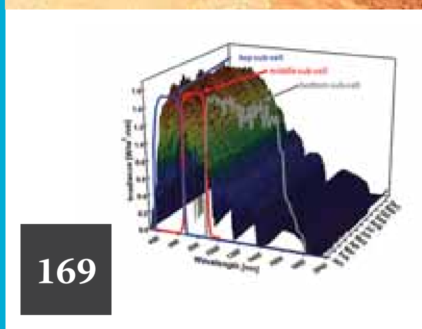


## Boston Consulting and Pike Research estimate 30% increase in use of battery technologies

Market research firms Boston Consulting and Pike Research have estimated a growth of more than US$10 billion over the next five years for the stationary energy storage market. This has been facilitated by the latest round of funding grant awards from the US Department of Energy's American Recovery and Reinvestment Act 2009 Storage Demonstration program enabling companies like EnerVault to complete its first installation. The company's 1MWh system will be installed with partner Raytheon Ktech at a solar installation near Turlock, California, US.

EnerVault has announced the completion of a US$15.5 million Series B financing round, bringing total funding to date to US$24.5 million. The company's investors include Mitsui Global Investment, Total Energy Ventures, 3M, TEL Venture, Commercial Energy of California, Oceanshore Ventures and US Invest. The investor funds complement the company's grant awards totalling US$5.5 million from the US DOE, California Energy Commission and New York State Energy Research and Development Authority.

Source: venturebeat

EnerVault is developing energy storage systems based on a novel redox flow battery technology and has been awarded US$15.5 million in Series B financing.



**Asia & Oceania News Focus**

## Solar Frontier helps power Mt. Komekura solar plant in Japan

Solar Frontier provided 10MW of its CIS thin-film solar modules to power the Mt. Komekura Solar Power Plant in Yamanashi Prefecture, Japan, which started operations on January 27. Shigeaki Kameda, president of Solar Frontier, was in attendance for the plant's opening celebration.

The facility is being hailed as one of the largest solar plants in Japan. It is operated by both Yamanashi Prefecture and Tokyo Electric Power and expected to produce nearly 12 million kWh of electricity per year.

Source: Meidensha

Solar Frontier provided 10MW of its CIS thin-film panels for the Mt. Komekura solar plant.

## Assyce and Sonnedix complete 7.5MW plant in Thailand

A 7.5MW solar plant worth €22.8million has been built in the north-west province of Nakhon Ratchasima, Thailand. Spanish company Assyce was responsible for engineering, installation, commissioning

Source: Sonnedix

**A 7.5MW solar plant worth €22.8million has been built in the north-west province of Nakhon Ratchasima, Thailand.**

and maintenance of the installation, alongside Dutch company, Sonnedix and Thai public company, Karnchang. First Solar provided 90,000 panels spread over an area of 20 hectares. Ingeteam, another Spanish company, has manufactured high-performance inverters for use in this plant.

Assyce and Sonnedix have further plans to construct a 9.5MW PV plant in Chiant Rai, northern Thailand in July 2013. The plant has already received investment of €30.3million.

## Kokusai Kogyo Holdings and Orix Corp to install two 2MW plants in Japan

Japan's Kagawa government in western Japan has announced that Kokusai Kogyo Holdings and Orix Corp will each build a solar power plant, to start operations in July and September. The plants will each have a capacity of 2MW.

Japan's new feed-in tariff has attracted the aerial surveying contractor Kokusai Kogyo and leasing company Orix. Electricity output generated by the plants will be sold to regional power provider, Shikoku Electric Power. Japan is keen to increase renewable power in the wake of the radiation crisis at the Fukushima nuclear plant.

## Europe News Focus

## ESU, Thames Water and Ennoviga construct 3.7MW installations to beat UK FiT

Europe Solar Utility (ESU) has announced the sale of one of the last solar PV installations to be completed under the UK's previous feed-in tariff to Ennoviga Solar. The three installations, totalling 3.7MW, have been built on land owned by water regulator Thames Water. The area is equivalent to 10 football pitches and will generate up to 3,500MWh, saving Thames Water around £100,000 a year.

The first phase was completed before the August 1, 2011 deadline qualifying it for the higher feed-in-tariff rate of £0.307kWh. The installation will provide 0.5% of its 1,180GWh – £80m annual energy requirement – for processing and transporting 2.6 billion litres of water a day and more than 4 billion litres of sewage a day. This is in addition to the 16% already generated from burning biomethane gas derived from sewage sludge using anaerobic digestion.

## Gehrlicher Solar and Masdar PV complete 7.7kWp rooftop installation in Belgium

Masdar PV and Gehrlicher Solar have completed a 7.7kWp rooftop installation in Belgium, claimed to be the second of its kind, for French company InnoVent.

Masdar's 5.7 m$^2$ thin-film solar modules

Source: Gehrlicher Solar

**Gehrlicher's GehrTec Intra substructure allowed Masdar PV's 5.7m$^2$ thin-film solar modules to be fully integrated into the sloping roof of the 19th century barn.**

have been fully integrated into the Gehrlicher's GehrTec Intra substructure, creating a completely rain-proof roof system.

Products from Masdar PV are currently being used in a variety of project planned by InnoVent in southern Africa. Gehrlicher Solar has recently built its largest PV plant in Spain, whilst continuing its expansion into the US solar market.

## Solarstrom expands portfolio by 1MWp

S.A.G. Solarstrom has announced the expansion of its current power plant portfolio by about 1MWp, effective December 31, 2011. The company has invested around €2 million in a 919kWp rooftop system of a logistics service provider in Dortmund, Germany. Solarstrom now have 88 systems in Germany and abroad with a total output of 26.1MWp and worth €78 million.

Source: S.A.G. Solarstrom

**Solarstrom's 999kWp Esposito solar farm in Italy.**

## Premier Power and Viasol enter agreement to provide 5MW to Scandinavian solar projects

Scandinavia is to receive 5MWp in equipment for solar projects from Premier Power Renewable Energy. The plants will be funded through an agreement with Danish firm, Viasol. Equipment will be shipped out this month, with all systems scheduled for completion by the end of 2012.

"We are continuing with our strategic expansion to European markets, in 2011 we expanded to the Bulgarian market and now we are expanding to the Scandinavian market." said Bjorn Persson, executive vice president of European operations at Premier Power.

## SPI continues European expansion with 1MW fixed-ground-mount solar facility in Greece

SPI Solar, the US-based EPC services provider, has announced its third Greek venture, having acquired the necessary paperwork. Working alongside local partners SDL Solar and Global Energy Services, the installation is expected to be a 1MW fixed-ground-mount solar facility, located in Rhodope Prefecture,

News

Source: CBS News

LDK will provide its high-performance solar modules to SPI's 1MW facility in Greece.

north-eastern Greece. The electricity will be purchased by Greek Public Power Corporation through a 20-year PPA.

Earlier this month SPI released its preliminary financial results, forecasting its net sales for this year to double 2011 levels. In January 2012, SPI announced the second project, a 2MW facility also located in the Evros region. The first project, announced in August 2011, was a 4.4MW plant in the Evros region.

Once completed, SPI intends to perform operations and maintenance of the facility over the term of the PPA. The plant will use LDK's high-performance solar modules.

## Americas News Focus

### Exelon and First Solar defer change of ownership of AVSR PV project

Exelon and First Solar have extended their deadline for initial funding of the DOE loan for the 230MW Antelope Valley Solar Ranch One (AVSR) project, in northern Los Angeles County, California. A revised construction permit has been approved but the delay could mean First Solar has to repurchase the project from customer Exelon from February 24, 2012, as federal loan and loan guarantees would not be released in time for the contract clauses to kick in.

The new deadline for initial funding of the DOE loan has been moved to April 6 2012 in order to allow the expected time for the initial funding to be in place. The extended deadline means the risk of First Solar repurchasing the project has diminished. Construction of AVSR has not been affected.

Source: First Solar

Exelon and First Solar have extended their deadline for initial funding of the DOE loan for the 230MW Antelope Valley Solar Ranch One project.

### Mars Chocolate launches 1.258MW solar garden in North America

Mars Chocolate, North America, has announced the installation of a solar garden at its Henderson chocolate factory, providing 100% of the factory's electrical energy. The solar garden features 2,112 ground-mounted solar panels on 4.4 acres. Mars claims its installation to be the largest by a food manufacturer in Nevada.

The installation generates 1,258MW of zero-emission electricity each year, offsetting 867 metric tons of greenhouse gases – the equivalent of removing approximately 170 vehicles from the road. The project will generate enough energy for 115 Nevada households' use annually.

### Apple to construct 20MW plant in North Carolina, US

Apple has announced its plans to construct the largest end user-owned, onsite solar array in the US, quashing rumours surrounding the technology company's renewable energy goals. The 20MW facility, in Maiden, North Carolina, will be installed on 100 acres of land, supplying 42 million kWh of renewable energy annually. Apple will also be building a fuel cell installation, powered by 100% biogas to provide more than 40 million kWh of baseload renewable energy annually.

### IKEA completes 15th solar installation in US

IKEA is continuing with its investment in solar power with a further system installed at its store in College Park, Maryland, US. REC Solar was chosen to develop, design and install the 1,196kW system, which consists of a 148,200 square foot PV array, built with 4,984 panels. It will produce approximately 1,571,800kWh of clean electricity annually, the equivalent of reducing 1,195 tons of $CO_2$, eliminating the emissions of 213 cars or powering 135 homes yearly.

IKEA owns and operates each of its solar PV energy systems in the US, with a further 22 more locations underway. The company claims this will make its eventual

Source: IKEA

The solar system consists of a 148,200 square-foot PV array, built with 4,984 panels.

# Every Day, The Sun Rises. And Every Day, We're There to Meet it.

ecobuild Visit us at Booth No. N3210

Visit us at Booth I1.2, Hall 7b SOLAREXPO

**Shouldn't a solar energy company be as dependable as the sun is?**

We think so. That's why we're taking on serious and growing energy challenges with innovative energy solutions. At Hanwha Solar, our scientists and engineers work tirelessly to bring this reliable and limitless resource to more of the world's people, more efficiently. From the manufacture of modules to the construction and financing of power plants, our knowledge is comprehensive while our commitment is unparalleled. When it comes to solar energy, you might say we're up to it.

Hanwha Solar

Trust in the Sun

US solar presence nearly 85% with a total generation of 30.8MW.

## Odersun PV honoured with iF gold award for BIPV modules

Odersun was one of 100 products or ideas to be selected for the iF gold award 2012, making it the first company from the solar sector to be chosen for the prize. The company's PV modules were additionally recognized for their aesthetics with an iF material design award 2012.

Source: Odersun

**Odersun is the first company from the solar sector to receive the iF gold award.**

The company's Solar Module Designer was also honoured with the iF communication design award. This is the second award for the online configuration tool, having been additionally been recognized at the red dot design awards.

# Africa & the Middle East

## Tenesol working on a €4.5 million solar telecoms project in Morocco

A €25 million project partnership between Tenesol and Morocco's National Electricity Office for will see the deployment of PV power systems across 26,000 rural homes in Morocco. Furthermore, the SunPower subsidiary is also currently working on a €4.5 million solar telecoms project in Morocco that will involve the company's supplying more than 4,500 PV panels to Maroc Telecom for use at 42 sites across the country. Overall, Tenesol claims to have installed 3,000 systems for the telecoms industry.

Source: Tenesol

**Tenesol is currently working on a €4.5 million solar telecoms project in Morocco.**

The use of PV in off-grid telecoms applications is also being used for charging mobile phones – a key challenge for mobile operators attempting to expand market footprint and address over 1.6 billion people living without electricity supply.

## Africa could alleviate poverty through renewable energy, says UN report

Sub-Saharan Africa could still be without electricity in 2030 if the continent does not take advantage of its wealth of untapped, domestic renewable energy, said a recent United Nations report. Government policies that facilitate private sector investment in energy markets are crucial to reducing poverty and encouraging sustainable development.

The UN report was produced by the UN Environment Programme in Nairobi to mark the African launch of the International Year of Sustainable Energy for All, which outlines how current obstacles to the scaling-up of sustainable energy solutions in Africa, such as the cost of electricity generation or difficult grid access, can be tackled.

The UN reports that in order to meet the continent's growing energy demands, the power sector in Africa needs to install an estimated 7,000MW of new generation capacity each year.

altestore.com

**Solar energy is plentiful in Africa, yet remains an untapped resource.**

The study gives examples of how policy incentives can help reduce the higher costs associated with electricity generation from renewable sources. For example, in Kenya, the government feed-in tariff offers production incentives for an estimated additional energy generation capacity of 1,300MW.

## GeoModel Solar releases new solar maps for South Africa

New solar maps for South Africa, Lesotho and Swaziland have been released by GeoModel Solar, showing the direct solar radiation on the African continent. "Uniqueness of these maps is reflected in their very high spatial resolution of 250 metres. As regards temporal resolution, the underlying solar database represents more than 18 years of historical data (1994 - to present) with a time step of up to 15 minutes," said Marcel Suri, managing director of GeoModel Solar.

Source: GeoModel

**New solar maps of South Africa, Lesotho and Swaziland have been developed by GeoModel Solar.**

"The solar radiation received in some regions can vary by up to 20% within a distance of 10 kilometres. Hence, it is very important to have access to data with high accuracy and spatial resolution, making it possible to predict a solar plant's output with greater confidence," Suri added.

Development of the maps was completed using data from GeoModel's SolarGIS, a program that was developed in partnership with the Centre for Renewable and Sustainable Energy Studies at Stellenbosch University. The new maps and data can be accessed through GeoModel's SolarGIS web platform.

# Product Reviews

## Amphenol

### DC cabling solution from Amphenol

**Product Outline:** Amphenol Industrial is offering a new active trunk and drop cabling solution, in conjunction with Ampt, a designer of active electronics for PV solar modules. The new cabling solution is claimed to reduce the cost of commercial and utility-scale PV systems.

**Problem:** Rapidly declining module prices are placing increasing pressure on BOS cost reduction. Providing a simplified alternative to conventional DC wiring in PV systems, by replacing conventional trunk wiring design would reduce installation costs significantly.

**Solution:** Comprised of one major cable conductor with a number of smaller cables connected to a PV panel, the new assembly allows for up to 40% more modules per string as well as lower current carrying requirements. When paired with Amphenol's ModLink junction box, the new active trunk and drop cabling solution also maximizes the output of each module, recovers degradation losses, removes the risk of module obsolescence, improves system run time and lowers energy costs. Providing a simplified alternative to conventional DC wiring in PV systems, Amphenol's active trunk and drop cabling replaces the typical trunk wiring design with its pre-fabricated wire harness assembly.

**Applications:** Commercial and utility-scale PV systems.

**Platform:** Integrated into Amphenol's ModLink junction box, Ampt's active electronics monitor power generation conducted down the trunk and drop cable assembly, while providing power monitoring and optimization for solar panels attached by a wire harness. The ModLink base can accept a range of smart modules such as DC/DC converters/optimizers, micro-inverters or monitoring modules.

**Availability:** February 2012 onwards.

## Anderson Power Products

### APP's multi-pin connector offers shorter PV system installation times

**Product Outline:** Anderson Power Products has introduced its Solar SPEC Pak, claimed to be the first multi-pin connector to meet PV industry requirements specified in UL 6703A, passing the same harsh environmental tests used to qualify solar panels.

**Problem:** Designed for wire-to-wire applications, Solar SPEC Pak is capable of handling up to four individual lines which reduces the number of traditional connectors needed in solar installation applications. Reducing the number of wire-to-wire connections can assist in minimizing the amount of space needed while simplifying and lowering installation costs.

**Solution:** Solar SPEC Pak has power handling capabilities up to 1000 volts and features a locking latch that complies with NEC 2008 section 690.33(C) requirements. The multi-pin connector is capable of handling up to four individual lines, whilst minimizing the amount of space needed.It is claimed to lower installation costs and will hold up to four Powerpole power contacts, 16 signal contacts or a combination of both. Individually, the power contacts are rated to 40 amps and are capable of handling wire sizes of 20 to 10 AWG (0.5 to 4mm$^2$).

**Applications:** Designed for wire-to-wire applications in PV module installations needing multi-pin connectors.

**Platform:** The Solar SPEC Pak, IP68-rated shell has a flammability rating of UL 94 V-0 and a weatherability rating of F1 per UL 746C. The housing is touch-safe per UL 1977 when used with Fingerproof Powerpole housing and has a temperature range of -40° to 105°C (-40° to 221°F).

**Availability:** January 2012 onwards through APP authorized distributor networks or direct from the factory.

## BISOL

### BISOL's PV power plant monitoring system provides 24/7 real-time analysis

**Product Outline:** BISOL Group has developed a complete and elaborate real-time monitoring system. By detecting faults and conveying them to the maintenance team and to the owner, the system enables a rapid response when a defect in the PV system occurs.

**Problem:** PV power plant owners may lose a substantial part of their earnings if their solar systems are not operating correctly. Due to the PV system's exposure to the outdoor elements, electrical grid problems, component wear and tear or poor maintenance, faults in performance may occur. Immediate response is essential for preventing loss of income for the owner.

**Solution:** In order to ensure a rapid response, BISOL Group has developed a central monitoring system, a graphically appealing and extensive web application that was fully developed in-house and provides 24/7 real-time monitoring. The application allows the owner to track daily, monthly and yearly energy yields and other ecologically relevant information. Web application allows the owner to follow BISOL news, manage the power plant picture gallery and publish the selected information about the solar system in the form of a public web page profile which can be shared with others.

**Applications:** Commercial and utility-scale PV power plants.

**Platform:** BISOL Group is also offering a mobile version of the application for the iPhone, iPad and android platforms. Moreover, the system sends immediate alerts via email and SMS to the owner and the maintenance team.

**Availability:** January 2012 onwards.

# Product Reviews



## Conergy

### Conergy's PowerPlus module now available in black

**Product Outline:** Conergy's PowerPlus Premium module is now available in black. As an alternative to the polycrystalline, classic blue module, the Hamburg-based company is now offering its "Edition Noir" as a second design option, with black cells and a black backsheet. Monocrystalline modules in four different performance classes, from 240 to 255W, will also be available in this new look. The Conergy SunTop mounting system is also available in this range.

**Problem:** There is a growing demand, especially in the US market for better-looking, less obvious rooftop PV system installations. Providing a black-on-black module is regarded as a more sophisticated look for rooftop systems.

**Solution:** Conergy's PowerPlus Premium module offering, Edition Noir, is a second design option, with black cells and a black backsheet. Performance features are not impacted as Conergy is supplying Edition Noir modules with positive performance tolerances up to +3%.

**Applications:** Residential and commercial rooftop installations.

**Platform:** Monocrystalline modules are available in four different performance classes, from 240 to 255W. The polycrystalline Conergy laminate also features a black back sheet, and thereby expands Conergy's module portfolio to include a roof-integrated option. The modules have a load capacity of 6,000 pascals and weigh in at 19.6 kilograms.

**Availability:** February 2012 onwards.

## GeoModel Solar

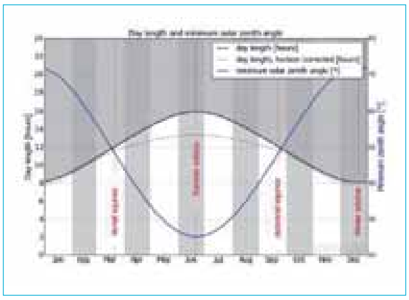

### GeoModel Solar's latest software suite plots PV projects potential

**Product Outline:** GeoModel Solar has launched a new generation of solar installation software – iMaps and pvPlanner. iMaps provides access to key solar resource parameters with a spatial detail of 250m, thus allowing for accurate site selection, while pvPlanner allows fast comparison of various sites and technology options.

**Problem:** PV project developers require quick and easily identified project sites that have high insulation to maximize electricity production and ensure the economic profitability of solar energy projects. Engineers, installers, financers, policy-makers and the wider community need to be able to use reliable, historical and up-to-date information before investments are made.

**Solution:** SolarGIS iMaps offer unlimited access to the relevant site-specific climate and geographic data required for prefeasibility studies, supported by the data reports and high-resolution interactive maps. Once a site is selected, PV electricity yield can be interactively estimated by SolarGISpvPlanner. The pvPlanner software simulates long-term electricity production of PV projects. For small- and medium-sized PV systems, pvPlanner reports are bankable benefiting from validated insulation resource data and state-of-the-art knowledge.

**Applications:** Industrial, commercial and utility-scale PV projects.

**Platform:** SolarGIS solar resource database is based on advanced numerical models and geoinformation infrastructure. It helps to optimize choice of different types of modules, inverters and mounting strategies. SolarGIS platform was first introduced in 2010 for Europe, Africa and Middle East, and also consists of other applications: iMaps, climData, and pvSpot.

**Availability:** January 2012 onwards.

## GreenPeak Technologies

### GreenPeak's wireless monitoring and controlling of PV modules

**Product Outline:** GreenPeak Technologies, a fabless semiconductor company, has introduced a wireless monitoring and control system solution for solar panel installations that will allow individual panel parameter tracking and control.

**Problem:** Currently, most residential solar panel systems only provide energy information on a monthly basis and do not allow individual panel monitoring. Improvement in the efficiency of solar systems and the need for a more developed understanding of solar panel performance, tracking and maintenance becomes increasingly important because of the rapid deployment of solar technologies in the marketplace.

**Solution:** The Smart Junction Box reference design utilizing its wireless chips provides a solution to monitor solar systems in more detail and to control the chain from a central unit or remote device. The GreenPeak solution also allows PV module manufacturers to comply with new upcoming legal requirements requiring that solar panels can be individually switched off in case of calamities. By adding wireless Smart Junction Boxes on every individual panel, up-to-the-minute status information on electricity generation of each panel can be provided.

**Applications:** Wireless monitoring and control system for PV modules.

**Platform:** The data collected from each individual panel can also be shown in a configurable GUI software application. When a problem in the solar panel system occurs, performance gradually declines or suddenly drops. Remote diagnosis and controlling via a mobile App on smart phone can be one of the use cases.

**Availability:** January 2012 onwards.

## Kyocera

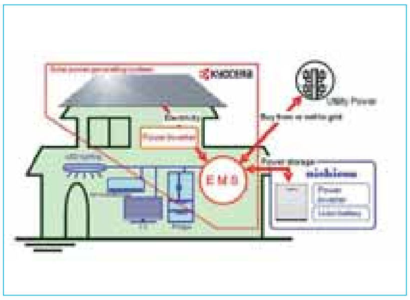


### Kyocera to add energy storage with PV modules in Japan

**Product Outline:** Kyocera and Nichicon will begin domestic sales this summer of a new energy management system (EMS) which combines Kyocera's solar power-generating systems with Nichicon's high-capacity lithium-ion battery storage units. Designed for the Japanese market, the new system responds to the growing demand for residential energy storage equipment following the March 2011 disasters. Kyocera will begin sales in Japan this summer.

**Problem:** Using and regulating a solar power-generating system with battery storage requires a power inverter and sophisticated energy-management technology. The EMS developed by Kyocera is thus effective in optimizing residential energy use from those systems and utility power from the electricity grid.

**Solution:** The new EMS system offers various operating modes to meet the energy use patterns and needs of various customers — whether their peak energy consumption occurs in the daytime or at night and for families who want to prioritize reducing their energy bill or those who place a premium on guaranteed electricity supply. The system automatically switches to independent operation in the event of a natural disaster or electricity black-out. In the event of a prolonged black-out, the battery can be charged directly by the solar modules during the day, allowing users to draw from the battery at night or during inclement weather.

**Applications:** Residential energy storage.

**Platform:** The system uses a lithium-ion battery, which is claimed to last roughly five times longer than conventional lead-acid batteries. The battery has a high capacity of 7.1kWh, weighs roughly 200kg and has a size of 120cm × 90cm × 35cm (H×W×D).

**Availability:** Summer 2012 in Japan only.

## Rainwise

### Weather station system from Rainwise offers continuous environmental data

**Product Outline:** Rainwise has recently released the PVmet Solar Energy Efficiency Monitor, a weather station designed to improve accurate monitoring of PV plant performance parameters. The monitoring system is said to be the first weather station to be recognized by SunSpec Alliance for compatibility with industry plant management systems and has already sold 500 units to two inverter manufacturers.

**Problem:** Understanding PV module and array performance characteristics are important for predicting and maximizing actual electrical production and panel maintenance. The current standard method for testing the performance of PV modules and arrays monitor performance in a single standard reporting condition set at an artificial uniform ambient temperature of 25°C. This standard reporting condition is unrepresentative of actual operating conditions.

**Solution:** RainWise's PVmet Solar Energy Efficiency Monitor weather station acquires continuous environmental data on installed panels. It includes a global solar irradiance sensor, a plane-of-array irradiance sensor, two back-of-module temperature sensors, an ambient air temperature sensor and a wind speed/direction sensor.

**Applications:** Commercial and utility-scale PV power plants.

**Platform:** Housed in a compact and easy to install unit, unique to the PVmet are the back-of-module temperature sensor and two key irradiance sensors that provide information fundamental to performing key panel efficiency calculations. It is also in three different models with options. Modbus RS-485 Communication and Sunspec Ver. 1.1 Compliant.

**Availability:** Currently available.

## Siko

### Siko's IK360 inclinometer provides precise solar tracking of modules

**Product Outline:** Siko has developed the IK360 inclinometer, which is claimed to provide ultimate accuracy in solar tracking with absolute measurement technology over 360°. The main area of application of the new IK360 from Siko is the alignment of heliostat or PV modules and the tracking of parabolic trough collectors or even Fresnel collectors.

**Problem:** Solar tracking has to be accurate to reach the best possible efficiency to provide the best IRR.

**Solution:** The absolute measurement technique of the IK360 makes reference runs after start-up or following a period of idle time unnecessary. The sensor uses the natural force of gravity to accurately map positions with a claimed system accuracy of +/- 0.1° in a 360° area. The compact IK360 also benefits from quick and easy installation and a variety of different interfaces.

**Applications:** Alignment of heliostat or PV modules and tracking of parabolic trough collectors or Fresnel collectors.

**Platform:** The IK360 rounds off Siko's portfolio of magnetic and non-contact measuring systems from the MagLine product range. Power consumption is less than 1W. Environmental conditions include operating accuracy of 0.1° (at -10°C +40°C) and works in 100% humidity condensation. Sensor response time 10ms (without filter). Protection category of IP69K (connected). Interface CAN according ISO 11898, galvanically isolated CANopen (profile 410).

**Availability:** Currently available.

# Product Reviews



## Trina Solar

### Trina Solar offers three-pronged service solution for rooftop installations

**Product Outline:** Trina Solar is offering a three-pronged service solution featuring complimentary design services, newly available high-performance 'Honey' modules and the rapid install 'Trinamount' racking system specifically for large rooftop PV installations in the North American market.

**Problem:** Compared to industry-standard 230W modules, Trina Solar claims that a typical flat rooftop system using comparably sized 260Wp Honey modules could produce over 18% more electricity per year from the same roof area. By combining high-performing Honey modules with the fast-mounting Trinamount system, customers can install Trinamount Honey systems up to 4.5 times faster while shaving installation costs by up to 10%.

**Solution:** Customers using Trina Solar modules can benefit from a complimentary design service that delivers preliminary system layouts and performance estimates for large rooftop installations. Trina Solar also offers its high-performance 60-cell, up to 260W Honey module series for North America.

**Applications:** Large rooftop PV installations.

**Platform:** Laboratory tests, confirmed by TÜV Rheinland in September 2011, demonstrated that a 60 Honey cell module set a world record for multicrystalline module power by reaching a 274W peak. In June 2011, Trina Solar broke ground with an industry-leading 25-year linear power warranty, a 10-year product warranty and a guaranteed positive power tolerance of 0/+3%.

**Availability:** January 2012, in the North American market only.

## Wagan Tech

### Wagan Tech has developed scalable off-grid solar power generators

**Product Outline:** Wagan Tech has launched new off-grid solar power generators. The 'Solar e Power' Cube 1500 and the 'Solar e Power' Case 450 are both plug and play solar generators providing instant access to AC power.

**Problem:** Access to electricity is either unreliable or non-existent in much of the developing world. Natural disasters such as earthquakes can disrupt power sources for considerable durations, while essential services often have most urgent need for safe, reliable electricity.

**Solution:** The larger and more powerful of the two units is the Solar e Power Cube 1500. It boasts a 1,500W AC inverter and a 55AH battery. The solar panels provide 80W of solar charging. The Solar e Power Case 450 features a 450W inverter and a 26AH battery. The 40W solar panel unit attaches to the side for easy transport.

**Applications:** In developing countries, as back-up power or for remote locations.

**Platform:** The two solar generators are self-contained power sources which makes setup quick and easy. They are equipped with solar panels, an AGM/Gel Hybrid battery and one of Wagan Tech's legacy power inverters, all packaged together in a rugged case. The Solar e Power Cube 1500 features 1500W AC inverter, 12-volt DC outlets and 2.1 amp USB power ports supported by a 55AH gel battery. Initial AC charge is up to 24 hours while the solar panel charging time is 16 hours in peak sunlight. The MSRP for the Solar e Power Cube 1500 is US$1,199.00. The Solar e Power Case 450 has an MSRP of US$799.00.

**Availability:** January 2012 onwards.

## TTi

### Mounting system from TTi is 100% watertight for shingle roofs

**Product Outline:** TTi has introduced its next generation of residential solar roof mounts, the patented TTi 'Flat Jack Comp Shingle Mount.' As a durable and reliable mount for installing PV panels on composition shingle roofs, the TTi Flat Jack now requires no shingle trimming or sealants, reduces labour costs and protects roofs.

**Problem:** Today, most houses in the US are designed with shingle roofs. As rooftop solar power systems become a more popular way for homeowners to cut their monthly energy expenses, the installation of solar panels on this type of roof can present a challenge for even the most experienced solar installer. A mistake means the homeowner is left with a leaky roof.

**Solution:** Made of galvanized steel and with only three primary components, the TTi Flat Jack anchors to the roof's rafters providing a solid foundation and converting a shingle roof into a solar platform. The system is engineered with a breakthrough design and is built to withstand heavy vertical loads and high winds. It is compatible with all standard PV rail systems and can support other roof installations including HVAC equipment, antennas, solar thermal or flagpoles.

**Applications:** Shingle-based roofs in the US.

**Platform:** The TTi 'Flat Jack Comp Shingle Mount is ICC certified for residential solar installations, compatible with standard PV rail systems to mount solar panels and comes with a 10-year warranty.

**Availability:** January 2012 onwards.

# Weighing the merits of solar power plants using concentration photovoltaics (CPV)

**Geoffrey S. Kinsey**, Amonix, Seal Beach, California, USA

## ABSTRACT

In endeavouring to introduce its relatively new technology to customers of traditional utilities, the photovoltaic industry often finds itself in the awkward position of trying to sell a product to a customer who may not want to buy. The upfront capital costs of new solar plants (which deliver power only intermittently) can be less than appealing. To facilitate large-scale grid integration there is a need for the development of PV technologies that more closely fit the profile of traditional power sources. In addition to low cost, things to consider include high capacity factors and the ability to better match demand during daylight hours. As a step towards satisfying these requirements, concentration photovoltaic (CPV) power plants are now being integrated into the grid at megawatt scales. By performing light collection using acrylic, silicone or glass optics instead of semiconductors, CPV fundamentally shifts the material cost balance. The world's most efficient solar cells can now be employed, and maintaining tracking of the sun becomes economically favourable across vast sunny locales worldwide. Offering AC system efficiencies in excess of 25%, the resulting CPV power plants produce high energy yields throughout the year and deliver the high capacity factors demanded by utility customers. Since semiconductors are a minority component cost, manufacturing capital costs are lower than for any other PV technology, allowing for rapid scale-up and field deployment. This paper describes the state of the art of CPV technology, field performance results and the outlook for near-term deployments.

## Introduction

Upfront capital costs mean that new solar plants, which deliver power only intermittently, can be unattractive as replacements for fossil-fuelled plants. Large-scale grid integration will be accelerated by PV technologies that best fit the profile of traditional power sources. Low dollar per watt cost is thus a necessary, though not a sufficient, condition. Photovoltaic power plants will also need to deliver higher capacity factors and the ability to better match demand, at least during daylight hours, than at present. This suggests the need for tracker-based systems (Fig. 1(a)).

While the benefits of tracking the sun to the horizon have been understood since the earliest days of PV, commercialization of tracking systems has been hampered by the higher upfront costs, operation and maintenance costs, and a market that has often incentivized rated power ($/W) over energy (¢/kWh). As the PV market has reached maturity, emphasis has shifted away from peak power ratings towards energy yield, as reflected in the adoption of feed-in tariffs in Europe, Japan, parts of the USA, China and elsewhere. With an eye on increasing the net cash flow of PV plants, migration towards tracker-based installations has accelerated. Tracker-based PV favours higher-efficiency modules for an energy yield that justifies the higher cost of installation and maintenance. For energy return on a tracker, there is no better technology than high-concentration photovoltaics (Fig. 1(b)).

Concentration photovoltaics (CPV) that operate at high concentration, above about 100×, rely on precise, dual-axis tracking. Such trackers have operated reliably for many years, but the upfront cost was a deterrent until around 2006, when the efficiency of III-V multijunctions reached 40%. Following a trajectory that

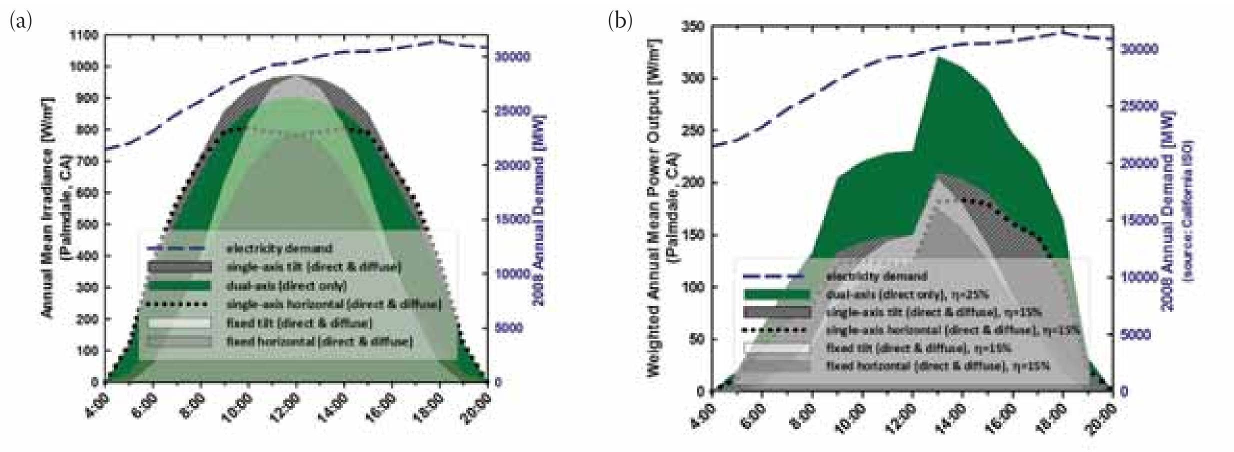


**Figure 1. (a) Use of the solar resource to meet grid demand depends on either single- or dual-axis tracking. (b) The benefit is more pronounced if the irradiance is weighted by time-of-day utility rates (source: Southern California Edison) and conversion efficiency is considered. As an illustration, an AC system efficiency of 25% was assumed for dual-axis (CPV) systems and 15% for all other systems.**

began more than a decade earlier in space applications, III-V multijunctions then proceeded to displace high-efficiency silicon cells in the CPV systems then under development. The move to III-V multijunctions delivers more than a 30% increase (relative) in AC system efficiency; dual-axis tracking maintains this high efficiency from sunrise to sunset. This combination makes a virtue out of necessity: the higher energy yield more than justifies the cost of dual-axis tracking, as well as the higher cost of the III-V multijunction cells.

## Economics

In conventional PV, large sheets of semiconductor material are needed to perform both light collection and energy conversion. The fundamental premise of CPV is that semiconductors need not be used for light collection: lower-cost materials serve this function. Substituting acrylic, silicone or glass optics for semiconductors separates the light collection from energy conversion and fundamentally shifts the cost balance of PV. The world's most efficient solar cells can now be put into service, and precision tracking becomes economically favourable across vast sunny locales worldwide. A dividend of CPV is that cell voltage rises logarithmically with light intensity; this is why cell efficiency increases with concentration. With AC system efficiencies now in excess of 25%, the resulting CPV power plants produce high energy yields throughout the year and deliver the high capacity factors demanded by utility customers. Since semiconductors are a minority component cost, manufacturing capital costs are lowered, allowing for rapid scale-up and field deployment.

"A dividend of CPV is that cell voltage rises logarithmically with light intensity; this is why cell efficiency increases with concentration."

The leveraging effect of efficiency and concentration is illustrated in Fig. 2. Applying cost assumptions for flat-plate and dual-axis tracking at production scales [1], CPV systems using cells with efficiencies of 40% or more are projected to deliver an upfront system cost below the range achievable for flat-plate systems employing single-crystal silicon cells. The outsized role that efficiency plays in CPV also leads to more headroom for innovation: improvements in performance and durability that would otherwise prove too expensive in less efficient designs typically pay for themselves in CPV. These advantages have provided the impetus for scaling up production of CPV power plants. Once CPV reaches the scale of other technologies, it is expected to deliver the lowest levelized cost of energy (Fig. 3).

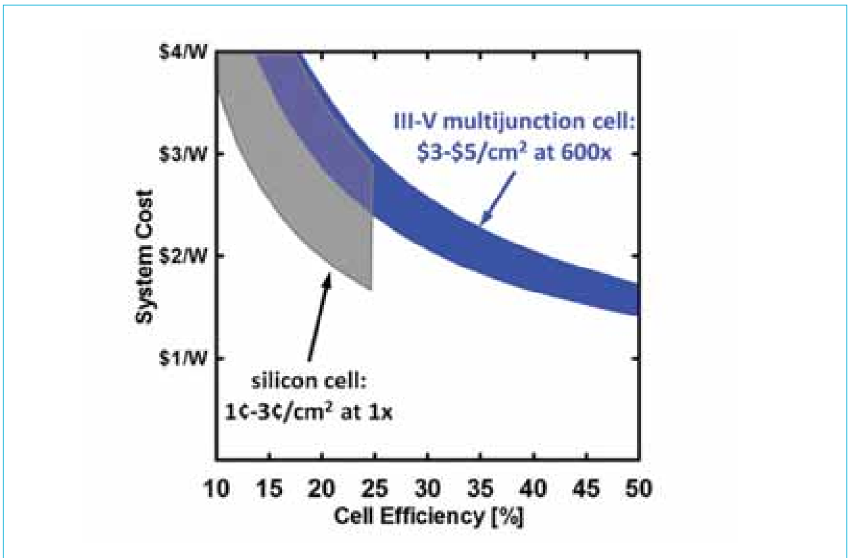


**Figure 2. With high efficiency and high concentration, low system costs are achieved despite the high cost of III-V multijunctions. Here, the world-record efficiency of 25% is assumed as an (optimistic) upper bound for commercial silicon cells. 1¢/cm² translates to about 40¢/W at 25% (DC) cell efficiency.**

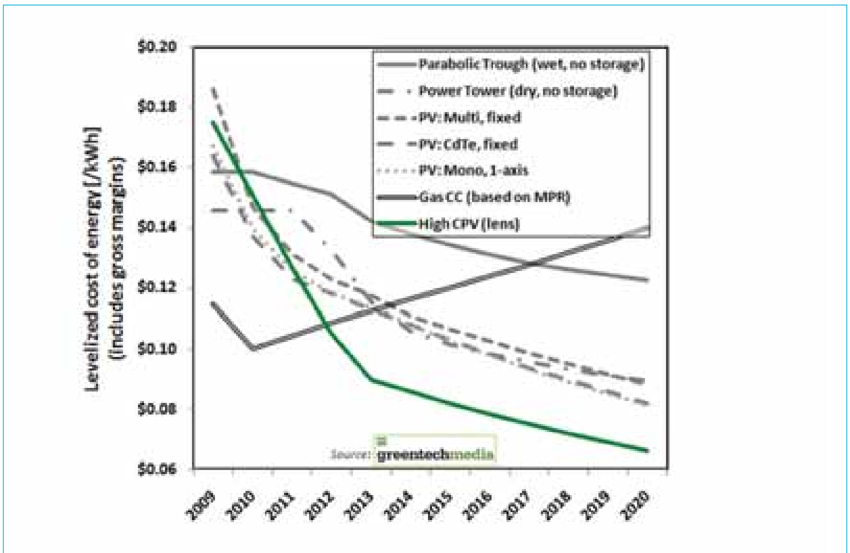


**Figure 3. At scale, CPV is expected to outrun rival technologies in delivering the lowest levelized cost of energy (LCOE) [2].**

The system economics of CPV favour maintaining the highest possible efficiency, so low cost of energy is obtained by making the most of the III-V multijunction cells. The cells that lie at the core of CPV power plants today are well equipped to take maximum advantage of the energy delivered to them via the concentrating optics. Commercially available cells now realize 40% efficiency under standard test conditions (25°C, 1000W/m$^2$, AM1.5 spectrum). The temperature coefficient of III-V multijunctions is less negative than for other semiconductors (such as CdTe and Si) and the magnitude decreases with increasing concentration [3]. When paired with properly designed optics, a passively cooled module above 500× concentration readily achieves DC efficiencies over 30% (Fig. 4(a)); AC system efficiencies greater than 25% have been demonstrated by several CPV companies (Fig. 4(b)).

## Ratings

The different methods used in rating cell, module and system efficiencies create some confusion. Standard test conditions (STC) of 25°C and 1000W/m$^2$ are used for the cell, but not for the module. Since CPV optics generally require outdoor (on-sun) testing, both modules and systems are usually measured under operating conditions instead, which are typically taken to be 20°C ambient and either 850W/m$^2$ (PVUSA) or 900W/

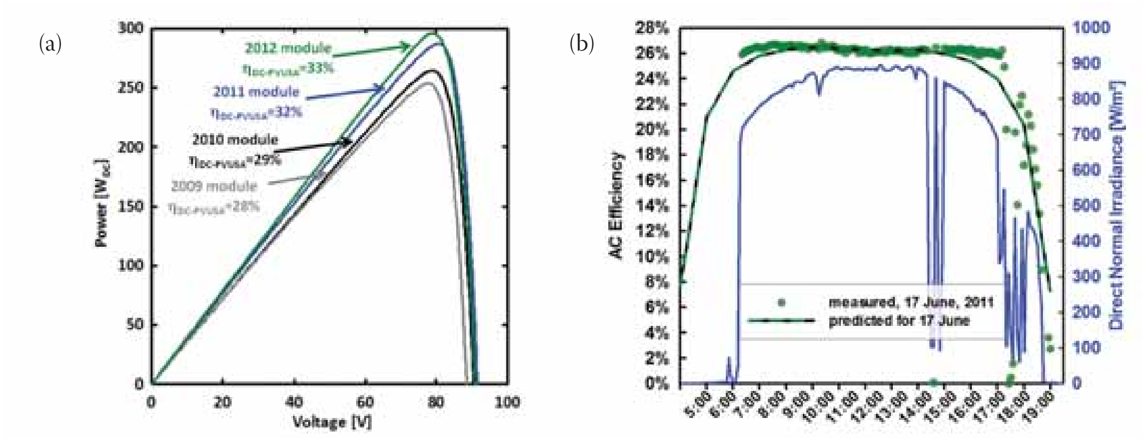


**Figure 4. Since the integration of III-V multijunctions, Amonix CPV module operating efficiency (a) and system efficiency (b) have continued to rise steadily. The generator in (b) is a 7700 from the 2MW plant at the University of Arizona Science & Technology Park (UASTP) in Tucson, USA.**

$m^2$ (IEC 62670, draft). Whereas many installers are accustomed to having PV modules in the field perform below their rating (under STC), CPV systems often perform above their (PVUSA) rating in locations with higher direct normal irradiance (DNI). The difference between standard and operating conditions accounts for about a 7% relative (3% absolute) decrease in rated efficiency from CPV cell to CPV system. The remaining loss is due to transmission and reflection losses from the optical elements, as well as string mismatch and inverter losses. Additional losses arise once real-world variations in the conditions are factored in. In order to translate high cell efficiency into high annual energy generation of a system, the design must balance tradeoffs involving variations in cell temperature, irradiance intensity, irradiance uniformity and spectrum variation. A cell designed for peak efficiency under STC is not likely to be optimized for maximum energy yield under lossy concentrating optics, at elevated temperature, over the course of a day or a year in the field.

## Energy prediction and results

To optimize a CPV system for actual field conditions, a predictive energy model has been developed that has proved successful in predicting both peak daily power and cumulative energy generation of existing installations [4,5]. The Typical Meteorological Year 3 (TMY3) database [6], established by NREL, is used as the source for the atmospheric and environmental conditions (air turbidity, precipitable water, ambient temperature, site pressure, etc.) that have an impact on the operation of III-V multijunctions. These inputs are used to generate representative spectra using the SMARTS radiative transfer model [7] (Fig. 5(a)). When combined with the spectral response of a III-V multijunction cell and losses due to the optics, the current available to each sub-cell is determined. Further corrections for the impact of intensity variation and temperature on voltage and fill factor, as well as the various (and variable) mismatch losses, result in a comprehensive, hour-by-hour prediction of CPV system output for any location in the TMY3 database. Though this is essentially a predictive model, a soiling correction based on the cleaning schedule is necessary to give expected peak daily power. For cumulative energy generation, an average soiling rate is sufficient and the model becomes entirely predictive.

This model has been applied to existing installations. The first Amonix generator using III-V multijunctions has been operating since January 2009 in Las Vegas, USA. Fig. 6 shows the effectiveness of the model in predicting the performance of this generator. Despite the vagaries of weather and season, peak power rises and falls much as expected. In Las Vegas, this

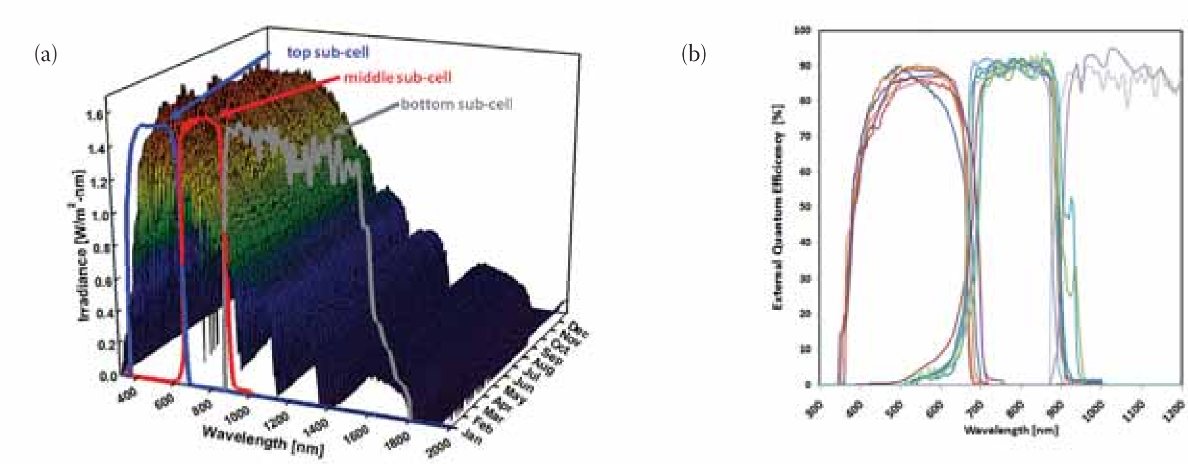


**Figure 5. (a) Hourly spectra generated using TMY3 inputs to SMARTS for a year in Las Vegas, USA. The spectral responses of the three sub-cells in a conventional III-V multijunction are also shown. (b) The variety of alloy compositions available provides the means for tuning the spectral response for increased energy generation in the field.**

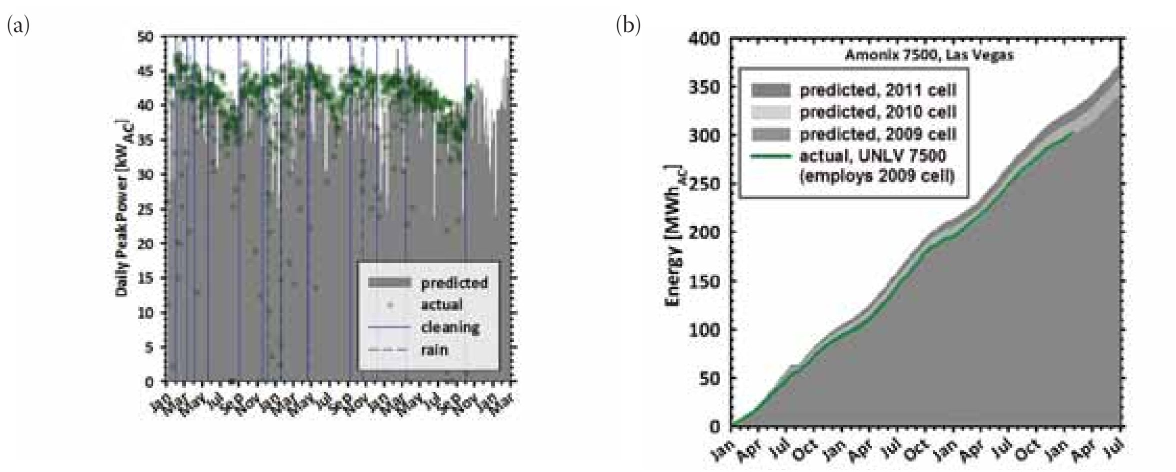


Figure 6. (a) Predicted vs. actual peak AC power of the 38kW$_{AC}$ Amonix 7500 operating in Las Vegas, USA, since January 2009. Actual cleaning and rain events were used to calculate the expected soiling losses in the prediction. (b) Corresponding cumulative energy generation. After more than 3 years in operation, the difference between predicted and actual energy (using 2009 cells) is less than 1%. The average energy yield over three years is 2600 kW-h/kW.

generator also typically operates above its 38kW$_{AC\text{-}PTC}$ rating. After more than 3 years of operation, which is 12% of the warranty lifetime, the cumulative energy is within 1% of the prediction. Any degradation is therefore below the threshold of detection.

## Designing for energy yield

The model in question is now being used to predict the energy yield of future power plants and make choices between competing design improvements. Opportunity for improvement has grown substantially in the last two years, as more advanced III-V multijunction designs have become available. The spectral response of III-V multijunctions has, until recently, been a limitation in increasing the energy yield. The spectral response is a result of the alloy composition of the III-V layers, but there is limited latitude for changing this alloy composition without compromising material quality. Fortunately, the accelerating interest in CPV that began in 2006 has germinated a host of new cell designs, from multiple vendors, that are now reaching commercial viability. The confusing mess of spectral response curves shown in Fig. 5(b) is a bounty for the CPV

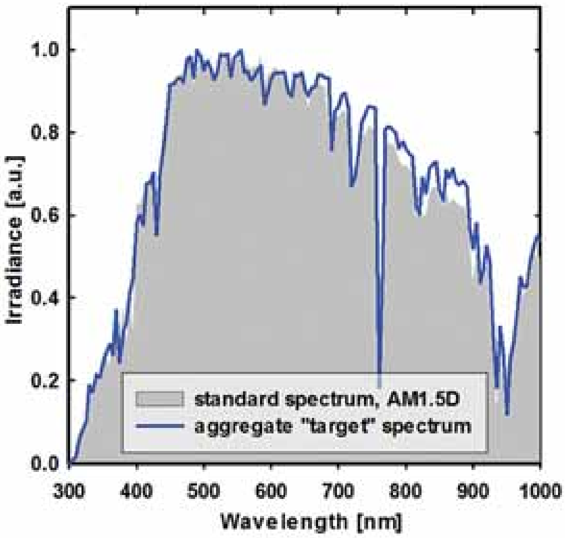


**Figure 7. Target spectrum compared with the standard AM1.5D reference. The target spectrum is a composite based on TMY3 data from six locations: Alamosa, CO; Las Cruces, NM; Las Vegas, NV; Palmdale, CA; Tucson, AZ ; and Denver, CO.**

system designer trying to squeeze more energy out of the next-generation systems. New designs include metamorphic materials [8], quantum structures [9] and grown bottom sub-cells that provide a higher voltage than the conventional germanium bottom sub-cell [10].

The greater flexibility afforded by these newer structures is already making its way into commercial CPV systems. Fig. 6(b) shows the increase in energy output predicted for an Amonix 7500 with the recent generations of cell designs. The ability to tune the spectrum response delivers a remarkable increase in energy generation with respect to cells available in 2009. Whereas the expected increase in efficiency for the latest cells under standard conditions is about 8% (relative), the increase in energy yield is about 14%. However, even more energy is available, as the current cell structures are still designed for maximum current output under the standard spectrum. Since the spectrum that reaches cells under optics in the field differs from the AM1.5D reference, further increases in energy are expected once cells are re-tuned for field conditions. Taking into account transmission losses from the optics, variation over the day and year in target locations, and weighting of the spectra with typical time-of-day (TOD) utility rates results in a new 'target' spectrum shown in Fig. 7. This composite spectrum is noticeably more 'red rich' than the AM1.5D standard. This implies that a typical III-V multijunction cell, designed for the standard AM1.5D spectrum, will, on average, have insufficient photons available for the top sub-cell. The movement by cell suppliers to re-balance cell structures for field conditions is now underway. Once cells are re-tuned, energy yield is expected to rise an additional 3–6%, depending on the cell technology [11].

Improving the III-V multijunction cell structure is just one of a host of design improvements beginning to reach commercialization now that CPV scale-up has begun. The III-V structure is currently grown on 100mm germanium wafers. The transition to 150mm wafers will take place in 2012, led by cell suppliers such as JDSU and Spectrolab, and will facilitate a cost reduction trajectory familiar in the semiconductor industry. The increase in the packing fraction of the cells, along with a decrease in the proportion of cells near the wafer edge, results in cell yields substantially higher than those corresponding to the 2.25× increase in area (Fig. 8).

"Improving the III-V multijunction cell structure is just one of a host of design improvements beginning to reach commercialization now that CPV scale-up has begun."

## Optics

The optics in CPV systems must satisfy multiple competing demands. The outer optical surface must be highly transmissive over the wide range of wavelengths converted by III-V multijunctions, but also robust under long-term exposure to UV radiation, temperature, humidity, soiling, occasional snow loads and hail, and resistant to abrasion from both windborne particles and cleaning. Two materials that meet these requirements are acrylic and tempered glass. Tempered glass has superior UV stability and abrasion resistance, but typically has lower optical transmission than acrylic. The shaped optic that collects and concentrates sunlight, known as the *primary optical element* (POE), can be either a refractor (e.g. Fresnel lens) or a reflector. In the case of a Fresnel lens, which is the most common POE in use today, the flat side of the lens also serves as the outer optical surface. The POE must have low loss (transmission/reflection above 90%), be formed with precision, maintain its shape under varying temperature and humidity, and be manufacturable at low cost. Reflective POEs are often back-surface mirrors to minimize degradation of the reflective surface, but this approach comes at the price of lower optical efficiency. Reflectors have an advantage over refractors, however, in terms of chromatic aberration, which can reduce the fill factor of a III-V multijunction cell.

Refractive POEs are typically Fresnel lenses, although all-glass convex lenses are also coming into use. Glass is generally too viscous to form the fine ridges needed for high optical efficiency in a Fresnel lens, so Fresnel POEs are composed of either acrylic or silicone-on-glass (SoG). Researchers at NREL have recently published a comprehensive study of the characteristics of Fresnel lens materials as they relate to CPV [12]. Acrylic has the virtues of low cost and high optical efficiency, and a lens composed of a single material experiences less distortion due to mechanical stresses. The principal disadvantage of acrylic is that it has less UV tolerance than glass, but long-term outdoor exposure studies of even the older acrylic materials have so far indicated that degradation rates are modest – less than 0.4% per year. Acrylics developed in the last decade, specifically for long-term outdoor exposure, fare even better. A compensating advantage of acrylic is that UV inhibitors and other additives can be combined with the acrylic backbone to increase UV resistance and enhance mechanical properties.

Newer acrylics now in production promise reduced degradation rates compared to the older acrylics tested in the field, with negligible impact on energy yield. In SoG lenses, the outer surface is glass, an excellent material for surviving long-term outdoor exposure. Antireflective coatings are also easier to obtain on glass than on acrylic. The lens pattern for SoG lenses is formed using UV-resistant silicones. This class of silicones is highly transparent, but relatively soft, so care must be taken to avoid dust accumulation on the inner lens surface. Since the silicone materials have higher expansion coefficients than glass, the silicone lens facets tend to become distorted under temperature. The index of refraction of the silicone also changes. As a result, it is more difficult to maintain

optical efficiency; highest efficiency is maintained by keeping the area of the lens elements relatively small. Long-term adhesion of silicone to glass must also be verified. Based on these tradeoffs, acrylic lenses remain the component of choice for Amonix generators. However, SoG lenses are a viable option for regions susceptible to sandstorms, for example.

In addition to the primary optical element, most CPV systems employ a secondary optical element (SOE). (Some systems even employ a tertiary optical element, but the optical losses of the additional optical 'bounce' are often prohibitive.) The SOE can be reflective or refractive, and is either in close proximity to, or in contact with, the surface of the cell. Reflective SOEs often function merely to increase the acceptance angle of the system by reflecting back light that strays off the cell aperture area. Refractive SOEs, on the other hand, can be designed to increase concentration and improve flux uniformity within the aperture, which increases the fill factor of the cell. From a pure performance standpoint, refractive SOEs are therefore superior. However, they are more expensive, and direct contact to the cell surface requires more delicate assembly. The adhesive must be strong enough to ensure a stable optical interface for the design life, yet compliant enough to avoid cracking the cell during temperature excursions. Whereas gradual soiling of a reflective SOE has a modest impact on performance, soiling of a glass SOE can lead to stress cracking that would compromise both the SOE and the cell.



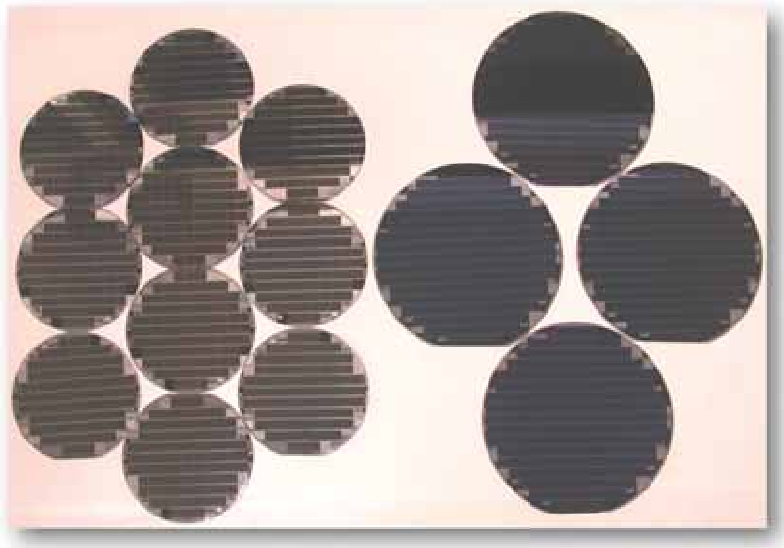

**Figure 8. The four 150mm wafers (right) contain the same number of cells as the ten 100mm wafers (left). Processing cost per cell is reduced, packing fraction is increased and the lower perimeter-to-area ratio results in higher yields.**

## Manufacturing and installation

Once these components are assembled into a module, high energy yield depends on precise tracking. Most high-concentration systems have an 'acceptance angle' of less than one degree. Should the module veer off track by more than this value, power loss would be in excess of 10%. Systems that deliver high energy yield are therefore designed to maintain their pointing vector to within a few tenths of a degree of the solar disc. This can be obtained with either electric gear drives or hydraulics. Gear drives may have lower upfront cost and require less routine maintenance, but often produce substantial backlash during tracking and reduced precision over time as the gears wear out. Hydraulics are generally favoured for larger systems and allow for rapid movement into stow position during wind gusts, for example.

"Once these components are assembled into a module, high energy yield depends on precise tracking."

Amonix generators offer one illustration of CPV for utility-scale power generation. The Amonix 7000 series is the seventh generation, but marks the first use of III-V multijunctions at Amonix. Design improvements in the cell and the rest of the power path have led to a 20% (relative) increase in efficiency since the first 7700s were installed using III-V multijunctions just two years ago. DC module efficiency now

(a) (b)

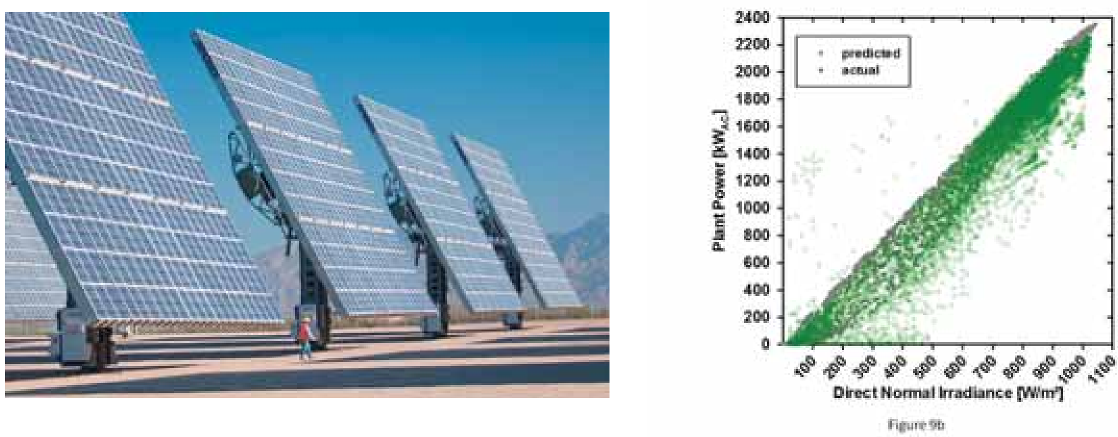


**Figure 9. (a) Five of the thirty-six generators that make up the 2MW installation at UASTP in Tucson, USA. (b) After six months of operation, the plant output closely matches prediction from the energy model.**

exceeds 33% under operating conditions (Fig 4a). Almost twice the size of any other PV system, the 7700 relies on hydraulics for its tracking. The MegaModule design reduces material and installation cost by ganging thirty-six module-sized components into a single rigid frame. Each MegaModule brings $10kW_{DC}$ into alignment at once and is mounted using four connection points. Most assembly is therefore relocated back to the level of MegaModule construction, in the controlled environment of a CPV factory. Since the semiconductor component is substantially reduced, a CPV factory is relatively low tech. New factories can be put into operation in just a few months, close to point of use, and at a fraction of the capital cost of technologies that are weighted more heavily by the semiconductor components.

Similar to other large-scale construction projects, installation of the CPV systems is highly mechanized. In the Amonix case, cranes now hoist about $70kW_{DC}$ into position with each array of seven MegaModules; megawatts can be installed in a day. This is a substantial advantage, particularly in remote locations, for an industry in which installation can make up the majority of the project cost. Panels mounted high off the ground also enjoy lower soiling rates. Wind buffeting can reduce energy yield, but the effects of wind loading in most target locations have been found to be acceptable. Compared to installations mounted close to the ground, CPV has a smaller effective footprint: it requires less site preparation and has a lower environmental impact during operation.

More than half a dozen CPV installations with individual capacities of over 1MW each have been commissioned in Europe and the USA by companies such as Amonix, Guascor Foton, Soitec and SolFocus [13]. All the installations since 2007 have employed III-V multijunction cells. One such recent installation is the Amonix plant at the University of Arizona's Science & Technology Park (Fig. 9(a)). The 2MW plant consists of thirty-six 7700s rated at $56kW_{AC}$. The performance of the plant, in operation since June, matches prediction (Fig. 4(b), Fig. 9(b)). A fall-off in peak power relative to prediction observable at levels of direct normal irradiation greater than $900W/m^2$ is primarily due to coincident temperatures that exceeded 40°C around solar noon during the summer. With more than a hundred generators online, Amonix now has over 100 unit-years of operating experience with III-V multijunction systems and will soon be adding more than a unit-year per day. A 30MW plant under construction in Alamosa, CO, will consist of the latest 7700 generators, rated at $60kW_{AC}$ each and expected to reach AC efficiencies of 27%.

## Conclusion

Recent CPV installations signal the commercial scale-up of an industry which is just beginning to gain economies of scale and travel down its experience curve. The high performance of existing systems represents merely the leading edge of a host of improvements already in the transition to production. CPV provides unparalleled energy generation that makes it ideal for deployment in the vast sunny and dry regions of the globe. The continuing installation of large-scale CPV power plants will accelerate the growth of photovoltaics in the world's energy mix.

### References


[1] Swanson, R.M. 2000, "The promise of concentrators", *Prog. Photovolt: Res. Appl.*, Vol. 8, pp. 93–111.

[2] Prior, B. and Seshan, C. 2011, "Concentrating photovoltaics 2011: Technology, costs, and markets", Greentech Media Research [available online at http://www.greentechmedia.com/research/report/concentrating-photovoltaics-2011].

[3] Kinsey, G.S. et al. 2008, "Concentrator multijunction solar cell characteristics under variable intensity and temperature", *Prog. Photovolt: Res. Appl.*, Vol. 16, pp. 503–508.

[4] Kinsey, G.S. and Edmondson, K.M. 2009, "Spectral response and energy output of concentrator multijunction solar cells", *Prog. Photovolt: Res. Appl.*, Vol. 17, pp. 279–288.

[5] Kinsey, G.S. 2010, "High-concentration, III-V multijunction cells", in Partain, L.D. and Fraas, L.M., Eds., *Solar Cells and Their Applications*, 2nd edn. Hoboken, NJ: Wiley & Sons, pp. 293–312.

[6] Typical Meteorological Year 3 (TMY3) database [available online at http://rredc.nrel.gov/solar/old_data/nsrdb/1991-2005/tmy3/].

[7] Gueymard, C. 2005, "SMARTS, a simple model of the atmospheric radiative transfer of sunshine: Algorithms and performance assessment", Technical Report No. FSEC-PF-270-95. Cocoa, FL: Florida Solar Energy Center.

[8] Al Taher, O. et al. 2010, "Qualificationtesting of 40% metamorphic CPVsolar cells", *Proc. 35th IEEE PVSC*, Honolulu, Hawaii, USA, pp. 1995–1998.

[9] Dobbin, A. et al. 2011, "Energy harvest predictions for a spectrally tuned multiple quantum well", *Proc. 7th Intl. Conf. Conc. PV Sys.*, Las Vegas, Nevada, USA.

[10] Olson, S. 2011. "NREL confirms world-record 43.5% efficiency on Solar Junction's CPV cell", PV-tech [available online at www.pv-tech.org/news/nrel_confirms_world_record_43.5_efficiency_on_solar_junctions_cpv_cell].

[11] Kinsey, G.S. et al. 2011, "Increasing Power and Energy in Amonix CPV Solar Power Plants", *IEEE Journal of Photovoltaics*, vol.1, no.2, pp.213-218

[12] Miller, D.C. and Kurtz, S.R. 2011, "Durability of Fresnel lenses: A review specific to the concentrating photovoltaic application", *Solar Energy Mater. & Solar Cells*, Vol. 95, pp. 2037–2068.

[13] CPV Consortium [available online at http://www.cpvconsortium.org/].


### About the Author


**Geoffrey S. Kinsey** is senior director of research and development at Amonix in Seal Beach, California, USA, where he leads the team for optimizing the operation of Amonix solar power generators using III-V multijunction cells. From 2001 to 2008, he was at Boeing-Spectrolab carrying out R&D of high-efficiency III-V multijunction cells for both space and terrestrial applications. Dr. Kinsey received his B.S. from Yale University and his Ph.D. from the University of Texas at Austin.

### Enquiries

Tel: +1 310 744 6002
Email: gkinsey@amonix.com

# Harmonized procedures for long-term energy yield measurements and performance evaluation of PV modules in outdoor conditions

**Vincent Helmbrecht[1], Diana Craciun[1], Abraham Ellis[2], Jennifer Granata[2], Stathis Tselepis[3], Anastasios Kyritsis[3] & Nikos Hatziargyriou[4]**
[1]European Distributed Energy Resources Laboratories (DERlab) e.V., Kassel, Germany;
[2]Sandia National Laboratories, Albuquerque, New Mexico, USA;
[3]Centre for Renewable Energy Sources and Saving (CRES), Pikermi, Greece;
[4]Institute of Communication and Computer Systems - National Technical University of Athens (ICCS-NTUA), Athens, Greece

ABSTRACT
As yet, procedures for long-term tests of photovoltaic modules in outdoor conditions have not been considered by international standardization committees. Although many laboratories perform long-term PV outdoor tests, a commonly agreed and standardized procedure has so far not been adopted. The European Distributed Energy Resources Laboratories' (DERlab) approach to filling the gap of international standardization has led to the development of a basic protocol that complies with European and international standards, while providing specific common guidelines and procedures for measuring the energy yield of PV modules for at least one year in outdoor conditions. The DERlab procedures for long-term PV module testing are described in this paper, and the range of analyses that can be derived from the data, such as module degradation, are discussed. The paper also presents the DERlab approach to measuring module performance in outdoor conditions, which can be used to complement energy-rating methods suggested in international standards. DERlab has created consistent measuring procedures that allow the direct comparison of the energy yield of solar modules taking into account the site-specific factors of different locations and varying climatic conditions, as well as a maintenance guideline.

## Why perform long-term outdoor tests on PV modules?

Among the issues affecting technical certification and reliability, the main parameter of interest concerning PV modules is the energy yield. For this reason, long-term PV module tests are carried out to give site-specific reports about the module performance. Long-term outdoor measurements are not repeatable like laboratory measurements, but they allow a direct comparison between the energy yields of different module types under varying weather conditions. In the interests of customers and of the industry, many PV laboratories perform long-term outdoor tests, but, because of the lack of international standardization, these tests are partly performed in accordance with internal procedures. The European Distributed Energy Resources Laboratories (DERlab) has reacted to the lack of standardization by setting up a protocol that provides specific requirements and guidelines for performing PV outdoor tests over a period of at least one year.

Another aspect to consider is the modelling of energy yield. There are numerous performance models and algorithms in existence, both commercially available (such as PVSyst [1] and the Sandia Array Performance Model [2]) and proprietary. The output of these models often drives technical and financial decisions regarding the modules to use in a system, and whether a system is worth financing. Performance data from controlled outdoor module testing, at both the module level as described in the DERlab proposal, and at the systems level, are highly useful for validating model algorithms and energy yield predictions [3].

> "DERlab has reacted to the lack of standardization by setting up a protocol that provides specific requirements and guidelines for performing PV outdoor tests over a period of at least one year."

## Outdoor measurements in international standardization

Statements about outdoor testing for various purposes can be partly found in international standards. The standards for design qualification and type approval of terrestrial PV modules – IEC 61215 for crystalline silicon and IEC 61646 for thin film – suggest an outdoor exposure of the test modules to an irradiation of 60kWh/m$^2$. The purpose of the outdoor test is to "make a preliminary assessment of the ability of the module to withstand exposure to outdoor conditions and to reveal any synergistic degradation effects which may not be detected by laboratory tests" [4,5].

Although the exposure time is very short for detecting long-term effects like degradation, the standards require no visible damage at the end of the exposure time; in addition, the drop in maximum output power may not exceed 5% of the measured value before the test, and the leakage resistance has to fulfil the same criteria as in the initial measurements. Furthermore, these standards allow the determination of the electrical power under standard test conditions (STC) (irradiance intensity: 1000W/m$^2$, module/cell temperature: 25°C, irradiation spectrum: AM 1.5 in accordance with IEC 61215) and the nominal operating cell temperature (NOCT) under natural sunlight [5]. However, the realization of these requirements in outdoor conditions is quite difficult and for most regions not practicable during the whole year. That is why most PV laboratories use a module-scale solar simulator. Procedures in natural sunlight are also given, to some extent, in

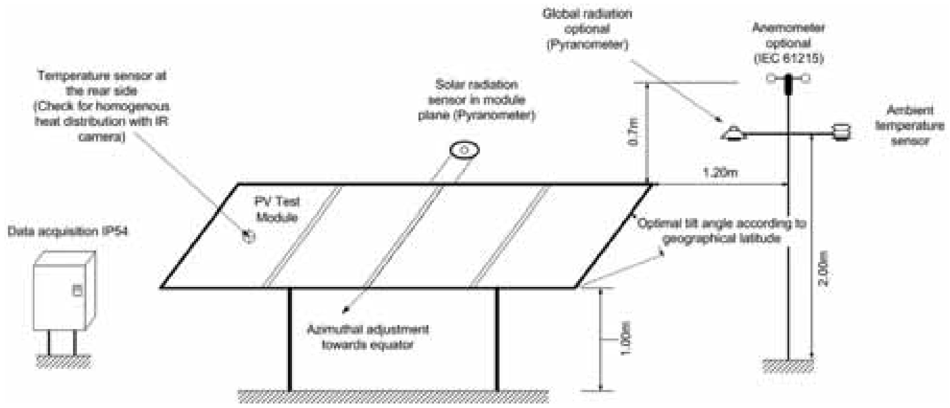


Figure 1. Typical plan of a standard testing setup [11].

the photovoltaic devices standards IEC 60904 Parts 1–10 [6].

As the procedures proposed in these standards are performed for various reasons, the requirements for measurement equipment and environmental conditions are specific to the performance of individual tests, and so the requirements can differ from test to test.

IEC 61853 provides guidelines on energy rating by calculating the energy yield on the basis of PV module characteristics and parameters, including irradiance, temperature, incident angle and spectral distribution. The calculations are performed using either given standard days or site-specific measured data. In the evaluation of site-specific data, the effort required of measurement equipment is enormous. In particular, the direct beam radiation $G_{dir}$ and the solar spectrum $E(\lambda)$ have to be measured among many other parameters. Compared to real outdoor measurements, the energy rating according to IEC 61853 leads to reasonable results [7,8]. IEC 61853 Part 1 (of 4) was published in January 2011.

IEC 61724 provides measurement procedures for the overall performance of PV systems and suggests a data analysis presentation [9]. In contrast to this monitoring standard for PV systems, DERlab is focusing on test procedures for measuring the energy yield under various meteorological conditions for a specific PV technology, or under the same conditions for different PV technologies, without taking into account the performance of the power electronics.

## The DERlab technical guidelines on long-term measurements

The common DERlab technical guidelines on long-term PV module outdoor tests were developed to harmonize outdoor testing procedures for energy yield measurements among different PV test laboratories. The document is meant to complement the above-mentioned standards by stipulating further criteria. It provides basic guidelines and procedures for the placement of measurement equipment and the requirements for the testing location as well as for the accuracy of the measurement equipment in measuring the energy yield of PV modules for at least one year. The DERlab technical guidelines do not address data evaluation and analysis.

Site-specific measurements imply natural influences on the tested modules and measurement equipment from flora and fauna, seasonal effects and regional climate. During the development of the test protocol, the maintenance of modules to remove impurities was (and still is) a controversial topic. As a justification for not cleaning the modules during the testing period, some laboratories suggest that the composition of the surface and framing of the module influences its self-cleaning mechanisms.

The DERlab document is clear in proposing a maintenance plan. It suggests that a general survey of the apparatus, and the cleaning actions of the measuring instruments and tested modules, as well as the calibration intervals for the various sensors used, should be noted for documentary and evaluation purposes.

The equipment for basic energy yield measurements records ambient temperature, module temperature, and irradiance in the module plane (plane of array); current and voltage measurements are taken at the maximum power point (MPP). The recording time interval is documented, with 15 seconds being a compromise between precision and applicability.

In accordance with ISO 9060 [10], irradiance is measured using a secondary standard pyranometer in the module plane. The sensitivity over a wide range of the solar spectrum allows a direct comparison of different module technologies to be made to a high accuracy. In the case of measurements of a single module technology, a reference cell of the same photovoltaic technology satisfying the IEC 60904-2 or IEC 60904-6 criteria is acceptable (see Fig. 1).

> "One important issue in the course of taking long-term energy yield measurements is the adequate operation availability of the transducers and data-logging apparatus."

## Initial experiences with taking measurements in accordance with DERlab guidelines

An indicative data analysis and visualization graphs are now presented and briefly discussed. One important issue in the course of taking long-term energy yield measurements is the adequate operation availability of the transducers and data-logging apparatus to avoid gaps that increase the uncertainty of the annual energy yield. An availability of at least 98% to 99% of the potential operation time per year of the PV module should be aimed for.

Long-term measurements include the continuous recording of meteorological and electrical data for at least one year. These data are required for modelling and for checking the module performance and energy yield in different conditions, such as low light or oblique illumination. Information about seasonal and long-term effects such as degradation can be given on the basis of these measurements.

In the following figures the data originate from a polycrystalline silicon module with an STC nameplate power output of 220Wp. The PV module is installed facing south in an optimal inclination angle of 30° at the Centre for Renewable Energy Sources and Saving (CRES) facilities in Pikermi. Raw

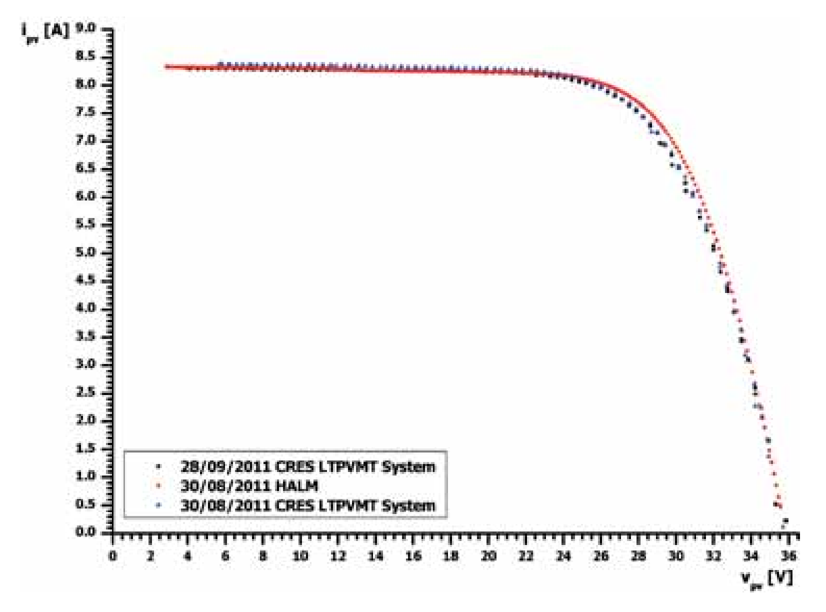


Figure 2. Polycrystalline PV module *I-V* curves, corrected for STC in accordance with IEC 60891.

| | HALM PV-CT-F1 PV Curve Tracer (30/08/2011) | CRES LTPVMT System (30/08/2011) | CRES LTPVMT System (28/9/2011) |
|---|---|---|---|
| $I_{sc}$ [A] | 8.333 | 8.331 | 8.317 |
| $V_{oc}$ [V] | 35.566 | 35.939 | 35.838 |
| $V_{mp}$ [V] | 28.12 | 27.391 | 27.871 |
| $I_{mp}$ [A] | 7.661 | 7.640 | 7.566 |
| $P_{mp}$ [W] | 215.44 | 209.28 | 210.88 |
| *FF* [%] | 72.69 | 69.89 | 70.75 |
| $\eta$ [%] | 13.21 | 12.83 | 12.93 |

Table 1. *I-V* curves of a polycrystalline Si PV module, corrected for STC using IEC 60891.

measurements taken every 15 seconds are averaged to 1-minute values. All parameters are calculated and presented for the time period between September 24th 2011 and October 8th 2011.

Once each month, a clear day with light wind is selected; the raw data of the *I-V* curve are retrieved and these data are then corrected for STC. The electrical output characteristics are determined in accordance with IEC 60891 [12]. This month-by-month analysis provides information about the module degradation over time.

Fig. 2 shows three *I-V* curves of the same polycrystalline Si PV module. Two *I-V* curves were taken on the first day of the test (August 30th 2011) using different photovoltaic curve tracers, with the objective of comparing the two outputs. The third *I-V* curve shown was taken one month later. All curves have been corrected for STC using the standard IEC 60891 to facilitate direct comparison.

More specifically, the *I-V* curves were taken on August 30th 2011 (at the beginning of the test) using: 1) a HALM PV-CT-F1 PhotoVoltaic Curve Tracer; and 2) an electronic load and analysis system that was designed and realized by CRES for long-term PV module testing. The third *I-V* curve was taken one month later, again using the CRES system, in order to investigate the PV module performance under the same conditions (STC). All the data were corrected to STC in accordance with the IEC 60891 procedure; the test results are summarized in Table 1.

Fig. 3 presents the PV module output power, as well as the field test meteorological conditions for a 15-day period (between September 24th 2011 and October 8th 2011), with 1-minute averaged

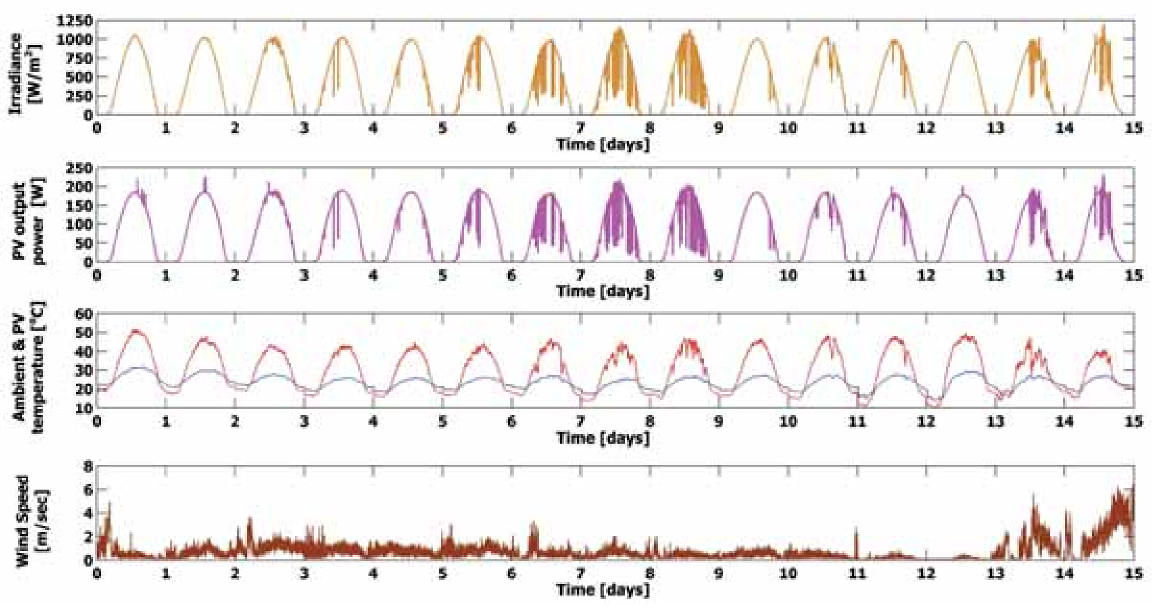


Figure 3. PV module output power and meteorological conditions analysis.

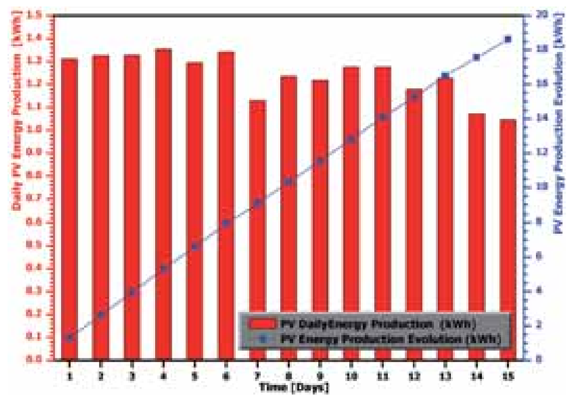


Figure 4. PV module daily and cumulative energy production.

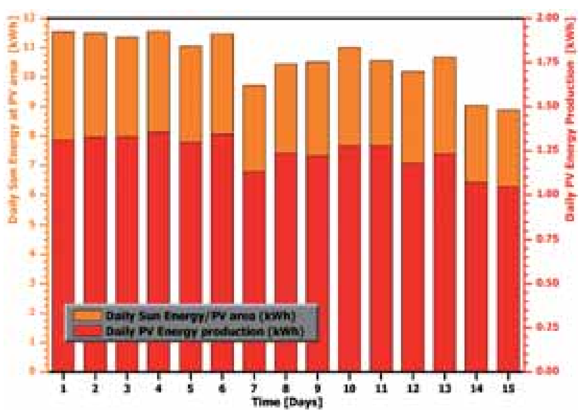


Figure 5. PV module daily energy production and average daily efficiency evolution.

recorded values and calculated parameters. A day is assumed to start at 05.00 and end at 21.00; the CRES electronic recorder system is shut down for the rest of the time.

The daily and cumulative energy production of the PV module is shown in Fig. 4; the module's daily energy production, relative to the available sun irradiation in the PV module plane, is shown in Fig. 5.

Fig. 6 illustrates the variation of the PV module efficiency during a 1-day period (day 13 in Fig. 3), with clear skies and light wind. The efficiency, as well as the PV module temperature, is plotted as a function of the irradiance for levels between 200W/m$^2$ and 1000W/m$^2$. Note how the PV module efficiency changes along the horizontal axis, going from left to right, corresponding to the morning, midday and afternoon hours.

## Model validation – real-time analysis of modelled and measured performance

Performance monitoring should involve measuring the power and energy output of the PV module or system, as well as intermediate variables such as $V_{mpp}$ and module temperature. Throughout the test period, it is recommended to regularly compare these data with the output of performance prediction tools used by industry and the financial community [1,2], given the observed weather and site conditions. An example of this approach for a system that performed well is shown in Fig. 7 in the form of a scatter plot of measured versus predicted DC power. Both approaches, either comparing modules with each other as outlined above or comparing the performance output with a model, allow performance problems to be identified. However, a comparison with an accurate model has the advantage of aiding in pinpointing the cause of the problem, which is valuable

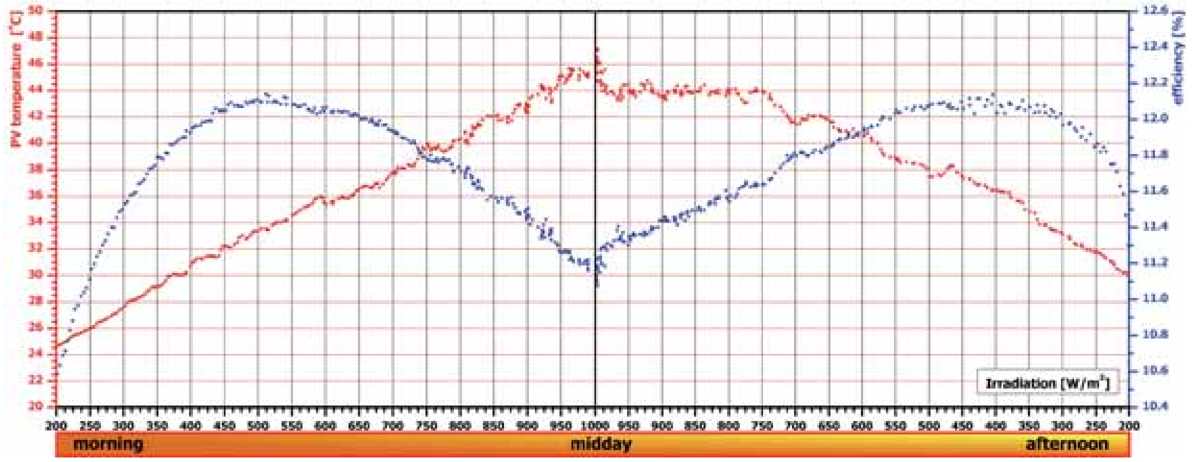


**Figure 6. PV module efficiency variation during a clear day with light wind.**

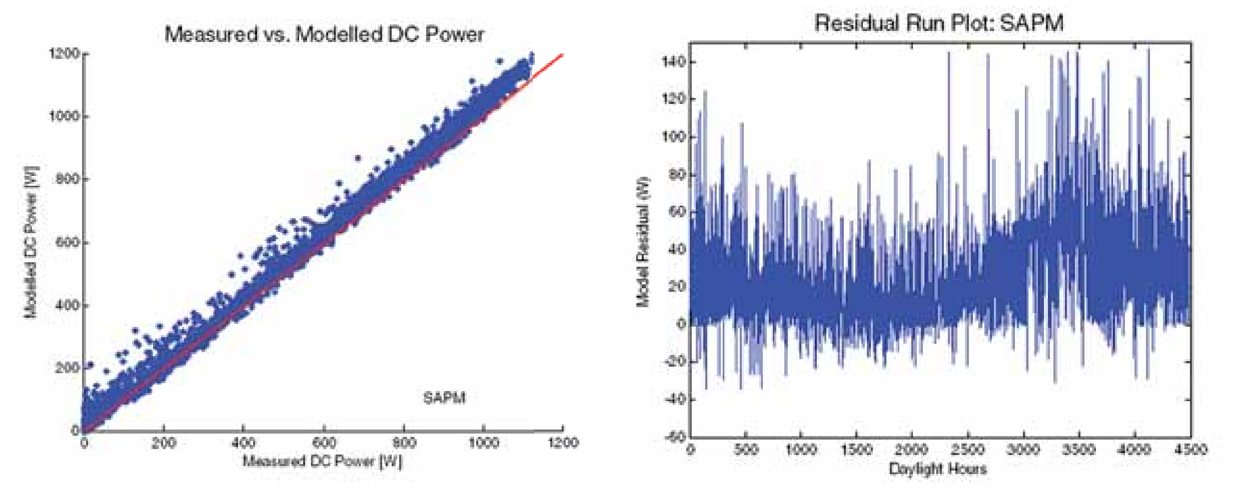


**Figure 7. Left: a comparison of measured and modelled hourly power output from a PV system that is performing as expected. Right: a plot showing residuals (modelled – measured) as a function of time [3].**

information for assessing overall system performance.

## Module degradation

Long-term outdoor testing is necessary for measuring module degradation rates. There are many challenges associated with accurately measuring degradation rates, particularly over a short time period. Module $P_{mpp}$ degradation rates of between 0.02%/year and 4%/year have been measured [13]. Most modules fall in the 0.5%/year to 1.5%/year range. Even with high-accuracy measurement equipment, it is a challenge to determine degradation rates over periods of less than three years. The DERlab approach can be used over multiple years (three or more) to measure module degradation, but in this case it is important to ensure that the modules and the irradiance equipment are cleaned prior to measuring *I-V* curves and that all the data are normalized to STC.

## Conclusion

The DERlab technical guidelines on long-term photovoltaic module outdoor tests contribute to the harmonization of testing procedures between institutes performing photovoltaic outdoor tests. Outdoor tests that are currently running and being carried out according to the aforementioned guidelines within the DERlab members' laboratories will be evaluated after a one-year time period. The experience gained from these tests will then further contribute to the harmonization of photovoltaic long-term outdoor testing. This paper has presented some examples of data evaluation with regard to performance analysis and model validation. As these data evaluations require a highly accurate database, the DERlab approach aims at increasing data accuracy by establishing comprehensive and well-defined testing procedures. With 21 partner laboratories at the moment, DERlab is working on pre-normative research in the field of distributed energy resources (DER) with a focus on smart grids integration and testing of DER technologies.

### Acknowledgements

The authors would like to thank the DERlab members for their contribution in the collection of data for this article.

### References

[1] Mermoud, A. & Lejeune, T. 2010, "Performance assessment of a simulation model for PV modules of any available technology", *Proc. 25th EU PVSEC*, Valencia, Spain.

[2] King, D.L. et al. 2004, *Photovoltaic array performance model*, Sandia National Laboratories SAND Report No. SAND2004-3535 [available online at http://www.sandia.gov/pv/docs/PDF/King%20SAND.pdf].

[3] Stein, J.S. et al. 2010, "A standardized approach to PV system performance model validation", *Proc. 35th IEEE PVSC*, Honolulu, Hawaii, USA.

[4] IEC 61646, 2008, Thin-film terrestrial photovoltaic (PV) modules – "Design qualification and type approval".
[5] IEC 61215, 2005, Crystalline silicon terrestrial photovoltaic (PV) modules – "Design qualification and type approval".
[6] IEC 60904 Parts 1–10, 1998–2011, Photovoltaic devices.
[7] IEC 61853-1, 2011, Photovoltaic (PV) module performance testing and energy rating – "Part 1: Irradiance and temperature performance measurements and power rating".
[8] Poissant, Y., Pelland, S. & Turcotte, D. 2008, "A comparison of energy rating methodologies using field test measurements", *Proc. 23rd EU PVSEC*, Valencia, Spain.
[9] IEC 61724, 1998, Photovoltaic system performance monitoring – "Guidelines for measurement, data exchange and analysis".
[10] ISO 9060, 1990, Solar energy – "Specification and classification of instruments for measuring hemispherical solar and direct solar radiation".
[11] DERlab 2011, "DERlab technical guidelines on long-term photovoltaic module outdoor tests", Reference No. 100-01.
[12] IEC 60891, 2009, Photovoltaic devices – "Procedures for temperature and irradiance corrections to measured I-V characteristics".
[13] Jordan, D.C. & Kurtz, S.R. 2011, "Photovoltaic degradation rates—an analytical review", *Prog. Photovolt: Res. Appl.*, doi: 10.1002/pip.1182.

## About the Authors

**Vincent Helmbrecht** is a research assistant for DERlab Network of Excellence in the field of photovoltaic standardization. He received his B.Eng. degree in renewable energy technologies from Nordhausen University of Applied Sciences in 2009. Vincent is currently working on his M.Sc. thesis at the University of Kassel, Germany.

**Diana Craciun** is a research coordinator within DERlab e.V. and a research engineer at Fraunhofer IWES. She completed her Ph.D. at the Grenoble Electrical Engineering Laboratory, Grenoble INP, France, on the modelling of dynamic equivalents of transmission and distribution power systems in the context of high DER penetration. Dr. Craciun received the diploma in power systems from the University 'Politehnica' of Bucharest, Romania.

**Abraham Ellis** has a Ph.D. in electrical engineering and power systems from New Mexico State University and is the technical head of Renewables Grid Integration at Sandia National Laboratories in Albuquerque, New Mexico, USA. He is the current chair of the WECC Renewable Energy Modeling Task Force and participates or leads several stakeholder groups in IEEE, NERC and IEC on the subject of wind and solar grid integration.

**Jennifer Granata** received her Ph.D. in physics from Colorado State University in 1999 and has been working in the PV field since beginning her graduate work in 1993. Dr. Granata currently leads the PV Reliability Team at Sandia National Laboratories in New Mexico and is developing infrastructure and protocols for large-scale systems testing.

**Stathis Tselepis** is the head of the Photovoltaic Systems and Distributed Generation Department at CRES in Greece. Dr. Tselepis is a member of various European organizations, such as EPIA and the European PV Technology Platform (WG3), a national expert in the European Electricity Grid Initiative (EEGI), and a member of the Solar European Industry Initiative (SEII) team for photovoltaic and concentrated solar power.

**Ch. Kyritsis Anastasios** received a Dipl. Eng. degree and a Ph.D. degree in electrical engineering from the University of Patras, Greece, in 2003 and 2009 respectively. Dr. Kyritsis is currently working in the PV System and DER Department of CRES. His research interests are power quality improvement and renewable energy source issues.



**Nikos Hatziargyriou** is deputy CEO of PPC, responsible for transmission and distribution networks, island DNO and the Center of Testing, Research and Prototyping. He has been with the Power Division of the School of Electrical Engineering of NTUA since 1984, and a full professor since 1995. Prof. Hatziargyriou is a member of CIGRE, the Convener of SCC6, a Fellow Member of IEEE, a past chair of the Power System Dynamic Performance Committee, a member of the board of directors of EURELECTRIC and a member of the EU Advisory Council of the Technology Platform on SmartGrids.

## Enquiries

**Vincent Helmbrecht**
DERlab e.V.
Tel: +49 561 7294 383
Email: vincent.helmbrecht@der-lab.net
Website: www.der-lab.net

**Diana Craciun**
DERlab e.V.
Tel: +49 561 7294 133
Email: diana.craciun@der-lab.net
Website: www.der-lab.net

# Market Watch

**Page 187**
**News**

**Page 190**
**Tariff Watch**
Nilima Choudhury,
*Photovoltaics International*

**Page 192**
**The global PV market – predictions for 2012**
Ash Sharma, Sam Wilkinson & Frank Xie, PV Research Group, IMS Research, Wellingborough, UK and Shanghai, China

**Page 195**
**The UK solar market's position worldwide in the face of changing FiT policy**
Emma Hughes, Solar Power Portal, London, UK


# News

## German government cuts FiT from March 9

Due to an aggressive FiT cut of between 20% for residential and 30% for large-scale PV installations, the German government has decided to introduce FiT cuts from March 9, 2012 to eliminate a rush of installations to beat the tariff change.

Tariff changes include 19.5€c per kWh for small-scale to 16.5€c per kWh for larger systems and only 13.5€c per kWh for 10MW or below utility plant-scale systems.

Cuts will also be made via a new mechanism each month starting in May 2012 of 15€c per kWh, while utility-scale projects over 10MW will have all incentives withdrawn after July 1, 2012.

The new tariff system is also said to eliminate the self-consumption bonus and effectively puts a cap to the subsidy per unit to 85% of electricity produced for small systems and 90% for large systems.

Source: Tory Aardvark

Due to an aggressive FiT cut of between 20% for residential and 30% for large-scale PV installations, the German government has decided to introduce the FiT cuts from March 9, 2012.



**Financial and Business News Focus**

## Main Street Power closes financing for 9MW of Toronto-based solar roof projects

Financing was recently closed for 9MW of solar rooftop projects for the Toronto area by MOM Solar, a limited partnership owned by Main Street Power and MS Solar Solutions with universal bank NORD/LB. The projects are located on large retail stores and have 20-year contracts with Ontario Power Authority. The credit facility is for CAD$35.4 million, which will finance the purchase of the completed projects from affiliates of MOM Solar.

Source: ithinqware

The credit facility totals CAN$35.4 million, which will finance the purchase of the completed projects from affiliates of MOM Solar.

## Suntech guides 2011 revenue topped US$3.13 billion; recorded impairment charges of US$571 million

Suntech Power Holdings released preliminary fourth quarter and full-year results early, highlighting better-than-expected module shipments in the fourth quarter but recorded impairment charges of US$571 million due to market conditions. Revenues in the fourth quarter of 2011 were said to be in the range of US$610 million to US$630 million. Gross margin is expected to be in the middle of the previously guided range of 9% to 11%. Suntech expects shipments in 2011 to be approximately 2.09GW, above previous guidance of 2GW. Full-year revenue is anticipated to be between US$3.13 and US$3.15 billion.

Suntech would seem to have benefited from the strong demand for modules seen in the fourth quarter, notably from Germany and the US. The company noted that it had significantly reduced accounts receivable and inventory by approximately US$450 million.

## Trina Solar's module shipments increase in Q4 but revenue and margins down

Trina Solar said that non-silicon manufacturing cost for its core raw materials to module production had declined faster than previously guided. Non-silicon costs reached approximately US$0.64 per watt, compared to its previously announced target of US$0.70 per watt by the end of 2011.

The faster-than-expected gain was said to be down to higher cell conversion efficiencies, as well as reduced supply chain costs created by increased on-site recycling of consumable and non-consumable materials.


Source: Trina Solar

Trina Solar also reported full-year PV module shipments had reached approximately 1.51GW, compared to previous guidance of 1.4GW, up 43.1% from 2010.

## SPI releases preliminary Q4 revenues of US$100 million

SPI Solar has released its preliminary financial results for Q4 2011. The company expects annual revenues to reach around US$100 million, better than its November business outlook. Additionally, SPI is forecasting that its net sales in 2012 will be double its 2011 levels as it furthers its domestic and international developments.

Source: Peak Days

SPI expects to post higher Q4 2011 revenues then earlier anticipated.

## Sunways sales almost halved in 2011 despite Q4 record module shipments

Weak demand that continued until the fourth quarter of 2011 led to Sunways' annual sales declining by almost 50% compared to 2010. Record module shipments in the fourth quarter did little to

Source: Star Solar

Sunways' preliminary full-year 2011 results show sales of €115.4 million, compared to €222.7 million in 2010.

dent the revenue declines as ASPs declined significantly compared to the previous year. Preliminary full-year 2011 results show sales of €115.4 million, compared to €222.7 million in 2010.

Sunways reported sales in the fourth quarter €31.2 million, compared to €55.5 million in the prior year period, despite achieving a new quarterly record of module shipments of 22.1MW, compared to 16.6MW in the previous period.

## AEG Power Solutions to be acquired in friendly takeover

AEG Power Solutions is to be acquired by Andrem Power, which is itself wholly owned by Nordic Capital Fund VII. Andrem Power said it had started a voluntary public takeover offer for all outstanding shares of 3W Power, AEG's parent company, for €4.35 in cash per share, a 40% premium on its average share price over the last three months.

3W Power reported recently that it had increased revenue in 2011 by 39.9% to €428.2 million, compared to €306.0 million in 2010. The closing of the transaction is expected in the second quarter of 2012, should the 95% of shares be acquired for the deal to be sanctioned.

Source: AEG Power

**Industrial power supplies and PV inverter specialist, AEG Power Solutions, is to be acquired by Andrem Power.**

## Canadian Solar shipments soar

Better-than-expected market demand across multiple regions in the fourth

Source: Canadian Solar

**The quarterly increase means full-year shipments are expected to be in the range of 1,316MW-1,326MW.**

quarter of 2011 has led to Canadian Solar's significantly increasing its module shipment guidance. Previously, the company guided fourth quarter shipments to be in the range of 340–360MW, in line with third-quarter shipment levels and in contrast to many of its tier 1 rivals. However, the company expects shipments to be in the range of 430–440MW.

The quarterly increase means full-year shipments are expected to be in the range of 1,316–1,326MW, compared to prior guidance in the range of 1,200–1,300MW.

## ESU completes sale of 3.7MW installations beating UK FiT

Europe Solar Utility (ESU) has announced the sale of one of the last solar PV installations to be completed under the UK's previous feed-in tariff, to an undisclosed investor. The three installations, which total 3.7MW, have been built on land owned by water regulator Thames Water. The area is equivalent to ten football pitches and will generate up to 3,500MWh – enough to run around 750 homes, saving Thames Water around £100,000 a year.

Source: ESU

**The three installations, which total 3.7MW, have been built on land owned by water regulator Thames Water.**

Construction of the projects was financed and managed by ESU, successfully completing the first phase of the project before the August 1, 2011, deadline qualifying it for the higher feed-in-tariff rate of £0.307kWh. The three installations, which total 3.7MW, have been built on land owned by water regulator Thames Water.

## BofA Merrill, GCL-Poly close initial transaction for funding of US solar developments

GCL-Poly Energy Holdings and Bank of America Merrill Lynch have closed the initial transaction to fund 15 solar power systems that will be developed by GCL-Poly's US subsidiary, GCL Solar Energy. The 15 solar sites will total 5MW of solar energy and serve the Palmdale School District in southern California.

The two companies acknowledged their desire for this initial funding to be the beginning of a long-term relationship that provides funding for a portion of the 1GW of solar projects under development by GCL Solar in the US.

**Market Trends & Developments**

## PV capacity in Ukraine could reach 500MW by the end of 2012

Solar PV capacity in the Ukraine is set to double in 2012 as a result of generous renewable incentives. Europe's second-largest country currently hosts Europe's biggest PV plant, a 100MW behemoth installed by Activ Solar GmbH last year, and is set to benefit from continued investment due to the scaling-back of feed-in tariff schemes across Europe.

Source: Clean Technica

**Activ Solar's 100MW solar park could mark the start of increased investment in the Ukrainian solar market.**

Ukraine offers the highest feed-in tariff rate of any European country. Currently, utility-scale projects benefit from a generous €0.46/kWh, fixed until 2030. The munificent FiT rate forms part of President Yanukovych's wider renewable energy ambitions. Yanukovych believes the nation's push towards self-sustaining energy production will help the country "earn and save money for decades to come." As a result, the president set an ambitious target of 1,000MW of installed solar capacity by 2015.

## IMS Research: Smarter use of BOS products to help push market to US$24 billion in 2016

The IMS Research report, "The World Market for PV Balance of System Equipment," noted that 40% of global BOS revenue in 2011 was contributed by PV inverters.

Nevertheless, the report identified that the fastest-growing segment is going to be tracker systems, with revenues for these products predicted to grow by nearly 30% per annum up until 2016.

A combination of factors is said to be responsible for this, including the high level of utility-scale PV project pipeline in the US, especially in high irradiation regions such as California. Another factor is the emergence of new utility-scale markets in South Africa and the Middle East, which would gain important advantages in using tracker systems to maximize system yields.

## Italian subsidies for PV systems on agricultural land cancelled by ministers

The Italian council of ministers has approved an amendment to the Quarto Conto Energia to cease the proviso of incentives for PV solar systems on agricultural land from 2013. However, the change will not apply to plants built within the next 12 months. The government is aiming to encourage and boost competition in the national economy, causing a boom in solar

Source: 123RF

**Agricultural land will no longer be available to PV manufacturers who seek a solar subsidy.**

PV-related manufacturing. Previously, the law demanded a 1MW limitation to installations on the condition that less than 10% of the land was covered with panels.

In turn, the Government has increased incentives for PV plants installed on greenhouses, by providing them the full tariff for rooftop PV plants instead of the currently applicable average between the tariffs for rooftop and ground-mounted facilities. Unlike the 2012 FiT, the 2013 amendment will already include the price for the sale of electricity roof installations costing €0.227kWh.

## Fourth quarter 2011 Japanese solar cell sales rise 30.7%

With only three out of 54 of Japan's nuclear power stations still functioning following the Fukushima crisis, sales of solar cells

Source: gstriatum.com

**Government subsidies have encouraged sales to top 1,000MW for the first time.**

were seen to rise by 30.7% last year. Government subsidies have encouraged sales to top 1,000MW for the first time.

Sales in the fourth quarter rose 30.4% from 2010 to 406.3MW. Solar cell exports for the whole of 2011 rose to 1,462.8MW, up 1.2% from a year earlier, although they fell 13.5% to 321.3MW in the last quarter of 2011.

## Leading manufacturers collaborate to update International Technology Roadmap for Photovoltaics

The 6th PV Fab Managers' Forum in Berlin will present the third edition of the International Technology Roadmap for Photovoltaics (ITRPV). Solar industry decision-makers as well as scientists and experts from research institutes and universities will gather to hear from leading European, American and Asian manufacturers of silicon wafers, solar cells and modules, who will contribute to the latest roadmap updates.

The information garnered could prove advantageous for all stakeholders, from materials suppliers to end-users. More than 20 participating companies will be setting aside their differences to make PV more competitive and ensure technological progress. They will discuss common manufacturing challenges and trends in business.

## DOE SunShot study examines potential for solar over the next several decades

The *SunShot Vision Study*, a report by the US Department of Energy's SunShot Initiative, has taken a look at the potential solar technologies have, over the next several decades, to provide a large share of electricity demand in the US. Looking at a scenario where the cost of solar technologies decreases by 75% between 2010 and 2020 and focusing on PV and CSP, the study reports on the pathways, barriers and implications that the actual achievement of the SunShot Initiative price reduction targets would have on market penetration levels.

The SunShot study utilized two models, the SunShot program and a reference scenario, developed by the National Renewable Energy Laboratory, to look and compare the possible outcomes. Among other conclusions, the study found that reaching the level of price reductions that the SunShot Initiative is promoting could result in solar energy meeting 14% of US electricity needs by 2030 and 27% by 2050. The study did note that reaching these levels did depend on a combined evolution and revolution of technological advances.

Furthermore, in addition to the prediction that the SunShot scenario would produce less carbon dioxide emissions than the reference scenario, the study also found that the SunShot scenario could support 290,000 new solar jobs by 2030 and 390,000 by 2050. The full report is available on the US DOE's SunShot Initiative website.


Source: US DoE

**The SunShot Initiative's proposals could result in solar energy meeting 14% of US electricity needs by 2030.**

News

## Europe

### Bulgaria

Last summer, Bulgaria was the land of opportunity to solar investors, despite amendments to the Energy Renewable Sources Act. With 30% cuts and renewable energy growth caps, it is easy to see why companies may be disinclined to invest in Bulgaria. However, Bulgaria currently has around 30MW of installed solar capacity. FiT rates are not regulated by law and set up on July 1 every year, which applies for 20 years, having been reduced from 25 years.

In light of plummeting prices for solar panels, the government has made considerable cuts. For instance, ground-mounted arrays larger than 200kW now receive approximately €0.29kWh, equivalent to a 19% reduction below the previous level. Roof arrays up to 200kW were cut by a more moderate 14.8% and are now eligible for €0.3049kWh. However, many sources have argued that these amendments may not have as adverse an effect on the industry as had been previously thought. Bulgarian solar irradiation ranges from 1,400 to 1,600kWh per $m^2$ annually, which would mean the new tariffs would still be considerably better than the comparable support in countries like Germany.

Prime Minister Boyko Borisov recently said: "It is not in the interest of Bulgarian citizens to see power rates rise constantly due to the expensive eco-friendly energy. The fact that we have a deadline by 2020 to comply with the target, by when the technologies will most probably be cheaper, defends the interests of Bulgarian citizens." Perhaps a contradiction, but we can still hope.

### Germany

In October 2011 it was announced that the FiT for PV installations for 2012 would be reduced by 15%, much higher than the originally anticipated 12%. However, Germany's Federal Minister of Energy and Environment, Norbert Röttgen, announced his intention to cut subsidies by as much as 29% starting on March 9th. FiTs will be reduced monthly by €0.15/kWh starting in May. Both the government and the solar industry were said to have agreed that FiTs should be cut every month, rather than the current six months, to avoid the last minute rush that, in 2011, created a record level of 7.5GW capacity; however, the momentum at which the government is moving has unions and various solar companies up in arms fearing a slump of 75%. Plants larger than 10MW will not receive any subsidies after July 1st.

### UK

The UK solar industry has been fighting an uphill struggle these last few months against the government. In January, the UK Court of Appeal upheld a High Court ruling that the Department of Energy and Climate Change acted illegally over planned cuts to FiTs. DECC has now proposed three options for FiT cuts, the most conservative of which would be 20% in July and the most extreme would see March tariff levels slashed by 35%.

*For more information on the UK PV market, see our special report on p. 195.*

### Spain

At the end of January, the nuclear-friendly, centre-right Popular Party made the controversial decision to cease renewable subsidies for new solar, wind, co-generation and waste incineration plants in the face of an ever-growing government budget deficit of €24 billion. Forty representatives of energy and environmental agencies presented a petition campaigning against the renewable energy moratorium. The petition expressed that alongside the government's disregard for the environment and rising $CO_2$ levels and loss of jobs, economically, the renewable energy sector contributes significantly to the wealth of Spain by encouraging investors.

Furthermore, on a legal note, it says the moratorium goes against the European Directives 2009/28/EC and 2010/30/EC for the energy efficiency of buildings.

The European Commission itself feels that such a seemingly rash judgment could have a devastating impact on investment opportunities and is therefore contrary to what the government wants to achieve.

### Greece

The Greek Ministry of Environment has published new FiTs for PV installations, effective February 1. The tariff for PV systems up to 100kW and for systems installed on non-interconnected islands has been reduced by 12.5% compared to the previous rate introduced in 2009. The new tariff will be further reduced by 7% every six months until August 2014.

The tariff will start at €0.328kWh in February and will eventually drop down to €0.229kWh in August 2014. From February 2015 onwards, the tariffs will be defined by a specific equation that will continue to gradually reduce the tariffs. Meanwhile, the tariff for rooftop PV systems up to 10kW will be reduced by 5% every six months. It has now been set at €0.495 and will end with a tariff of €0.383 in 2014.

## Asia & Oceania

### Malaysia

Malaysia is the latest Asian country to launch a renewables subsidy scheme with the intention the FiT will help it develop more than 3GW of new renewable capacity by 2020. The Sustainable Energy Development Authority (SEDA) expects PV to account for more than a third of this number.

SEDA has started accepting applications from PV project developers to participate in its new FiT programme. Tariffs range from €0.31 per kWh for the smallest installations to €0.21 for systems between 10MW and 30MW. The programme offers 21-year contracts and successful bidders will need to complete their systems by 2014.

### India

India's Jawaharlal Nehru National Solar Mission (JNNSM) was approved on January 11, 2010, by the National Action Plan on Climate Change, the JNNSM aims to establish India as a global solar leader, with the goal of reaching a target of 20GW of solar capacity by 2022 from the 81MW currently being produced. JNNSM is divided into three phases with the ultimate goal of reaching grid parity with coal by 2030.

- Phase I
  Date to be achieved: 2012 and 2013
  Target capacity: 1,100MW

- Phase II
  Date to be achieved: 2013 to 2017
  Target capacity: 3,000–10,000MW

- Phase III
  Date to be achieved: 2017 to 2022
  Target capacity: 20,000GW

The three main regional solar policies in India are:

**Gujarat Solar Policy**
The state of Gujarat was the first to launch its own solar policy in 2009, with the intention of remaining operative until 2014. The initial target was to achieve 500MW; however, given the level of interest, the government has allocated projects worth 935MW. For projects commissioned before January 28, 2011, tariffs for the first 12 years are €0.22kWh and then €0.08kWh for the following 13 years. For projects commissioned post January 28, 2011, tariffs start at €0.18kWh and then drop to €0.10kWh for the next 13 years.

**Rajasthan Solar Policy**
Launched in July 2011, Rajasthan's plan has a target of 12GW to be installed by 2022. In the first phase, PV projects worth 300MW will be awarded through a competitive bidding process which took place at the end of 2011 and will need to be installed by 2013.

**Karnataka Solar Policy**
Also announced in July 2011, this policy has a target of 350MW by 2016. Karnataka is looking to attract investors that are interested in developing smaller plants for a more decentralized energy supply.

### China

**The BIPV subsidy program:**
This was China's first solar subsidy program. Announced in March 2009, this offered RMB20 (€2.40) per watt for BIPV systems and RMB15 (€1.80) per watt for rooftop systems.

**The Golden Sun Program:**
This February, the Chinese Ministry of Finance cut subsidies by 22% claiming this will speed up the domestic large-scale application process to steadily develop the PV industry. In 2012, owners of PV installations relying on crystalline silicon modules and silicon thin-film modules will receive a tariff of €0.84 per watt. Previously, investors received €1.09 per watt for crystalline silicon modules and €0.97 per watt for silicon thin-film modules.

China had recently raised the target of solar energy to 15GW by 2015 from 10GW and is continuing to flourish despite accusations of dumping by American solar companies.

### Japan
It may be a new year, but the word Fukushima remains on everyone's lips. Previous efforts to bring renewable energy sources online have been hampered by the monopoly of Japan's electrical utilities. However, due to political pressure, a condition of Prime Minister Naoto Kan's resignation was to rush through a feed-in tariff policy, expected to come into force in July 2012. Aimed mainly at the residential market, for systems up to 10kW, the revised policy offers up to €0.20 per kWh and will last for about 15 years.

While the proposals have been welcomed by the renewables industry, fears remain that Japan could experience the same 'bubble' that forced many European countries to cut their subsidy schemes. A review of the finalized rates will take place in 2015 and every three years thereafter.

Currently, the tariff has been set at €0.41 per kWh for residential systems of less than 10kW and €0.39 per kWh for non-residential systems and residential systems of 10 kW and above.

## Africa & Middle East

### Israel
Around 43% of Israel's energy needs come from coal and 37% from gas; renewable energy sources represent only 0.1% of total capacity. The government has set 2014 as the year by which 5% of the country's electricity needs should be sourced from renewable energy, increasing to 10% by 2020. The government believes this target will result in €4 billion of investment in the industry and deliver 2.76GW of renewable electricity capacity by 2020.

In June 2008, the Public Utility Authority approved an FiT policy to cover small domestic and commercial plants for both solar and wind. However, in October 2011, the mid-sized FiT was cut by 25%. Last year's rates fell to €0.20/kWh for solar with new aggregate caps set at 460MW for large solar fields and 100MW for rooftop PV arrays.

Fortunately, additional subsidy mechanisms are available for renewable energy, including tax cuts, tax exemptions, facilitation of land availability and investment grants.

### South Africa
South Africa's 20-year master energy plan, the IRP, was finalized in March 2011. The plan allocates 8,400MW of solar PV to be built by 2030, rolling out 300MW a year of large-scale PV from 2012 onwards.

Currently, the FiT stands at €0.228 for ground-mounted installations greater than 1MW; for 2013, the tariff will rise to €0.230.

### Ethiopia
The Ethiopian government's Climate Resilient Green Economy Initiative, a five-year growth and transformation plan, aims to increase renewable energy production from 2,000MW to 10,000MW by the end of 2015. To fulfil this, the government is currently in the process of drafting an FiT bill to be released sometime this year.

### Botswana
Currently, Botswana imports 72% of its electricity from South Africa. The country will now introduce a renewable energy feed-in tariff next month which will apply to projects under 5MW. All other projects will need to go through power purchase agreements with Botswana Power Corporation.

## Americas

### Canada
The Ontario Power Authority has advised that rooftop projects of less than 10kW will be given a tariff of €0.61 and on the opposite end of the spectrum, more than 500kW is €0.41. For ground-based projects, the tariff is €0.49 for more than 10kW and €0.34 for less than 10MW. This will last for 20 years.

Ontario has recently been criticized by Japan and the EU who claim that the country's feed-in tariff's clause regarding domestic content requirements discriminates against imported products and violates key elements of international trade law.

Passed in 2009 by the Liberal Party, Ontario's Green Energy Act FiT program covers biomass, biogas, landfill gas, on-shore wind, solar PV and waterpower. According to government figures, it has created 13,000 jobs and attracted CAD$20 billion in private-sector investment.

Compiled by Nilima Choudhury
*Web and Publications Editor,*
*Solar Media Ltd.*

# The global PV market – predictions for 2012

**Ash Sharma**, **Sam Wilkinson** & **Frank Xie**, PV Research Group, IMS Research, Wellingborough, UK and Shanghai, China

ABSTRACT
Predicting what will happen to the global PV market is very nearly an impossible task. Its underlying principles are very similar to the dozens of other electronics markets that IMS Research studies, but the key difference in the PV industry is the very close link to, and ultimate dependence on, government policy. In a few years' time, the introduction, halting or change (or rumoured change) of a single government's PV policy will have little effect on the global industry, and the huge swings in demand will be less common and less severe. The reasons for this are clear. First, because of geographic diversification in the industry, a single country will account for a smaller portion of the global total (unlike in 2011, when Germany and Italy accounted for more than half of global demand) and thus individual governments' policy changes will have a smaller impact. Second, if system prices continue to drop rapidly (and IMS Research believes they will), a growing number of regions will achieve the 'holy grail' of grid parity and will thus no longer depend solely on government policy to drive their markets.

## Installation demand to grow but fragment in 2012

Although in 2011 IMS Research predicted a 30% growth in installation demand (this forecast was perhaps the highest of all industry analysts'), we still under-called the market. Despite the incredibly challenging conditions throughout 2011, installations still soared by some 40% – exceeding the expectations of everyone in the industry. At the time of writing this paper (early February 2012), the task of producing our annual forecast of 2012's global PV installations has not got any easier. In recent weeks major incentive cuts have been mooted by some of the industry's biggest markets, including Germany, Italy, Spain, Greece, the UK and China. These markets alone accounted for nearly 70% of global demand in 2011 and so these cuts will undoubtedly have a major effect on the outlook for global demand.

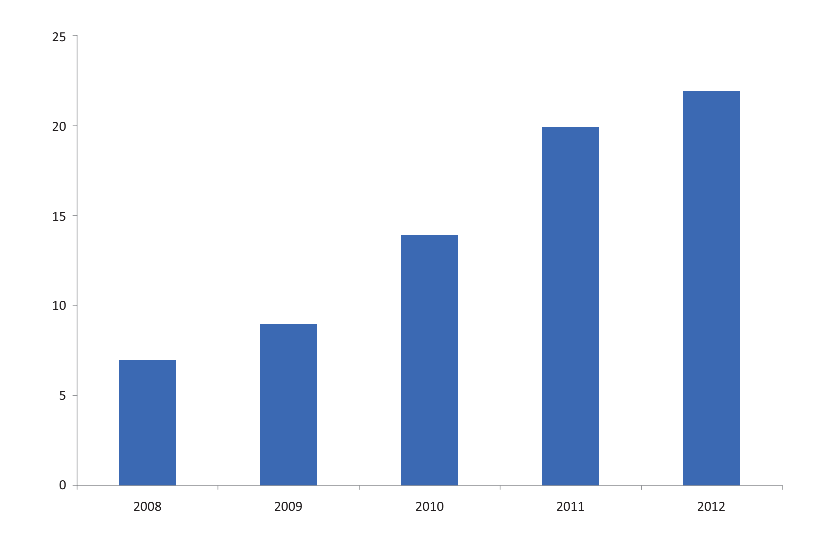


*Source: IMS Research – www.PVMarketResearch.com (Feb 2012)*

**Figure 1. Number of PV markets installing more than 100MW annually.**

> "IMS Research's latest forecasts predict that 26–29GW of new PV capacity will be added in 2012."

IMS Research's latest forecasts predict that 26–29GW of new PV capacity will be added in 2012. This would imply an increase of up to 10% over 2011. This may now seem unlikely given the harsh cuts being introduced; however, these cuts will lead to more rapid system price reductions throughout the supply chain and will allow respectable returns on investment to be achieved as well as industry growth.

Despite the growing number of countries that now have incentives in place, and despite the fact that more than 20 countries will install at least 100MW of new capacity this year, the fate of the industry will still remain closely tied to just a handful of markets. Germany and Italy are the two largest factors in the equation, and, unsurprisingly, both markets are predicted to fall considerably in 2012 following their record year in 2011. Given that these two countries have been the European PV industry's growth engine, it is also not surprising that the European market is predicted to shed around 4GW of demand this year. In view of this, the industry will need the Americas and Asia to come to its rescue, and IMS Research predicts that these regions can more than make up for Europe's shortfall.

### The US market

The US market is again projected to grow considerably in 2012, with large commercial and utility-scale plants driving the market. Its growth would, however, have been even more spectacular had lobby groups successfully achieved an extension of the 1603 policy for renewable energy projects. Ironically, the expiration of the 1603 programme will still drive huge PV deployment in 2012 as IMS Research identified massive stockpiling of modules and inverters towards the end of 2011, since systems can still qualify for the scheme in 2012, provided some of the components were purchased in 2011. These components will of course need to be installed in 2012, and installers and integrators will most likely not want to be sitting on large inventories if prices start falling rapidly again.

The biggest uncertainty facing the US market is of course the ongoing trade dispute, initiated by SolarWorld and others, with Chinese module manufacturers. At the time of writing, no decision had been made, but the introduction of steep tariffs on imports to the USA looks increasingly likely and

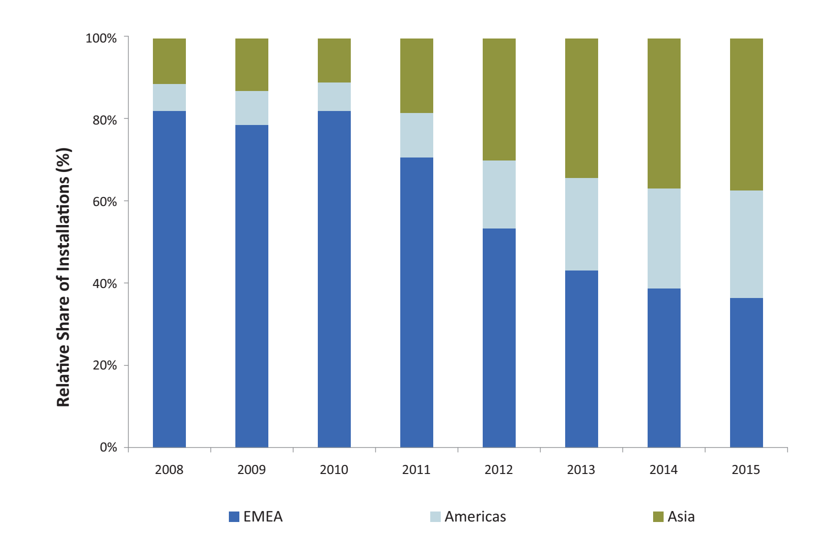


**Figure 2. PV installations in EMEA, Americas and Asia – relative share of global installations.**

*Source: IMS Research – www.PVMarketResearch.com (Feb 2012)*



could have a serious negative effect on its market's development.

> "Within Asia, and perhaps globally, China is the biggest wild card for the PV industry."

### Asia's role

Asia will play an increasingly significant role in the global PV industry in 2012, with three countries (China, Japan and India) almost certain to add more than a GW of capacity each, and with another three countries adding at least 150MW each. Within Asia, and perhaps globally, China is the biggest wild card for the PV industry. While its government recently announced tariff cuts for Golden Sun projects completed in 2012, it will undoubtedly step up aid for domestic deployment to support its huge supplier base while overseas markets are faltering. IMS Research believes that a 5GW market could well be possible in 2012, even with current incentives, and that this may even be a pessimistic prediction. As it proved in 2011, when more than 2GW was installed (despite only having a FiT mid-way through the year), the Chinese market can move quickly and is able to soak up excess supply.

Two main hindrances to the development of the Chinese PV market are the problems developers face in getting projects grid connected (due to infrastructure issues and resistance from utilities) and in moving away from only developing vast MW-scale plants in remote regions, to instead deploying PV closer to major cities that actually consume the electricity. Being able to successfully promote rooftop and smaller ground-mount systems could prove crucial in establishing China as a stable market for PV deployment and not just for supply.

## Cost – the PV industry's focus for 2012

For module suppliers, 2011 will certainly be remembered for one thing – being the year that prices were in free fall. In early 2011 all suppliers accepted that prices would fall over the course of the year. At that time, most Chinese suppliers conceded that their average selling prices (ASPs) would probably have to hit around $1.40/W by the end of the year. In reality, by the middle of Q3, they would have been delighted to have sold their modules at that price, and they ended the year with ASPs around the one dollar per watt mark. Most people predicted strong price pressure in 2011; very few, if any, predicted that prices would fall anywhere near as much as they actually did.

Much has been written about this spectacular decline in prices, but the simple version of events is that demand in Europe stopped abruptly in early 2011, largely due to the temporary cancellation of Italy's FiT, but capacity expansions continued. The result was that, though in 2010 modules could easily be sold at almost any price, in 2011 the market suddenly became very competitive. With a surplus of modules flooding the market, and very little to differentiate one from the other, competitiveness unsurprisingly came down to price. Crystalline prices at the end of 2011 were a massive 45% lower than they had been at the end of 2010, exceeding even the most aggressive forecast for price reductions.

> "So now, at the start of 2012, the PV module industry must focus on one thing – costs."

So now, at the start of 2012, the PV module industry must focus on one thing – costs. The unfortunate truth is that, in order to significantly reduce prices (and survive), it is necessary to significantly reduce costs as well, and this has certainly not been the case. No suppliers were able to reduce their cost structures at the same rate as their prices in 2011, and margins throughout the industry have certainly suffered the consequences. Average gross margins for crystalline PV module suppliers have fallen into single digits, having been in the high twenties 18 months ago.

This was highlighted by a number of high-profile exits from the industry in 2011. Easily the most talked about casualty of 2011 was the US CIGS supplier Solyndra. Although the benefits of its unique product and technology allowed it to make some progress in the industry and secure a half-billion-dollar government-backed loan guarantee, the company filed for bankruptcy in September 2011.

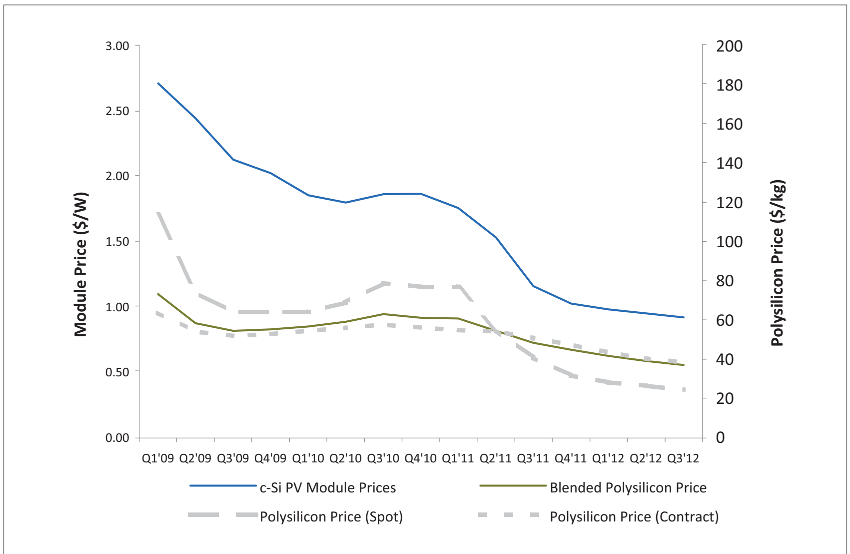


**Figure 3. Crystalline PV module prices ($/W) – contract, spot and blended average polysilicon prices ($/kg).**

*Source: IMS Research – www.PVMarketResearch.com (Feb 2012)*

Many official and unofficial statements can be read concerning the company's failure, but, put simply, it had to concede that – with prices falling as far and as fast as they did, and the high cost and price of its unique cylindrical-shaped modules – the chances of achieving profitability in the short, mid or even long term were not good. The discussion over what Solyndra's failure means for the rest of the industry continues even today, but it can clearly be seen as a warning shot to investors and PV start-ups.

A similar shot was fired across the industry's bows later in 2011 when BP Solar, one of the world's largest energy companies and one of PV industry's oldest manufacturers, announced it would leave the industry. BP has a balance sheet more than capable of riding out a few years of tight margins if the company thought this was worthwhile, but it did not.

What this means in 2012 is that investors are nervous, and the window of opportunity for small but ambitious start-up suppliers is narrowing at a fast pace. Despite the shutting of some factory doors in 2011, capacity still far outweighs demand in 2012 and so the reality is that consolidation is likely to continue, and small companies with high costs are the most vulnerable.

> "For crystalline module manufacturers, the biggest difficulty in reducing costs lies in the comparatively stubborn pricing of polysilicon."

For crystalline module manufacturers, the biggest difficulty in reducing costs lies in the comparatively stubborn pricing of polysilicon. While much has been reported of polysilicon prices declining rapidly and reaching record lows, particularly in the second half of 2011, the reality is that the silicon being offered at these low prices is from lower-tier suppliers and sold on the spot market. As the majority of silicon is sold under long-term contracts, fluctuations in spot pricing have only a small effect on the actual average price at which suppliers are buying polysilicon. With the majority of leading suppliers securing most of their polysilicon under contract, they have seen only relatively small reductions in the price that they are paying for it.

With incentive levels already starting to be pared back considerably in 2012, module suppliers' cost structures remain at the mercy of stubborn long-term polysilicon prices, and hopes for future cost reductions are understandably pinned on polysilicon prices falling. This is likely to happen in 2012, especially given that the capacity expansions of Tier 1 suppliers (originally put in motion several years ago) are due to come online during the year. Tier 1 capacity for polysilicon is predicted to reach close to 300,000MT in 2012 – enough to serve over 40GW of installations; yet installations are forecast to be broadly flat at 26–29GW. With Tier 1 polysilicon capacity alone enough to serve the entire market, and suppliers claiming cash costs are reaching close to US$20/kg, things are likely to get a lot more competitive for the big polysilicon players. This will create some much-needed breathing room for downstream manufacturers' cost structures.

With impending polysilicon price drops likely, many manufacturers have begun accepting penalty charges for cancelling long-term supply contracts in order to purchase polysilicon, wafers and cells on the spot market instead, or to renegotiate new contracts, another trend that is likely to continue in 2012.

## Conclusion

Looking back at 2011, there are certain similarities to 2009 that can be seen: changes in government subsidies causing a sharp slowdown in demand, leading to oversupply, falling prices and consequently a strong end to the year and many being surprised that installations grew. However, there is one clear difference – it will not be followed by another year of massive demand like 2010, and 2012 will undoubtedly be a lot tougher for suppliers.


### About the Authors

**Ash Sharma** is the senior research director of IMS Research's PV Research Group, overseeing the entire group's activities in this field and leading a team of analysts based in the UK, the USA and China. Now a well-known speaker and industry expert within the PV field, Ash has been involved in research for more than 10 years and joined IMS Research in 2004. Prior to this he was employed by a London-based research firm, and gained an honours degree in physics from the University of Leicester.

**Sam Wilkinson** is a senior analyst within IMS Research's PV Group, and has been heavily involved in researching the polysilicon-to-module supply chain, working closely with leading global suppliers. He has also been responsible for establishing primary research reports and benchmarking services for global system integrators and EPCs. Before joining IMS Research, Sam worked as a structural engineer for one of Europe's leading engineering firms. He has a degree in engineering from the University of Nottingham.

**Frank Xie** is a senior analyst based in IMS Research's China offices. Prior to joining IMS, he worked as an industry research and business development manager in a major Chinese chemicals company, and has also worked as an industry research manager at Frost & Sullivan. Frank has completed dozens of syndicated research reports and customized projects on sectors such as biofuels, petrochemicals, adhesives and coatings. He holds a B.A. in medical English from West China Medical Centre of Sichuan University and has a background in accounting and financial basics.

### Enquiries

IMS Research Europe (Headquarters)
3–5 Huxley Close
Wellingborough
NN8 6AB
UK
Tel: +44 (0) 1933 40 22 55
Email: pv@imsresearch.com

# The UK solar market's position worldwide in the face of changing FiT policy

**Emma Hughes**, Solar Power Portal, London, UK

ABSTRACT
The solar photovoltaics market in the United Kingdom was virtually non-existent until April 2010, when the long-awaited feed-in tariff scheme was implemented. Yet, despite coming late to the game, the UK's solar industry took off immediately, installing more than 80MW in the first 12 months alone. Now, just two years down the line, the market is placed as the world's eighth largest. This paper will take a look back at how the UK got to this point as well as considering just how bright the future of this fast-paced market will realistically be.

## A victim of its own success

When the UK government first introduced a feed-in tariff (FiT), the rate was extremely attractive. Paying out 41.3p (49.3 euro cents) per kilowatt hour of solar energy produced for systems up to 4kW, the incentive prompted a large amount of interest. In fact, in the first three months of the scheme more than 6MW of microgeneration was added to the Ofgem Central FiT Register.

Yet it wasn't long before the UK solar market became a victim of its own success. The new coalition government – which took office after the implementation of the FiT scheme – soon realized that because solar component prices were falling so dramatically, the incentive rate was simply too high. This, coupled with the fact that the UK FiT is index-linked and therefore due to increase annually, prompted the UK's first experience of feed-in tariff cuts.

At this point, feed-in tariff reductions were occurring worldwide as the cost of PV components continued to decrease. In most cases the markets affected by cuts were mature enough to cope with the changes, and therefore adapted and continued on. Examples of this were seen in Germany, Italy and France, where alterations were made in order to compensate for current market conditions. These three countries still rank among the world's top five.

However, the UK government, which was not as familiar with the photovoltaics industry as its European neighbours, resolved to impose drastic feed-in tariff cuts without consulting industry beforehand. The decision was made to dramatically decrease the tariff for larger-scale solar – above 50kW – in a bid to stunt the growth of this end of the market. On August 1, 2011, those installing systems of 5MW saw the FiT drop from 30.7p/kWh down to just 8.5p/kWh.

The UK's climate change and energy minister, Greg Barker, explained: "I want to drive an ambitious roll-out of new green energy technologies in homes, communities and small businesses and the FiT scheme has a vital part to play in building a more decentralized energy economy.

"We have carefully considered the evidence that has been presented as part of the consultation and this has reinforced my conviction of the need to make changes as a matter of urgency. Without action, the scheme would be overwhelmed. The new tariffs will ensure a sustained growth path for the solar industry while protecting the money for householders, small businesses and communities and will also further encourage the uptake of green electricity from anaerobic digestion."

This striking reduction prompted investor, market and industry uncertainty all at the same time.

At this point it seemed that large-scale solar was to be scarcely installed in the UK, as the upfront cost simply outweighed the return offered by the feed-in tariff. However, while the future looked bleak for the larger installations, the feed-in tariff rates for systems smaller than 50kW had been left untouched until the first scheduled scheme review in April 2012. These incentive rates were still considerably attractive to those working in the UK solar industry, and many began to ramp up installations.

By the end of the first FiT year, more than 73MW had been installed at microgeneration level, and this success was set to continue.

As the end of 2011 came into sight, the UK government realized the error of its ways in slashing the feed-in tariff rate for systems over 50kW while leaving the smaller system rates at the original level. As it turned out it was really this sector that needed reviewing, as the UK government's passion for small-scale generation coupled with a generous incentive rate prompted a huge amount of uptake.

Before long, the success of the smaller-scale systems prompted fears that there were more cuts on the horizon. As it turned out, these fears were well-founded.

## Small-scale slashing

On October 31, 2011 the UK's Department of Energy and Climate Change (DECC) announced its intention to reduce the feed-in tariff rates for solar PV installations up to 50kW by as much as 50%. DECC also revealed that it planned to introduce these cuts from April 1, 2012, but with a reference date of December 12, 2011 – giving installers just six weeks to install at the higher rates.

"The plummeting costs of solar means we've got no option but to act so that we stay within budget and not threaten the whole viability of the FiT scheme. Although I fully realize that adjusting to the new lower tariffs will be a big challenge for many firms, it won't come as a surprise to many in the solar industry who've themselves acknowledged the big fall in costs and the big increase in their rate of return over the past year," explained minister Barker.

"My priority is to put the solar industry on a firm footing so that it can remain a successful and prosperous part of the green economy, and so that it doesn't fall victim to boom and bust."

This proposal again prompted a huge amount of backlash from those working in the UK solar industry, as many felt that the government had again acted without consulting those at ground level. This time the proposal was held up in a courtroom, where the December deadline was deemed "unlawful". DECC appealed against this ruling to the Supreme Court, though the final judgment is yet to be announced.

Though the UK solar industry expressed the concern that these cuts would restrict the market, DECC maintained that the proposed new tariff rates will still offer

| Band | Original feed-in tariff rate (pence/kWh) | Post large-scale cuts feed-in tariff (pence/kWh) | Post microgeneration cuts feed-in tariff (pence/kWh) | Duration (years) |
|---|---|---|---|---|
| ≤4kW (new build) | 37.8 | 37.8 | 21 | 25 |
| ≤4kW (retrofit) | 43.3 | 43.3 | 21 | 25 |
| 4kW–10kW | 37.8 | 37.8 | 16.8 | 25 |
| 10kW–50kW | 32.9 | 32.9 | 15.2 | 25 |
| 50kW–100kW | 32.9 | 19 | 12.9 | 25 |
| 100kW–150kW | 30.7 | 19 | 12.9 | 25 |
| 150kW–250kW | 30.7 | 15 | 12.9 | 25 |
| 250kW+ | 30.7 | 8.5 | 8.5 | 25 |
| Standalone | 30.7 | 8.5 | 8.5 | 25 |

**Table 1. UK feed-in tariff rates before and after the cuts take place.**



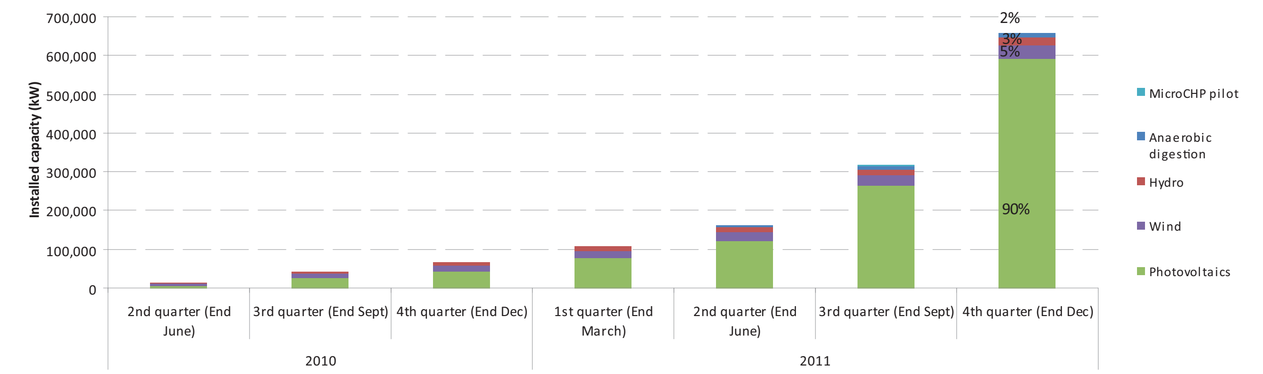


Source: DECC

**Figure 1. Installations by technology – cumulative installed capacity (kW).**

a rate of return of around 4.5% to 5% for "well-situated solar PV – broadly comparable to that intended when the scheme was set up."

While these returns are indeed profitable, those working in the industry were used to an ROI of 10% or even 20% and therefore rushed to complete as many installations as possible at the higher rate, prompting a gold rush in the solar market.

In the fourth quarter of 2011, in the two months between the October announcement and the December deadline, more than 63MW of solar was installed.

While the feed-in tariff fiasco had generated a lot of uncertainty in the UK solar industry, it also prompted a great amount of solar enthusiasm. By January 2012, the UK solar industry had installed more than 910MW, from 1kW installations right through to large-scale solar parks. This places the UK in eighth position worldwide, where previously the UK was not even recognized as a solar player.

## The UK vs. the global market

According to the European Photovoltaics Industry Association (EPIA), global PV installations reached 27.7GW in 2011, marking a 70% increase from the numbers recorded in 2010. The leading markets, including Italy, Germany, China, US, France and Japan, reached more than 1GW of additional capacity during this period. The two biggest markets in 2011, Italy and Germany, accounted for nearly 60% of global market growth during the past year. These results were achieved despite several rounds of feed-in tariff cuts in both locations.

In 2012 alone, feed-in tariff cuts have been announced in Germany, Italy, Spain, Switzerland and Greece as well as in China. The difference between most of these cuts and those occurring in the UK is that they have been implemented as a direct result of market conditions as opposed to knee-jerk reactions that have become so synonymous with the UK.

## Leading by example

In a bid to move its solar market beyond feed-in tariff furore and further uncertainty, the UK government has now pledged to step up its commitment to solar technology by working alongside – instead of against – those in the solar industry. This method has been tried and tested in successful solar markets around the world, including Germany.

Since the UK solar industry has been forced to deal with unexpected and

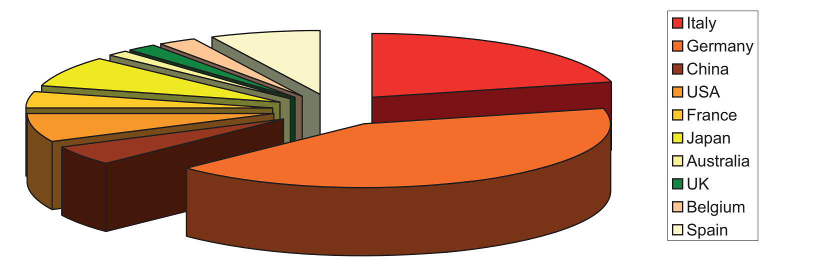


**Figure 2. Top 10 solar markets by global cumulative installed capacity (MW).**



Figure 3. Howbery Business Park in Wallingford Oxfordshire.



somewhat rash decision-making in the past, the future success of its market depends largely on government following through with this commitment.

Leading by Germany's example, the UK government has therefore set up two focus groups where members of DECC, including the minister of state for energy and climate change, can meet with representatives of the UK solar industry in order to discuss policy decisions before they are implemented. One of these groups will focus solely on the UK's solar strategy, while the other will involve members of the PV manufacturing industry, who will be able to offer advice on PV cost declines, which are likely to impact the rates of return possible in the UK. This is very similar to the way things are done in Germany, where the Federal Solar Industry Association (BSW-Solar) has regular meetings with the government.

Furthermore, after much contemplation, the UK government has also decided to implement a feed-in tariff degression model, similar to the system currently in place in Germany. DECC proposes that such a scheme is necessary to allow the British solar industry to operate within its tightly constrained budget.

Instead of targeting a specific a specific rate of return, DECC has decided that, from July 1, the tariff level should be set at a rate that "returns broadly within the range of 4.5–8% under central cost assumptions."

DECC proposes that the starting tariff levels for July 1 should be set dependent on the levels of actual deployment of solar in March and April. As a result, DECC has modelled for three different scenarios depending on the level of capacity installed in March and April.

DECC's proposed July 1 tariff rates are outlined in Table 2.

The most conservative option released by DECC would see FiT rates slashed by over 20% in July, while Option A will see March tariff levels slashed by 35%. A further 5% reduction on the July level of tariff will be enacted in October 2012, with 10% reductions being introduced every six months thereafter.

## Conclusion

For a market that is only two years old, the UK solar sector has gained a lot of experience. Having faced two rounds of harsh feed-in tariff cuts in the space of just a few months, the industry has been forced to quickly adapt to changing environments. Indeed, many have discovered how to bounce back and continue profitably despite an abundance of uncertainty. The government has also had to make changes in order to cement the future success of PV in the UK. Learning from the more experienced markets, DECC is now expected to work in partnership with the solar sector to keep key players informed of upcoming decisions as well as tracking PV price declines by communicating with experienced manufacturers.

2012 is not expected to be as tumultuous as the previous two years. As a result, the installation figures will be lower. Yet, as the market levels off, the industry is expected to pick up and work consistently to the point where grid parity is achievable and feed-in tariffs can be left in the past. Since the leading PV markets in Europe have had a considerable head-start, the UK solar sector is not projected to overtake or compete in the coming years; it will, however, be recognized as a serious contender at last.

| Band (kW) | April 1 tariff | Option A | Option B | Option C |
|---|---|---|---|---|
| ≤4kW | 21p | 13.6p | 15.7p | 16.5p |
| >4kW–10kW | 16.8p | 10.9p | 12.6p | 13.2p |
| >10–50kW | 15.2p | 9.9p | 11.4p | 11.9p |
| >50–150kW | 12.9p | 7.7p | 9.7p | 10.1p |
| >150–250kW | 12.9p | 5.8p | 8p | 10.1p |
| >250–5000kW | 8.9p | 4.7p | 6.8p | 7.1p |
| Standalone | 8.9p | 4.7p | 6.8p | 7.1p |

Table 2. Tariff rates for July 1, 2012, as proposed by DECC.


### About the Author

**Emma Hughes** is editor of news and information website Solar Power Portal and bi-monthly magazine *Solar Business Focus UK*. She has been covering the UK's solar industry since its inception in 2010, and has spent several years working in the semiconductor, consumer technology and photovoltaics industries. Emma has also presented at several global solar events and is widely regarded as one of the most influential solar technology journalists in the UK.

### Enquiries

Email: ehughes@solarpowerportal.co.uk

# Advertisers & Web Index


| ADVERTISER | WEB ADDRESS | PAGE NO. |
|---|---|---|
| 27th EU PVSEC | www.photovoltaic-conference.com | 31 |
| 3S Modultec | www.3-s.ch | 133 |
| AESCUSOFT GmbH Automation | www.aescusoft.de | 173 |
| Air Products and Chemicals, Inc. | www.airproducts.com/sunsource2 | 37 |
| ASYS Solar | www.asys-solar.com | 71 |
| BASF | www.basf.com | 87 |
| BERGER Lichtechnik GmbH & Co. KG | www.bergerlichtechnik.de | 149 |
| BTU International | www.btu.com | 69 |
| BYD New Energy | www.bydenergy.com | 179 |
| Coveme S.p.A. | www.covemephotovoltaic.com | 4, 5 |
| DEHN Surge Protection (Shanghai) Co., Ltd | www.dehn.cn | 183 |
| Dow Corning | www.dowcorning.com/solarsealants | 127 |
| Ecoprogetti S.r.l. | www.ecoprogetti.it | 131 |
| Garbo S.r.l. | www.garbosrl.net | 61 |
| GBR Schmid | www.schmid-group.com | 77, 83 |
| GfE Metalle und Materialien GmbH Fremat | www.gfe.com | 109 |
| Grenzebach Maschinenbau GmbH | www.grenzebach.com | 103 |
| GT Advanced Technologies, Inc. | www.gtat.com | IFC |
| Hanwha SolarOne | www.hanwha-solarone.com | 163 |
| H.C. Starck | www.hcstarck.com | 105 |
| Heraeus PV Business Unit | www.pvsilverpaste.com | 89 |
| Hermann Otto GmbH | www.otto-solar.com | 151 |
| Hyundai | www.hyundaisolar.com | 27 |
| IEEE PVSC | www.ieee-pvsc.org | 111 |
| Indian Solar 2012 | ww.solarsummitindia.com | 29 |
| Intersolar Europe | www.intersolar.de | 55 |
| Intevac, Inc. | www.intevac.com | 93 |
| Isovoltaic AG | www.isovoltaic.com | 25 |
| Kipp + Zonen B.V. | www.kippzonen.com | 175 |
| Komax Solar, Inc. | www.komaxsolar.com | 121 |
| Kuka Systems GmbH | www.kuka-systems.com | 9 |
| Linde Group | www.linde.com/electronics | 15 |
| LPKF SolarQuipment GmbH | www.lpkf-solarquipment.com | 95 |
| Madico | www.madico.com | 129 |
| Manz AG | www.manz.com | OBC |
| MBJ Solutions GmbH | www.mbj-solutions.com | 131 |
| MacDermid, Inc. | www.macdermid.com/photovoltaics | 41 |
| Merck | www.isishape.com | 75 |
| Meyer Burger Technology Ltd | www.meyerburger.com | 11 |
| Mondragon Assembly S. Coop. | www.mondragon-assembly.com | 137 |
| Nordson EFD | www.nordsonefd.com/ads/pvi-2011 | 85 |
| Pasan SA | www.pasan.ch | 145 |
| Pfeiffer Vacuum GmbH | www.pfeiffer-vacuum.com | 109 |
| PVA TePla AG | www.pvatepla.com | 53 |
| REC Silicon ASA | www.recgroup.com/silane | 3 |
| Rena Solar GmbH | www.rena.com | 95 |
| Robert Bürkle GmbH | www.buerkle-gmbh.de | 143 |
| Roth & Rau | www.roth-rau.de | 75 |
| Schott Solar | www.schottsolar.com/solar-yield | 161 |
| SEMI PV Group | www.semi.org | 45 |
| SENTECH Instruments GmbH | www.sentech.de | 115 |
| Shandong Linuo Power | www.linuopower.com | 159 |
| SIKO GmbH | www.siko.de | 171 |
| Silicon PV Conference | www.siliconpv.com | 57 |
| SNEC PV Power Expo | www.snec.org.cn | 19 |
| Solar Expo | www.solarexpo.com | 99 |
| Solar Power UK 2012 | www.solarpowerukevents.org | IBC |
| Solarch | www.sol-arch.eu | 181 |
| Somont GmbH | www.somont.com | 123 |
| Spire Corporation | www.spirecorp.com | 17 |
| Sputtering Components | www.sputteringcomponents.com | 105 |
| Strama – MPS Maschinenbau GmbH & Co. KG | www.strama-mps.de | 79 |
| Tempress Systems | www.tempress.nl | 83 |
| Testbourne Ltd. | www.testbourne.com | 103 |
| Tonsan Adhesive, Inc. | www.tonsan.com | 137 |
| Umicore SA Thin Film Products | www.thinfilmproducts.umicore.com | 115 |
| Umicore Substrates | www.substrates.umicore.com | 171 |
| Varian Solion | vsea.com/solion | 97 |
| Vitronic | www.vitronic.com | 127 |

**Photovoltaics** International

**DON'T MISS:** Accelerated aging of CIGS cells | Silicon ingot production | Tax issues in solar leasing agreements

I would like to purchase a subscription.

Price: ☐ 1 x Issue **$59.00 USD** (includes international delivery)
☐ 4 x Issue **$199.00 USD** (includes international delivery) Please start my subscription with edition ...........

Method of payment: ☐ Credit Card ☐ Bank Transfer

Name: ....................
Job Title: .................... Job Function: ....................
Company: .................... Div/Dept: ....................
Street Address: ....................
City: .................... Post Code/Zip: ....................
Country: ....................
Telephone Number: .................... Web URL: ....................
E-mail: ....................
For the purposes of our circulation audit, please indicate the last digit of your birth year (YYYY): ....................

**Company Activity (tick where appropriate):**

☐ PV Manufacturer (inc. Thin Film & Module) ☐ Materials Supplier ☐ Equipment Supplier

If you ticked any of the above three options, please indicate the company technology type by ticking one or more of the boxes below:

☐ Si Cell ☐ Thin Film ☐ Module ☐ Concentrator ☐ Emerging ☐ Polysilicon ☐ Ingot/Wafer

☐ University ☐ Energy Utility Supplier ☐ Government Agency
☐ R&D Facility ☐ Financial Community ☐ Other (please specify ....................)

**In order to continually improve Photovoltaics International we require your feedback. We would be very grateful if you would answer the following questions:**

(Q) Which section(s) of the publication are of interest to you? (please tick)

☐ Fab + Facilities ☐ Materials ☐ Cell Processing ☐ Thin Film
☐ PV Modules ☐ Power Generation ☐ Market Watch

(Q) What technical subjects do you wish to see in future editions?....................

....................

Signature:.................... Date ....................

**Payment Details:**

**Fax on +44 (0) 20 7871 0101 or email info@pv-tech.org:**

Type of credit card: ☐ VISA ☐ MasterCard ☐ American Express

Card Number: ....................
Expiry Date: ....................
3 Digit CVV Code (back of card): ....................
Cardholder's name: ....................

**Post:** Make cheques payable to **"Solar Media Ltd."**
Photovoltaics International, Trans-World House,
100 City Road, London EC1Y 2BP, UK
**Online:** PayPal - visit **www.photovoltaicsinternational.com/subscriptions**

**To request an invoice please call on 020 7871 0148**
or **email:** subscriptions@pv-tech.org

**Bank Transfer Details:**

| | |
|---|---|
| Account Name: | Solar Media Ltd. |
| Account Number: | 80686832 |
| Sort Code: | 20-39-53 |
| Swift Code: | BARC GB 22 |
| IBAN Number: | GB 42 BARC 203953 80 68 68 32 |
| Bank: | Barclays Bank Plc, 10 Hart Street, Henley-on-Thames, Oxon, RG9 2AX. |

*All invoices are calculated in Pounds Sterling.*

*Any payments made in US$ must be made according to the appropriate exchange rate at the time of payment.*

# CIGS finance - the end of the [credit] line for VCs?

2011 was hardly a vintage year for thin-film solar in the US. Doubts about revenue-ready technologies based on copper, indium, gallium and selenide coalesced around the Solyndra bankruptcy in August. In December, First Solar decided it could not replicate its success in cadmium telluride and shuttered its CIGS division.

So far this year, companies such as Stion and SoloPower, both in San Jose, California, are forging ahead with new manufacturing plants in Korea, Mississippi and Oregon. MiaSolé's future remains secure for now as the CIGS startup searches for a company to partner with and two of Silicon Valley's largest venture capital companies, Kleiner Perkins Caulfield Byers and VantagePoint, are unlikely to watch their thin-film darling get shot down in flames, taking around US$350 million with it.

But have venture capitalists spread their bets too widely when it comes to this particular emerging technology and inadvertently created barriers to high volume manufacturing? At least one industry insider thinks so.

Markus Beck was Solyndra's chief scientist until 2007. First Solar snapped up the former National Renewable Energy Laboratory scientist to lead the US$37.7 million R&D facility in Santa Clara, California.

"I want us to be frank about the mistakes that we've made in the past and preconceptions that we have that are often times wrong and not data driven," Beck told a PHOTON conference in San Francisco last week. "If we addressed those reasons, we would have been a lot smarter and could actually move CIGS where it belongs."

VC-backed startups had been experimenting too widely with sputtering, evaporation, ink printing and substrates such as glass, steel and polyimide, Beck said.

Beck claimed to have patented an optimal covaporation technique on glass substrate that could scale more cheaply and easily to high-volume manufacturing. He said that at the time of its collapse, Solyndra still had the best technology in the industry with a 20.5% lab efficiency using a 3-stage covaporation technique.

Solar Frontier, Global Solar, Solibro and Avancis have opted for an evaporation process while Stion and MiaSolé use sputtering. Having won a Department of Energy loan for US$197 million last August, SoloPower is now under pressure to prove out its pioneering electrodeposition process on flexible steel at its new 300MW facility in Portland.

Pallavi Madakasira, a CIGS engineer who left MiaSolé in 2006, and is now a Lux Research analyst said that technological diversity is good for the industry. "Evaporation and sputtering are probably going to be the two more mainstream methods that will get companies to where they want to be. It's a question of time and not everybody is patient."

But the investor profile for CIGS has already begun to alter from VCs to conglomerate acquisitions or strategic partnerships. Global Solar now sells its shingle PowerFLEX Technology to Dow and Avancis last year announced a joint venture to produce up to 400MW by 2015 with Hyundai last year.

Madakasira said: "Strategic partnerships will more likely shape the future of the CIGS industry because they are not looking to have an IPO. They have the patience because they've developed technology before and want to transfer their knowledge. They are more focused on technology improvements as opposed to an IPO or acquisition."

Contrary to conventional wisdom of VC-backed startups, technical teams at large companies may also be more ready to adapt to the rapidly changing dynamics that are particular to the CIGS market, said Beck.

"CIGS has been plagued. The biggest problem in CIGS is with discipline and funding. It's not a technology problem it's a financing problem - it's a curse. Once you go to a VC, they want to hear that this is the holy grail, this is a gamechanger. You can't change course. If you do, you're doomed. You have to stick with the idea."

Beck also claimed that before leaving Solyndra, he implored the chief executive, Chris Gronet, to ditch the cattle grid design. But Gronet apparently told him that VCs had bought into the design that ultimately proved an expensive novelty that added no efficiency.

"I told him that the design was flawed he freaked out because there was too much money invested in the company," said Beck. "I told him that we should switch to flat glass - but that would have killed the idea."

Madakasira authored last month's report from Lux Research, Sorting through the Maze of CIGS Technologies: Who Will Cash in on the Breakout Year, which identified winners who have already peeled away from the pack, while the losers would be those who had not gone far enough beyond the science project stage.

Madakasira said they had tracked around 18 CIGS companies and five came out on top. "Solar Frontier is clearly the outright winner now in terms of scale," she said.

"It's a huge advantage to be a subsidiary of a large company or in a strategic partnership with a large conglomerate, especially given the dynamics in the solar industry. In CIGS there is a huge amount of risk and liability because the technology is new and is largely unproven on a commercial or industrial scale."

Madakasira is convinced that there is still room for venture-backed innovation in CIGS, such as AQT's announcement last month of a sputter deposited copper-zinc-tin-sulfide (CZTS) process. But even though AQT recently secured US$18.7 million in venture funding, investments in CIGS may become an increasingly attractive technology proposition for large companies.

Around 85% of the solar market will continue to be dominated by silicon until at least 2025, according to IHS Emerging Energy Research. Dominance by incumbents makes it all but impossible for newcomers to enter the polycrystalline market, forcing them to seek investments in emerging technologies such as CIGS, which Lux Research estimates will reach 2.3GW with US$2.35 billion in revenue by 2015.

*This column is a revised version of a blog that originally appeared on PV-Tech.org.*

Felicity Carus is a regular freelance blogger for PV-Tech.